

WestminsterResearch

<http://www.westminster.ac.uk/research/westminsterresearch>

Characterization of MC₃ and the other melancortin receptors (MC) in the hypothalamo-pituitary-gonadal system of the mouse

Monika Dowejko

Faculty of Science and Technology

This is an electronic version of a PhD thesis awarded by the University of Westminster. © The Author, 2014.

This is an exact reproduction of the paper copy held by the University of Westminster library.

The WestminsterResearch online digital archive at the University of Westminster aims to make the research output of the University available to a wider audience. Copyright and Moral Rights remain with the authors and/or copyright owners.

Users are permitted to download and/or print one copy for non-commercial private study or research. Further distribution and any use of material from within this archive for profit-making enterprises or for commercial gain is strictly forbidden.

Whilst further distribution of specific materials from within this archive is forbidden, you may freely distribute the URL of WestminsterResearch: (<http://westminsterresearch.wmin.ac.uk/>).

In case of abuse or copyright appearing without permission e-mail repository@westminster.ac.uk

**CHARACTERIZATION OF MC₃ AND THE OTHER
MELANOCORTIN RECEPTORS (MC) IN THE
HYPOTHALAMO-PITUITARY-GONADAL SYSTEM
OF THE MOUSE**

Monika Dowejko

**A thesis submitted in partial fulfilment of the
requirements of the University of Westminster
for the degree of Doctor of Philosophy**

May 2014

Abstract

Melanocortin receptors (MC, MC₁–MC₅) are GPCRs, activated with different affinities by the melanocortin peptides (α -, β -, γ -MSH and ACTH). MC₃ has well characterised roles in both the central regulation of energy metabolism and peripheral inflammatory responses. The functions and distribution of MC₃ and the other MC in tissues of the reproductive system are unclear. Compared to wild type mice (WT), an apparent decrease in fertility of MC₃ null mice (MC₃^{-/-}) has been observed and hence it was the aim of this series of studies to characterize MC₃ and the other MC in tissues of the mouse hypothalamo-pituitary-gonadal (HPG) system.

The relative mRNA expressions of the MC have been identified at each level of the HPG axes in both male and female mice. It appeared that the MC mRNA expression may be regulated by the reproductive state of an animal and may change with age. Two different forms of POMC mRNA have been confirmed in the reproductive axes of both genders implicating local melanocortin production. Localization of MC₃ protein was unsuccessful due to a lack of specificity of all the antibodies applied. Ablation of MC₃ led to a decrease in the total pituitary hormone content in both male and female mice. The histology of testes of MC₃^{-/-} mice at different ages were abnormal compared to WT. *In vitro* incubation of hemi-sected testes of Balb/c or C57BL/6 mice in varying concentrations of selective MC₃ agonist had modulatory, although non-significant, effects on testosterone production. However, MC₃ activation during an inflammatory-like state in the testis, inhibited nitrite production but had no effects on the release of cytokines. The inhibitory action of MC₃ agonist on nitrite release was also apparent in the K9 Leydig cell line, which expresses all five isoforms of MC.

MC₃ may be both directly and/or indirectly implicated in the control of the mouse HPG system. The anti-inflammatory action of testicular MC₃ activation could lead to possible clinical applications of MC₃ agonists in the treatment of inflammatory situations associated with the loss of fertility.

Table of contents

Abstract	1
Table of contents	2
List of figures	6
List of tables	10
Acknowledgements	11
Declaration	12
List of abbreviations	13
1 General Introduction	16
1.1 <i>The role of inflammation in male idiopathic infertility</i>	16
1.2 <i>The melanocortin system</i>	23
1.2.1 Melanocortins.....	24
1.2.2 Melanocortin receptors (MC)	26
1.2.2.1 Agonists	28
1.2.2.2 Antagonists.....	28
1.2.2.3 Melanocortin receptors signalling	29
1.2.2.4 Melanocortin 1 receptors (MC ₁)	29
1.2.2.5 Melanocortin 2 receptors (MC ₂)	29
1.2.2.6 Melanocortin 3 receptors (MC ₃)	30
1.2.2.7 Melanocortin 4 receptors (MC ₄)	31
1.2.2.8 Melanocortin 5 receptors (MC ₅)	31
1.2.3 Anti-inflammatory potential of MC	32
1.3 <i>Expression and role of MC in the HPG system</i>	34
1.3.1 Hypothalamus	34
1.3.2 Pituitary	42
1.3.3 Gonads.....	46
1.3.3.1 Testis	46
1.3.3.2 Ovary	49
1.4 <i>Aims of the research</i>	52
2 Expression of MC in the HPG systems of both male and female mice	53
2.1 <i>Introduction</i>	53
2.2 <i>Materials and Methods</i>	54
2.2.1 Animals	54

2.2.2	Expression of MC mRNA in the HPG system.....	55
2.2.2.1	RNA extraction.....	55
2.2.2.2	cDNA synthesis	56
2.2.2.3	RT- PCR	57
2.2.2.4	Gel Electrophoresis	58
2.2.2.5	Sequencing of PCR products.....	58
2.2.2.6	Quantitative RT-PCR (qRT-PCR)	59
2.2.2.6.1	Primer amplification efficiency	61
2.2.2.6.2	Reference genes selection	62
2.2.2.6.3	Relative gene expression analysis.....	67
2.2.3	Expression of MC ₃ protein in the HPG system.....	68
2.2.3.1	Western blot.....	68
2.2.3.2	Immunostaining	73
2.2.3.2.1	Tissue preparation.....	73
2.2.3.2.2	Immunohistochemistry (IHC)	74
2.2.3.2.3	Immunofluorescence (IF).....	75
2.2.4	Statistics.....	78
2.3	<i>Results</i>	78
2.3.1	Expression of MC mRNA in the HPG systems of both male and female mice.....	78
2.3.1.1	Relative mRNA expression of MC in the HPG systems of Balb/c and C57BL/6 male mice.....	79
2.3.1.2	Relative mRNA expression of MC in the HPG systems of C57BL/6 male mice at different ages.	84
2.3.1.3	Relative mRNA expression of MC in the HPG systems of male and female (14 weeks) C57BL/6 mice.	88
2.3.1.4	Relative mRNA expression of MC in the HPG systems of C57BL/6 female mice (14 weeks) at different stages of pregnancy.	92
2.3.1.5	Relative mRNA expression of MC in the HPG system of a MC ₃ null male mouse.....	98
2.3.2	Expression of POMC mRNA in C57BL/6 male and female mice.	100
2.3.3	Expression of MC ₃ protein in the HPG system.....	102
2.3.3.1	MC ₃ protein characterization.....	102
2.3.3.2	Antibody characterization using recombinant MC ₃	103
2.3.3.3	Immunoreactive MC ₃ -like protein expression.....	105

2.3.3.4	Expression pattern of immunoreactive MC ₃ -like protein in testis of sexually mature (14 weeks) C57BL/6 mice.	107
2.4	<i>Discussion</i>	113
3	Comparison of Wild Type and MC₃ null mice	122
3.1	<i>Introduction</i>	122
3.2	<i>Materials and Methods</i>	123
3.2.1	Comparison of pituitary hormone content.....	123
3.2.1.1	Animals	123
3.2.1.2	Radioimmunoassays (RIAs) for pituitary hormones	124
3.2.2	Histological comparisons of testes from WT and MC ₃ ^{-/-} mice.....	128
3.2.2.1	Haemotoxylin and Eosin (H&E) staining	128
3.2.2.2	Staining Visualisation.....	128
3.2.2.3	Histological comparisons	129
3.2.2.4	ImageJ analyses.....	129
3.2.2.5	Quality Controls	130
3.2.3	Statistics.....	130
3.3	<i>Results</i>	131
3.3.1	The effects of MC ₃ gene ablation on total pituitary	131
3.3.2	The effects of MC ₃ gene ablation on testicular histology.....	134
3.4	<i>Discussion</i>	145
4	The effects of MC₃ activation in normal and LPS-stimulated mouse testicular tissue	154
4.1	<i>Introduction</i>	154
4.2	<i>Materials and Methods</i>	156
4.2.1	<i>In vitro</i> incubation of testicular tissue.....	156
4.2.1.1	Tissue collection and incubation	156
4.2.1.2	Radioimmunoassay (RIA) for testosterone	159
4.2.1.3	Biochemical Assays	162
4.2.1.3.1	Griess Assay	162
4.2.1.3.2	ELISA IL-1β	163
4.2.1.3.3	ELISA KC (CXCL1).....	165
4.2.2	The K9 Leydig cell line	166
4.2.2.1	Maintenance of the K9 Leydig cell line	166
4.2.2.2	<i>In vitro</i> stimulation of the K9 Leydig cell line	166
4.2.2.3	RT – PCR	167

4.2.2.3.1	RNA extraction	167
4.2.2.3.2	cDNA synthesis	167
4.2.2.3.3	PCR and gel electrophoresis	168
4.2.3	Statistics.....	168
4.3	<i>Results</i>	169
4.3.1	Comparison of testosterone production by the testicular tissue of Balb/c and C57BL/6 mice.....	169
4.3.2	Effects of [D-Trp ⁸]- γ ₂ -MSH under various conditions on <i>in vitro</i> testosterone and inflammatory markers production.....	170
4.3.2.1	Balb/c mice	170
4.3.2.1.1	<i>In vitro</i> testosterone production	170
4.3.2.1.2	<i>In vitro</i> nitrite production	173
4.3.2.1.3	<i>In vitro</i> IL-1 β production	176
4.3.2.1.4	<i>In vitro</i> KC production	179
4.3.2.1.5	Correlations	182
4.3.2.2	C57BL/6 mice	185
4.3.2.2.1	<i>In vitro</i> testosterone production	185
4.3.2.2.2	<i>In vitro</i> nitrite production	188
4.3.2.2.3	<i>In vitro</i> IL-1 β production	191
4.3.2.2.4	<i>In vitro</i> KC production	194
4.3.2.2.5	Correlations	197
4.3.3	Comparison of nitrite and cytokine production by LPS-stimulated testicular tissues of Balb/c and C57BL/6 mice.....	200
4.3.4	The K9 Leydig cell line	205
4.3.4.1	Relative mRNA expressions of MC in the K9 Leydig cell.....	205
4.3.4.2	Effects of γ ₂ -MSH on <i>in vitro</i> nitrite production of the LPS-stimulated K9 Leydig cell line.....	208
4.4	<i>Discussion</i>	210
5	General discussion	222
5.1	<i>Recommendations for future work</i>	228
6	References	230
7	Appendices	254
7.1	<i>Appendix 1: Image J instructions</i>	254
7.2	<i>Appendix 2: Ethics forms</i>	257

List of figures

Figure 1.1 Neuroendocrine control of the hypothalamo-pituitary-gonadal axis.	21
Figure 1.2 Processing of proopiomelanocortin (POMC) hormone precursor.	26
Figure 1.3 A model of melanocortin receptors structure	27
Figure 1.4 Proposed model of mechanism(s) through which the melanocortin system may affect the GnRH release.....	41
Figure 2.1 Primer amplification efficiency.....	61
Figure 2.2 The average expression stability value (M) of 12 reference genes.....	65
Figure 2.3 Determination of the optimal number of reference genes.	66
Figure 2.4 Example of a standard curve generated to determine the protein content in samples of interest.....	69
Figure 2.5 Relative mRNA expression of MC in hypothalami of 8 weeks old Balb/c and C57BL/6 male mice.	80
Figure 2.6 Relative mRNA expression of MC in pituitaries of 8 weeks old Balb/c and C57BL/6 male mice.	81
Figure 2.7 Relative mRNA expression of MC in testes of 8 weeks old Balb/c and C57BL/6 male mice.	82
Figure 2.8 MC mRNA expression in tissues from C57BL/6 and Balb/c 8 weeks old male mice.....	83
Figure 2.9 Relative mRNA expression of MC in hypothalami of 8 and 14 weeks old C57BL/6 male mice.	85
Figure 2.10 Relative mRNA expression of MC in pituitaries of 8 and 14 weeks old C57BL/6 male mice.	86
Figure 2.11 Relative mRNA expression of MC in testes of 8 and 14 weeks old C57BL/6 male mice.	87
Figure 2.12 MC mRNA expression in tissues from 14 weeks old male and female C57BL/6 mice.	89
Figure 2.13 Relative mRNA expression of MC in hypothalami from male and female (14 weeks) C57BL/6 mice.	90
Figure 2.14 Relative mRNA expression of MC in pituitaries from male and female (14 weeks) C57BL/6 mice.	91

Figure 2.15 Average mRNA expression level of reference genes (ACTB and ATP5B) in all female samples.	93
Figure 2.16 Relative mRNA expression of MC in hypothalami of 14 weeks old C57BL/6 female mice at different stages of pregnancy.	94
Figure 2.17 Relative mRNA expression of MC in pituitaries of 14 weeks old C57BL/6 female mice at different stages of pregnancy.	95
Figure 2.18 Relative mRNA expression of MC in ovaries of 14 weeks old C57BL/6 female mice at different stages of pregnancy.	96
Figure 2.19 Relative mRNA expression of MC in uteri of 14 weeks old C57BL/6 female mice at different stages of pregnancy.	97
Figure 2.20 Relative mRNA expression of MC in tissues from 14 weeks old wild type and MC ₃ null male mice.	99
Figure 2.21 MC mRNA expression in tissues from 14 weeks old MC ₃ null male mouse.	100
Figure 2.22 POMC mRNA expression in mice tissues	101
Figure 2.23 The effects of different denaturing conditions on detection of immunoreactive MC ₃ -like protein in tissue homogenates.	103
Figure 2.24 The effects of Enzo antibody preincubation with recombinant MC ₃	104
Figure 2.25 The effects of Abcam antibody preincubation with recombinant MC ₃	105
Figure 2.26 Immunoreactive MC ₃ -like protein expression in male and female mice tissues.	106
Figure 2.27 Immunohistochemical staining for Sertoli (Wilm's Tumour 1, WT-1) and Leydig cells (3β-HSD) in mice testes	108
Figure 2.28 Expression of immunoreactive MC ₃ -like protein (Enzo) in mice testes. ...	109
Figure 2.29 Expression of immunoreactive MC ₃ -like protein and 3β-HSD in mice testes.	110
Figure 2.30 Expression of immunoreactive MC ₃ -like protein and 3β-HSD in testes of wild type and MC ₃ null mice.	111
Figure 2.31 Expression of immunoreactive MC ₃ -like protein in testes of wild type and MC ₃ null mice.	112
Figure 2.32 Anti-MC ₃ antibodies – amino acid sequences and recognition sites.	120
Figure 3.1 Total pituitary hormone content in wild type (blue bars) and MC ₃ null (black bars) male mice.	132

Figure 3.2 Total pituitary hormone content in wild type (pink bars) and MC ₃ null (black bars) female mice.	133
Figure 3.3 Microscopic images of testes from Wild Type (WT) and MC ₃ null mice (MC ₃ ^{-/-}) at different ages.....	138
Figure 3.4 Examples of seminiferous tubules depleted of germ cells (arrow) in both WT (left) and MC ₃ ^{-/-} (right) mice at 3-4 weeks of age.	138
Figure 3.5 Area (%) occupied by the tissue.....	139
Figure 3.6 Average area (µm ²) of interstitial islets.....	141
Figure 3.7 Tubule diameter (µm).....	142
Figure 3.8 Average area (µm ²) of tubules.	143
Figure 3.9 Tubule thickness (µm).....	144
Figure 4.1 Dose response effect of hCG (mIU/ml) on <i>in vitro</i> testosterone production in Balb/c (left) and C57BL/6 (right) mice testes.	157
Figure 4.2 Dose response effect of LPS (µg/ml) on <i>in vitro</i> testosterone production in Balb/c mice testes.....	158
Figure 4.3 Dose response effect of SHU9119 (µg/ml) on <i>in vitro</i> testosterone production in Balb/c mice testes.	158
Figure 4.4 Dose response effect of SHU9119 (µg/ml) on <i>in vitro</i> testosterone production in C57BL/6 mice testes.	159
Figure 4.5 Example of a standard curve used for determination of nitrite concentrations.	163
Figure 4.6 Example of a standard curve used for determination of IL-1β concentrations.	165
Figure 4.7 Effects of hCG (50 mIU/ml) on <i>in vitro</i> testosterone production in Balb/c and C57BL/6 mice testes.....	169
Figure 4.8 Effects of [D-Trp ⁸]-γ ₂ -MSH in the presence or absence of various compounds on <i>in vitro</i> testosterone production in Balb/c mice testes.....	172
Figure 4.9 Effects of [D-Trp ⁸]-γ ₂ -MSH in the presence or absence of various compounds on <i>in vitro</i> nitrite production in Balb/c mice testes.	175
Figure 4.10 Effects of [D-Trp ⁸]-γ ₂ -MSH in the presence or absence of SHU9119, LPS and hCG on <i>in vitro</i> KC production in Balb/c mice testes.	181
Figure 4.11 Relationship between testosterone, nitrite, KC and IL-1β release from <i>in vitro</i> incubated testicular tissue of Balb/c mice.....	184

Figure 4.12 Effects of [D-Trp ⁸]- γ_2 -MSH in the presence or absence of LPS and hCG on <i>in vitro</i> testosterone production in C57BL/6 mice testes.....	187
Figure 4.13 Effects of [D-Trp ⁸]- γ_2 -MSH in the presence or absence of hCG and LPS on <i>in vitro</i> nitrite production in C57BL/6 mice testes.....	190
Figure 4.14 Effects of [D-Trp ⁸]- γ_2 -MSH in the presence or absence of hCG and LPS on <i>in vitro</i> IL-1 β production in C57BL/6 mice testes.....	193
Figure 4.15 Effects of [D-Trp ⁸]- γ_2 -MSH in the presence or absence of LPS and hCG on <i>in vitro</i> KC production in C57BL/6 mice testes.	196
Figure 4.16 Relationship between testosterone, nitrite, KC and IL-1 β release from <i>in vitro</i> incubated testes of C57BL/6 mice.....	199
Figure 4.17 Effects of LPS (10 μ g/ml) on <i>in vitro</i> nitrite and cytokines production in testicular tissue of Balb/c and C57BL/6 mice.	202
Figure 4.18 Relative mRNA expression of MC in the K9 Leydig cell line.	206
Figure 4.19 3 β -HSD and iNOS mRNA expression in the K9 Leydig cell line.	207
Figure 4.20 Dose response effect of LPS on nitrite release by the K9 Leydig cell line.	208
Figure 4.21 Effects of γ_2 -MSH on LPS-induced nitrite release by the K9 Leydig cell line.	209

List of tables

Table 1.1 Summary of melanocortin receptors distribution, functions and ligands	24
Table 2.1 Primer sequences used for RT-PCR.	57
Table 2.2 PCR conditions used for each set of primers.....	58
Table 2.3 A list of primers including their catalogue numbers and amplicon sizes used in qRT-PCR.	59
Table 2.4 Cycling conditions for qRT-PCR.....	60
Table 2.5 Primer specific amplification efficiencies.	62
Table 2.6 List of primers used in the geNorm analysis.	63
Table 2.7 Samples included in the geNorm analysis.	64
Table 2.8 qPCR cycling conditions.....	64
Table 2.9 List of primary and secondary antibodies used in Western blot.	72
Table 2.10 Concentrations and manufacturers of primary and secondary antibodies used in IHC.....	77
Table 2.11 Concentrations and manufacturers of primary and secondary antibodies used in IF.....	78
Table 3.1 Sample preparation for pituitary hormones RIAs.	126
Table 3.2 Initial antibody concentrations used in each of the pituitary hormones RIAs	126
Table 3.3 Summary of pituitary hormones RIA protocol.	127
Table 3.4 Coefficients of variations (CVs)	130
Table 3.5 Intertubular space (%) in testes from WT and MC ₃ ^{-/-} mice at different ages.	140
Table 4.1 Compounds used in <i>in vitro</i> studies.....	161
Table 4.2 Summary of testosterone RIA protocol.....	161
Table 4.3 Effects of [D-Trp ⁸]- γ ₂ -MSH on testosterone, nitrite, IL-1 β and KC production by testicular tissue of Balb/c and C57BL/6 mice under various treatment conditions.	203
Table 4.4 Effects of various treatments on testosterone, nitrite, IL-1 β and KC production by testicular tissue of Balb/c and C57BL/6 mice.	204

Acknowledgements

I would like to take this opportunity to express my deepest gratitude to the following people who helped me in one way or another during the course of this PhD project.

My supervisors Dr Caroline Smith, Dr Stephen Getting, Dr Paul Le Tissier and particularly my Director of Studies Dr Joanne Murray, for all their invaluable support and continuous guidance during development of this research.

To Professor Mauro Perretti, Dr Trinidad Montero-Melendez and Dr Leonard Cheung for their generosity and help with tissue collection.

To the technical and academic staff as well as colleagues at the University of Westminster for their assistance in various aspects of this project.

A special note of thanks to my family and friends for their support and encouragement, and to my husband to whom I dedicate this thesis.

Declaration

I declare that the research presented in this thesis is my own, except where otherwise indicated, and that it has not been submitted anywhere for any award.

List of abbreviations

A	ampere
Axxxnm	absorbance at xxx nm
ABP	androgen-binding protein
AGRP	agouti-related protein
α -, β -, γ - MSH	melanocyte stimulating hormone
ACTH	adrenocorticotrophic hormone
β -, γ -LPH	lipotrophin
bp	base pair
cDNA	complementary DNA
CNS	central nervous system
DHT	dihydrotestosterone
GH	growth hormone
GnRH	gonadotrophin-releasing hormone
h	hour(s)
hCG	human Chorionic Gonadotrophin
HPG	hypothalamo–pituitary–gonadal
HRP	horse-radish peroxidase
ELISA	enzyme–linked immunosorbant assay
FGF2	fibroblast growth factor 2
FSH	follicle stimulating hormone
FSH-R	FSH receptor
ICV	intracerebroventricular
IF	immunofluorescence
IGF1	insulin-like growth factor 1
IHC	immunohistochemistry
IL–1 β	interleukin 1 beta
INF– γ	interferon gamma
InsI3	insulin-like 3

KC	CXCL1; chemokine (C-X-C motif) ligand 1
kDa	kilo dalton
LH	luteinizing hormone
LPS	lipopolysaccharide
MC	melanocortin receptors
MC ₁₋₅	melanocortin receptor
MC ₃ ^{-/-}	melanocortin 3 receptor null mice
MCH	melanocyte concentrating hormone
µg	microgram
µl	microliter
mg	milligram
min	minute(s)
ml	millilitre
mRNA	messenger ribonucleic acid
NO	nitric oxide
NOS	nitric oxide synthase
ng	nano gram
nm	nanometer
no-RT	no reverse transcriptase control
POA	preoptic area
POMC	proopiomelanocortin protein
RIA	radioimmunoassay
rpm	rotations per minute
RT	reverse transcriptase
RT-PCR	reverse transcriptase – polymerase chain reaction
qRT-PCR	quantitative RT-PCR
SCF	stem cell factor
sec	second(s)
SEM	standard error of the mean
SD	standard deviation

SGP n	sulphated glycoproteins n
TNF- α	tumor necrosis factor alpha
TSH	thyroid stimulating hormone
WB	Western blot
WT	Wild Type
w/v	weight/volume
v/v	volume/volume
V	volt

1 General Introduction

1.1 *The role of inflammation in male idiopathic infertility*

Reproduction is a vital requisite for the survival of all living organisms. In mammals, reproduction is regulated by the evolutionarily conserved hypothalamo-pituitary-gonadal (HPG) system (Figure 1.1). Gonadotrophin releasing hormone (GnRH), synthesised primarily in cell bodies located in the medial preoptic area and arcuate nucleus of hypothalamus, is a key molecule in this control circuit. The production of this decapeptide hormone is modulated by other neuronal pathways; including, Kisspeptin (KISS1) neurones as well as neurotransmitters (GABA, noradrenaline, opiate peptides, dopamine *et cetera*) and peripheral hormones (for example, leptin). GnRH is released in a pulsatile manner, approximately one pulse per hour, into the hypophyseal portal circulation from the terminals located in the external zone of the median eminence and is delivered to the anterior pituitary lying in the hypophyseal fossa of the sphenoid bone. GnRH binds to its receptors located on one subset of anterior pituitary cells called gonadotrophs. This activation stimulates the secretion of luteinizing- (LH) and follicle-stimulating hormones (FSH). These glycoprotein hormones consist of two distinct subunits, an α subunit common to both LH and FSH as well as thyroid stimulating hormone (TSH) and human chorionic gonadotropin (hCG), and a unique β subunit. The two gonadotrophins in turn regulate gonadal functioning, including gametogenesis and steroidogenesis, in both sexes. Other anterior pituitary hormones namely prolactin and growth hormone released from lactotrophs and somatotrophs, respectively, as well as posterior pituitary oxytocin can influence gonadal functioning. Prolactin, for example, is particularly important in rodents where it

stimulates the generation of the LH surge and maintains the corpus luteum in females as well as potentiates the steroidogenic effect of LH on Leydig cells in males (Johnson, 2007).

In the ovary, FSH stimulates follicle maturation whilst LH promotes ovulation and corpus luteum formation. The primordial follicles are the fundamental components of the ovary and are derived from clusters of oocytes arrested in meiotic prophase I (Rajkovic *et al.*, 2006). Each primordial follicle consists of primary oocyte (arrested in the dictyate stage of the first meiotic prophase) surrounded by mesenchymal cells (granulosa cells). All follicles are embedded in the interstitial tissue of the ovary. During development, each primordial follicle becomes first a primary, secondary and preantral follicle, then an antral follicle and finally a preovulatory follicle, from which an oocyte will be extruded during the process of ovulation. In humans, this entire process of the primordial follicle development takes several months whilst in rodent only 3 weeks (Rajkovic *et al.*, 2006). Recruitment of primordial follicles into growing follicles begins prenatally, however, follicular maturation throughout childhood does not proceed beyond the preantral stage and follicles undergo atresia. It is following puberty that a preantral follicle may develop into an antral and then into preovulatory follicle. The transition from one stage to another of a follicle is governed by intra- and extra-ovarian factors. The early stage of follicular development, up to the preantral follicle, is facilitated by a number of auto- or para-crine factors including insulin-like growth factor 1 (IGF1), stem cell factor (SCF) and fibroblast growth factor 2 (FGF2). In the late preantral and early antral follicles there appear FSH and LH receptors in the granulosa and theca interna cells (differentiated from stroma cells surrounding follicle into theca interna and externa), respectively. FSH stimulates initial follicular growth whilst

LH assists further antral expansion. The gonadotropins stimulate synthesis of follicular inhibins influencing release of the FSH, the ratio of inhibin A to inhibin B increases with increasing stage of follicle maturation, with inhibin B predominating in the follicular phase and inhibin A in the luteal phase. Oestrogen is another product of ovarian LH and FSH stimulation. It is produced via two routes: de novo from theca cells following LH stimulation or through aromatization from theca-derived androgens in granulosa cells mediated by FSH. The balance between the two pathways is species dependent, but the latter route seems to be significantly more important. Ovarian oestrogens themselves stimulate granulosa cell proliferation, hence exerting positive feedback, which leads to increased production of steroids. The increase in oestrogens, approximately 200 – 400 % above normal concentrations, in the late stage of antral expansion in turn exerts positive effects on both the release of pituitary LH and locally on the appearance of LH-binding-sites on the outer layers of granulosa cells. The increased number of LH receptors in the theca and granulosa cells and coinciding short surge of LH lead to the oocyte's expulsion from the follicle during the process of ovulation. The follicle itself becomes corpus luteum releasing high concentrations of progestagens, which negatively feedback on the release of LH and FSH from pituitary. However, if fertilization does not occur the corpus luteum degrades after approximately 14 days and progestagen concentrations drop. This decrease leads to menstruation, which indicates the beginning of a new menstrual cycle. The approximate length of the menstrual cycle in human is 28 days. This is in contrast to rodents as their reproductive cycle, called the estrous cycle, lasts for about 4 to 5 days and resembles a shortened version of that present in large farm animals. The length of the estrous cycle in rodent can be altered by

mating. The luteal phase of a female mice mating with an infertile male at the time of ovulation lasts for 11 to 12 days and is called a pseudopregnancy. However, if a female does not mate at the time of ovulation the luteal phase is shortened to approximately 2 to 3 days. The prolonged luteal phase during an infertile mating is caused by a regular release of prolactin stimulated by the CNS. The stimulus is relayed from the sensory nerves of the cervix activated during coitus by the mechanical stimulus of the penis in the cervix (Johnson, 2007).

In the testis, similarly to the ovary, FSH promotes spermatogenesis whilst LH stimulates release of androgens. The testis displays two major compartments: the interstitial and the seminiferous tubule compartment. The interstitial compartment contains the blood and the lymphatic vessels. The interstitial islets contain mainly Leydig cells and other cells, predominantly macrophages. Leydig cells are the major source of androgens, notably testosterone, and variety of other steroids or proteins such as oestrogens, oxytocin and insulin-like 3 (Insl3). The steroids are synthesized from acetate or cholesterol in response to stimulation with LH acting through its receptors located on the surface of Leydig cells. Additionally, prolactin and inhibin facilitate the stimulatory effects of LH. Synthesized testosterone is secreted from the testis via blood and lymphatic vessels to enter systemic circulation. It can negatively feedback on pituitary and hypothalamus to decrease the release of LH and to a smaller extent FSH. Additionally, smaller concentrations of testosterone enter the seminiferous tubules, bind to androgen-binding protein and flow into the excurrent ducts. Intratesticularly produced testosterone binds to androgen receptor expressing cells such as Leydig, myoid and Sertoli cells. In the first cell type it acts in an autocrine manner to exert negative feedback. In Sertoli cells testosterone is

converted to more active dihydrotestosterone (DHT) by the action of 5 α -reductase. In contrast to the interstitial tissue, the seminiferous tubule has no blood and lymphatic vessels and is separated from the interstitial compartment by an acellular basal membrane surrounded externally by myoid cells and fibrocytes. There is restricted exchange between the two compartments, hence they differ in the fluid composition of ions, proteins, charged sugars and secreted products. The main components of the seminiferous tubules are germ cells at different stage of development. Spermatogonia located in the basal compartment are the stem cells from which the A1 spermatogonia emerge after a round of mitosis. Each A1 spermatogonia also undergoes a limited number of mitotic divisions giving rise to morphologically distinct spermatogonia type A1 to A4 at each mitotic division and hence increase the number of cells entering spermatogenesis. After the subsequent fifth division the spermatogonia type B are produced, which undergo meiotic division to form spermatocytes. Each spermatocyte rapidly enters the second meiotic division to yield haploid spermatids. These in turn undergo cytodifferentiation to form mature spermatozoa. As germ cells mature they move from the basal toward the adluminal compartment between Sertoli cells which provide nutrients for developing sperm cells. Sertoli cells are the prime site of FSH receptor (FSH-R) expression in the testis, which mediates production of androgen receptors. FSH and androgens regulate production of proteins and cytokines by Sertoli cells including androgen-binding protein (ABP), transferrin and stem cell factor which influence spermatogenesis. Sertoli cells also release sulphated glycoproteins 1 and 2 (SGP1 and 2) as well as activin A and inhibin B, which inhibits the release of FSH from the pituitary. The tight junctional complexes between the adjacent Sertoli cells create the blood-testis barrier, which prevents leakage of

spermatozoa into the systemic circulation as they are capable of eliciting an immune response. This barrier is absent prepubertally, but develops before the initiation of spermatogenesis. The process of spermatogenesis is tightly coordinated in temporal and spatial manner and is species specific. This regulation is probably mediated internally by the Sertoli cells (Russell *et al.*, 1990).

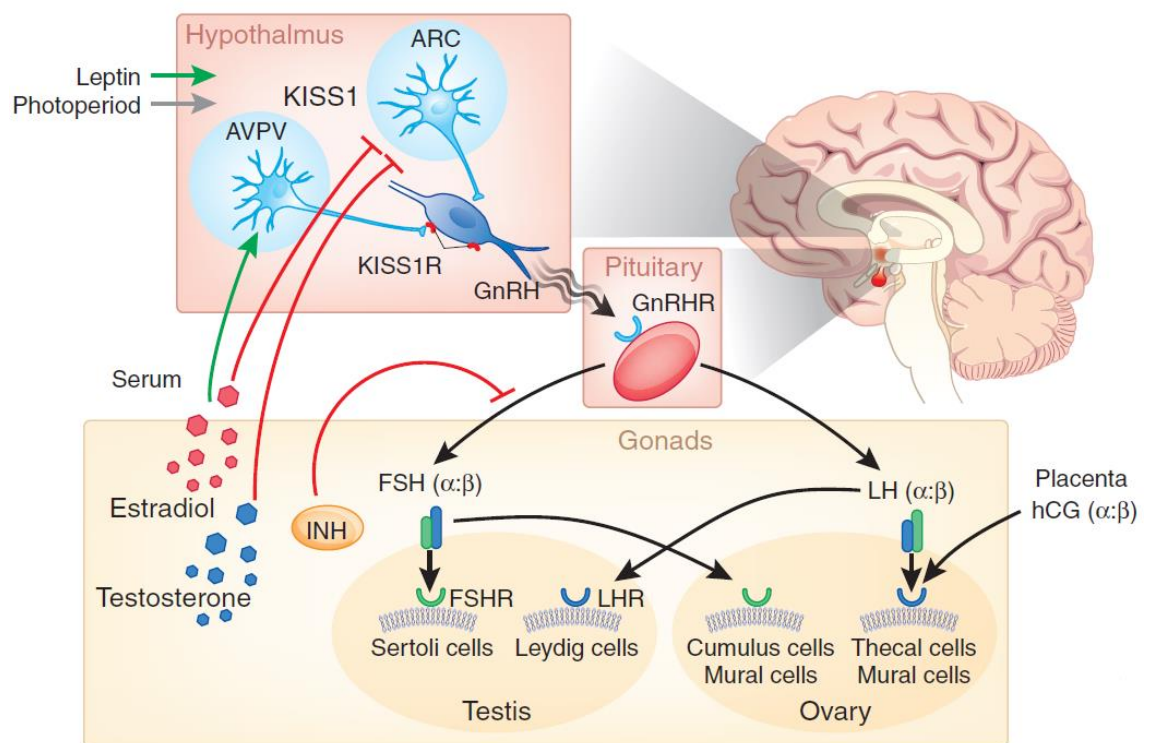


Figure 1.1 Neuroendocrine control of the hypothalamo-pituitary-gonadal axis.

Description in text; KISS1 (kisspeptin); ARC (arcuate nucleus); AVPV (anteroventral periventricular nuclei); KISSR1 (kisspeptin receptor); GnRHR (GnRH receptor); FSHR (FSH receptor); LHR (LH receptor); hCG (human chorionic gonadotropin); INH (inhibin) (Adapted from Matzuk and Lamb, 2008).

Disruption at any level of the hypothalamo - pituitary - gonadal axis may lead to infertility. Recently, the incidence of infertility has reportedly increased and it now affects one in seven couples in the United Kingdom (NICE, 2013). There are many definitions of infertility (Ray *et al.*, 2012) but according to the National Institute for Health and Clinical Excellence (NICE), infertility is defined as a failure to conceive after a period of 1 year of frequent and unprotected sexual intercourse (NICE, 2013). Nearly half of all infertility cases are due to a male factor (Forti and Krausz, 1998) and can be associated with different congenital or acquired etiologies including Klinefelter syndrome, genetic abnormalities, cryptorchidism, varicocele, genital infection, endocrine disturbances or immunological factors (Jungwirth *et al.*, 2013). Nevertheless, approximately 44 % of infertile men are categorized as having idiopathic infertility; that is, no demonstrable cause. These men appear normal on physical and endocrine examination but have a reduction in spermatozoa number, motility and normal morphology (Jungwirth *et al.*, 2013). The exact mechanisms driving these abnormalities are unclear but they are thought to be associated with factors such as genetic or epigenetic abnormalities, reactive oxygen species or environmental pollution (Nieschlag *et al.*, 2010). The contribution of testicular inflammatory cells, previously underestimated, has also been recognized and may account as an etiological factor in 40 % of idiopathic infertility cases (Moghissi *et al.*, 1980; Nieschlag *et al.*, 2010). Both humoral (antibody-mediated) and cellular immune responses are involved in immunologic infertility, although the latter type have received considerably less attention (Turek and Lipshultz, 1994). An influx of leukocytes has been detected in many testicular pathologies, such as orchitis (Trojjan *et al.*, 2009) or torsion associated with ischemia-reperfusion injury (Rodriguez *et al.*, 2006; Pellati *et al.*, 2008). It was

demonstrated, that pro-inflammatory cytokines released from activated inflammatory cells can affect normal testicular steroidogenesis and gametogenesis (Hales *et al.*, 1999). Tumor necrosis factor alpha (TNF- α), for example, impairs the motility and ability of spermatozoa to penetrate an ovum (Perdichizzi *et al.*, 2007). There is little known about the importance of testicular immune imbalance in idiopathic infertility (Nieschlag *et al.*, 2010). Treatment for this condition is usually conducted empirically with minimal scientific evidence, hence it is often ineffective and patients are recommended assisted reproduction techniques (ART) to achieve pregnancy in their partner without treatment of the underlying causes (Hamada *et al.*, 2011; Jungwirth *et al.*, 2013). New avenues in understanding testicular inflammation have to be explored to help determine possible etiologies of idiopathic infertility in male patients and develop novel diagnostic and treatment options. One such avenue would be to investigate the anti-inflammatory properties of some of the melanocortin receptors in testicular inflammation.

1.2 The melanocortin system

The melanocortin system was first identified nearly 90 years ago by the effects of what is now known as α -MSH (melanocyte stimulating hormone) on the darkening of amphibians' skin. Later, in the early 1960s these effects were also evident in human (Lerner and McGuire, 1961). However, it was not until the cloning of the first melanocortin receptor (MC₁) (Chhajlani and Wikberg, 1992; Mountjoy *et al.*, 1992) and subsequent discovery and cloning of the other four melanocortin receptors (Roselli-Rehfuss *et al.*, 1993; Gantz *et al.*, 1993a;

Chhajlani, 1996) that an interest in melanocortin signalling in mammalian physiology grew. The melanocortin receptors can be activated with different affinity by the melanocortin peptides [α -, β -, γ -MSH and adrenocorticotrophic hormone (ACTH)] or antagonized by endogenous agouti and agouti-related protein (AGRP) (Table 1.1).

	MC ₁	MC ₂	MC ₃	MC ₄	MC ₅
Expression	Melanocytes, Endothelial cells, Fibroblasts, Monocytes,	Adrenal cortex, Adipocytes	Brain, Heart, Macrophages, Gut, Kidney	Brain, Adipose tissue	Lymphocytes, Exocrine glands, Brain, Adipocytes
Function	Pigmentation, Anti-inflammatory Anti-pyretic	Steroidogenesis, Lipolysis	Cardiovascular Anti-inflammatory, Energy homeostasis	Energy homeostasis, Appetite regulation, Anti-inflammatory	Immunoregulatory functions, Lipolysis, Control of sebaceous secretion
Agonist	α -MSH > β -MSH \geq ACTH γ -MSH	ACTH	γ -MSH, β -MSH \geq ACTH, α -MSH	β -MSH \geq α -MSH, ACTH > γ -MSH	β -MSH \geq α -MSH \geq ACTH > γ -MSH

Table 1.1 Summary of melanocortin receptors distribution, functions and ligands (rank order of ligands potency based on Fong *et al.*, 2013).

1.2.1 Melanocortins

Melanocortins are derivatives of a larger precursor molecule of approximately 31 kDa called proopiomelanocortin protein (POMC). This protein is the source of ACTH, α - β - and γ -MSH as well as opiate peptides such as β -endorphin, from which the name pro-opio-melanocortin was derived. A short sequence of pituitary POMC is evolutionary conserved across all vertebrate classes and

dates back some 450 or more million years ago to common ancestors of both teleosts and mammals (Bumaschny *et al.*, 2007).

Although first identified in the anterior and intermediate lobes of the pituitary, POMC mRNA can also be found in the hypothalamus (arcuate nucleus), brainstem (solitary tract), hippocampus and cortex of the brain, as well as in peripheral organs (including skin, adrenal glands, gastrointestinal tract, immune system, ovary, testis and placenta) where its derivatives act as paracrine factors (as reviewed by Wikberg *et al.*, 2000; Bicknell, 2008).

The POMC molecule is composed of three main domains: the N-terminal with γ -MSH, the central containing ACTH and the C-terminal generating β -lipotrophin (as reviewed by Bicknell, 2008) (Figure 1.2). The core amino acid sequence, His-Phe-Arg-Trp (HFRW), is common to all melanocortins and is required for receptor binding and activation (as reviewed by Getting, 2006a). POMC protein is postrationally processed by prohormone convertases, PC1 and PC2, at dibasic cleavage sites (Gantz and Fong, 2003). PC1 leads to cleavage of ACTH, whilst PC2 generates smaller POMC peptides such as α -MSH which is derived from the first 13 amino acids of ACTH (as reviewed by Wikberg *et al.*, 2000). The expression of PC1 and PC2 mRNA shows tissue-specific variations leading to the formation of different POMC derivatives (Wilkinson, 2006). In the mouse pituitary, for example, both PC1 and PC2 are expressed in the intermediate lobe melanotrophs generating mainly α -MSH (Marcinkiewicz *et al.*, 1993). In contrast, the anterior lobe corticotrophs, synthesizing mainly ACTH, express principally PC1 and minor levels of PC2 mRNA (Marcinkiewicz *et al.*, 1993). The majority of circulating melanocortins, primarily α -MSH and ACTH, are thought to be of pituitary origin (as reviewed by Bicknell, 2008).

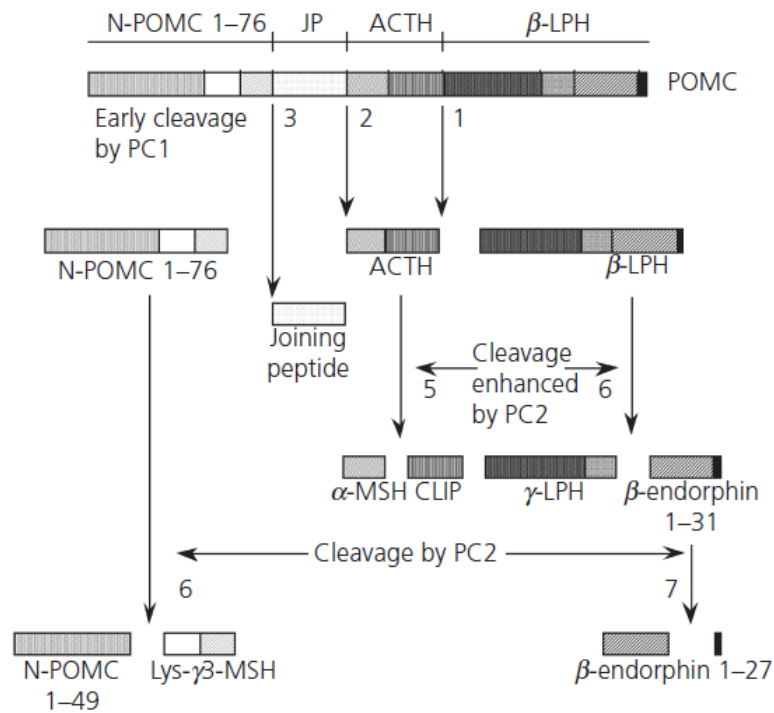


Figure 1.2 Processing of proopiomelanocortin (POMC) hormone precursor. The specific order of POMC cleavage process is illustrated by the numbers. POMC preprohormone is first processed by PC1 into N-POMC1-76, JP, ACTH and β-LPH. Further cleavage of N-POMC1-76 generates N-POMC1-49 and γ3-MSH, ACTH, and β-LPH. PC2 generates α-MSH and CLIP from ACTH, and γ-LPH and β-END from β-LPH. ACTH, adrenocorticotrophin; CLIP, corticotrophin-like intermediate peptide; JP, joining peptide; LPH, lipotrophin; MSH, melanocyte-stimulating hormone. (Adapted from Bicknell, 2008).

1.2.2 Melanocortin receptors (MC)

The melanocortin receptors (MC; MC₁-MC₅) belong to a class of small (rhodopsin) seven-transmembrane (TM) domain receptors coupled to protein G (G-protein-coupled receptors; GPCRs). They consist of a single polypeptide that is 291 – 361 amino acids long. The intracellular amino- and extracellular carboxyl- terminals as well as the second extracellular loop of MC are very short

(Figure 3; Yang, 2011). As in other GPCRs, MC contain palmitoylation sites at the C-terminus, phosphorylation sites in the 1st and 3rd intracellular transmembrane domain and potential sites for N-glycosylation at the N-terminus (Yang, 2011). Additionally, they contain a number of cysteine residues in various regions of the receptors including extracellular loops, which may lead to formation of disulfide bonds and in turn to possible receptor dimerisation (Rediger *et al.*, 2012). There is very close, approximately 42-67 % homology in the amino acids sequences between the MC (Wikberg, 1999). The majority of endogenous melanocortins bind to MC at the orthosteric receptor site but reports indicate the presence of a functional allosteric site, which alters receptor biological activity and enables increased selectivity across MC subtypes as well as selectivity across various signalling pathways (Yang, 2011). This feature of MC receptors is particularly important considering the low selectivity of known MC agonists and antagonists.

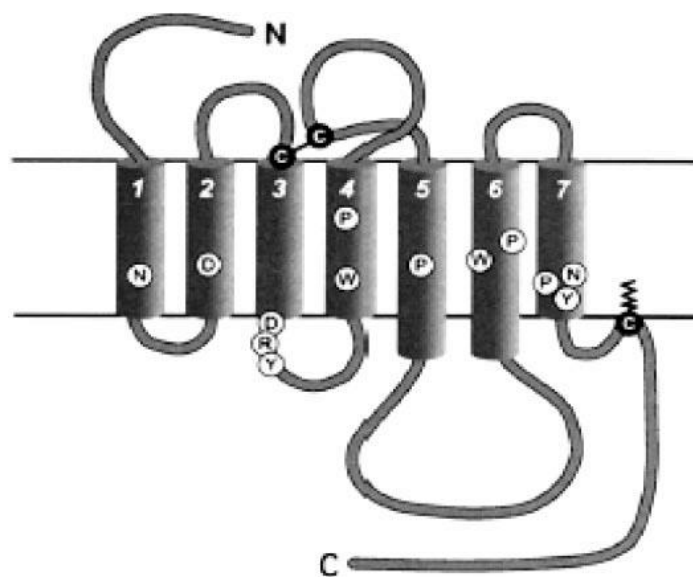


Figure 1.3 A model of melanocortin receptors structure indicating the presence of extracellular N-terminus, 7-transmembrane domains and intracellular C-terminus (Adapted from Catania *et al.*, 2004).

1.2.2.1 Agonists

Melanocortins are endogenous agonists for MC and include ACTH, α - β - and γ -MSH. Both ACTH and α -MSH activate all MC with the exception of MC₂ (ACTH only receptors). γ -MSH, in contrast, has the highest affinity for MC₃, this peptide exists in three forms, γ_1 -MSH, γ_2 -MSH and γ_3 -MSH (22-31aa), the latter variant occurs most readily in mammals (Eberle, 2000). A number of research groups attempted to generate selective MC ligands, however with different degrees of success. Available ligands include: MS05 with selectivity for MC₁ (Szardenings *et al.*, 2000), [D-Trp⁸]- γ_2 -MSH for MC₃ (Grieco *et al.*, 2000), THIQ for MC₄ (Sebhat *et al.*, 2002) and PG-901 for MC₅ (Grieco *et al.*, 2002). Nevertheless, there is still a need for more selective compounds as independent testing often demonstrates low selectivity of proposed ligands (as reviewed by Renquist *et al.*, 2011).

1.2.2.2 Antagonists

Agouti and agouti-related protein (AgRP) are the two endogenous peptides exhibiting antagonistic action on MC. They act as inverse agonists suppressing constitutively active MC as opposed to competitive antagonists, which only compete for the binding place on the receptors but do not change their biological activity (Adan, 2006). Agouti and AgRP are the only known naturally found inverse agonists for GPCRs (as reviewed by Milligan, 2003). Synthetic compounds with antagonistic action at MC are also available: HS024 (MC₁, MC₃, MC₄, MC₅) (Kask *et al.*, 1998), SHU9119 (MC₃, MC₄) (Adan *et al.*, 1999) and HS014 (MC₄, MC₃) (Schieth *et al.*, 1998), although their selectivity is not always satisfactory.

1.2.2.3 Melanocortin receptors signalling

Activation of MC leads to cAMP accumulation through activation of adenylyl cyclase in the target cell (Wikberg *et al.*, 2000). Other signal transduction pathways have also been implicated including activation of inositol triphosphate (Konda *et al.*, 1994) and protein kinase C, suggesting that melanocortins may modulate a range of signalling pathways, possibly in a tissue-specific manner (Wachira *et al.*, 2003).

1.2.2.4 Melanocortin 1 receptors (MC₁)

MC₁ was the first MC to be cloned (Chhajlani and Wikberg, 1992; Mountjoy *et al.*, 1992). This receptor subtype is almost exclusively expressed in melanocytes (Chhajlani and Wikberg, 1992) and has a well defined role in pigmentation (Abdel-Malek, 2001). This 317 amino acid protein can also be found in inflammatory cells; including, dendritic cells, neutrophils, B lymphocytes and macrophages (Star *et al.*, 1995; Taherzadeh *et al.*, 1999). It is believed to mediate anti-inflammatory and immunomodulatory effects in these cells (Catania *et al.*, 2004). The most potent MC₁ agonist is α -MSH, which also activates MC₃, MC₄ and MC₅ (Abdel-Malek, 2001). β -MSH, ACTH and γ -MSH also have potency at this receptor (Fong *et al.*, 2013).

1.2.2.5 Melanocortin 2 receptors (MC₂)

MC₂ consists of 297 amino acids and is unique as it is selectively activated by ACTH (Catania *et al.*, 2004). It has been identified in the zona glomerulosa and fasciculata of the adrenal cortex where it is involved in secretion of mineralocorticoids and glucocorticoids, respectively (Mountjoy *et al.*, 1992). MC₂ has also been shown to stimulate lipolysis in murine adipocytes (Noon *et*

al., 2006). This receptor isoform requires melanocortin 2 receptor accessory protein (MRAP) for trafficking to the cell surface (Chung *et al.*, 2008). Mutations in this component lead to defective MC₂ function and are associated with the occurrence of Familial Glucocorticoid Deficiency (FGD) characterised by glucocorticoid deficiency.

1.2.2.6 Melanocortin 3 receptors (MC₃)

The MC₃ gene encodes a protein of 361 amino acids. γ -MSH has more than 100-fold affinity and 45-fold higher potency at MC₃ as compared to the other MC (as reviewed by Renquist *et al.*, 2011). β -MSH, α -MSH and ACTH can bind to it with comparable affinity to each other. The determination of the molecular basis of MC₃ ligand binding and receptor signalling is incomplete but potential amino acid sequences in transmembrane domains have been identified (Chen *et al.*, 2006).

The greatest expression of MC₃ is in the brain, where it has been found in more than 30 different regions including the hypothalamus (arcuate nucleus, dorsomedial part of the ventromedial nucleus and medial preoptic nucleus), hippocampus and thalamus (Gantz *et al.*, 1993; Roselli-Rehfuss *et al.*, 1993). There are species differences in the pattern of MC₃ expression. In the chicken, for example, the receptor is absent in the brain but was instead found in the adrenal gland (Takeuchi and Takahashi, 1999). The peripheral expression of MC₃ has been demonstrated in a range of human tissues including gut, placenta, kidney, heart, immune cells, ovary and testis (Chhajlani, 1996).

Although this receptor subtype was identified nearly twenty years ago, its physiological functions remain largely enigmatic. Centrally expressed MC₃ is thought to participate in regulation of food intake as deduced from the knockout

model (Butler *et al.*, 2000; Chen *et al.*, 2000). In heart, MC₃ plays a protective role in myocardial ischemia-reperfusion injury (Getting *et al.*, 2004). Furthermore, in kidney, MC₃ and its potent agonist γ -MSH have an important function in sodium homeostasis as disruption of this system leads to salt-sensitive hypertension (Ni *et al.*, 2003). Activation of MC₃ in B lymphocytes (Cooper *et al.*, 2005) and macrophages (Getting *et al.*, 1999) has clear anti-inflammatory and immunomodulatory effects, which have been applied in modulating a range of disease pathologies (as reviewed by Catania *et al.*, 2004; Getting, 2006a).

1.2.2.7 Melanocortin 4 receptors (MC₄)

MC₄ consists of 332 amino acids and, similarly to MC₃, is primarily expressed in the central nervous system (CNS) including the hypothalamus, thalamus and hippocampus (Gantz *et al.*, 1993b; Chhajlani, 1996). MC₄ mRNA is located in paraventricular nucleus (PVN), including both the parvocellular and magnocellular neurones of the hypothalamus in the adult rat brain (as reviewed by Tao, 2010). Peripheral expression of MC₄ is nearly absent and most functions are attributed to the centrally expressed receptors. MC₄ is involved in the regulation of food intake and energy expenditure (Catania *et al.*, 2004). In the human, mutations of this receptor subtype lead to severe obesity (Vaisse *et al.*, 2000). There are also reports indicating that activation of centrally expressed MC₄ modulates erectile function and sexual behaviour (Van der Ploeg *et al.*, 2004).

1.2.2.8 Melanocortin 5 receptors (MC₅)

MC₅ consists of 325 amino acids and is distributed primarily in the periphery although brain expression has also been reported (Fathi *et al.*, 1995). Other

sites of expression include: the exocrine glands - sebaceous, preputial, lacrimal and Harderian (Chen *et al.*, 1997), rodent adipocytes (Møllera *et al.*, 2011) and bovine adrenal gland (Liakos *et al.*, 2000). The key function of this receptor is in the regulation of exocrine gland secretions (Chen *et al.*, 1997).

1.2.3 Anti-inflammatory potential of MC

Melanocortins comprise an ancient system, with their key role being protection and restoration of baseline conditions of the host whenever it is exposed to pathogens such as bacterial endotoxins, UV light or affected by overactivity of inflammatory mediators (Sarkar *et al.*, 2003). The anti-inflammatory properties of melanocortins were first discovered by the effects of α -MSH on suppression of inflammation induced by urate crystals (Denko and Gabriel, 1985) and fever (Rheins *et al.*, 1989). Further evidence of the anti-inflammatory effects of this and other melanocortin peptides has accumulated over years and triggered interest as potential therapeutics for the treatment of various forms of inflammation (as reviewed by Catania *et al.*, 2004; Getting, 2006a).

The anti-inflammatory effects of melanocortins are exerted through activation of MC on peripheral inflammatory cells leading to reduction in inflammatory mediators release and cell migration, as well as indirectly through binding of melanocortins within the brain and affecting the neural anti-inflammatory pathways (Lipton and Catania, 1997). α -MSH is known to inhibit activation of transcription factor NF- κ B induced by inflammatory stimuli, which leads to subsequent suppression of the gene transcription of pro-inflammatory mediators (Manna and Aggarwal, 1998).

MC₁ is the prime MC involved in the anti-inflammatory effects of melanocortins. This MC subtype has the greatest affinity for α -MSH and is expressed in

macrophages (Star *et al.*, 1995; Rajora *et al.*, 1996), neutrophils (Catania *et al.*, 1996) and mast cells (Artuc *et al.*, 1999). MC₁ expression is upregulated in response to inflammation (Bhardwaj *et al.*, 1997) and anti-MC₁ antibodies can attenuate the suppressive effects of α -MSH on TNF- α release from human monocytic cell line (Tahezadeh *et al.*, 1999).

In addition to MC₁, evidence exists that activation of MC₃ also exerts anti-inflammatory effects. Its expression was determined in murine (Getting *et al.*, 1999) and human (Tahezadeh *et al.*, 1999) macrophages. Furthermore, natural and synthetic agonists for this receptor subtype had anti-inflammatory effects in a model of experimental gout induced by urate crystals (Getting *et al.*, 2001). In this model, systemic administration of γ ₂-MSH and MTII suppressed accumulation of KC and IL-1 β as well as reduced migration of neutrophils: this effect was blocked by SHU9119 (MC₃/MC₄ antagonist). MC₃ activation also displays protective effects following ischemia-reperfusion injury characterised by influx of leukocytes. In a model of myocardial ischaemia, administration of selective and non-selective agonists for MC₃ reduced incidence of ventricular fibrillation, tachycardia, and death (Mioni *et al.*, 2003) as well as inhibited the release of inflammatory markers (Getting *et al.*, 2004).

Since the expression of MC₅ was also detected in human monocytes (Tahezadeh *et al.*, 1999), mast cells (Artuc *et al.*, 1999) and in B lymphocytes (Buggy, 1998) involvement of this receptor subtype in the immunomodulatory effects of MC cannot be excluded.

1.3 Expression and role of MC in the HPG system

1.3.1 Hypothalamus

MC₃ and MC₄, as aforementioned, are the most abundantly expressed MC in the hypothalamic nuclei. They are thought to play a key role in regulating appetite and energy balance as deduced from their knockout mice models. The MC₃ null mice (MC₃^{-/-}) exhibited a complex obesity syndrome characterised by an increase in adipose mass in parallel with reduced lean mass as well as a higher ratio of weight gain to food intake (Butler *et al.*, 2000; Chen *et al.*, 2000). It was suggested that the increase in fat mass may be due to abnormalities in food partitioning as it was exacerbated in mice placed on a high-fat diet (Ellacott *et al.*, 2007). In contrast to other mouse models with similar levels of adiposity, MC₃^{-/-} mice do not exhibit marked insulin resistance or accumulation of fat in the liver, possibly due to reduced inflammatory response to obesity (Ellacott *et al.*, 2007).

Conversely, MC₄ null (MC₄^{-/-}) mice have a phenotype comparative to that of diet-induced obese (DIO) mice, characterised by increase in body weight due to hypometabolism and hyperphagia (Huszar *et al.*, 1997). These mice develop metabolic syndrome with insulin resistance and fatty liver disease (Huszar *et al.*, 1997) associated with an increase in expression of pro-inflammatory genes (Ellacott *et al.*, 2007).

The obesity phenotype of MC₃^{-/-} and MC₄^{-/-} mice occur by distinct mechanisms. Mutations in MC₄ gene in humans led to the phenotype observed in MC₄^{-/-} mouse, and account for 5 % of all monogenic cases of severe obesity (Vaisse *et al.*, 2000). In contrast, nine different mutations in the MC₃ gene have been

reported to date in human but their relevance to obesity is still unclear (Yang and Tao, 2012).

Although high body growth due to increased intake of nutrients at a young age is known to advance sexual maturation, in adulthood overnutrition may inhibit reproductive functioning. In men, obesity leads to reduction in circulating testosterone (Giagulli *et al.*, 1994) and low spermatozoa concentration (Hammoud *et al.*, 2008), whilst in females it is associated with irregular menstrual cycles (Douchi *et al.*, 2002). The effects of alterations in food intake, under- or over-nutrition, on reproductive function in humans are documented, however, the exact mechanism(s) are still being established.

As described above, MC₃ and MC₄ regulate energy balance as their absence leads to various forms of metabolic abnormalities. The central melanocortin system is not only composed of MC₃ and/or MC₄ expressing neurones but also includes neurones expressing MC agonists, POMC (POMC neurones), or MC antagonists, agouti gene-related protein (AgRP neurones), originating primarily in the arcuate nucleus (Liotta *et al.*, 1984; Haskell-Luevano *et al.*, 1999). The posttranslational processing of POMC leads to production of active melanocortin peptides in this region including α - and γ -MSH (Liotta *et al.*, 1984). The sites of MC₃ and MC₄ expression in the arcuate nucleus receive projections from both the anorexigenic POMC and the orexigenic AgRP neurones (Roselli-Reh fuss *et al.*, 1993; Mountjoy *et al.*, 1994; Bagnol *et al.*, 1999). Additionally, MC₃ but not MC₄, has been localized in both the POMC and the AgRP neurones (Bagnol *et al.*, 1999; Jegou *et al.*, 2000). MC₃ expressed in the cell bodies of the POMC neurones is thought to serve as an auto-inhibitory receptor to decrease the activity of POMC neurones (Jegou *et al.*, 2000; Cowley *et al.*, 2001). Long-term stimulation of MC₃ using [DTrp⁸]- γ 2-MSH by

intracerebroventricular (ICV) infusion decreases expression of POMC mRNA (Lee *et al.*, 2008). The inhibitory effect of MC₃ on the anorexigenic POMC neurones becomes even more intriguing considering the complex obesity syndrome in MC₃^{-/-} mice and the importance of MC₃ in adaptations to restricted feeding (Sutton *et al.*, 2010; Begriche *et al.*, 2012).

The prime site of POMC and AgRP neurones expression, the arcuate nucleus, is positioned between the median eminence and the 3rd ventricle and hence has direct exposure to factors from blood (Liotta *et al.*, 1984; Haskell-Luevano *et al.*, 1999). This collection of POMC and AgRP neurones receives and integrates a number of blood-borne signals; including adipostatic hormones leptin and insulin, as well as hunger and satiety signals from ghrelin and peptide YY (PYY) (as reviewed by Cone, 2005). The integration of neuronal inputs from other brain circuits as well as that of blood-derived factors plays an important role in maintaining the energy balance by regulating food intake and energy expenditure. An increasing body of evidence indicates that the central melanocortin system can convey physiological signals or information from other brain regions to GnRH neurones to control the reproductive system. In support of this statement, two examples will be described in more detail.

Oestrogen has a well-described role in the functioning of the reproductive system. In females, the hypothalamic action of oestrogen exhibits positive or negative feedback depending on the phase of the reproductive cycle (Brawer and Naftolin, 1978). The main sites of oestrogen receptor expression, both ER α and ER β , in the hypothalamus include the arcuate and ventromedial nucleus (Shupnik, 2002). A direct action of oestrogens on the release of GnRH neurones has already been described, however oestrogens also affect neurones in close proximity to GnRH cells including POMC and GABAergic

neurones (Herbison and Pape, 2001). Oestrogens target POMC neurones presynaptically (Blum *et al.*, 1989) and can modulate their G-protein-coupled inwardly rectifying potassium channels (GIRKs) (Kelly *et al.*, 2003). This modulation of POMC activity by oestrogens is thought to indirectly affect reproductive and other systems regulated by the hypothalamic neurones.

Another extensively researched potential candidate affecting the GnRH neurones through the melanocortin system is leptin. It is an adipocyte-derived hormone with well-defined anorexigenic effects characterised by inhibition of food intake and increase in energy expenditure. Leptin mediates its effects by binding to cytokine receptors, which activate the JAK-STAT pathway (as reviewed by Huang and Li, 2000). Leptin receptors are expressed in the hypothalamus and were localized in the POMC and AgRP neurones (Munzberg *et al.*, 2003; Balthasar *et al.*, 2004). Furthermore, administration of leptin increases the frequency of POMC action potentials (Cowley *et al.*, 2001) and expression of POMC gene, hence reversing the obese and diabetic phenotypes of the leptin-deficient mice (Mizuno *et al.*, 2003). In addition to the anorexigenic effects, leptin was reported to have important effects on reproductive function. Administration of physiological concentrations of leptin recovered preovulatory surges of LH and prolactin in food deprived female rats (Watanobe *et al.*, 1999). Similarly in starved male rats, infusions of leptin increased prolactin concentrations. The exact mechanism of LH regulation by leptin is not clear as leptin receptors are absent in the GnRH neurones, suggesting an indirect action on GnRH release (Quennell *et al.*, 2009). The involvement of centrally expressed MC₃ and MC₄ have been postulated as administration of MC antagonists, SHU9119 and HS014, resulted in inhibition of LH and prolactin surges in female rats (Watanobe *et al.*, 1999). In male rats, however, the effects

of MC antagonists are controversial as stimulatory (Stanley *et al.*, 1999) or no effects (Raposinho *et al.*, 2000) on the basal release of LH, FSH and testosterone have been reported. Furthermore, previous experiments using non-selective MC agonists, such as α -MSH, *in vivo* have been performed but the effects on GnRH and/or gonadotrophin release are inconsistent: stimulatory (Newman *et al.*, 1985), no effect (Khorram and McCann, 1986) or inhibitory effects (Scimonelli and Celis, 1990) have been reported.

Understanding of both the exact downstream mechanisms of the melanocortin system on GnRH release and the involvement of MC₃ and MC₄ receptors are still rudimentary. It has been established that POMC and AgRP neurones located in the arcuate send their projections to the medial preoptic area (POA) and are in close apposition to perikarya and dendrites of GnRH neurones (Naftolin *et al.*, 1996). Moreover, studies presented evidence of potential synaptic transmission between POMC and GnRH cell bodies (Leshin *et al.*, 1988; Naftolin *et al.*, 1996).

Different research groups are actively working to determine the exact MC receptor mediating the postsynaptic effects of POMC on GnRH neurones. Expression of both MC₃ and MC₄ were identified in immortalized GnRH-releasing GT1-1 and GT1-7 neuronal cell lines (Khong *et al.*, 2001; Stanley *et al.*, 2003). Both receptors were functional as stimulation with α -MSH dose-dependently increased GnRH release in GT1-1 (Khong *et al.*, 2001) and GT1-7 (Stanley *et al.*, 2003) neuronal cell lines. In support of this effect, α -MSH directly excited the majority of GnRH neurons of mice through postsynaptic activation of both MC₃ and MC₄ (Roa and Herbison, 2012). This group reported that other MC₃ or MC₄ selective agonists also increased the GnRH neuronal firing. Stanley and others (2003) reported that *in vivo* administration of γ ₂-MSH, an agonist

with the greatest affinity for MC₃, into the medial preoptic area of rat resulted in significant increases in plasma LH concentrations. Recently, MC₄ expression was identified in some GnRH neurones located in the preoptic area of the hypothalamus and their activation by MTHL caused an increase in action potential firing of GnRH neurones (Israel *et al.*, 2012). There is, however, evidence implying that although MC₃ has not yet been found in the GnRH neurones, it may work upstream of MC₄ in the control of GnRH release. MC₃ is the dominant receptor expressed in the arcuate and is present on both the POMC and the AgRP neurones. This receptor subtype may create a type of neuronal circuit between the two populations of neurones and regulate the release of melanocortins, thus modulating the activity of MC expressed on the GnRH neurones.

Most of the studies investigating the central effects of melanocortin system concentrated on MC₃ and MC₄ as the prime MC expressed in the brain. Evidence exists, however, that the fifth MC named MC₅ is also expressed in the brain (Chhajlani *et al.*, 1993; Griffon *et al.*, 1994) and its distribution pattern corresponds to that of MC₃ and MC₄ (Fathi *et al.*, 1995). Hypothalamic MC₅ is mainly expressed in rostral and medial parts of the medial preoptic area (Murray *et al.*, 2002). Furthermore, Murray and colleagues (2006) suggested that melanocyte concentrating hormone (MCH) stimulates LH release, at least in part, by activating MC₅ in the preoptic area of rat hypothalamus. MCH is a ligand for MCH-1R or MCH-2R receptors but previous work indicated that MC₅ transfected into HEK cells respond to MCH stimulation by releasing IP₃ (Murray *et al.*, 2000). The hypothalamic MCH fibres are in close vicinity to that of both GnRH and POMC neurones (Murray *et al.*, 2006; Ward *et al.*, 2009), thus further supporting the postulate that MC₅ may mediate some of the effects of

MCH on the release of GnRH, although this receptor subtype still has not been identified in the GnRH neurones.

Finally, the melanocortin system may also act on other populations of neurones, which have established influence on GnRH release, to modulate reproductive function. Backholer and colleagues (2009) suggested that melanocortins exert stimulatory effects on LH release during the luteal phase of ewes, possibly via kisspeptin cells in the POA and/or orexin cells in the dorsomedial hypothalamus, as mRNA expression of these neurones was upregulated following treatment.

The MC₃, MC₄, MC₅ and POMC seem to play a redundant role in the modulation of GnRH activity, as none of these knockout models appeared to be infertile. Based on presented evidence it is feasible to postulate that the GnRH release is controlled by integrated modulation from various neuronal populations; including, POMC, AgRP, Kiss1 or MCH expressing neurones, which are in very close apposition to each other and most importantly to GnRH neurones (Ward *et al.*, 2009; Roa, 2013). The exact role of the melanocortin system in this neuronal network is an as-of-yet unresolved but important issue. The summary of known effects of the melanocortin system on GnRH release and proposed mechanism is presented below (Figure 1.4).

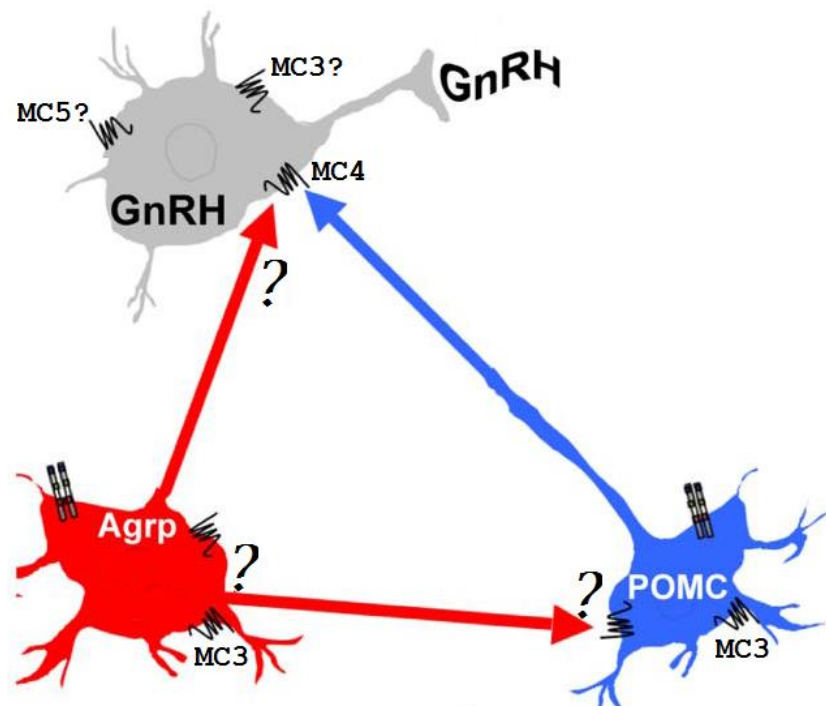


Figure 1.4 Proposed model of mechanism(s) through which the melanocortin system may affect the GnRH release Description in text (Modified from Israel *et al.*, 2012).

In addition to the effects of the melanocortin system on the GnRH release, centrally expressed MC stimulate sexual behaviour in both males and females upon activation by endogenous or exogenous ligands. One of the first effects of melanocortins on sexual function were reported by Bertolini and co-workers in 1965, who observed repeated episodes of spontaneous full penile erections in male rabbits and dogs after ICV injection of ACTH (Argiolas, 1999; Bertolini *et al.*, 2009). Copulatory behaviour was also observed after injections of either α -MSH or γ -MSH into laboratory animals (Gonzalez *et al.*, 1996). Currently, a number of highly selective agonists at MC are being developed for the treatment of a range of pathological conditions; including reduced sexual arousal and desire in women as well as erectile dysfunction and hypoactive

sexual desire disorder (HSDD) (Hadley, 2005). A synthetic analogue of α -MSH, PT-141, produced by Palatin Technologies is a novel candidate for the treatment of male and female sexual dysfunctions and is currently in Phase 2 of development (Rosen *et al.*, 2004; Palatin Technologies, 2014).

1.3.2 Pituitary

The melanocortin system may also affect reproductive function at the level of the pituitary. There are substantial species differences in pituitary MC expression. In the human, three subtypes were detected: MC₁, MC₄ and MC₅ (Chhajlani, 1996). Expressions of both MC₃ and MC₅ were identified in the anterior and intermediate lobes of the rat pituitary (Lorsignol *et al.*, 1999), whereas in mouse only MC₃ has been detected (Morooka *et al.*, 1998). The expression of MC₃ mRNA in the mouse pituitary was localized to the intermediate lobe as well as in anterior lobe lactotrophs and some somatotrophs (Matsumura *et al.*, 2003). The role of MC₃ in the anterior pituitary received particularly high attention due to the stimulatory effects on lactotrophs following administration of γ ₃-MSH, an agonist with the highest potency at MC₃ (Roudbaraki *et al.*, 1999; Matsumura *et al.*, 2003), hence this MC subtype will be mainly described here.

Age and gender differences are thought to exist in the expression pattern of MC₃. In adult life MC₃ is mainly present in lactotrophs (Matsumura *et al.*, 2003) whilst in immature rats MC₃ mRNA was located in pituitary cells expressing multiple mRNAs; that is, prolactin, growth hormone, POMC, or thyrotropin stimulating hormone- β , in various combinations (Roudbaraki *et al.*, 1999). These findings suggest that MC₃ may play a role in postnatal development, as it is present in a subpopulation of pituitary cells containing more than one hormone mRNA, which can be crucial during conditions of higher demand for a

specific hormone. Furthermore, Matsumura and colleagues (2003) indicated that the number of MC₃ mRNA transcripts present in anterior pituitary of adult female mice is higher compared to adult males. The reason for this observation can be explained by the fact that the proportion of lactotrophs is lower in male mice. Lorsignol and colleagues (1999) reported that MC₃ was expressed in a functional state in anterior pituitary cells of immature rats, as it increased Ca²⁺ concentrations in response to γ -MSH stimulation. This effect was partially blocked by administration of SHU9119 (MC₃/MC₄ antagonist), suggesting primary involvement of MC₃, since expression of MC₄ in the mouse pituitary had previously not been reported (Lorsignol *et al.*, 1999).

The presence of precursor for melanocortin peptides and their generation in the pituitary of various species has been well documented (as reviewed by Wikberg *et al.*, 2000; Bicknell, 2008). The majority of α -MSH but also small quantities of γ -MSH peptides are known to be released in the intermediate lobe of the pituitary (as reviewed by Wikberg *et al.*, 2000). In the anterior lobe, both α - and γ -MSH release has been reported from corticotrophs and lactotrophs, where they act in an auto- or paracrine manner on nearby populations of pituitary cells (Marcinkiewicz *et al.*, 1993). The stimulatory effects of α -MSH on *in vivo* and *in vitro* prolactin release were determined in both mice (Matsumura *et al.*, 2003) and rats (Ellerkmann *et al.*, 1992; Hill *et al.*, 1993). Administration of α -MSH increased the responsiveness of lactotrophs to other stimuli such as thyrotropin releasing hormone (TRH), known to stimulate prolactin secretion (Nunez and Frawley, 1998), and directly stimulated the release of prolactin in oestradiol-primed female rats or mice (Ellerkmann *et al.*, 1992; Morooka *et al.*, 1998). Additionally, studies in rats suggested that α -MSH is involved in the regulation of suckling-induced prolactin release in lactating females (Hill *et al.*, 1993).

Further experiments using an adult male mouse model showed that α -MSH was able to stimulate lactotroph proliferation and prolactin release (Matsumura *et al.*, 2003). The outcomes of these reports suggest that α -MSH may serve as a prolactin releasing factor. The receptor mediating the effects of α -MSH in lactotrophs is thought to be MC₃. There are several lines of evidence supporting this statement. First, MC₃ is the only MC receptor found to be expressed in both rat and mice, which served as a model in the above studies (Morooka *et al.*, 1998; Larsingol *et al.*, 1999). The effects of α -MSH can be blocked by SHU9119 *in vitro* (Matsumura *et al.*, 2003). Expression of MC₃ in anterior pituitary of mice increases in response to oestrogen (Matsumura *et al.*, 2004), which is in accordance with the α -MSH-mediated increase in prolactin release in oestradiol-primed rats and mice (Ellerkmann *et al.*, 1992; Morooka *et al.*, 1998). Furthermore, Tilemans and others (1997) demonstrated that γ ₃-MSH, the melanocortin peptide with the highest potency at MC₃, induced DNA replication in lactotrophs and prolactin release in cell aggregates from immature rats pituitaries.

Some reports, however, suggest that another receptor, different from the classic melanocortin receptors, is involved in mediating the effects on lactotrophs. Langouche and colleagues (2004) demonstrated that γ ₃-MSH as well as Ala⁸- γ ₂-MSH, a very weak agonist at MC₃, increased prolactin mRNA expression in pituitary cells of immature rats, and this effect was not reduced following administration of agouti-related protein (endogenous MC_{3/4} antagonist). Additionally, the rat GH3 cell line (which resembles lactotrophs) responded to stimulation with γ ₂-MSH and Ala⁸- γ ₂-MSH by an increase in [³⁵S] GTP γ S binding however none of the known MC were identified in this cell line (Langouche *et*

al., 2004). No further reports describing the novel receptor have been published since then.

It can be concluded, that the involvement of melanocortin system in regulation of reproductive function at the level of pituitary is primarily exerted by regulation of prolactin release. The effects of prolactin on reproductive physiology in the mammalian female vary according to the reproductive state such as the stage of the oestrous/menstrual cycle, mating, pregnancy or lactation. An increase in prolactin secretion stimulated by oestradiol during the afternoon of proestrus leads to a preovulatory surge coinciding with the LH surge (as reviewed by Gregerson, 2006). In contrast, suckling-induced prolactin release during lactation inhibits LH secretion by gonadotrophs and thus results in amenorrhea (Sortino and Wise, 1989). It is worth mentioning that prolactin is essential in maintaining the implantation of corpora lutea during early pregnancy of rodents (as reviewed by Gregerson, 2006). Therefore, it can be concluded that episodic release of prolactin is crucial for maintaining normal reproductive functions of mammalian females. However, chronically elevated levels of prolactin are associated with disrupted cyclicity and infertility in females (Voogt *et al.*, 1987). In male mice, prolactin exerts stimulatory effects on a number of aspects of testicular growth and function, hence lack of prolactin signalling, as deduced from prolactin receptor null mice (PRL-R-KO) leads to reduced fertility (as reviewed by Bartke, 2004).

Evidence of a direct role of the melanocortin system on the functioning of gonadotrophs exists but has not been fully elucidated. POMC expression was identified in 35-80 % of rat gonadotrophs between days 4-11 postnatally (Childs *et al.*, 1982). Furthermore, Marcinkiewicz and others (1993) reported the presence of prohormone-converting enzyme 1 (PC1) in this population of

anterior pituitary cells suggesting the possibility of further POMC cleavage into smaller peptides. Gonadotrophs responded to GnRH stimulation by releasing N-terminal 10 and 12 kDa POMC peptides, which were shown to stimulate lactotroph recruitment and prolactin mRNA expression during lactotroph development (Van Bael *et al.*, 1996). Thus far, no reports of autocrine actions of secreted peptides on gonadotrophs and MC expression in this population of cells exist.

Increased circulating concentrations of α -MSH (possibly of pituitary origin), however were reported in the late follicular phase of the menstrual cycle in women, when gonadotropin secretion is correspondingly high, suggesting possible direct effects on LH and FSH release (Mauri *et al.*, 1990). The direct role of melanocortins and their receptors on gonadotrophs and their secretions remains to be clearly defined.

1.3.3 Gonads

1.3.3.1 Testis

Expressions of four MC subtypes: MC₁, MC₂, MC₃, MC₅, were identified in human testes (Chhajlani, 1996). Detectable levels of MC₅ mRNA were also found in adult mice testes (Fathi *et al.*, 1995). In fetal mice, testicular expressions of MC₂ and MC₅ were reported during embryonic days 13.5 to 18 (Nimura *et al.*, 2006). Expressions of mRNA for MC₂ as well as MC₃ and MC₄, but not MC₅ were detected in fetal testes and none of the MC were identified in adult mice testes (O'Shaughnessy *et al.*, 2003). The significant age-related decrease in this study was further confirmed by real-time PCR for the MC₂ subtype (O'Shaughnessy *et al.*, 2003).

POMC derivatives, including α -MSH, γ -MSH and ACTH, were reported in the Leydig cells of rodent testes (Bardin *et al.*, 1984; Chen *et al.*, 1984). Both α -MSH and ACTH were shown to be secreted by Leydig cells into testicular interstitial fluid (Bardin *et al.*, 1984). Melanocortins are thought to regulate Sertoli cell growth (Bardin *et al.*, 1984) and function in a paracrine fashion by increasing Sertoli cell sensitivity to FSH stimulation (Morris *et al.*, 1987). Melanocortins have also been reported to affect both aromatase (converts androgens to oestrogens) and plasminogen activator (urokinase; local fibrinolysis, essential for mammalian spermatogenesis) activities: two parameters of Sertoli cell function (Boitani *et al.*, 1989).

The expression of MC₂ and MC₅ in the Leydig cells of fetal or neonatal mice renders the possibility of an autocrine effect on steroidogenesis (Johnston *et al.*, 2007). Incubation of fetal, neonatal or adult testes with α - or γ -MSH had no effect on testosterone release (O'Shaughnessy *et al.*, 2003). ACTH incubation, however, significantly increased androgen production in fetal or neonatal mouse testicular tissue but had no effect in adult mouse testicular tissue. The response mediated by ACTH was comparable to that of human chorionic gonadotropin (hCG; luteinizing hormone analogue) suggesting that both LH and ACTH may regulate Leydig cells steroidogenesis in a redundant fashion during postnatal life of mice (O'Shaughnessy *et al.*, 2003). This is in agreement with reports indicating that steroidogenesis during fetal life can be gonadotropin independent (O'Shaughnessy *et al.*, 1998). The fact that ACTH and not α - or γ -MSH stimulates androgen production indicates that MC₂, the ACTH only receptor, is likely to mediate the described ACTH effects in fetal mouse testicular tissue. Further experiments determined that testicular MC₂ is functional as activation with ACTH led to an immediate increase in cAMP release, and similarly to hCG,

it increased mRNA expression of the steroidogenic acute regulatory protein (StAR) suggesting that both mediators can act on Leydig cells through the same signalling pathway (Johnston *et al.*, 2007).

In contrast to fetal mice, acute administration of pharmacological levels of ACTH in adult rabbits and pigs increased testicular testosterone release *in vivo* (Juniewicz *et al.*, 1988). This indicates involvement of the melanocortin system in testicular functioning in later life in these species. The discrepancies between the two studies may be due to either species differences or possible variation of POMC expression influenced by reproductive stage. Bardin and co-workers (Bardin *et al.*, 1987a) reported that the amount of POMC peptides as well as POMC mRNA changes at different stages of reproductive development in both the mouse and the hamster. POMC derivatives were detectable in Leydig cells of mice by day 16 of gestation and increased in fetal life, after birth, however, their concentrations gradually declined until puberty period at around 40 days of life. These results suggest that POMC expression is dependent upon gonadotropin secretion and increases during periods of testosterone release in fetal life and at puberty (Bardin *et al.*, 1987b). The possibility exists that expression of receptors for POMC derivatives may also be influenced by gonadotropin secretion and change at certain periods during reproductive development.

In addition to the effects in Leydig cells, Nimura and colleagues (2006) reported the presence of MC₂ and particularly MC₅ in spermatogonia of fetal mice suggesting their possible involvement in cell division during the fetal period. Gizang-Ginsberg and Wolgemuth (1987) proposed that POMC derivatives may serve as a link between germ and Leydig cells. The group reported that POMC mRNA expression was particularly high in Leydig cells located in association

with seminiferous tubules at spermatogenic stages IX-XII, which contain germ cells at later stages. Interestingly, POMC mRNA was undetectable in the testis of mutant mice devoid of germ cells, thus emphasizing the importance of paracrine interactions between germ and Leydig cells. Although the presence of POMC in germ cells is still questionable (Gizang-Ginsberg and Wolgemuth, 1987), expression of MC in these cells (Nimura *et al.*, 2006) indicates a possible paracrine action.

Testicular expression of mRNAs for the other three subtypes MC₁, MC₃ and MC₄, (Chhajlani, 1996; O'Shaughnessy *et al.*, 2003), although still not localized, indicates that the melanocortin system may be involved in other activities enabling normal testicular functioning.

1.3.3.2 Ovary

Similarly to the testis, expression of MC in the ovary has been reported in a number of species at different ages. Nimura and colleagues (2006) determined the expression of MC₂ in the ovaries of fetal mice from embryonic day 13.5 to 18.5 by immunohistochemistry. MC₂ mRNA was also reported to be expressed in the ovary of the juvenile nonmammalian vertebrate rainbow trout (*Oncorhynchus mykiss*) (Aluru and Vijayan, 2008), whilst MC₅ cDNA was determined in human ovaries (Chhajlani, 1996). Amweg and co-workers (2010) localized the expression of mRNAs for MC₁, MC₂ and MC₃ in theca cells at different stages of follicular development and in corpora lutea of adult cows. Interestingly, POMC derivatives such as γ -MSH were identified in large antral follicles and corpora lutea of cycling or pregnant mice but no immunostaining was reported in immature animals (Shaha *et al.*, 1984). The mRNA for POMC was also absent in ovaries from immature rats but increased markedly during

pregnancy or in response to stimulation with gonadotropins (Chen *et al.*, 1986). The fact that some MC are co-expressed with POMC suggests an auto- or paracrine roles in ovaries, similarly to the male gonads.

The effects of ovarian MC activation by their agonists vary depending on the concentration and frequency of administration. The early studies on the effects of exogenous administration of ACTH in laboratory animals, mainly rodents, aimed at determining the effects of stress-associated cortisol release on reproductive physiology. Christian (1964) reported an increase in follicular atresia in immature female rats after chronic administration of ACTH. Similarly, repeated administration of synthetic ACTH during the proestrous phase in sows disturbed follicular development and prolonged the oestrous cycle (Einarsson *et al.*, 2007). McKinney and Pasley (1974) showed that subcutaneous administration of exogenous ACTH *in vivo* reduced uterine and ovarian weights in juvenile female rats and delayed sexual maturation, however, histological examination of the ovaries did not reveal obvious differences in the number of maturing or atretic follicles. The above studies still did not provide an evidence of a direct effect of ACTH on the ovary.

In contrast, acute ACTH administration facilitated ovulation in the presence of moderate or high oestrogen concentrations (Baldwin *et al.*, 1974; Putnam *et al.*, 1991). This effect is supported by the fact that both MC and POMC are expressed in antral follicles and corpora lutea (Chen *et al.*, 1986; Amweg *et al.*, 2010) and that MC₄-deficient mice have reduced number of corpora lutea, linked to a decrease in ovulation rate (Sandrock *et al.*, 2009).

ACTH was also reported to exert direct effects on steroidogenesis, as pharmacological doses of this peptide stimulated the secretion of 17 β -oestradiol

and progesterone by ovaries primed with gonadotropins *in vivo* (Varga *et al.*, 1986). Likewise, a single administration of ACTH alone or in combination with human chorionic gonadotropin increased synthesis of progesterone in rat luteal cells *in vitro* (Horvath *et al.*, 1986). The group suggested that this effect was mediated by prostaglandins E, which were released after binding of ACTH to a specific receptor located on the membrane of luteal cells. MC₂ is the prime candidate mediating the effects of ACTH on ovary, however some groups suggested involvement of other MC with lower affinity for ACTH than MC₂ (Horvath *et al.*, 1986). This observation was further supported by work of Durando and Celis (1998) who reported significant increases in progesterone release from prepubertal rat ovaries in response to α -MSH administration *in vitro*. There have been very few reports using selective MC ligands hence the exact receptor(s) mediating the described effects on follicular development, steroidogenesis, ovulation and luteal function are yet to be determined.

1.4 Aims of the research

The aims of this research were to determine the mRNA and protein distribution pattern of MC₃ at each level of the hypothalamo-pituitary-gonadal system in male and female mice, including the potential co-expression of the other four MC when possible. The other aims were to ascertain the role of MC₃ in reproductive physiology using the MC₃^{-/-} mouse model and an *in vitro* testicular culture.

The above aims were addressed by the following objectives:

- To determine MC mRNA expression in the reproductive axes of male and female mice at different ages and physiological states
- To establish the exact MC₃-expressing cells in mice testes using different anti-MC₃ antibodies
- To ascertain the possibility of local melanocortin peptides production by determining POMC mRNA expression in the reproductive tissues of male and female mice
- To compare the pituitary hormone content of MC₃^{-/-} to wild type mice
- To compare the morphology of testes from MC₃^{-/-} to wild type mice at different ages
- To examine the effects of MC₃ activation/inhibition on *in vitro* steroidogenesis and immune responses in testicular tissues from C57BL/6 and Balb/c mice
- To characterise the MC expression and effects of γ -MSH on nitrite production in the K9 Leydig cell line

2 Expression of MC in the HPG systems of both male and female mice

2.1 Introduction

Melanocortin receptors are widely expressed throughout the body and can be found in the central nervous system as well as in the periphery. Since the discovery of the first melanocortin receptor (MC₁) in skin in 1992 (Chhajlani and Wikberg, 1992), the main expression sites of another four receptors were determined. The primary cell type expressing MC₁ are melanocytes (Chhajlani and Wikberg, 1992) but dendritic cells, neutrophils, B lymphocytes and macrophages (Star *et al.*, 1995; Taherzadeh *et al.*, 1999) also synthesize this protein. MC₂ was found to be present in the zona glomerulosa and fasciculata of the adrenal cortex (Mountjoy *et al.*, 1992) and adipocytes (Noon *et al.*, 2006). The prime locations of MC₃ and MC₄ expression lie in the central nervous system and include the hypothalamus, hippocampus and thalamus (Gantz *et al.*, 1993; Roselli-Reh fuss *et al.*, 1993; Chhajlani, 1996). Peripheral expression of these two receptors has also been demonstrated: MC₃ was found in gut, placenta, kidney, heart, immune cells, ovary and testis (Chhajlani, 1996), whilst MC₄ is expressed in adipose tissue (Ellacott *et al.*, 2007). MC₅ is also present in the hypothalamus (Griffon *et al.*, 1994) but it is primarily expressed in peripheral exocrine glands including the sebaceous, preputial, lacrimal and Harderian glands as well as adipocytes (Chen *et al.*, 1997; Møllera *et al.*, 2011) and the adrenal gland (Liakos *et al.*, 2000).

MC are activated with different affinities by melanocortin peptides, which are derivatives of the POMC protein. The main sites of POMC expression are the anterior and intermediate lobes of the pituitary but high expression can also be

found in the hypothalamus, particularly in the arcuate nucleus (as reviewed by Bicknell, 2008). In the periphery, POMC is detectable in organs such as the adrenal medulla, skin and neurones of the intestine, where it is thought to have paracrine action (as reviewed by Wikberg *et al.*, 2000).

The (co-)expression of MC₃ and the other four receptor isoforms as well as POMC in the reproductive tissues, particularly gonads, has been reported, but not extensively studied. The factors that could influence (induce or inhibit) mRNA expression of MC and the melanocortin precursor molecule are unknown. Additionally, expression of MC₃ is usually determined at the level of mRNA and it is not always clear whether it becomes translated into protein.

The aim of this series of studies was to determine the expression of MC and POMC at the level of mRNA, and protein when possible, in tissues involved in the control of reproductive function in both male and female mice. The influences of age, gender and reproductive state, particularly in the female, were examined. Additionally, the expression of MC in two different mice strains namely Balb/c and C57BL/6, which are known to differ with regard to the steroidogenic activity and immune responses, were also determined.

2.2 *Materials and Methods*

2.2.1 *Animals*

Tissues from 3-24 weeks old wild type C57BL/6 or Balb/c mice were provided by Dr Le Tissier (National Institute for Medical Research, London, UK). Tissues from MC₃^{-/-} mice (3-24 weeks) with C57BL/6 background were obtained from Professor Perretti (William Harvey Research Institute, London, UK). All animals

were collected from animal houses licensed by the Home Office and killed using a schedule 1 procedure (cervical dislocation) by licensed personnel. Following removal from an animal, tissues were either frozen on dry ice and stored at -80 °C (until used for mRNA, protein extraction or radioimmunoassay) or fixed in 4 % paraformaldehyde (PFA; PROL294474L, VWR, UK; for immunostaining).

2.2.2 Expression of MC mRNA in the HPG system

2.2.2.1 RNA extraction

RNA was extracted using the Qiagen RNeasy kit (74004, Qiagen, UK) following the manufacturer's instructions. Frozen tissues (approximately 5 mg) from C57BL/6 or Balb/c mice (whole hypothalamus, whole pituitary, whole ovary, whole testis, pieces of the uterus removed from the junctions of both the oviduct and the cervix) were weighed and homogenized using a pestle and mortar in 350 µl of RLT lysis buffer. Tissues greater than 5 mg (testis and hypothalamus) were aliquoted and the RLT lysis buffer was added to the total volume of 350 µl. Solid material from tissue homogenate was separated by centrifugation for 5 min at full speed (13,000 rpm) in IEC Micromax microcentrifuge (DJB Labcare, UK). The supernatant was transferred to a new tube and one volume (approximately 350 µl) of 70 % ethanol added. Each sample was placed in a spin column in collection tube and spun for 15 sec at 10,000 rpm. The flow-through was discarded and the spin column membrane washed (with 350 µl of wash buffer RW1 by centrifugation for 15 sec at 10,000 rpm) in a microcentrifuge. To ensure removal of residual genomic DNA, the RNA preparations were treated with deoxyribonuclease. Briefly, 10 µl of DNase I stock solution (27 Kunitz units) were mixed with 70 µl resuspension buffer RDD and added directly to the membrane and incubated for 15 min (20 – 30

°C). The membrane was washed with 350 µl of wash buffer RW1 and 500 µl of wash buffer RPE (both by centrifugation for 15 sec at 10,000 rpm). In the final step 500 µl of 80 % ethanol were added and spun for 2 min at 10,000 rpm. The membrane was further dried by centrifuging an open spin column for 5 min at full speed (13,000 rpm). The RNA was eluted in 14 µl of RNase-free water (with centrifugation for 1 min at 13,000 rpm). The concentration and purity of each mRNA preparation were estimated spectrophotometrically at 260 nm and 280 nm using the Nanodrop 1000 (Thermo Scientific, UK). A 260 nm/280 nm absorbance ratio higher than 2.0 was considered as pure mRNA.

2.2.2.2 cDNA synthesis

The first strand of cDNA was synthesized in a 20 µl reaction mixture containing: total RNA (<500 ng), 150 ng random hexamers and 40 µM deoxyribonucleotides (dNTPs), and incubated for 5 min at 65 °C. First strand cDNA synthesis buffer (4 µl) (250 mM Tris-HCl [pH 8.3 at room temperature], 375 mM KCl, 15 mM MgCl₂) and 7.5 mM dithiothreitol (DTT) were added and incubated for 2 min at 25 °C followed by the addition of 1 µl SuperScript II reverse transcriptase (RT; 200 U/µl). The mix was further incubated for 10 min at room temperature. Reactions were then incubated at 42 °C for 50 min and inactivated for 15 min at 70 °C with cDNA stored at -20 °C until required. All reagents used in the synthesis of cDNA were from a SuperScript II Reverse Transcriptase Kit (18064-014, Invitrogen, UK). A non-template negative control for each of the mRNA preparations contained no SuperScript II reverse transcriptase (no-RT control) and served as a control for the assessment of genomic DNA removal. Prepared cDNA served as a template for regular PCR and/or quantitative PCR.

2.2.2.3 RT- PCR

Each PCR was carried out using 1 µl cDNA in a final volume of 20 µl using 0.5 µM forward and reverse primers in a Taq PCR Master Mix containing 1 U Taq polymerase, 1.5 mM MgCl₂ and 0.2 mM dNTP (201443, Qiagen, UK). The POMC, iNOS, 3β-HSD and β-actin (housekeeping gene) primer sequences are presented in Table 2.1 and PCR conditions in Table 2.2. Primer sequences were based on published literature.

Name		Sequence (5'-3')	Amplicon size (bp)
3β-HSD	forward	TATTCTCGGTTGTACGGGCAA	348
	reverse	GTGCTACCTGTCAGTGTGACC	
iNOS	forward	CAGATCGAGCCCTGGAAGAC	249
	reverse	CTGGTCCATGCAGACAACCT	
POMC	forward 1	GCTGGTGCCTGGAGAGCAGCCAGTG	F1&R-562; F2&R-509
	forward 2	TGCATCCGGGCCTGCAAACCTCGACCTCT	
	reverse	TGGCTCTTCTCGGAGGTCATGAA	
β-actin	forward	AGCCATGTACGTAGCCATCC	228
	reverse	CTCTCAGCTGTGGTGGTGAA	

Table 2.1 Primer sequences used for RT-PCR.

primer name	initial denaturation	denaturation	annealing	extension	final extension	number of cycles
iNOS, 3 β -HSD, β -Actin	94 °C for 5 min	94 °C for 45 s	60 °C for 30 s	72 °C for 1 min	72 °C for 10 min	40
POMC	95 °C for 5 min	94 °C for 1 min	60 °C for 1 min	72 °C for 1 min	72 °C for 10 min	30

Table 2.2 PCR conditions used for each set of primers.

2.2.2.4 Gel Electrophoresis

Amplification products were separated by electrophoresis on a 1.5 % - 2 % weight/volume (w/v) agarose gel at 100 V in Tris-Acetate-EDTA (TAE; 2 M Tris-Acetate and 100 mM Na₂EDTA in distilled/deionized water, pH 8.3) (EC-872; GeneFlow, UK) buffer for 60 min and then stained with ethidium bromide (0.5 μ g/ml) (E1510; Sigma-Aldrich, UK) for 20 min. The PCR products were visualised under UV light using an UVIPRO Silver transilluminator (UVITEC, UK). The sizes of the DNA fragments were determined by comparison to a molecular weight marker (100 bp – 5000 bp; L3-0015; GeneFlow, UK).

2.2.2.5 Sequencing of PCR products

The products of anticipated size were excised from the gels and purified using a Gel Extraction Kit (GeneClean® Turbo, 1102-200, MPBiomedicals, UK). The sequencing of purified products was performed as a service by the sequencing facility at the University College London (London, UK). The facility uses an AB

sequencer and the appropriate forward and reverse primers were supplied. Sequencing data were then further analysed using NCBI Blast.

2.2.2.6 Quantitative RT-PCR (qRT-PCR)

qRT-PCRs were performed on aliquots of cDNAs diluted to a working concentrations of 12.5 ng/μl of initial mRNA. The final reaction volume was 20 μl and contained 25 ng of mRNA and either 1.6 μl of forward and reverse primers mix for MC₁-MC₅ or 2 μl of forward and reverse primers mix for GAPDH, ATP5B and ACTB in Rotor-Gene SYBR Green PCR Master Mix (HotStarTaq DNA Polymerase, PCR Buffer and dNTP mix; 204074, Qiagen, UK). The catalogue numbers for the primers used are listed in Table 2.3. Each mRNA was run in duplicate or triplicate using Rotor-Gene Q Light Cycler (Qiagen, UK). The cycling conditions using the Rotor-Gene SYBR Green PCR Master Mix are presented in Table 2.4.

Company	Primer name	Catalogue number	Amplicon size (bp)
Qiagen	MC ₁	QT00305011	110
Qiagen	MC ₂	QT00260967	67
Qiagen	MC ₃	QT00264404	108
Qiagen	MC ₄	QT00280861	106
Qiagen	MC ₅	QT01166494	90
Qiagen	GAPDH	QT01658692	144
PrimerDesign	ATP5B	ge-PP-12	112
PrimerDesign	ACTB	ge-PP-12	84

Table 2.3 A list of primers including their catalogue numbers and amplicon sizes used in qRT-PCR.

Step	Time	Temperature °C
PCR initial activation	5 min	95
Two-step cycling		
Denaturation	5 sec	95
Combined annealing/extension	10 sec	60
Number of cycles		
	40	

Table 2.4 Cycling conditions for qRT-PCR.

Melting curve analyses of the PCR products were performed to verify their specificity and identity. The melting curve began at a temperature of 60 °C and rose by one degree every 95 sec up to the final temperature of 95 °C. To ensure accurate estimation of the gene of interest (GOI) expression, the specificity of qRT-PCR was tested in reactions using 'cDNA' prepared without SuperScript reverse transcriptase (no-RT control). The Ct values for no-RT reactions were at least five cycles greater (32-fold less) than those for reactions with RT (Laurell *et al.*, 2012). The specificities of the PCR products were additionally verified by agarose gel electrophoresis.

The initial analyses were performed using Rotor-Gene Q Series Software 1.7. The threshold for all amplification plots was set within the exponential phase, equal to 0.03 of the fluorescence level, to determine the crossing point (Ct), a tool for the calculation of gene expression.

2.2.2.6.1 Primer amplification efficiency

Standard curves were generated for every primer pair to determine amplification efficiencies for relative gene expression quantifications. Standard curves were prepared by two fold dilutions of testis and/or hypothalamus cDNAs, with an initial concentration of 100 ng/reaction mRNA. Each dilution series was then amplified in qRT-PCR and Ct values obtained were used to construct standard curves (Figure 2.1). The amplification efficiency, E value, for each target was calculated according to the following equation: $E = 10(-1/S) - 1$, where S is the slope of the standard curve (Table 2.5).

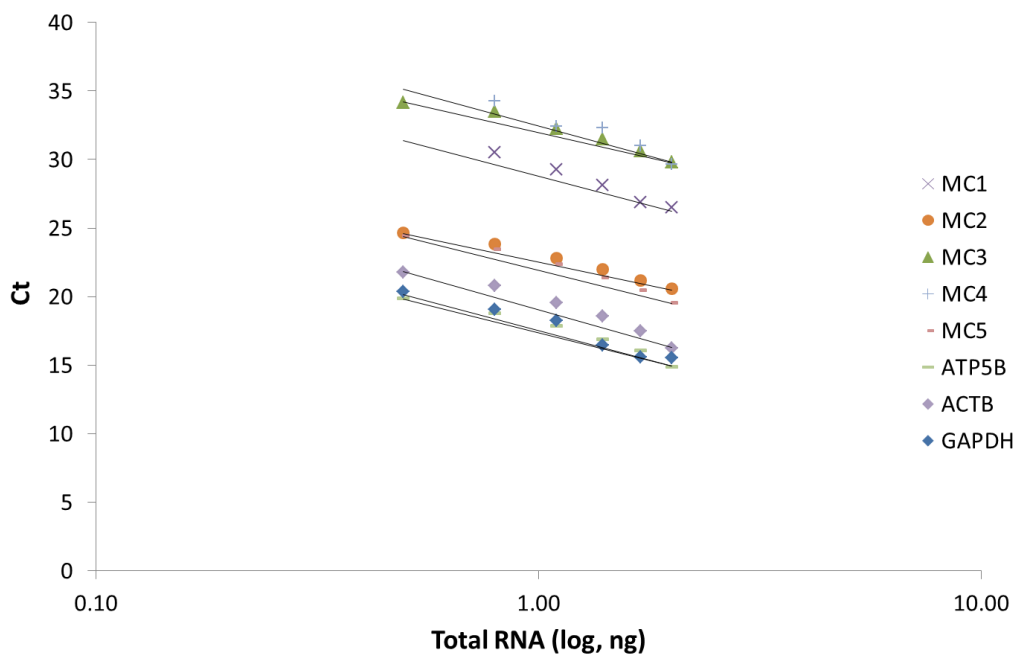


Figure 2.1 Primer amplification efficiency. Standard curves were constructed by plotting the Ct values against the logarithm of RNA template amount for each primer pair. The amplification efficiencies were then calculated using the slope of the curve.

Primer Name	Slope	E Value	Efficiencies (%)
MC ₁	-3.4293	1.9160	93
MC ₂	-2.7575	2.6265	93.85
MC ₃	-2.9494	2.3905	130.49
MC ₄	-3.5555	1.8125	118.3
MC ₅	-3.2615	2.0661	91.1
ATP5B	-3.2512	2.0758	107.52
ACTB	-3.6802	1.6971	86.08
GAPDH	-3.4788	1.8746	86.95

Table 2.5 Primer specific amplification efficiencies.

2.2.2.6.2 Reference genes selection

The most stable reference genes were selected from a panel of 12 genes (PerfectProbe geNorm 12 gene kit, ge-PP-12; PrimerDesign, UK). This was used to ensure accurate gene quantification by normalising the target genes' Ct to genes with the least variance in gene expression between samples. The expression of 12 reference genes (Table 2.6) was measured in a representative set of 13 tissue samples (Table 2.7). The final qPCR reaction volume was equal to 20 µl containing 25 ng of mRNA, 300 nM of forward and reverse primers in PrimerDesign Precision qPCR Mastermix. The qPCR cycling conditions are presented in Table 2.8.

Species	Primer name	Accession number	Product Tm (°C)	Amplicon size (bp)
Mouse	18S	NR_003278.3	82.9	93
Mouse	ACTB	NM_007393.3	90.2	84
Mouse	ATP5b	NM_016774.3	89.8	112
Mouse	B2M	NM_009735.3	84.7	120
Mouse	CANX	NM_007597.3	86.3	105
Mouse	CYC1	NM_025567.2	92.1	141
Mouse	EIF4A2	NM_013506.2	84.4	152
Mouse	GAPDH	NM_008084.2	90.8	127
Mouse	RPL13A	NM_009438.5	91.0	130
Mouse	SDHA	NM_023281.1	87.1	133
Mouse	UBC	NM_019639.4	96.8	129
Mouse	YWHAZ	NM_011740.3	87.8	141

Table 2.6 List of primers used in the geNorm analysis.

Gender	Strain	Age	Tissue
Male	Balb/c	8 weeks	Hypothalamus
Male	Balb/c	8 weeks	Pituitary
Male	Balb/c	8 weeks	Testis
Male	C57BL/6	8 weeks	Hypothalamus
Male	C57BL/6	8 weeks	Pituitary
Male	C57BL/6	8 weeks	Testis
Male	C57BL/6	14 weeks	Hypothalamus
Male	C57BL/6	14 weeks	Pituitary
Male	C57BL/6	14 weeks	Testis
Female	C57BL/6	14 weeks	Hypothalamus
Female	C57BL/6	14 weeks	Pituitary
Female	C57BL/6	14 weeks	Ovary
Female	C57BL/6	14 weeks	Uterus

Table 2.7 Samples included in the geNorm analysis.

Step	Time	Temperature °C
PCR initial activation	10 min	95
Two-step cycling		
Denaturation	15 sec	95
Combined annealing/extension	60 sec	60
Number of cycles	50	

Table 2.8 qPCR cycling conditions.

Melt curve analyses were performed following the cycles and the Cts for the samples were calculated at a threshold of 0.03 using Qiagen Rotor-Gene software as described before.

The stability of each gene's expression was analysed and ranked using geNorm incorporated in the qbase^{plus} software (Basic, Biogazelle, Belgium) provided with the kit (Figure 2.2). The two most stable genes in tissues from C57BL/6 and Balb/c male and female mice were ACTB and ATP5B.

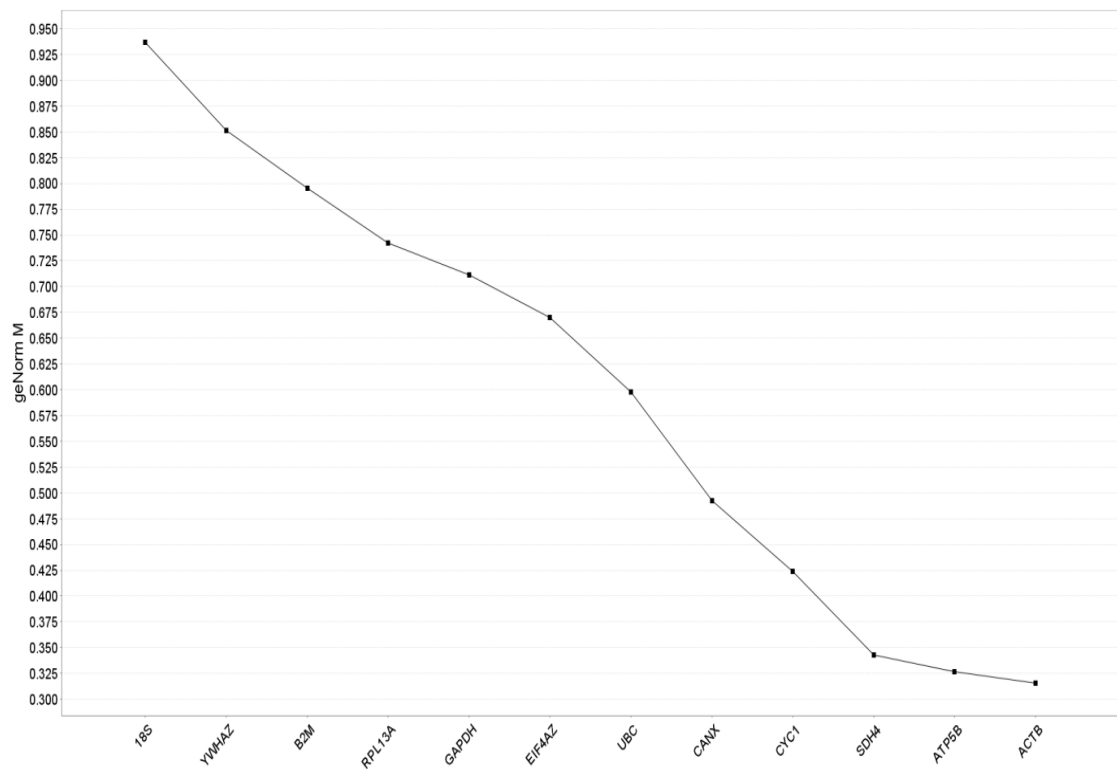


Figure 2.2 The average expression stability value (M) of 12 reference genes for hypothalami, pituitaries and testes taken from C57BL/6 and Balb/c wild type male and female mice. The M value was calculated at each step during stepwise exclusion of the least stably expressed reference gene. The least stable genes are indicated to the left of the curve, whilst the most stable are to the right.

The optimal number of reference genes was determined by calculation of a pairwise variation, $V(n/n+1)$, based on the variation in average stability of the reference genes (Figure 2.3). The geometric mean of the two most stable reference genes ATP5B and ACTB was sufficient to give a high quality normalization factor because the outcome of pairwise variation calculation is lower than the threshold value ($V < 0.15$).

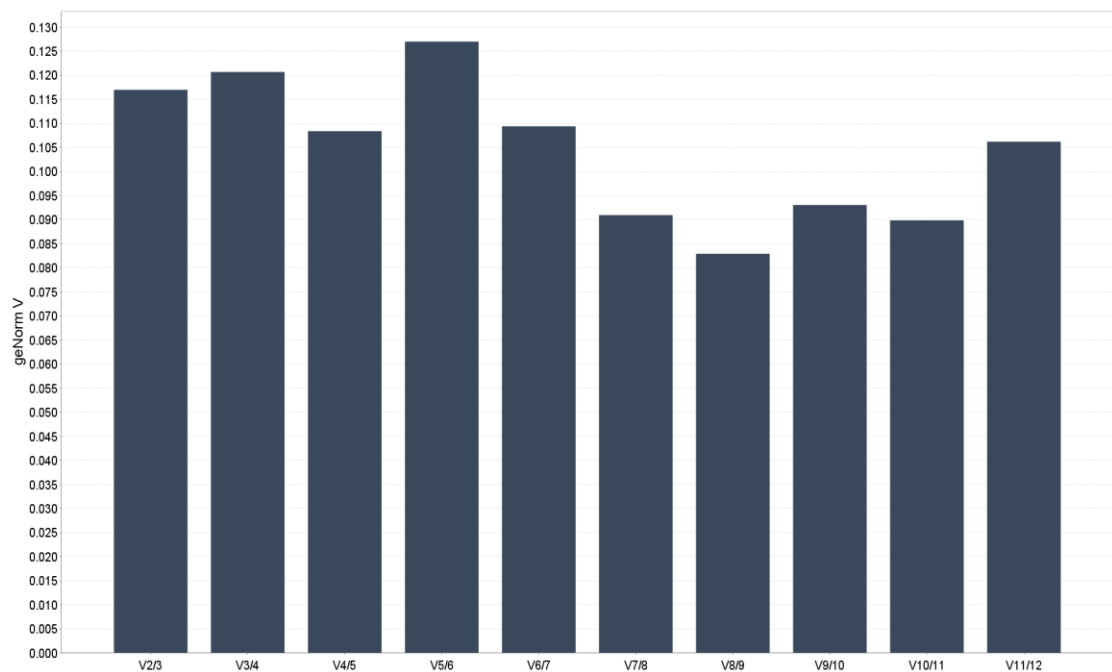


Figure 2.3 Determination of the optimal number of reference genes. The figure shows sequential addition of each reference gene starting with the two most stably expressed genes on the left with the inclusion of a 3rd, 4th, 5th gene *et cetera*, moving to the right. The optimal number of reference genes n is found when $V(n/n+1)$ drops below 0.15 and in this case an average of the two most stable genes would give a high quality normalising signal.

2.2.2.6.3 Relative gene expression analysis

The analyses of the relative gene expression level were performed using qbase^{plus} software (Basic, Biogazelle, Belgium). This is based on the $\Delta\Delta Ct$ method but with a number of improvements (Hellemans *et al.*, 2007; Hellemans and Vandesompele, 2011). First, qbase^{plus} calculates ΔCt for each gene in each sample by comparing the Ct of a given sample ($Ct_{sampleA}$) with the average Ct across all samples for that gene (\overline{Ct} ; equation 1). The Relative Quantities (RQ) are calculated based on the primer specific PCR amplification efficiency (E; equation 2; Table 2.5). The RQ was then normalized by dividing it by the geometric mean Ct of a set of selected reference genes, in this case ACTB and ATP5B, which results in the Normalized Relative Quantity (NRQ; equation 3). All of the data for the presented experiments were scaled to the average expression level of a gene across all samples as a reference. The scaling only changes the scale of the data, but not the fold changes between the samples. The NRQ for each reference was calculated in the same manner as the NRQ for a target gene by dividing the RQ of a single reference gene by the geometric mean of two reference genes. The NRQ values for both reference genes approach 1 indicating similarity, hence stability.

Equation 1 $\Delta Ct = \overline{Ct} - Ct_{sampleA}$

Equation 2 $RQ_A = E^{\Delta Ct}$

Equation 3 $NRQ = \frac{E_{goi}^{\Delta Ct_{goi}}}{E_{ref}^{\Delta Ct_{ref}}} = \frac{RQ_{goi}}{RQ_{ref}}$

RQ_{goi} = Relative Quantities for Gene Of Interest

RQ_{ref} = Relative Quantities for Reference Gene

$$\text{Multiple reference genes } NRQ = \frac{RQ_{goi}}{\text{geometric mean } (RQ_{refs})}$$

$$NF = \frac{1}{\text{geometric mean } (RQ_{refs})}$$

2.2.3 Expression of MC₃ protein in the HPG system

2.2.3.1 Western blot

Frozen tissue samples (whole hypothalami, whole pituitaries, whole ovaries, whole testes, pieces of the uterui removed from both the junctions of the oviduct and the cervix) from C57BL/6 mice were homogenised on ice in 1 ml of RIPA buffer (150 mM sodium chloride [S9888; Sigma-Aldrich, UK], 1 % volume/volume (v/v) Triton X-100 [T8787; Sigma-Aldrich, UK], 0.5 % w/v deoxycholic acid [D5670; Sigma-Aldrich, UK], 0.1 % w/v sodium dodecyl sulphate [SDS: BP166; Fisher, UK]) containing 1 % v/v of a cocktail of protease inhibitors (BPE 9707-1; Fisher Scientific, UK) using a mortar and pestle. Samples were then spun for 20 min at 4 °C at 14,000 rpm in a microcentrifuge and supernatants removed for further analysis. The protein contents were determined using the Bicinchoninic Acid Protein Assay Kit (BCA1 & B9643; Sigma-Aldrich, UK) in a 96 well plate. Protein standards 5 µg/ml – 1 000 µg/ml were prepared in duplicate using bovine serum albumin (BSA) (P0834-10X1ML; Sigma-Aldrich, UK) and their absorbance values were used to plot a standard curve (Figure 2.4). Absorbance was measured at 562 nm using a Versa Max microplate reader (Molecular Devices, UK) and analysed by SoftMaxPro 5.2 software (Molecular Devices, UK).

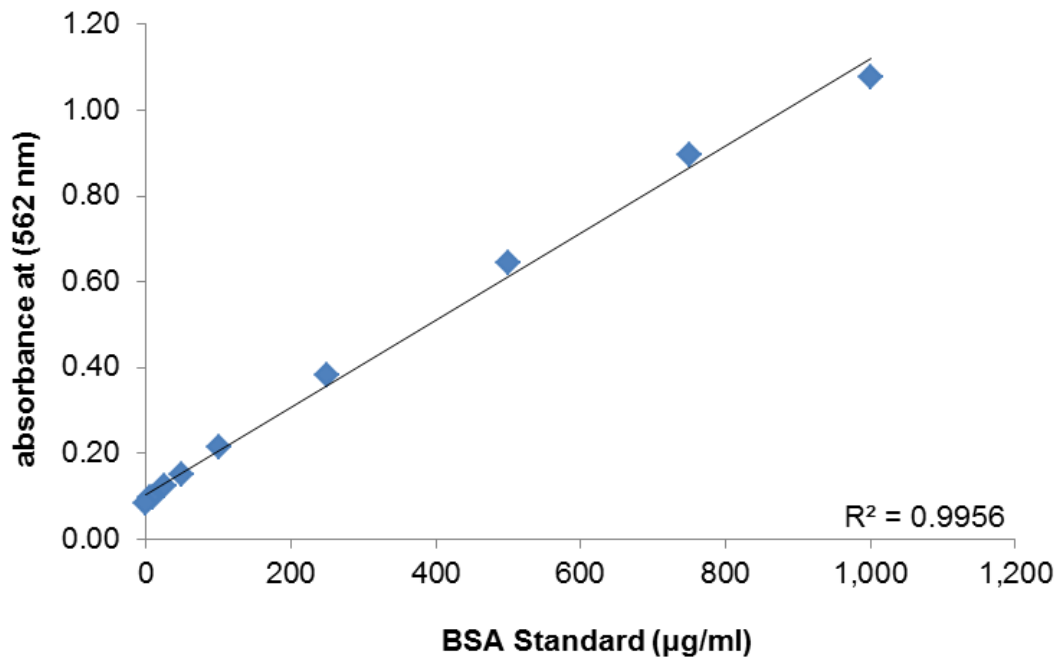


Figure 2.4 Example of a standard curve generated to determine the protein content in samples of interest. Value R^2 is displayed on the graph.

Protein (20 - 40 µg) was mixed with SDS-PAGE loading buffer (S3401-10VL; Sigma-Aldrich, UK) followed by heating for 5 min at 99 °C, vortexing and loading (15 µl) onto 10 - 12 % sodium dodecyl sulphate-polyacrylamide gel (SDS-PAGE). Protein ladder (5 µl) was also loaded onto each gel (BPE3603-500; Fisher, UK). The protein was separated by electrophoresis in a Bio-Rad Mini-PROTEAN® Tetra Cell electrophoresis system in Tris-Glycine-SDS Running Buffer pH 8.3 (250 mM Tris base [BP152; Fisher, UK], 1920 mM glycine [G8898; Sigma-Aldrich, UK], 1 % w/v SDS) for 35 min at 200 V.

Following electrophoresis, the gel was incubated in ice-cold cathode buffer pH 9.4 (25 mM Tris-base, 10 % v/v methanol [34860; Sigma-Aldrich, UK], 40 mM glycine) for 5 min in preparation for semi-dry protein transfer. The electrotransfer unit was organised in the following order starting from the anode electrode plate: two filter papers wetted in cold anode buffer I pH 10.4 (0.3 M

Tris base, 10 % v/v methanol), one filter paper wetted in cold anode buffer II (25 mM Tris base, 10 % v/v methanol), Immun-Blot™ PVDF Membrane (0.2 µm) (162-0175; Bio-Rad, UK) (prepared by placing in methanol for 30 sec, rinsed in deionized H₂O [dH₂O] and then incubated in anode buffer II for 5 min), gel and three filter papers wetted in cathode buffer. The semi-dry protein transfer was done for 30 min at 100 A using a Geneflow (Fradley, UK) transfer system.

The gel was stained for 30 min in Coomassie stain (0.25 % Coomassie brilliant blue [BP101-25, Fisher, UK] in Coomassie destain) followed by three washes in Coomassie destain (10 % v/v acetic acid [10001BT; VWR, UK] and 10 % v/v methanol). The membrane was then incubated in 5 % milk solution (5 % w/v milk powder [0.1 % fat skimmed milk powder, Sainsbury's, UK] in TBS-T : pH 7.4; 50 mM Tris base, 150 mM sodium chloride, 0.05 % v/v Tween® 20 [233362500; Acros Organics, UK]) for 1 h at room temperature on a rocking platform in order to prevent non-specific antibody binding. Blocking solution was removed and the membrane incubated in the primary antibody diluted in 5 % milk solution (concentrations of each primary antibody are presented in Table 2.9) at 4 °C overnight. Following incubation, the primary antibody solution was removed and membrane washed (3 x 5 min with TBS-T). The blot was placed in the corresponding secondary antibody conjugated to horseradish peroxidase (HRP, Table 2.9) for 1 h at room temperature and then washed as before (3 x 5 min with TBS-T).

To determine antibody specificity, a mix of particular antibody (0.5 µg) and recombinant MC₃ protein (1 µg, H00004159-P01; Abnova, UK) or Enzo blocking peptide (for Enzo antibody only) was pre-incubated for 1 h at room temperature before applying the mixture onto the membrane and incubating overnight at 4 °C.

Specific antibody binding was detected in the dark using a Chemiluminescence Detection Kit (K1-0170; Geneflow, UK) according to manufacturer's instructions. Briefly, equal volumes of EZ-ECL Solution A and Solution B were mixed, applied onto the membrane and incubated for 5 min. Excess detection mix was drained off and the membrane was placed in a Hypercassette™ (Amersham Pharmacia Biotech, Buckinghamshire, UK) and exposed to CL-XPosure™ X-ray film (34090; Fisher Scientific, Loughborough, UK) for 5 min, 2 min or 30 sec. The films were developed by incubation for 5 min in Kodak® GBX developer/replenisher (P7042; Sigma-Aldrich, UK), washed in dH₂O for 1 min and then fixed in Kodak® GBX fixer/replenisher (P7167; Sigma-Aldrich, UK). The size of detected protein bands were determined by comparison to a protein ladder (BPE3603-500; Fisher Scientific, Loughborough, UK).

Following detection, bound antibodies were removed by incubating the membrane in acidic glycine solution (0.2 M glycine, 3.47 mM sodium dodecyl sulphate, 1 % v/v Tween 20, pH 2.2) twice for 10 min, and then washing with phosphate buffered saline (PBS, P4417; Sigma-Aldrich) (2 x 10 min) and TBS-T (2 x 5 min) at room temperature. This was followed by blocking in 5 % milk solution for 1 h at room temperature. The membranes were subsequently reprobed for the detection of other proteins, such as α -tubulin (housekeeping protein).

To determine the efficiency of the transfer and protein separation on the gel the membrane was stained for 1 min with Coomassie solution, then destained with Coomassie destain three times for 5 min, dried in air and kept for future record.

primary antibody/ concentration	primary antibody manufacturer/ catalogue number	species reactivity	Molecular weight (kDa)	immunogen	secondary antibody/ concentration	secondary antibody manufacturer/ catalogue number
MC ₃ -rabbit polyclonal/ 1:1000	Sigma/M4937	Rat, Mouse (predicted)	40	N-terminal region of rat MC ₃ (amino acids 15-33) (highly conserved in mouse MC ₃ ; 89% identity)	goat anti-rabbit IgG-HRP/ 1:5000	BIO-RAD/170- 6515
MC ₃ -rabbit polyclonal/ 1:500	Abcam/ab2123 1	Human, Rat, Mouse	55	Unique C-terminal epitope, conserved in several species	goat anti-rabbit IgG-HRP/ 1:4000	BIO-RAD/170- 6515
MC ₃ -rabbit polyclonal/ 1:1000	Enzo Life Sciences /BML-SA640	Human, Rat, Mouse	70	Synthetic peptide corresponding to aa 102- 117 of rat MC ₃	goat anti-rabbit IgG-HRP/ 1:5000	BIO-RAD/170- 6515
α -tubulin-rat monoclonal/ 1:3000	Abcam/ab6160	Human, Mouse, <i>Caenorhabditis elegans</i> , Fruit fly, Pig, <i>Saccharomyces cerevisiae</i> ,	53	recognises short amino acid sequence Glu-Glu- Phe(OH) which can be inserted into the C- terminal domain of fusion proteins	goat anti-rat IgG-HRP/ 1:5000	Santa Cruz Biotechnology/s c-2032

Table 2.9 List of primary and secondary antibodies used in Western blot.

2.2.3.2 Immunostaining

2.2.3.2.1 Tissue preparation

Testes of male mice were excised immediately following death and placed in 4 % PFA for approximately 7 h at room temperature. Tissues were then transferred into PBS and stored at 4 °C. Fixed testes were placed in plastic histology cassettes, dehydrated first in 30 % and then 50 % ethanol (32221, Sigma-Aldrich, UK) for 1 h each at 4 °C, followed by an overnight incubation in 70 % ethanol at 4 °C. The tissues were further dehydrated in 90 %, 95 % and twice in 100 % ethanol for 1 h each at 4 °C before being cleared in 100 % xylene (4099-0025, Fisher Scientific, UK) once for 1 h and then 30 min at room temperature. Finally, tissues were incubated in infiltrating wax (1:1 paraffin wax/xylene) for 1 h at 56 °C and in 100 % paraffin wax (706043, VWR, UK) three times for 30 min at 56 °C. After wax infiltration, tissues were transferred to plastic moulds, embedded in paraffin wax and allowed to set before being stored at 4 °C overnight.

Sections were cut from the wax blocks using a microtome (Anglia Scientific, UK) at a thickness of 6 µm but initially at 10 µm, placed briefly in water bath at 21 °C and then mounted onto gelatine coated glass slides. The sections were thoroughly dried on a heating plate at 45 to 50 °C and placed in an oven overnight at 37 °C. Prepared slides were stored at room temperature prior to being processed for haematoxylin and eosin staining or immunohistochemistry.

2.2.3.2.2 Immunohistochemistry (IHC)

Unless otherwise indicated all washes were done by incubating the slides three times for 5 min in PBS on a rocking platform. Sections were first dewaxed with xylene and then rehydrated through an alcohol gradient followed by washes in PBS as described for haematoxylin and eosin staining (section 3.2.2.1). If antigen retrieval was required (as for Abcam MC₃ and WT-1 antibodies), the sections were kept in a Coplin jar containing citrate buffer (10mM citric acid, 0.05 % Tween 20, pH 6.0) in boiling water for 5-20 min, then cooled down at room temperature for 20 min and washed. Sections were then treated with 3 % H₂O₂ (v/v) (UN2014; VWR, UK) in methanol (34860; Sigma-Aldrich, UK) for 10 min at room temperature to block endogenous peroxidase activity. After washing, sections were incubated in 0.03 % Triton X-100 (TX-100: T8787; Sigma-Aldrich, UK) for 30 min at room temperature and rinsed before blocking in 10 % normal serum (serum was the same as the species that the secondary antibody was raised in, as opposed to the species of the primary antibody) in PBS for 30 min at room temperature. Slides were then placed in a humidified chamber, to prevent the sections from drying, and incubated in the specific primary antibody in 1 % serum in PBS (Table 2.10) for 1 h at room temperature followed by an overnight incubation at 4 °C. Sections were washed and incubated for 1 h at room temperature in the relevant biotinylated secondary antibody (Table 2.10). Following incubation sections were washed and left for 1 h at room temperature in Vector A + B solution (SK-4100; Vector Laboratories, UK). Slides were then washed in PBS 2 x 5 min and Tris buffer (10 mM Tris base, pH 7.4) for 5 min, followed by incubation in 3,3-diaminobenzidine (DAB) solution (SK-4100; Vector Laboratories, UK) for 5 min to visualise the antigen-antibody complex. Slides were further washed in Tris buffer (3 x 5 min) and

counterstained with Gill's haematoxylin for 4 min. Following rinsing in tap water, incubation in acid rinse solution and bluing solution, sections were dehydrated through an alcohol gradient 30 to 100 % (as described in section 3.2.2.1 but eosin omitted). Finally, slides were incubated with xylene (2 x 5 min) and mounted with DPX mounting media. Sections immunostained in the absence of the relevant primary antibody (1 % normal serum in 0.1 % TX-100 in PBS) served as negative controls.

2.2.3.2.3 Immunofluorescence (IF)

As for immunohistochemistry (section 2.2.3.2.2), sections were deparaffinised and rehydrated through an ethanol gradient. Following three washes for 3 min in PBS (the same wash for all steps unless indicated) slides were incubated in 0.03 % Triton X-100 for 30 min at room temperature. After rinsing, sections were placed in humidified chamber and blocked in 10 % normal serum containing 0.5 mg/ml of RNase A (19101; Qiagen, UK) in PBS for 30 min at room temperature to remove the cytoplasmic RNA and prevent background staining with nuclear stain. Slides were then incubated in first primary antibody (MC₃; antibody concentrations for IF are presented in Table 2.11) in 1 % normal serum in PBS at 4 °C overnight. Following washing, sections were covered with the secondary antibody, usually conjugated to Texas Red, in PBS for 1 h at room temperature in the dark. For double immunostaining, slides were washed and incubated with a second primary antibody (3 β -HSD) at an appropriate dilution (Table 2.11) in PBS for 3 h at room temperature in the dark. Sections were then washed and incubated with a fluorescein conjugated secondary antibody in PBS for 1 h at room temperature in the dark. To block intrinsic fluorescence present in some tissues, particularly the testis, sections were

rinsed and covered with 0.3 % Sudan Black B (w/v) (199664; Sigma, UK) in 70 % ethanol at 37 °C for 5 or 10 min in the dark (Yang and Honaramooz, 2012). Finally, slides were washed and incubated with 1 µM TO-PRO-3 Iodide (T3605; Life Technologies, UK) in PBS for 30 min at room temperature in the dark to stain nuclei. After rinsing, slides were mounted and stored in the dark at 4 °C.

2.2.3.2.4 Staining visualisation

Immunohistochemically stained sections were visualised using a Leica DM2000 light microscope with a Leica DFC420 camera attachment. Images were acquired using Leica Application Suite software (Leica Microsystems, Version:V5.0 R222, Switzerland). Images for the slides with the fluorescent label were acquired by sequential scanning using a Leica TCS SP2 confocal system (Leica Microsystems, Milton Keynes, UK), with emission spectra set for green (max 515 nm), red (615 nm) and blue (661 nm).

primary antibody/ concentrations	primary antibody manufacturer/ catalogue number	secondary antibody/ concentration	secondary antibody manufacturer/ catalogue number	serum used	serum manufacturer/ catalogue number
MC ₃ -rabbit polyclonal/ 1:200, 1:400, 1:800	Sigma/ M4937	goat biotinylated anti-rabbit IgG/1:300	Vector Laboratories/B A-100	normal goat serum	Vector Laboratories/ S-100
MC ₃ -rabbit polyclonal/ 1:100, 1:200, 1:400, 1:800	Abcam/ ab21231	goat biotinylated anti-rabbit IgG/1:300	Vector Laboratories/B A-100	normal goat serum	Vector Laboratories/ S-100
MC ₃ -rabbit polyclonal/ 1:200, 1:400, 1:800	Enzo Life Sciences /BML-SA640	goat biotinylated anti-rabbit IgG/1:300	Vector Laboratories/B A-100	normal goat serum	Vector Laboratories/ S-100
3 β -HSD (P-18) goat polyclonal/1:200 and 1:400	Santa Cruz Biotechnology/ sc-30820	horse biotinylated anti-goat IgG/1:300	Vector Laboratories/B A-9500	normal horse serum	Vector Laboratories/ S-200
WT-1 rabbit polyclonal (c-19)/ 1:50, 1:100, 1:200	Santa Cruz Biotechnology/ sc-192	goat biotinylated anti-rabbit IgG/1:300	Vector Laboratories/B A-100	normal goat serum	Vector Laboratories/ S-100

Table 2.10 Concentrations and manufacturers of primary and secondary antibodies used in IHC.

primary antibody/ concentrations	primary antibody manufacturer/ catalogue number	secondary antibody/ concentration	secondary antibody manufacturer/ catalogue number	serum used	serum manufacturer /catalogue number
MC ₃ -rabbit polyclonal/ 1:200 and 1:400	Enzo Life Sciences /BML-SA640	goat texas red conjugated anti-rabbit /1:300	Vector Laboratories/ TI-1000	normal horse serum	Vector Laboratories/ S-200
3 β -HSD (P-18) goat polyclonal/ 1:200 and 1:400	Santa Cruz Biotechnology/ sc-30820	rabbit fluorescein conjugated anti-goat /1:300	Vector Laboratories/ FI-5000	normal horse serum	Vector Laboratories/ S-200

Table 2.11 Concentrations and manufacturers of primary and secondary antibodies used in IF.

2.2.4 Statistics

Comparison between the relative mRNA expression of MC in C57BL/6 and Balb/c male mice tissues were performed using unpaired Student's *t*-test (two-tailed) (Excel, Microsoft Office 2010). For all statistical analyses P value is given.

2.3 Results

2.3.1 Expression of MC mRNA in the HPG systems of both male and female mice.

2.3.1.1 Relative mRNA expression of MC in the HPG systems of Balb/c and C57BL/6 male mice.

Expressions of each of the five MC were detected in the male hypothalami, pituitaries and testes of both C57BL/6 and Balb/c mice. Each of the receptors appeared to be expressed at different level in each of these tissues, however comparisons of expression between each of the receptors will only be inferred from the number of cycles required for amplification as the exact receptor copy number per tissue was not determined. The size of each PCR product was confirmed by electrophoretic separation on an agarose gel (Figure 2.8, 2.12 and 2.21). In general, the relative expressions of MC mRNAs were highest in the hypothalami, intermediate in the pituitaries and lowest in the testes of both C57BL/6 or Balb/c mice. MC₃ and MC₄ appeared to be the two dominant receptors in the hypothalami of both strains of mice (Figure 2.5). There were no significant differences in hypothalamic MC mRNA expression between the two strains but the relative expression of MC₅ was 50 % lower in C57BL/6 compared to Balb/c mice (*t*-test, *p*=0.11). MC₃ was likely to be by far the most highly expressed receptor subtype in the pituitary of both strains (Figure 2.6). In contrast, the relative mRNA expression of MC₂ in pituitaries was very low (Balb/c mice) or not detectable (C57BL/6 mice). Expression of MC₃, MC₅ and MC₁ was 2-, 9- and 13-fold greater in pituitaries of C57BL/6 compared to Balb/c mice, respectively (*t*-test; MC₃ *p*=0.17, MC₅ *p*=0.09 and MC₁ *p*=0.16; Figure 2.6). MC₂ appeared to have the highest mRNA expression level in testes of both strains and its expression was 50 % greater in Balb/c compared to C57BL/6 mice (*t*-test; *p*=0.12; Figure 2.7). Similarly, testicular expression of MC₅ was 60 % higher in Balb/c than in C57BL/6 mice (*t*-test; *p*=0.12; Figure 2.7).

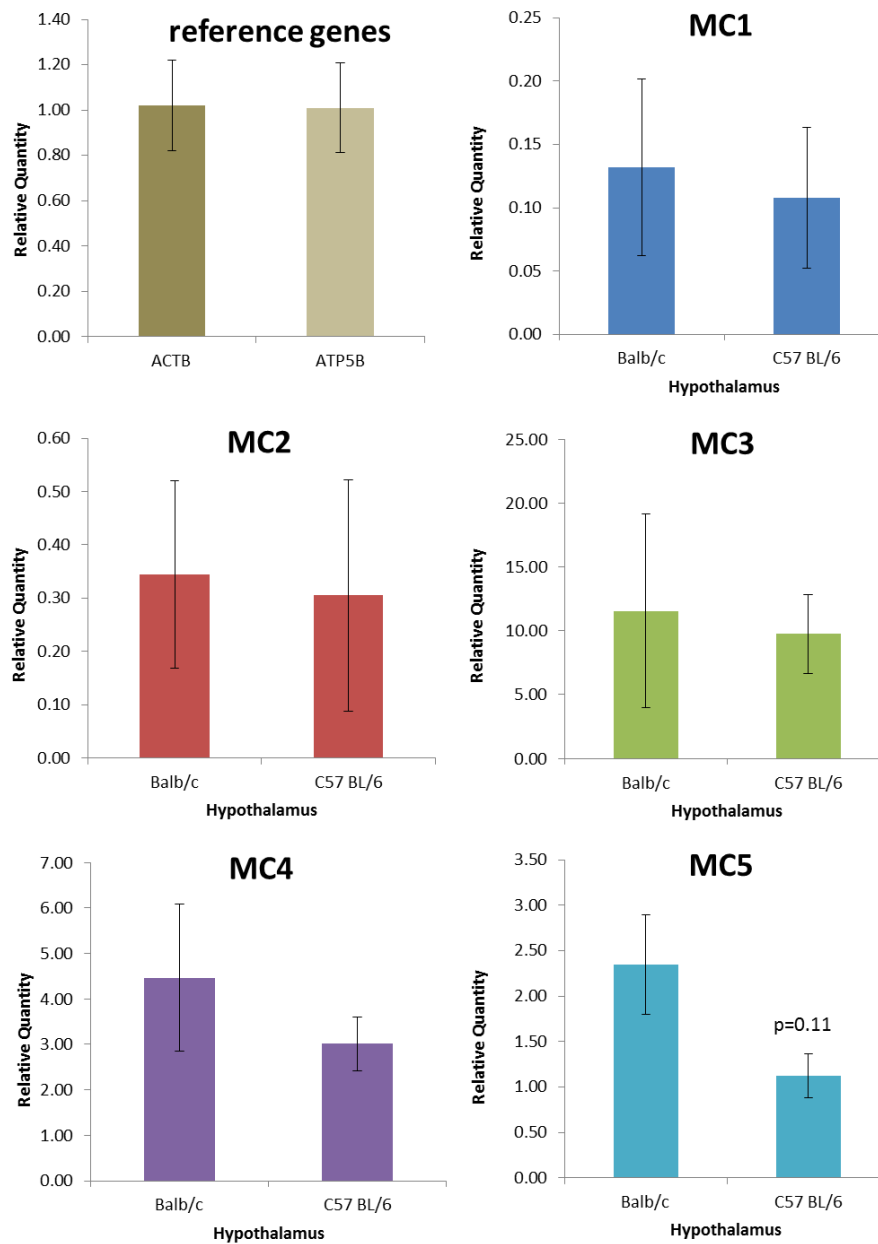


Figure 2.5 Relative mRNA expression of MC in hypothalami of 8 weeks old Balb/c and C57BL/6 male mice. Relative expression was determined by qPCR and results were analysed using qBase plus software including target specific amplification efficiencies. Data normalisation was performed using geometric mean of two reference genes ACTB and ATP5B (first panel). To ensure accurate estimation of gene of interest (GOI) expression, the specificity of qRT-PCR was tested in reactions without reverse transcriptase (SuperScript; no-RT control). Data are presented as mean \pm SEM of three independent samples. There are no significant differences between MC expression in Balb/c and C57BL/6 male mice (*t*-test).

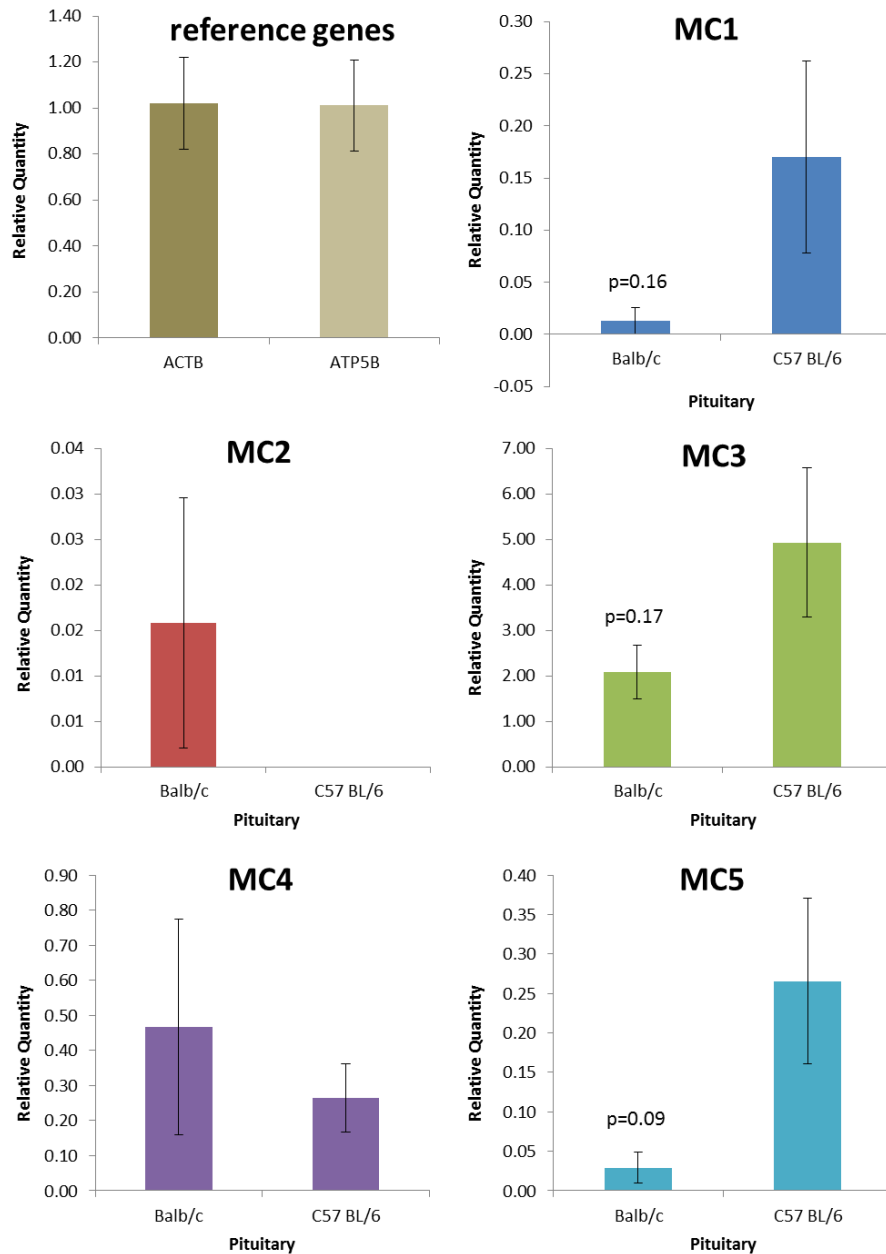


Figure 2.6 Relative mRNA expression of MC in pituitaries of 8 weeks old Balb/c and C57BL/6 male mice. Relative expression was determined by qPCR and results were analysed using qBase plus software including target specific amplification efficiencies. Data normalisation was performed using geometric mean of two reference genes ACTB and ATP5B (first panel). To ensure accurate estimation of gene of interest (GOI) expression, the specificity of qRT-PCR was tested in reactions without reverse transcriptase (SuperScript; no-RT control). Data are presented as mean \pm SEM of three independent samples. There are no significant differences between MC expression in Balb/c and C57BL/6 male mice (t -test).

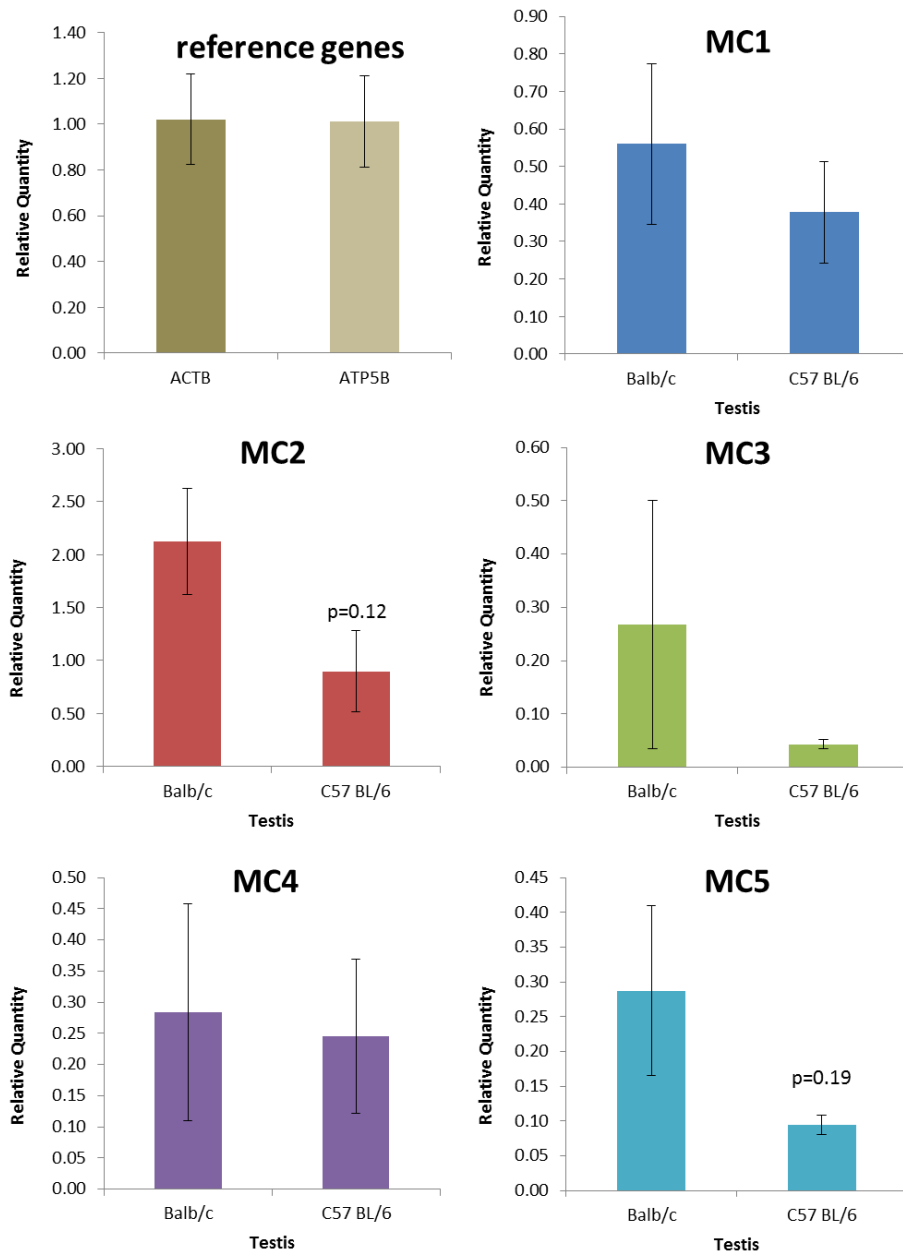


Figure 2.7 Relative mRNA expression of MC in testes of 8 weeks old Balb/c and C57BL/6 male mice. Relative expression was determined by qPCR and results were analysed using qBase plus software including target specific amplification efficiencies. Data normalisation was performed using geometric mean of two reference genes ACTB and ATP5B (first panel). To ensure accurate estimation of gene of interest (GOI) expression, the specificity of qRT-PCR was tested in reactions without reverse transcriptase (SuperScript; no-RT control). Data are presented as mean \pm SEM of three independent samples. There are no significant differences between MC expression in Balb/c and C57BL/6 male mice (t -test).

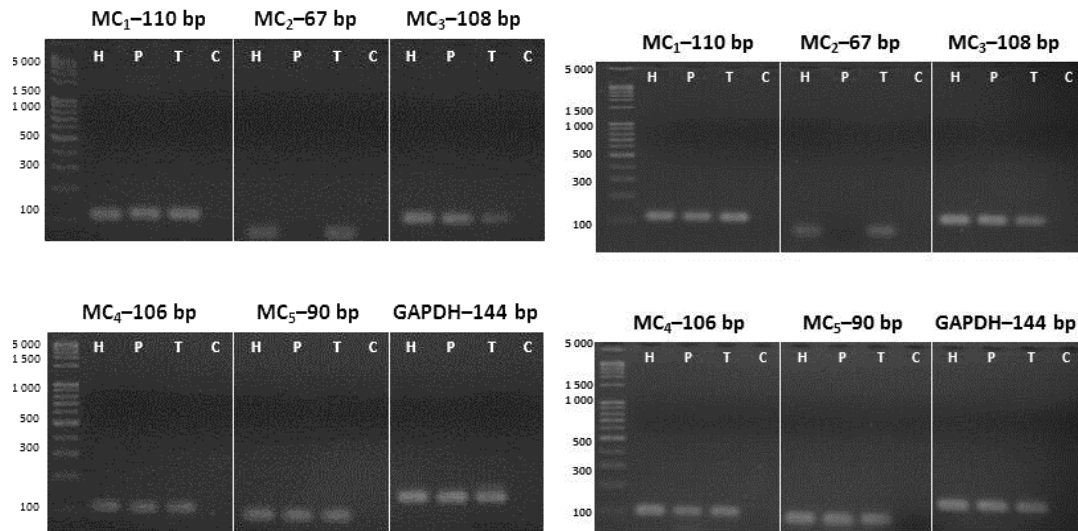
A: C57BL/6**B: Balb/c**

Figure 2.8 MC mRNA expression in tissues from C57BL/6 and Balb/c 8 weeks old male mice. In both animal strains (panels A and B): MC₁ - 110 bp; MC₂ - 67 bp; MC₃ - 108 bp; MC₄ - 106 bp; MC₅ - 90 bp; GAPDH - 144 bp. In all panels: H=hypothalamus, P=pituitary, T=testis, C=Control, no cDNA. Amplification products were separated on 2 % agarose gel. Representative images of three independent qPCRs.

2.3.1.2 Relative mRNA expression of MC in the HPG systems of C57BL/6 male mice at different ages.

The relative expressions of mRNAs for each MC in 14 weeks old male C57BL/6 mouse were based on a single mouse due to lack of animals supply, hence no statistical tests were performed but observed differences will be described. Expressions of all MC in the hypothalamus were 82-95 % greater in 14 weeks old compared to 8 weeks old male mice (Figure 2.9). In the pituitary, the mRNA levels of MC₃ and MC₄ were more than 2- and 3-fold, respectively, lower in the younger animals (Figure 2.10). MC₂ mRNA expression was below detection level in 8 weeks old mice using this method. Conversely, the relative pituitary MC₅ mRNA level was 60 % lower in 14 weeks old mouse (Figure 2.10). Testicular MC₂ mRNA was two fold lower in the younger mice (Figure 2.11). The relative mRNA expressions of MC₃ and MC₄ were 35 % and 90 %, respectively, higher in testes of 8 weeks old mice compared to 14 weeks.

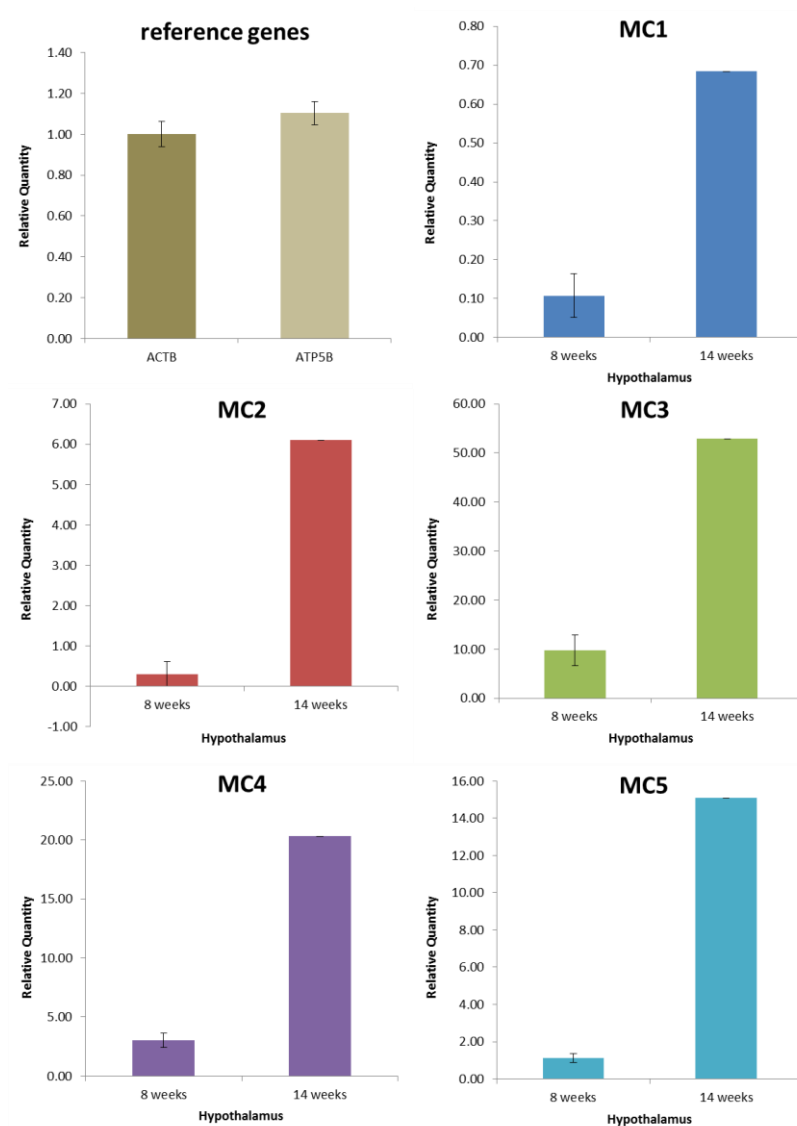


Figure 2.9 Relative mRNA expression of MC in hypothalami of 8 and 14 weeks old C57BL/6 male mice. Relative expression was determined by qPCR and results were analysed using qBase plus software including target specific amplification efficiencies. Data normalisation was performed using geometric mean of two reference genes ACTB and ATP5B. The average expression level for the two reference genes in all samples is shown in the first panel. To ensure accurate estimation of gene of interest (GOI) expression, the specificity of qRT-PCR was tested in reactions without reverse transcriptase (SuperScript; no-RT control). In 8 weeks old C57BL/6 male mice data are presented as mean \pm SEM of three independent samples. In 14 weeks old C57BL/6 male mouse data are presented as mean of one sample only.

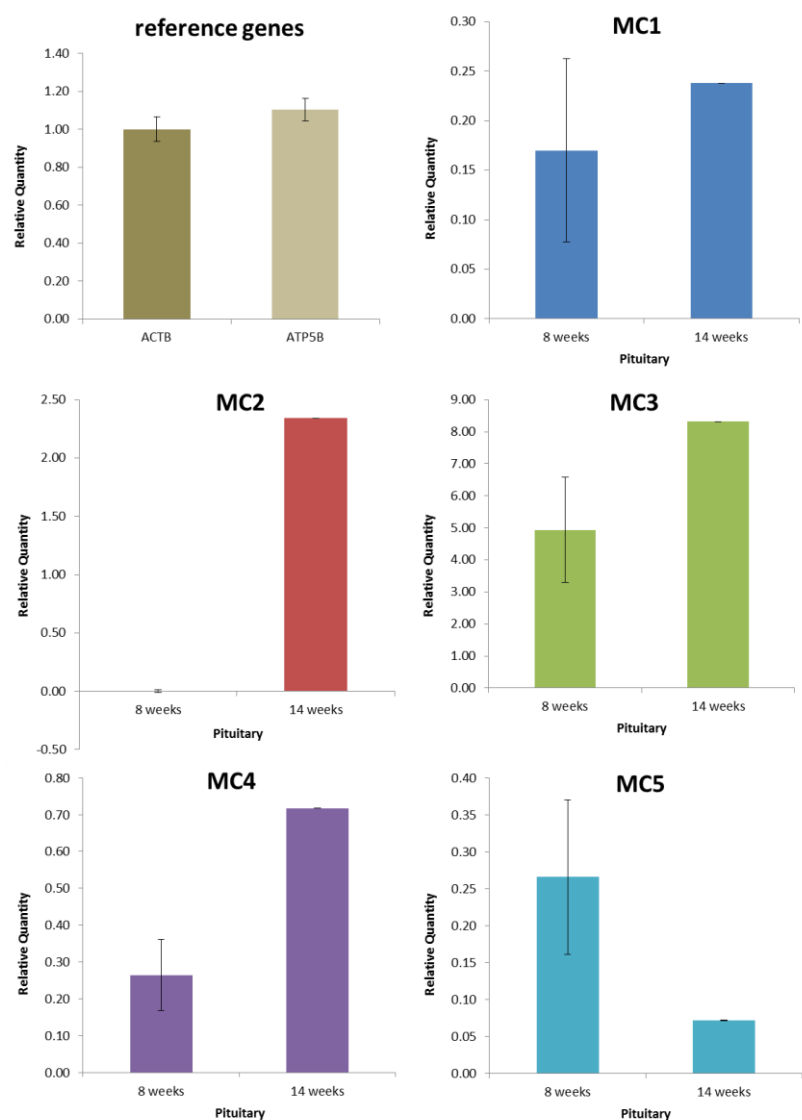


Figure 2.10 Relative mRNA expression of MC in pituitaries of 8 and 14 weeks old C57BL/6 male mice. Relative expression was determined by qPCR and results were analysed using qBase plus software including target specific amplification efficiencies. Data normalisation was performed using geometric mean of two reference genes ACTB and ATP5B. The average expression level for the two reference genes in all samples is shown in the first panel. To ensure accurate estimation of gene of interest (GOI) expression, the specificity of qRT-PCR was tested in reactions without reverse transcriptase (SuperScript; no-RT control). In 8 weeks old C57BL/6 male mice data are presented as mean \pm SEM of three independent samples. In 14 weeks old C57BL/6 male mouse data are presented as mean of one sample only.

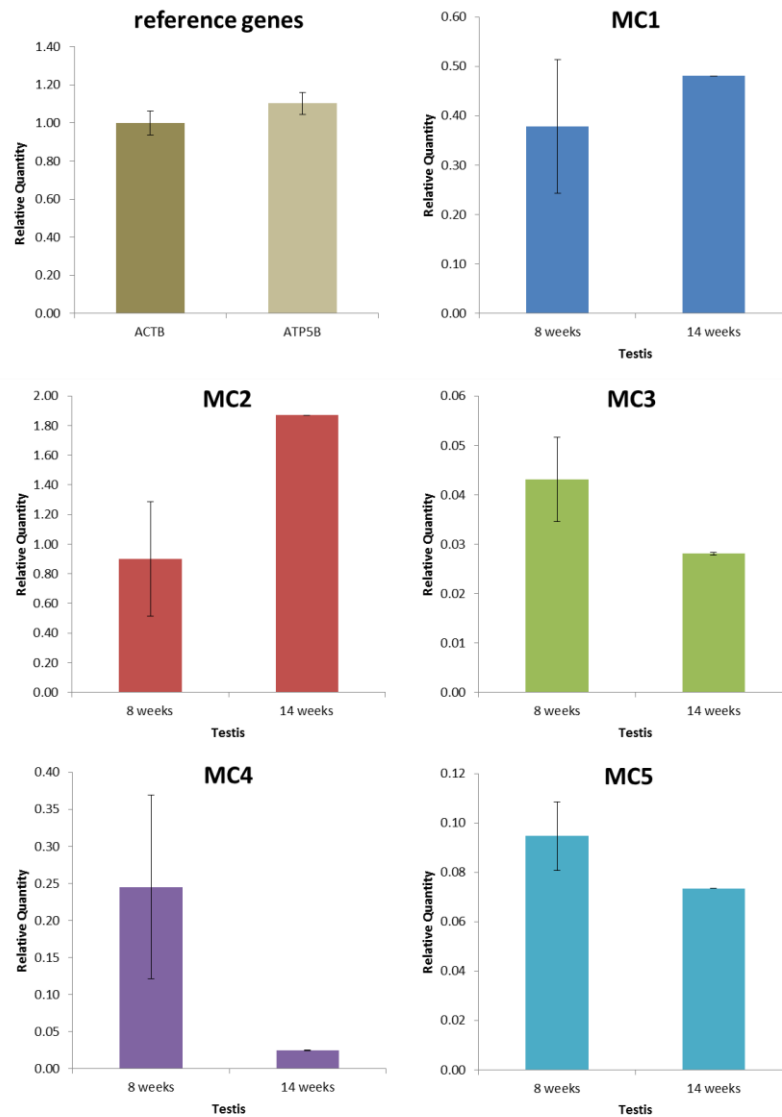


Figure 2.11 Relative mRNA expression of MC in testes of 8 and 14 weeks old C57BL/6 male mice. Relative expression was determined by qPCR and results were analysed using qBase plus software including target specific amplification efficiencies. Data normalisation was performed using geometric mean of two reference genes ACTB and ATP5B. The average expression level for the two reference genes in all samples is shown in the first panel. To ensure accurate estimation of gene of interest (GOI) expression, the specificity of qRT-PCR was tested in reactions without reverse transcriptase (SuperScript; no-RT control). In 8 weeks old C57BL/6 male mice data are presented as mean \pm SEM of three independent samples. In 14 weeks old C57BL/6 male mouse data are presented as mean of one sample only.

2.3.1.3 Relative mRNA expression of MC in the HPG systems of male and female (14 weeks) C57BL/6 mice.

There was approximately 2- to 3-fold higher mRNA expression of MC₂, MC₃ and MC₅ as well as 10-fold greater for MC₄ in male hypothalamus compared to that of female using this method (n=1 in both genders; Figure 2.13). Expression of MC₂ was undetectable and MC₄ was 80 % lower in the pituitary of female mouse (Figure 2.14). Pituitary MC₃ mRNA expression was nearly 2-fold higher in female than in male mouse (Figure 2.14). There were no gender differences in the expression of MC₁ in both the hypothalamus and the pituitary (Figure 2.13 and Figure 2.14).

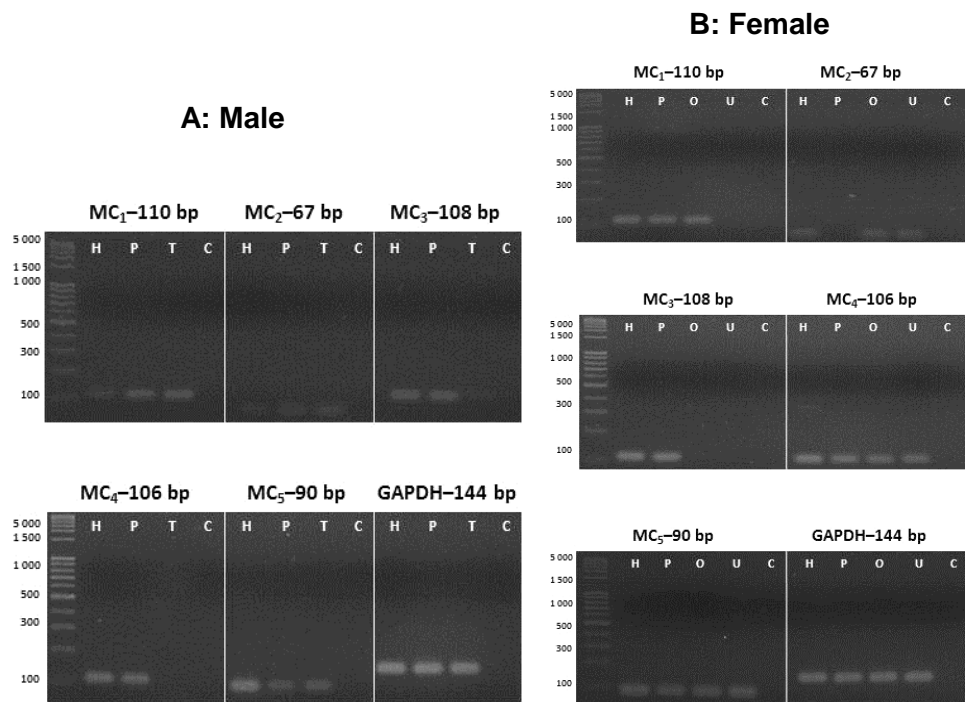


Figure 2.12 MC mRNA expression in tissues from 14 weeks old male and female C57BL/6 mice. In both genders (panels A and B): MC₁ - 110 bp; MC₂ - 67 bp; MC₃ - 108 bp; MC₄ - 106 bp; MC₅ - 90 bp; GAPDH - 144 bp. H=hypothalamus, P=pituitary, T=testis, O=ovary, U=uterus, C=Control, no cDNA. Amplification products were separated on 2 % agarose gel. Representative images of one qPCR.

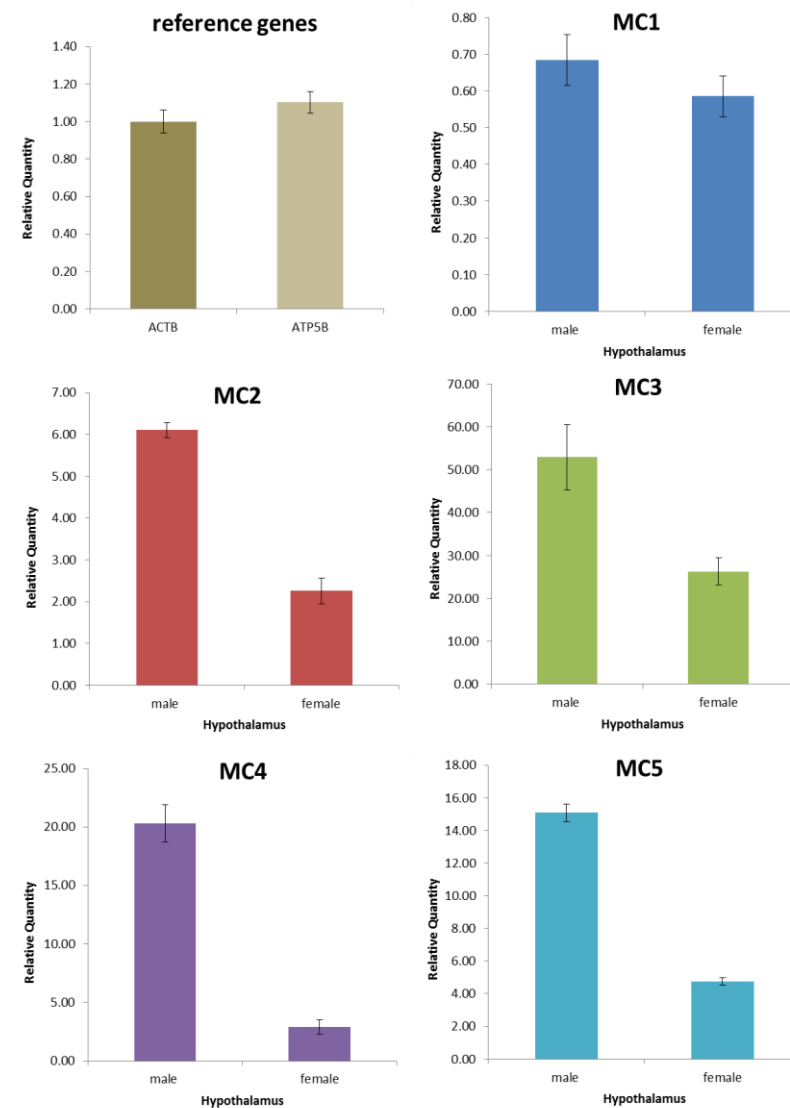


Figure 2.13 Relative mRNA expression of MC in hypothalami from male and female (14 weeks) C57BL/6 mice. Relative expression was determined by qPCR and results were analysed using qBase plus software including target specific amplification efficiencies. Data normalisation was performed using geometric mean of two reference genes ACTB and ATP5B. The average expression level for the two reference genes in all samples is shown in the first panel. To ensure accurate estimation of gene of interest (GOI) expression, the specificity of qRT-PCR was tested in reactions without reverse transcriptase (SuperScript; no-RT control). Data are presented as mean \pm SD (for technical replicates) of one sample.

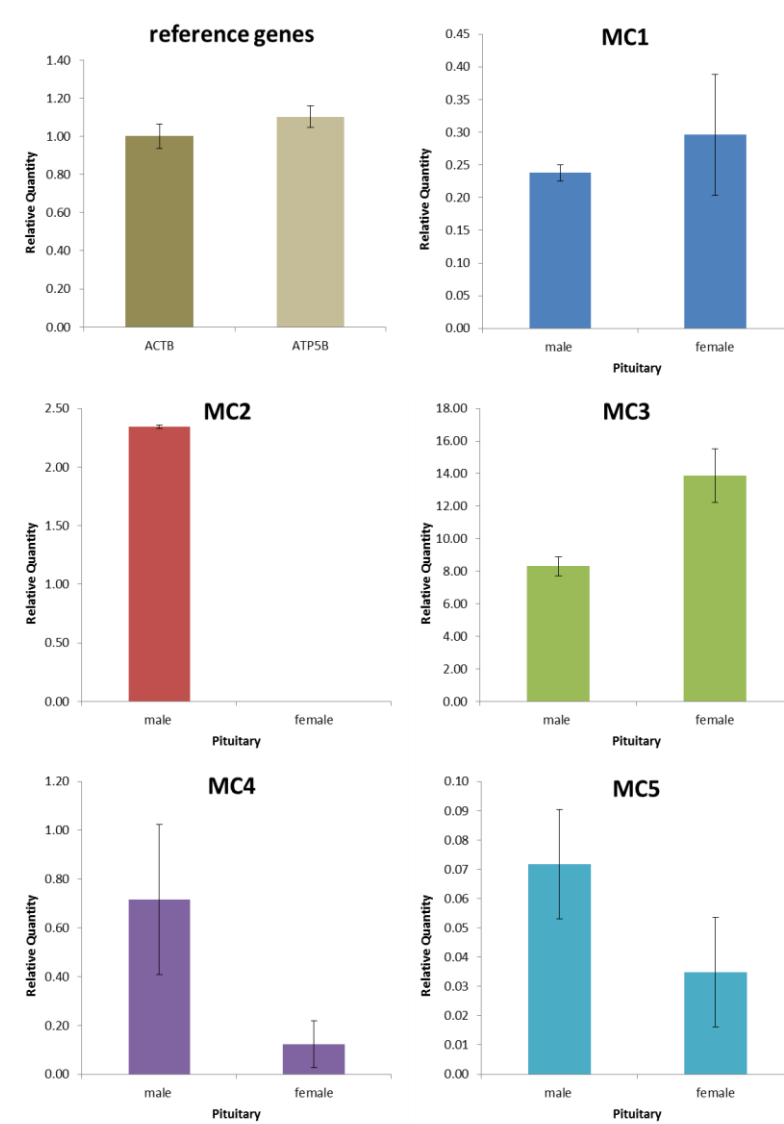


Figure 2.14 Relative mRNA expression of MC in pituitaries from male and female (14 weeks) C57BL/6 mice. Relative expression was determined by qPCR and results were analysed using qBase plus software including target specific amplification efficiencies. Data normalisation was performed using geometric mean of two reference genes ACTB and ATP5B. The average expression level for the two reference genes in all samples is shown in the first panel. To ensure accurate estimation of gene of interest (GOI) expression, the specificity of qRT-PCR was tested in reactions without reverse transcriptase (SuperScript; no-RT control). Data are presented as mean \pm SD (for technical replicates) of one sample.

2.3.1.4 Relative mRNA expression of MC in the HPG systems of C57BL/6 female mice (14 weeks) at different stages of pregnancy.

To determine whether reproductive state affects MC expressions as it did for POMC mRNA (Chen *et al.*, 1986), female mice at different stages of pregnancy (one in each group) were obtained and their tissues were analysed for the relative expressions of MC mRNAs.

Expressions of mRNAs for MC₄ and MC₅ were more than 2-fold and that for MC₁ was approximately 10-fold greater in hypothalami of females at days 7 or 14 of pregnancy compared to non-pregnant animals (n=1 for each group; Figure 2.16). In contrast, hypothalamic MC₃ mRNA expression was approximately 70 % lower in pregnant animals compared to non-pregnant ones.

The relative mRNAs expressions of MC₁ and MC₅ in pituitaries of pregnant animals were more than 1,000-fold higher compared to non-pregnant animals (Figure 2.17). Similarly, pituitary MC₄ mRNA was 300-fold greater at days 7 or 14 of pregnancy. Expression of MC₃ mRNA was 70 % higher in the pituitary of a 14 days pregnant female compared to mice at earlier stages of pregnancy or non-pregnant.

The pattern of MC expressions in ovary and uterus seemed almost identical. Relative expressions of mRNAs for MC₁ and MC₅ were more than 300-fold greater in ovaries of 7 days pregnant and more than 1,500-fold higher in ovaries of 14 days pregnant female compared to non-pregnant animals (Figure 2.18). Ovarian MC₄ mRNA was 90- and 300-fold greater in 7 and 14 days pregnant mice, respectively. Uterine mRNA expressions of both MC₁ and MC₅ were more than 100- or 1,000-fold greater in 7 or 14 days pregnant females compared to non-pregnant, respectively (Figure 2.19). The relative mRNA level of MC₄ in the

uterus was 29-fold higher in 7 days and 140-fold greater in 14 days pregnant female than in non-pregnant mice. The relative mRNA for MC₃ was very low in the ovary and undetectable in the uterus using this procedure. Due to insufficient sample volume, MC₂ expression was not studied in tissues from all 14 weeks old female mice.

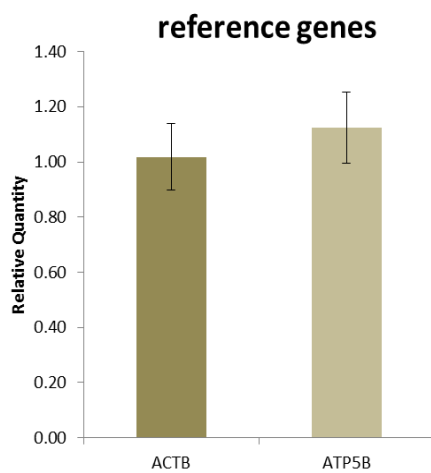


Figure 2.15 Average mRNA expression level of reference genes (ACTB and ATP5B) in all female samples. Relative expression was determined by qPCR and results were analysed using qBase plus software including target specific amplification efficiencies. The two reference genes were used to determine the normalised expression level of genes of interest (GOI). Data are presented as mean \pm SEM.

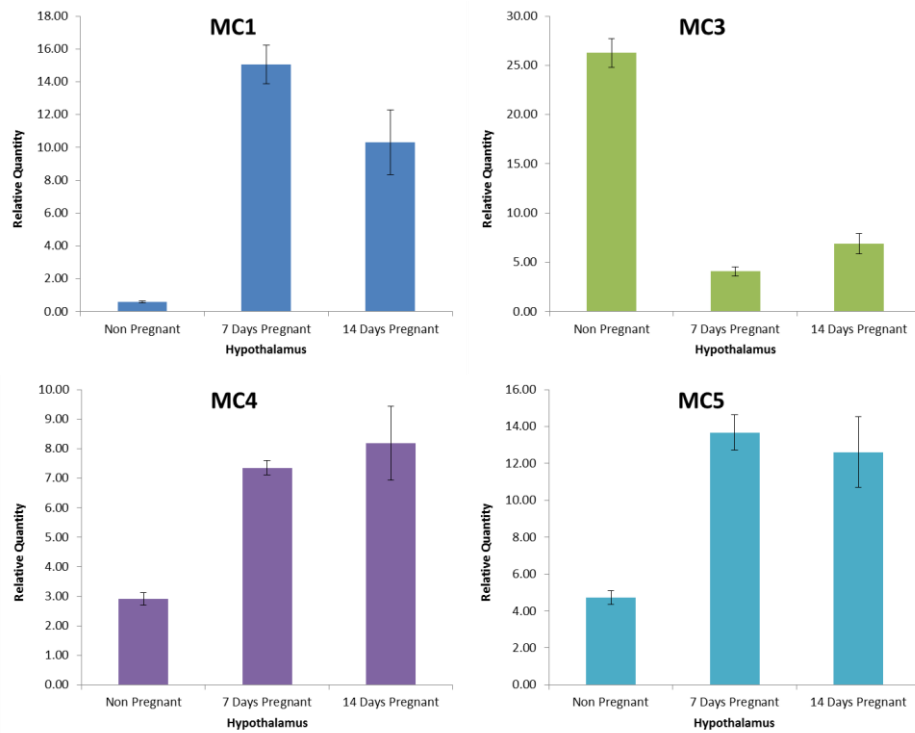


Figure 2.16 Relative mRNA expression of MC in hypothalami of 14 weeks old C57BL/6 female mice at different stages of pregnancy. Relative expression was determined by qPCR and results were analysed using qBase plus software including target specific amplification efficiencies. Data normalisation was performed using geometric mean of two reference genes (ACTB and ATP5B). To ensure accurate estimation of gene of interest (GOI) expression, the specificity of qRT-PCR was tested in reactions without reverse transcriptase (SuperScript; no-RT control). Data are presented as mean \pm SD (for technical replicates) of one sample for each physiological state.

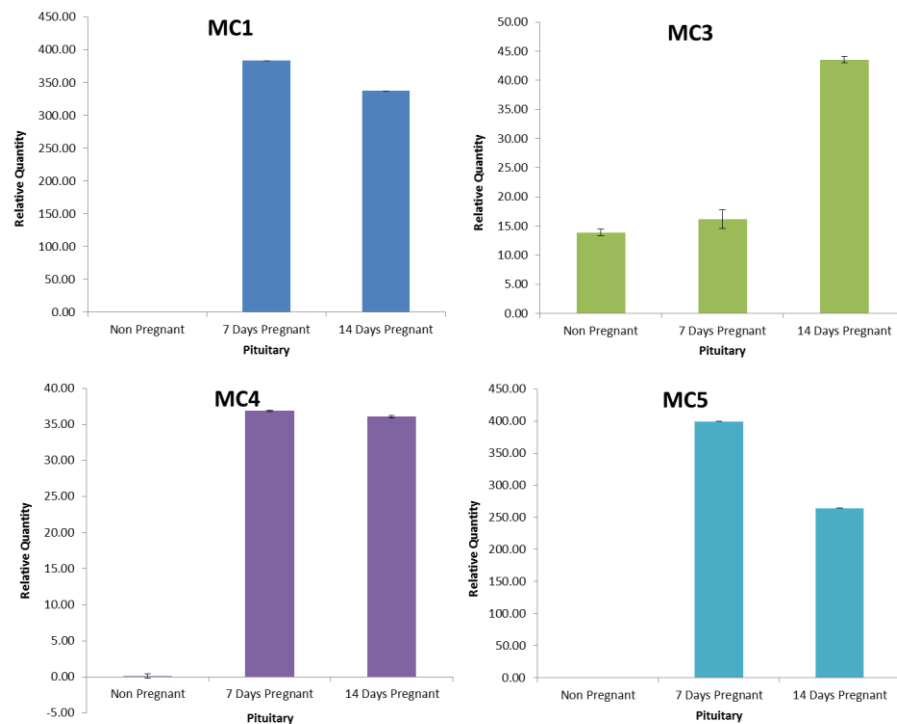


Figure 2.17 Relative mRNA expression of MC in pituitaries of 14 weeks old C57BL/6 female mice at different stages of pregnancy. Relative expression was determined by qPCR and results were analysed using qBase plus software including target specific amplification efficiencies. Data normalisation was performed using geometric mean of two reference genes (ACTB and ATP5B). To ensure accurate estimation of gene of interest (GOI) expression, the specificity of qRT-PCR was tested in reactions without reverse transcriptase (SuperScript; no-RT control). Data are presented as mean \pm SD (for technical replicates) of one sample for each physiological state.

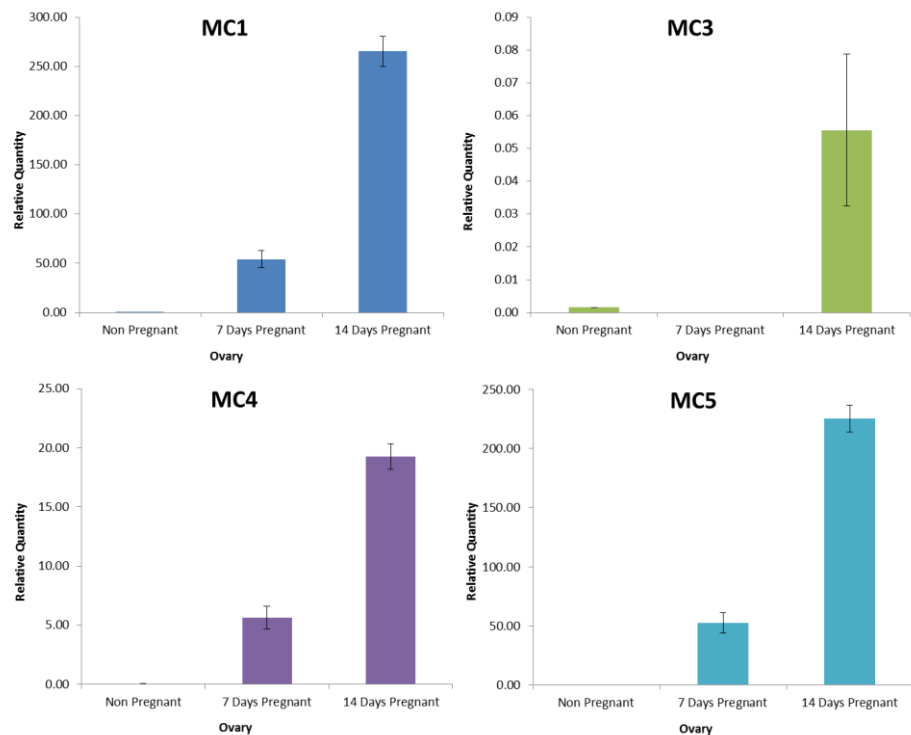


Figure 2.18 Relative mRNA expression of MC in ovaries of 14 weeks old C57BL/6 female mice at different stages of pregnancy. Relative expression was determined by qPCR and results were analysed using qBase plus software including target specific amplification efficiencies. Data normalisation was performed using geometric mean of two reference genes (ACTB and ATP5B). To ensure accurate estimation of gene of interest (GOI) expression, the specificity of qRT-PCR was tested in reactions without reverse transcriptase (SuperScript; no-RT control). Data are presented as mean \pm SD (for technical replicates) of one sample for each physiological state.

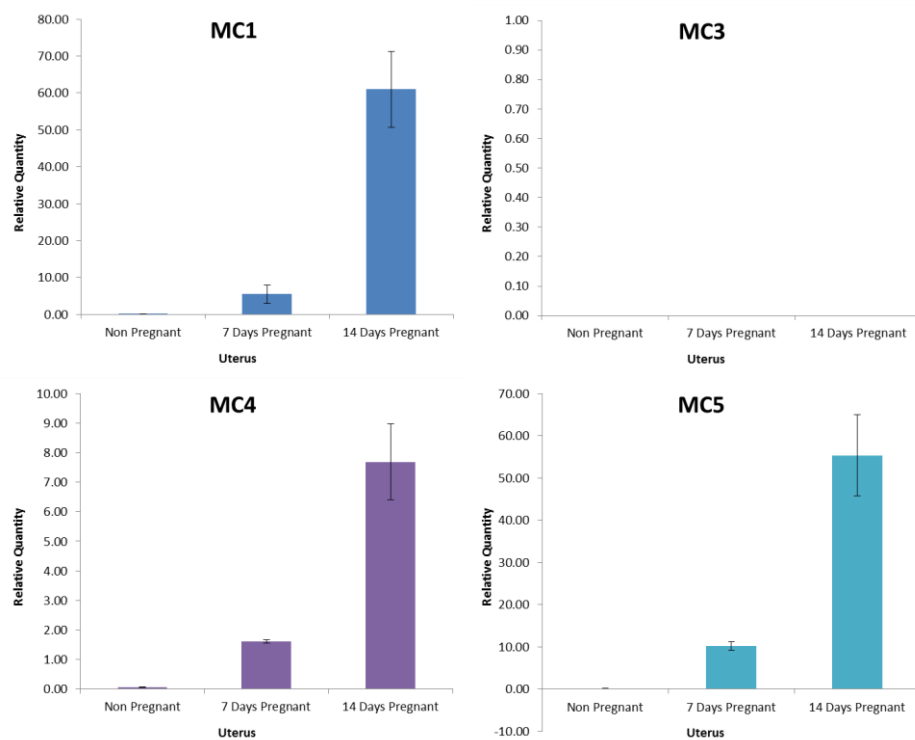


Figure 2.19 Relative mRNA expression of MC in uteri of 14 weeks old C57BL/6 female mice at different stages of pregnancy. Relative expression was determined by qPCR and results were analysed using qBase plus software including target specific amplification efficiencies. Data normalisation was performed using geometric mean of two reference genes (ACTB and ATP5B). To ensure accurate estimation of gene of interest (GOI) expression, the specificity of qRT-PCR was tested in reactions without reverse transcriptase (SuperScript; no-RT control). Data are presented as mean \pm SD (for technical replicates) of one sample for each physiological state.

2.3.1.5 Relative mRNA expression of MC in the HPG system of a MC₃ null male mouse.

qPCR was also performed on cDNA from a hypothalamus, pituitary and testis of a 14 weeks old MC₃^{-/-} mouse in order to confirm ablation of MC₃ gene and ensure that data obtained using this animal model are valid. There was a complete ablation of MC₃ mRNA in all tissues tested compared to a wild type mouse. Some differences in the relative expression levels of the other four melanocortin receptors seem to exist, however, due to small sample size no statistical comparisons were made (Figure 2.20). Marked decreases in the relative expressions of the majority of MC were observed in the hypothalamus and pituitary of a MC₃^{-/-} mouse. In the testis, there was at least a 10 % increase in the expression of MC₁, MC₄ and MC₅ in the absence of MC₃.

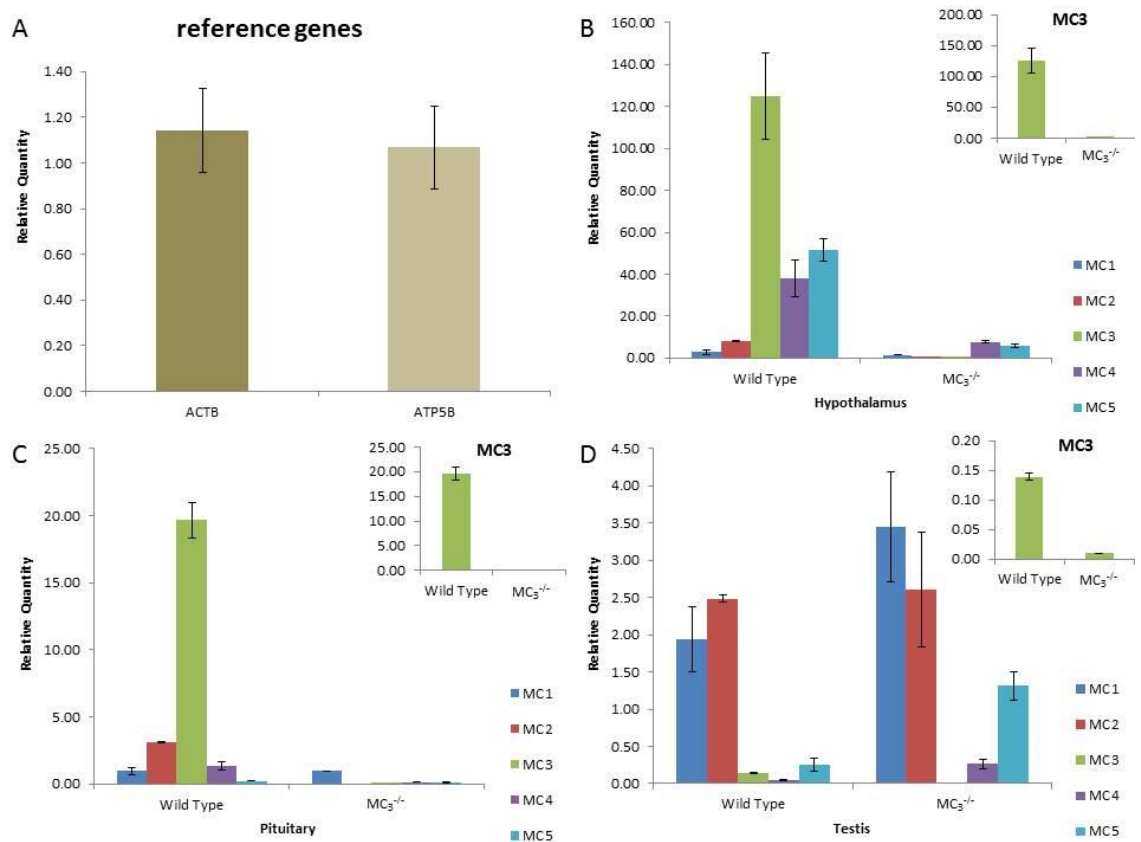


Figure 2.20 Relative mRNA expression of MC in tissues from 14 weeks old wild type and MC₃ null male mice. Relative expression was determined by qPCR and results were analysed using qBase plus software including target specific amplification efficiencies. Data normalisation was performed using geometric mean of two reference genes, ACTB and ATP5B. The average expression level for the two reference genes in all male samples is shown in panel A. To ensure accurate estimation of gene of interest (GOI) expression, the specificity of qRT-PCR was tested in reactions without reverse transcriptase (SuperScript; no-RT control). The inset in the top right corner of panels B-D shows the ablation of MC₃ mRNA expression in tissues of MC₃^{-/-} compared to WT mouse, differences in the scales should be noted. Data are presented as mean ± SD (for technical replicates) of one sample.

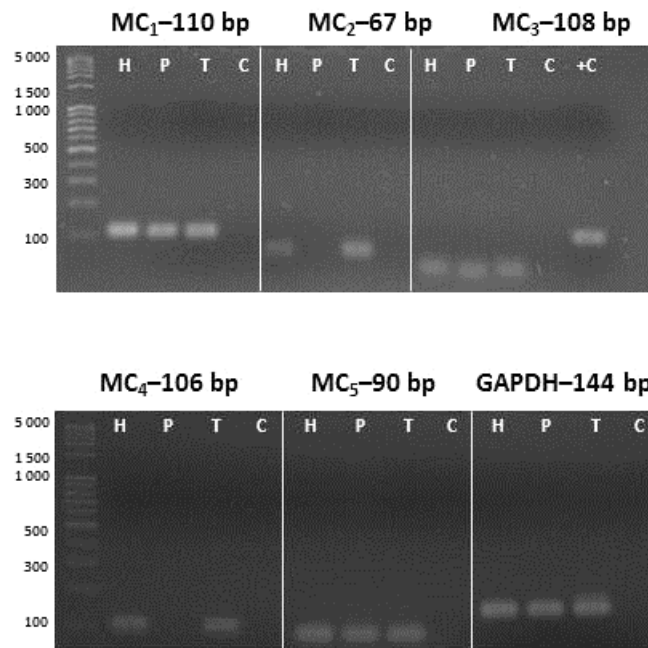


Figure 2.21 MC mRNA expression in tissues from 14 weeks old MC_3 null male mouse. qPCR products separated on 2 % agarose gel. In all panels: H=hypothalamus, P=pituitary, T=testis, C=Control, no cDNA and +C= positive control. MC_1 - 110 bp; MC_2 - 67 bp; MC_3 - 108 bp; MC_4 - 106 bp; MC_5 - 90 bp; GAPDH - 144 bp. Image of one qPCR.

2.3.2 Expression of POMC mRNA in C57BL/6 male and female mice.

Distribution of POMC mRNA, a precursor of melanocortin peptides, has also been determined. The results indicate presence of a full length POMC mRNA in male and female hypothalami and pituitaries as well as in the ovary, which also had a second, smaller weight band (Figure 2.22 a, b). There was no detectable product in the testis. However, using a different set of primers amplifying the region specific for all exon 3-containing POMC transcripts, a truncated product was identified in male gonads but not in the ovary or uterus (Figure 2.22 c, d). The identities of the full length POMC PCR products were confirmed by sequencing (98 % homology with mouse sequences).

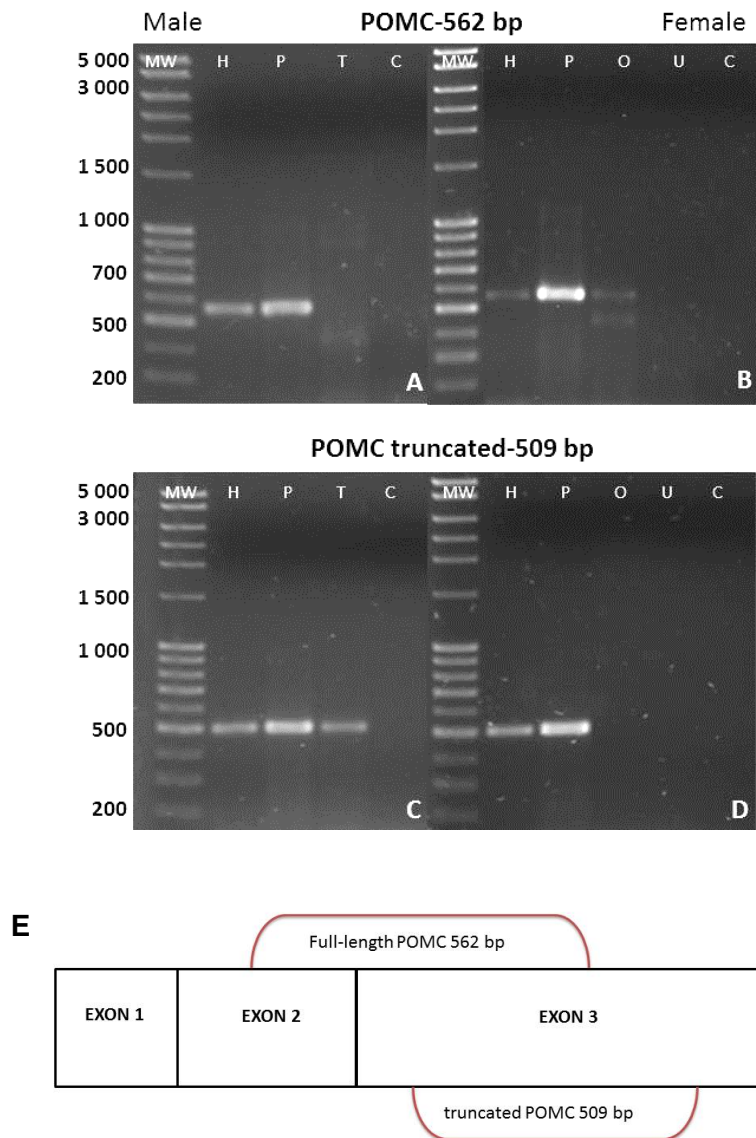


Figure 2.22 POMC mRNA expression in mice tissues. PCR for full-length (top panel) and truncated (bottom panel) POMC mRNA in male (A, C) and female (B, D) as well as approximate primers binding sites (E). Expected product length is 562 bp. Bottom panel - RT-PCR for truncated POMC mRNA in male (C) and female (D). Expected product length is 509 bp. In both panels: MW= molecular weight marker, H=hypothalamus, P=pituitary, T=testis, O=ovary, U=uterus, C=no cDNA. No PCR products were detected in parallel control samples using mRNA preparations without SuperScript - reverse transcriptase. Amplification products were separated on 1.5 % agarose gel. Representative images of three independent PCRs.

2.3.3 Expression of MC₃ protein in the HPG system

2.3.3.1 MC₃ protein characterization

Mouse MC₃ is a 35,800-Da protein containing a number of glycosylation sites, which impair its migration during SDS-PAGE separation leading to the detection of a band of higher molecular weight. This may explain why the lowest detectable band for immunoreactive MC₃-like protein was approximately 70 kDa, which is 30 kDa higher than the expected size (Figures 2.23-2.26). Surprisingly, other bands, of even greater molecular weights were also detected. It is known that MC₃ may form aggregates hence it was of interest to determine the exact form of MC₃ protein in tissue homogenates. Exposure of hypothalamus homogenate to various denaturing conditions led to differential protein(s) bond breakdown, which were visualised in a form of different molecular weight bands (Figure 2.23). Under no or mild denaturing conditions bands between 95 and 130 kDa were mostly detectable (Figure 2.23, lane 1 and 2). Exposure of tissue samples to additional denaturation by boiling for 5 or 15 min resulted in breakdown of additional covalent bonds (disulphide bonds for dimers) and immunoreactive MC₃-like protein detection at lower molecular weight, approximately 70 kDa (Figure 2.23, lanes 3-6). This suggests that the native MC₃ protein may be present as a homo- or heterodimer in these tissues.

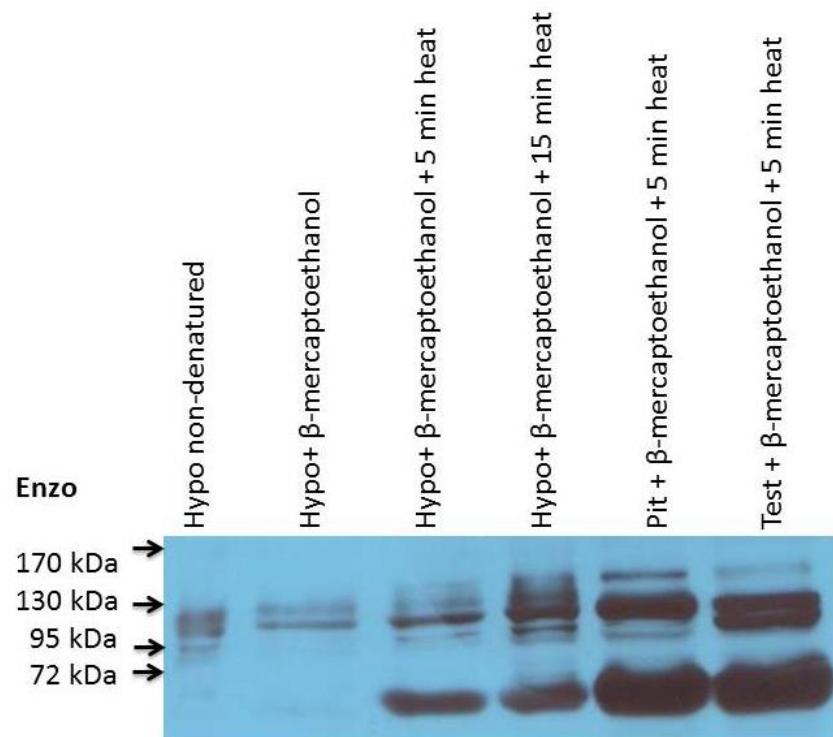


Figure 2.23 The effects of different denaturing conditions on detection of immunoreactive MC₃-like protein in tissue homogenates. Male mouse hypothalamus homogenate was exposed to different denaturing conditions: Lane 1 – hypothalamus sample loading buffer with no β-mercaptoethanol; Lane 2 - hypothalamus sample loading buffer with β-mercaptoethanol; Lane 3 - loading buffer with β-mercaptoethanol, hypothalamus sample boiled (99 °C) for 5 min; Lane 4 - loading buffer with β-mercaptoethanol, hypothalamus sample boiled (99 °C) for 15 min; Lane 5 - loading buffer with β-mercaptoethanol, pituitary sample boiled (99 °C) for 5 min; Lane 6 - loading buffer with β-mercaptoethanol, testis sample boiled (99 °C) for 5 min. Samples were separated on 10 % SDS-PAGE, immunoreactive MC₃-like protein was detected using anti-MC₃ antibody from Enzo.

2.3.3.2 Antibody characterization using recombinant MC₃

MC₃ detection was attempted using three anti-MC₃ antibodies from Enzo Life Sciences, Abcam and Sigma. First, the specificities of the antibodies were tested by preincubating them with either blocking peptides (immunogenic sequence against which the antibody was raised), if available, as in case of

Enzo or with human recombinant MC₃ (H00004159-P01, Abnova, UK). The preincubation with blocking peptide completely blocked immunoreactive MC₃-like protein detection by the Enzo antibody (Figure 2.24 c). Recombinant MC₃ decreased but did not block completely immunoreactive MC₃-like protein detection by the Enzo (Figure 2.24 b) and Abcam antibodies (Figure 2.25 b). The two antibodies from Enzo and Abcam detected recombinant MC₃ by Western Blot (data not shown). The Sigma antibodies do not bind to human MC₃ hence none of the experiments using recombinant MC₃ were successful.

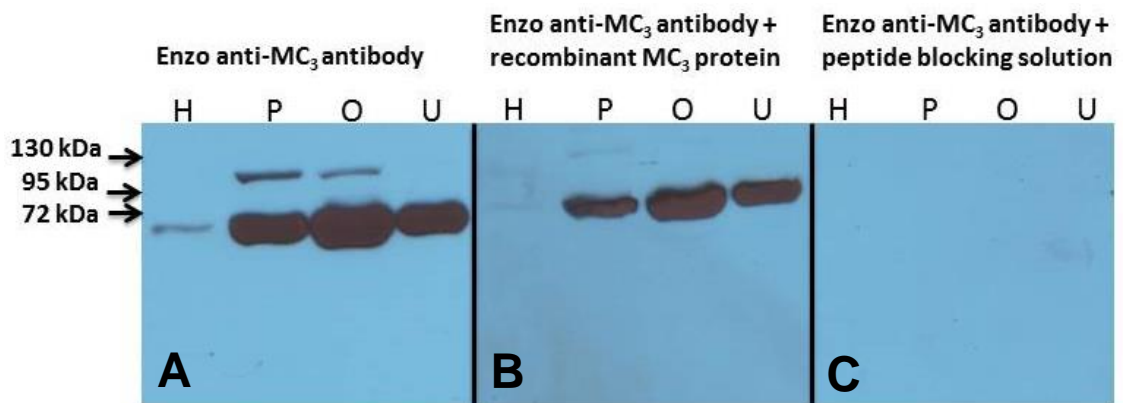


Figure 2.24 The effects of Enzo antibody preincubation with recombinant MC₃ protein or blocking peptide on immunoreactive MC₃-like protein detection in tissue homogenate by Western blot. The Enzo antibody was pre-incubated for 1h at room temperature with either recombinant MC₃ protein (Abnova, UK; panel B) or with peptide blocking solution (panel C) before applying it onto a membrane. The concentration of the antibody was 50 % lower than that of the recombinant MC₃ protein or blocking peptide. The experiment was performed in parallel for a membrane incubated with the Enzo antibody only (panel A). In all panels: H=hypothalamus, P=pituitary, O=ovary, U=uterus. Samples were separated on 10 % SDS-PAGE.

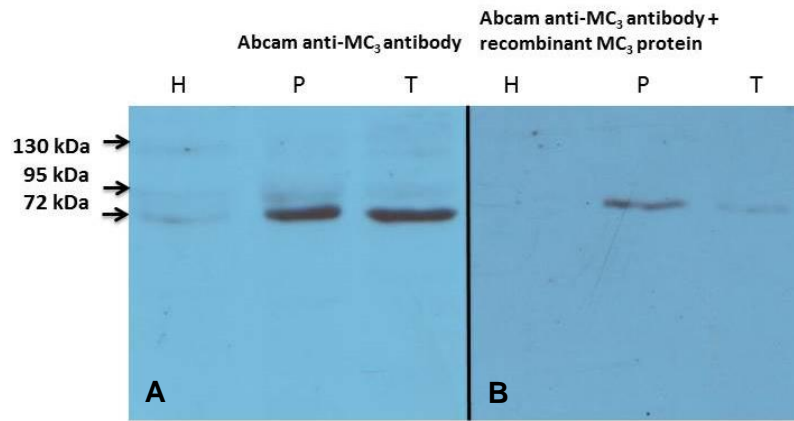


Figure 2.25 The effects of Abcam antibody preincubation with recombinant MC₃ protein on immunoreactive MC₃-like protein detection in tissue homogenate by Western blot. The Abcam antibody was pre-incubated for 1 h at room temperature with recombinant MC₃ protein (Abnova, UK; panel B) before applying it onto a membrane. The concentration of the antibody was 50 % lower than that of the recombinant MC₃ protein. There was no blocking peptide available for this antibody. The experiment was performed in parallel for a membrane incubated with the Abcam antibody only (panel A). In both panels: H=hypothalamus, P=pituitary, T=testis. Samples were separated on 10 % SDS-PAGE.

2.3.3.3 Immunoreactive MC₃-like protein expression

Immunoreactive MC₃-like protein was detected with varying band intensities and molecular weights in all tissues tested using three anti-MC₃ antibodies. The Enzo antibody detected a band of 70 kDa and one or two higher molecular weight band(s) of approximately 110 kDa in tissues from both male and female mice (Figure 2.26). Similarly, Abcam antibody identified immunoreactive MC₃-like protein at a weight of 75 kDa, although according to Abcam the expected MW is 55 kDa, and less intense bands between 95 -130 kDa in tissues from both genders (Figure 2.26). The Sigma antibody detected a band of 40 kDa, which is the expected molecular weight, in addition to many other bands of varying weights, indicating a lack of specificity (Figure 2.26). Additionally,

immunoreactive MC₃-like protein was detected using all three antibodies in samples of MC₃^{-/-} mice, which were incorporated in Western blot following IHC experiments.

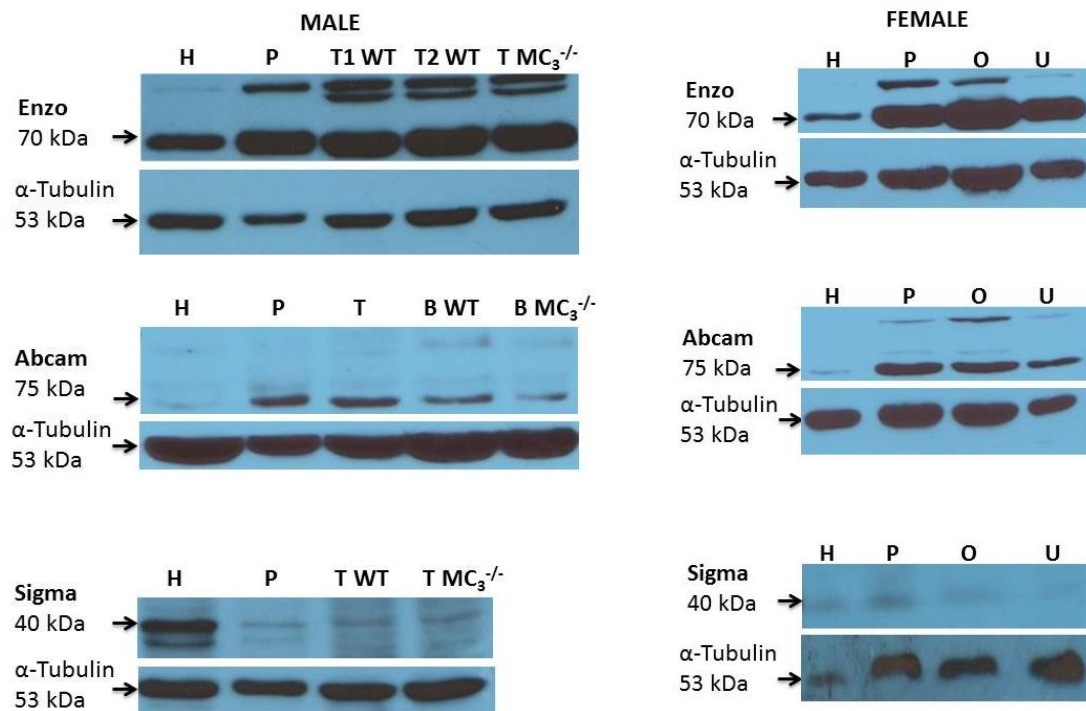


Figure 2.26 Immunoreactive MC₃-like protein expression in male and female mice tissues. In both Male and Female: Panel A- Western blot using anti-MC₃ antibodies produced by Enzo Life Sciences (70 kDa); Panel B -Western blot using anti-MC₃ antibodies produced by Abcam (expected - 55 kDa, detected - 75 kDa); Panel C - anti-MC₃ antibodies from Sigma-Aldrich (40 kDa). Anti- α -tubulin (housekeeping protein) (53 kDa) present in all panels. The amount of protein loaded for each tissue was 20 μ g. Abbreviations: H=hypothalamus, P=pituitary, T (number)=testis (number), B=brain, WT=wild type, MC₃^{-/-}=MC₃ null mouse, O=ovary, U=uterus. Proteins separated on 10 % SDS-PAGE. Representative images of five independent Western blots.

2.3.3.4 Expression pattern of immunoreactive MC₃-like protein in testis of sexually mature (14 weeks) C57BL/6 mice.

IHC was performed following the initial WB experiments using the Enzo antibody since it had appeared to detect immunoreactive MC₃-like protein in the homogenate of a mouse hypothalamus with a certain degree of specificity (Figure 2.23). The aim of IHC experiments was to specifically detect the exact cell type expressing immunoreactive MC₃-like protein in mouse tissues involved in reproductive function. The testis was the first tissue examined and it was chosen to further inform the *in vitro* testicular tissue steroidogenesis studies (Chapter 4). To aid in identification of the different cell types in the testis, two different cell markers were applied: namely Wilm's Tumour, which binds to Sertoli cells, and 3 β -HSD, a marker of Leydig cells (testosterone secreting cells) (Figure 2.27). The Enzo antibody detected immunoreactive MC₃-like protein in the interstitial islets and seminiferous tubules of testis from sexually mature mouse (Figure 2.28). To determine whether immunoreactive MC₃-like protein is expressed in the Leydig cells of interstitial islets, triple IF was performed (Figure 2.29 A-C). Due to high autofluorescence in the testis, which was not fully blocked by the use of Sudan Black B, the results are not a true representation of the immunoreactive MC₃-like protein and 3 β -HSD expression pattern. Instead the IHC using the two antibodies separately provided a more accurate representation (Figure 2.29 D-F).

The pattern of immunoreactive MC₃-like protein in the testis detected by the Enzo antibody was then compared to that detected by the Sigma and Abcam antibodies. Testes from MC₃^{-/-} were used as a negative control tissue. All antibodies detected immunoreactive MC₃-like protein, although at different intensity, in the testis of WT and, most importantly, in MC₃^{-/-} regardless of the antibodies concentrations (Figure 2.30 and 2.31).

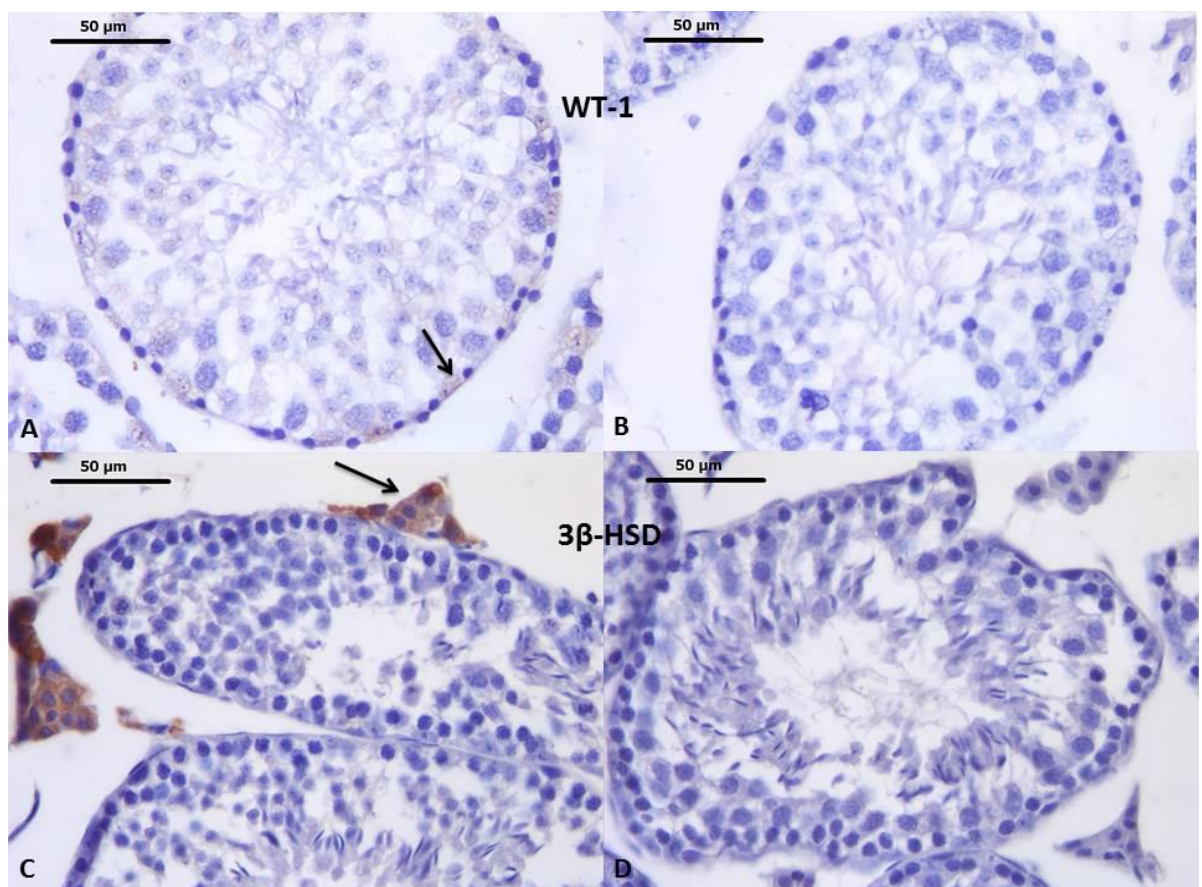


Figure 2.27 Immunohistochemical staining for Sertoli (Wilm's Tumour 1, WT-1) and Leydig cells (3 β -HSD) in mice testes of 14 weeks old C57BL/6 mice. Images A and B show staining for WT-1 (1 in 100 antibody dilution), a marker of Sertoli cells, whilst images C and D present staining for 3 β -HSD (1 in 200 antibody dilution), a marker of Leydig cells. Positive staining of cells is indicated by a brown precipitate (see arrows). There was no positive immunostaining in tissue sections incubated with secondary antibody only (negative controls, images B and D). Images are representative of the results of three independent experiments.

The Sigma antibody had the highest intensity of staining and, at the same time, it was least specific compared to the other two antibodies in both animal types. In contrast, Abcam antibody detected very little, if any, immunoreactive MC₃-like protein in testis, even following the antigen retrieval step. The Enzo antibody appeared slightly more specific, although the fact that it gave positive staining in the MC₃^{-/-}, discouraged its further use. Presented results confirm that the three anti-MC₃ antibodies lack specificity, hence all further protein work was terminated at this stage.

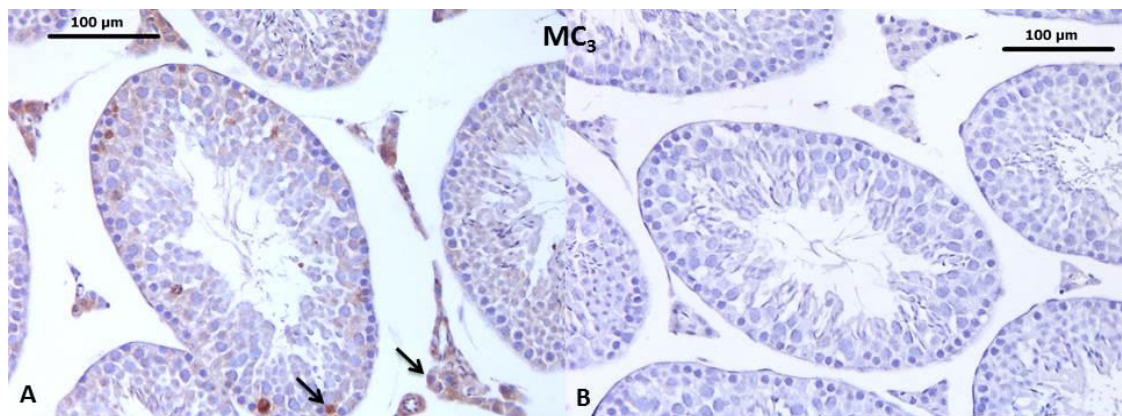


Figure 2.28 Expression of immunoreactive MC₃-like protein (Enzo) in mice testes. Results of immunohistochemical staining in the testes of 14 weeks old wild type C57BL/6 mice for MC₃ using anti-MC₃ antibodies from Enzo (1 in 200 antibody dilution). Positive staining of cells is indicated by a brown precipitate (see arrows). There was no positive immunostaining in tissue sections incubated with secondary antibody only (negative control, image B). Images are representative of the results of four independent experiments.

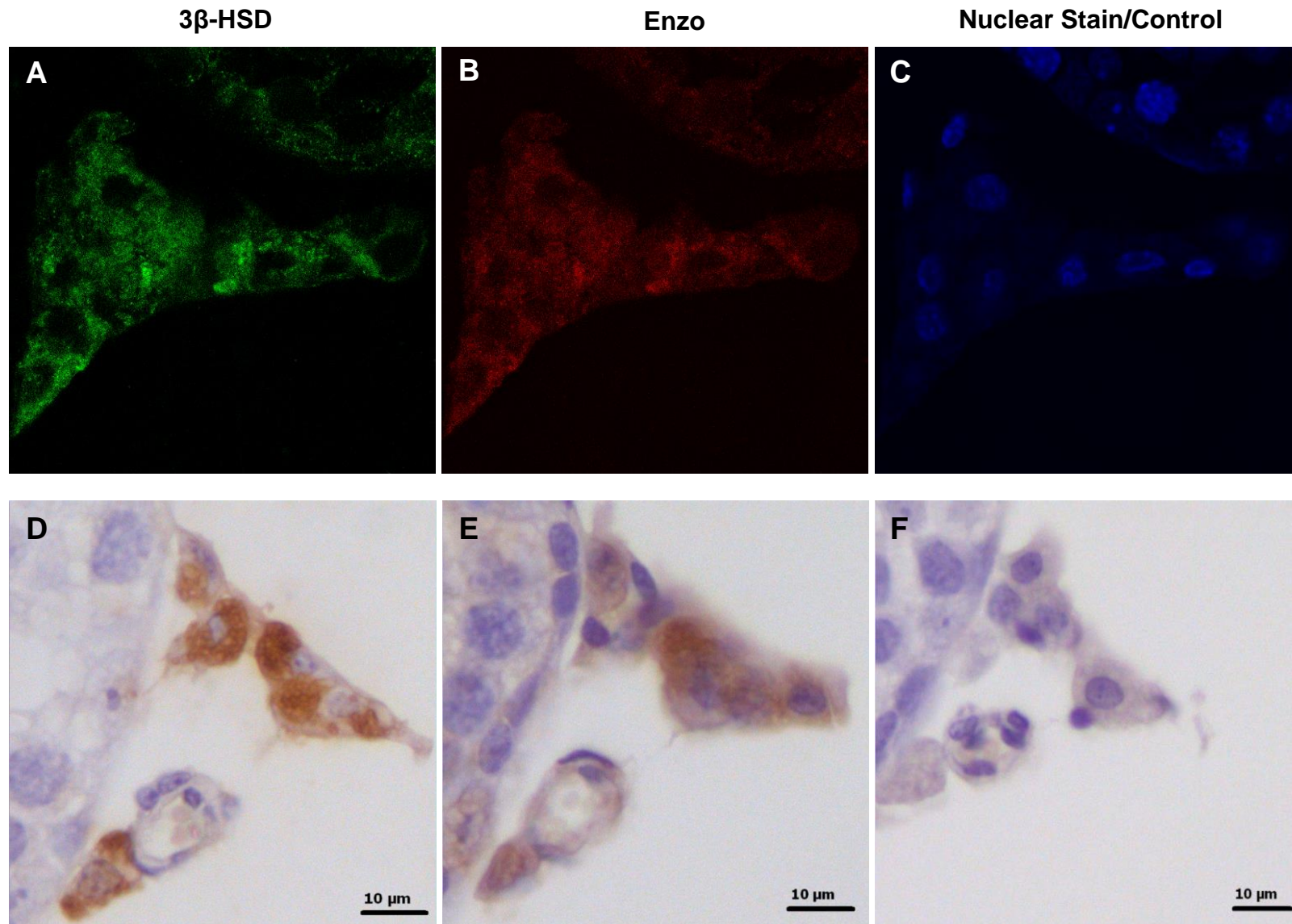


Figure 2.29 Expression of immunoreactive MC₃-like protein and 3β-HSD in mice testes. Results of immunofluorescent (IF, top panel) immunohistochemical (IHC, bottom panel) staining in testes of 14 weeks old wild type C57BL/6 mice for 3β-HSD (column 1) and MC₃ using anti-MC₃ antibodies from Enzo (column 2). Positive staining of cells is indicated by a fluorescent signal (IF) or brown precipitate (IHC). Nuclear staining (ToPro3) for IF (image C) and control staining (secondary antibody only) for IHC (image F) are present in column 3. Images are from adjacent sections and represent the results of three independent experiments.

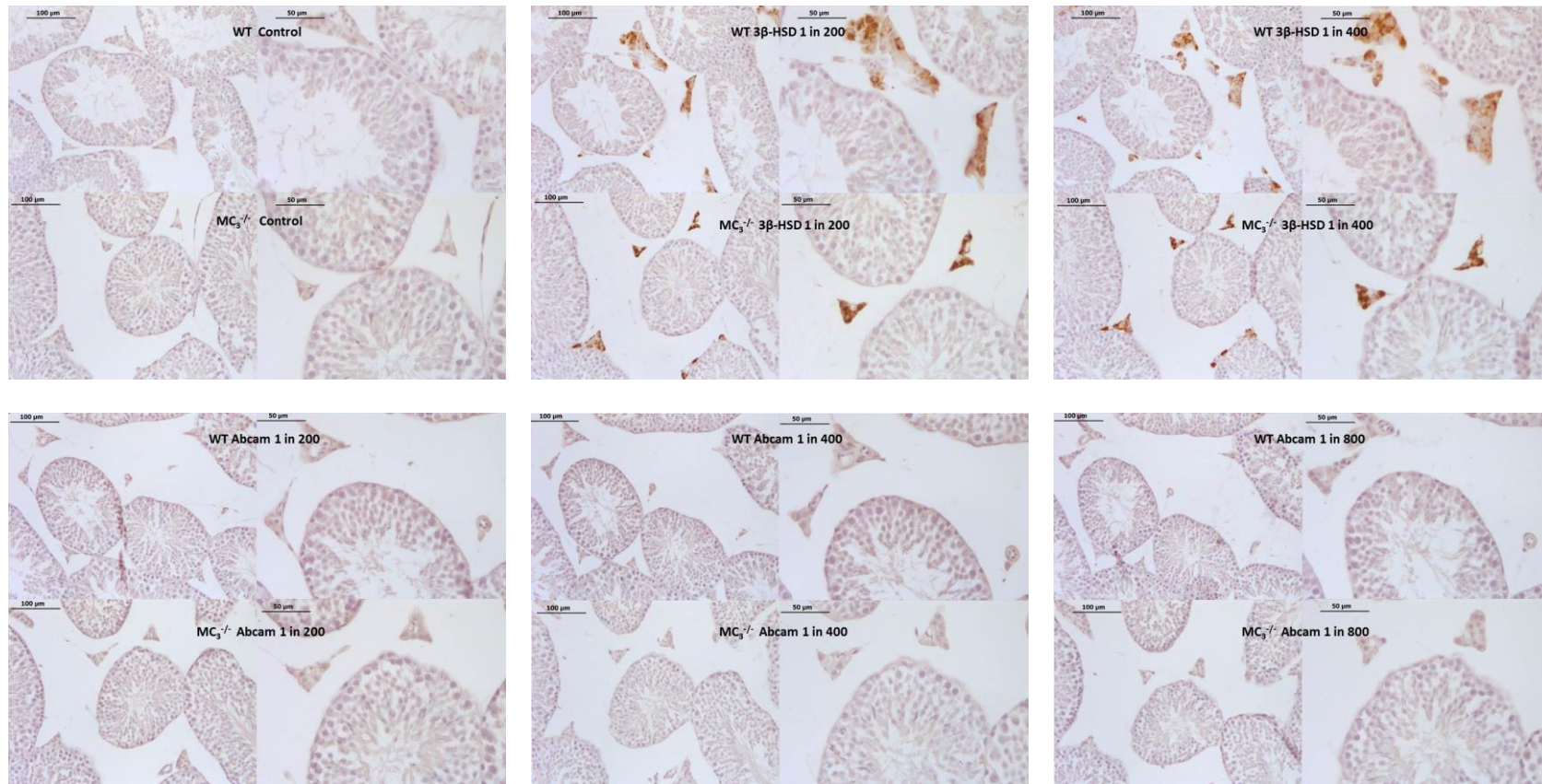


Figure 2.30 Expression of immunoreactive MC₃-like protein and 3β-HSD in testes of wild type and MC₃ null mice. Results of immunohistochemical staining in the testes of 14 weeks old wild type C57BL/6 and MC₃ null mice for 3β-HSD (top panel) and MC₃ using anti-MC₃ antibodies from Abcam (bottom panel). Positive staining of cells is indicated by a brown precipitate. Antibody dilution factor is indicated at the top of each image. There was no positive immunostaining in testes from tissue sections incubated with either PBS alone or normal goat serum diluted in PBS, control (first image, top panel). Images are from adjacent sections and represent the results of three independent experiments.. Scale bar is present in the top right corner of each image.

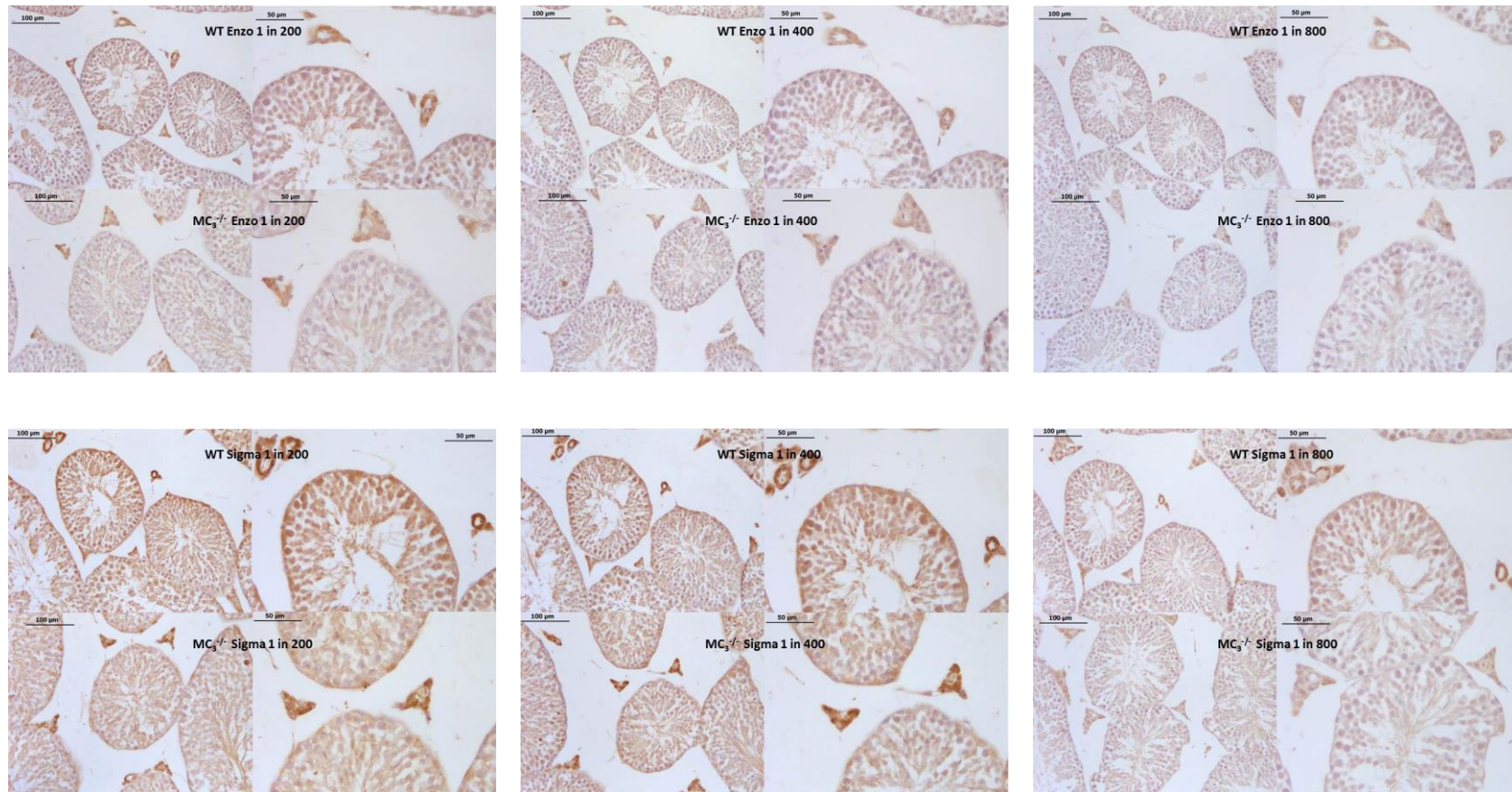


Figure 2.31 Expression of immunoreactive MC₃-like protein in testes of wild type and MC₃ null mice. Results of IHC staining in the testes of 14 weeks old wild type C57BL/6 and MC₃ null mice for MC₃ using anti-MC₃ antibodies from Enzo (top panel) and Sigma (bottom panel). Positive staining of cells is indicated by a brown precipitate. Antibody dilution factor is indicated at the top of each image. There was no positive immunostaining in testes from tissue sections incubated with either PBS alone or normal goat serum diluted in PBS, control (see previous page). Images are from adjacent sections and represent the results of four independent experiments. Scale bar is present in the top right corner of each image.

2.4 Discussion

The mRNAs for the majority of MC are expressed at each level of the hypothalamo-pituitary-gonadal system. Preliminary data indicate that MC expression may be regulated by both age and the reproductive state in the examined tissues. POMC mRNA is co-expressed with MC suggesting autocrine and/or paracrine action of melanocortins. Localization of MC₃-expressing cells in the testis is still questionable as commercially available anti-MC₃ antibodies lack specificity.

Expression of mRNAs for all five receptors were detected in the hypothalamus. The mRNA levels of MC₃, MC₄ and MC₅ appeared to be relatively higher than that for MC₁ and MC₂ in both C57BL/6 and Balb/c mice (Figure 2.5). These findings are in agreement with published literature as mRNAs for both MC₃ and MC₄ were identified primarily in the brain (Gantz *et al.*, 1993 a, b). Hypothalamic MC₃ was mainly localized in the arcuate nucleus, dorsomedial part of the ventromedial nucleus and medial preoptic nucleus (Gantz *et al.*, 1993a; Roselli-Reh fuss *et al.*, 1993). MC₄ mRNA was detected in the paraventricular nucleus (PVN), including both parvicellular and magnocellular neurones of the hypothalamus in the adult rat brain (as reviewed by Tao, 2009). Hypothalamic expression of MC₅ was previously detected (Griffon *et al.*, 1994), and localized to the rostral and medial parts of the medial preoptic area (Murray *et al.*, 2002). Both MC₁ and MC₂ seemed to be expressed at very low levels in the male hypothalamus (Figure 2.5). Previously, MC₁ was detected in the whole brain extract of Balb/c mice by RT-PCR (Rajora *et al.*, 1997) but the hypothalamic expression of MC₁ has only been determined in fish (Klovins *et al.*, 2004). Similarly, the presence of MC₂ in the hypothalamus has been observed in

rainbow trout (Aluru and Vijayan, 2008), whilst in the mammalian brain MC₂ expression was reported only during fetal life (Nimura *et al.*, 2006). There were no statistically significant differences in MC expression between Balb/c and C57BL/6 mice but mRNA level of MC₅ was lower in C57BL/6 mice.

It appeared that the most highly expressed MC gene in the pituitary was MC₃ (Figure 2.6). This supports the results of Morooka and others (1998), who reported that MC₃ may be the predominant MC receptor present in this gland in mice. MC₃ mRNA was previously detected in the anterior and intermediate lobes of rat (Lorsignol *et al.*, 1999) and mouse (Morooka *et al.*, 1998; Roudbaraki *et al.*, 1999) pituitaries. Expression of MC₃ mRNA in the anterior pituitary was localized mainly to lactotrophs and some somatotrophs (Matsumura *et al.*, 2003). Low levels of expression were measured for MC₁, MC₄ and MC₅, and even lower or no detectable signal for MC₂ using this qPCR methodology (Figure 2.6). Expression of MC₁ and MC₄ were previously only detected in human pituitary (Chhajlani, 1996), whereas MC₅ has been detected in both human (Chhajlani, 1996) and rat (Lorsingol *et al.*, 1999) pituitaries. The mRNA levels of MC₃, MC₁ and MC₅ seemed to be relatively higher in C57BL/6 compared to Balb/c mice (Figure 2.6).

In contrast to the pituitary, MC₂ is likely to be the dominant receptor in the testis, followed by MC₁ (Figure 2.7). Expression of the other isoforms, MC₃, MC₄ and MC₅ seemed to be considerably lower (Figure 2.7). All MC except for MC₄ were reported in human testes with expression intensity being the highest for MC₅ > MC₁ > MC₃ > MC₂ (Chhajlani, 1996). Other groups have detected MC₂, MC₃, MC₄ and MC₅ in fetal mice testes (O'Shaughnessy *et al.*, 2003; Nimura *et al.*, 2006; Johnson *et al.*, 2007).

In general, there appeared to be noticeable, although non-significant, differences between C57BL/6 and Balb/c in all tissues examined, particularly in pituitary and testis (Figures 2.5–2.7). Physiologically, the two mouse strains are different. Bartke (1974) performed a detailed comparison of C57BL/6 mice to other strains, in which he described them as hypoandrogenic. The *in vitro* steroidogenic activity in these mice is 40 % less than in Balb/c (Chapter 4, section 4.3.1). Interestingly, C57BL/6 mice breed significantly more efficiently than Balb/c mice possibly due to increased copulatory behaviour (Batty, 1978; Silver, 1995).

Age and gender are another two factors influencing MC expression. Hypothalamic mRNAs for all MC were more than five fold greater in 14 compared to 8 weeks old male mice (Figure 2.9). Kistler-Heer and colleagues (1998) reported an increase in centrally expressed MC₃ mRNA in the postnatal life of the rat. It also appeared that the dominant MC in the pituitary (MC₃) and the testis (MC₂) were two fold lower in 8 compared to 14 weeks old mice (Figure 2.10 and 2.11). Additionally, O'Shaughnessy and others (2003) reported that MC₂ expression in fetal mice testes was 100-fold higher than in the adult mice. Although the changing pattern of MC expressions during life span is still unclear, it seems that it may be related to the reproductive development of an animal. The preliminary results also suggest that some differences may exist between MC mRNAs in male and female mice. It appeared that the expressions of four MC (MC₂, MC₃, MC₄ and MC₅) were at least two fold greater in male compared to female hypothalami (Figure 2.13). In the pituitary, however, the relative mRNA expression of MC₃ seemed to be 50 % higher in female compared to male mice (Figure 2.14), which is in agreement with previous

reports and may be due to a higher proportion of lactotrophs, known to express MC₃, in female mice (Matsumura *et al.*, 2003).

Theoretically, loss of one receptor isoform should lead to overexpression of the other members from this receptor family to maintain normal physiology. This scenario was expected in MC₃^{-/-} mice, and indeed preliminary data indicate that absence of testicular MC₃ may result in a slight increase in the relative mRNAs expressions of the other MC subtypes (Figure 2.20 D). Conversely, MC₃ ablation in the hypothalamus and pituitary led to an apparent reduction in the majority of MC (Figure 2.20 B, C). This preliminary data suggest that expression of MC may be (co)-dependent and that it is tissue specific. As far as we are aware, this is the first study investigating the relative expression pattern of all the MC in the MC₃^{-/-} mice model but it still has to be reexamined.

The second aim of this series of studies was to determine the expression of the melanocortin precursor molecule, POMC, in the reproductive axis in order to establish whether these peptides can act on MC in a paracrine manner. To address this question, the expression of POMC mRNA was examined using two different primer pairs by RT-PCR. The POMC gene is expressed from 3 exons with approximate mRNA length equal to 1100 bp (Drouin *et al.*, 1985). The first combination of primers used results in a product that should span across the exon 2/exon 3 boundary and thus detect full length POMC transcripts composed of three exons. The second primer pair combination corresponds to the exon 3 region and is specific for all exon 3-containing POMC transcripts. Both forms, full and truncated POMC mRNA, were identified in hypothalami and pituitaries of male and female mice and thus confirm local production of ligands for MC (Figure 2.22).

Expression of testicular POMC mRNA in this study was found using the primer pair specific for all exon 3-containing POMC transcripts, but not using the primers for the full length functional transcript, suggesting that the major form of POMC mRNA is truncated (Figure 2.22 A, C). These aberrant transcripts are products of gonadal specific alternative transcription initiation in the intron 2-exon 3 boundary and thus lack the regions corresponding to exons 1 and 2 (Ivell *et al.*, 1988). Exon 1 includes a 5' non-coding region, whilst exon 2 encodes the signal peptide essential for entering the intracellular secretory pathway (Ivell, 1994). Theoretically, the truncated POMC gene transcripts may be functionally defective. However, the previously reported presence of POMC peptides in the gonads (Morris *et al.*, 1987) suggests that either the full-length version of POMC mRNA, although expressed at much lower concentration, significantly contributes to the synthesis of POMC peptides, or they are derived from the systemic circulation.

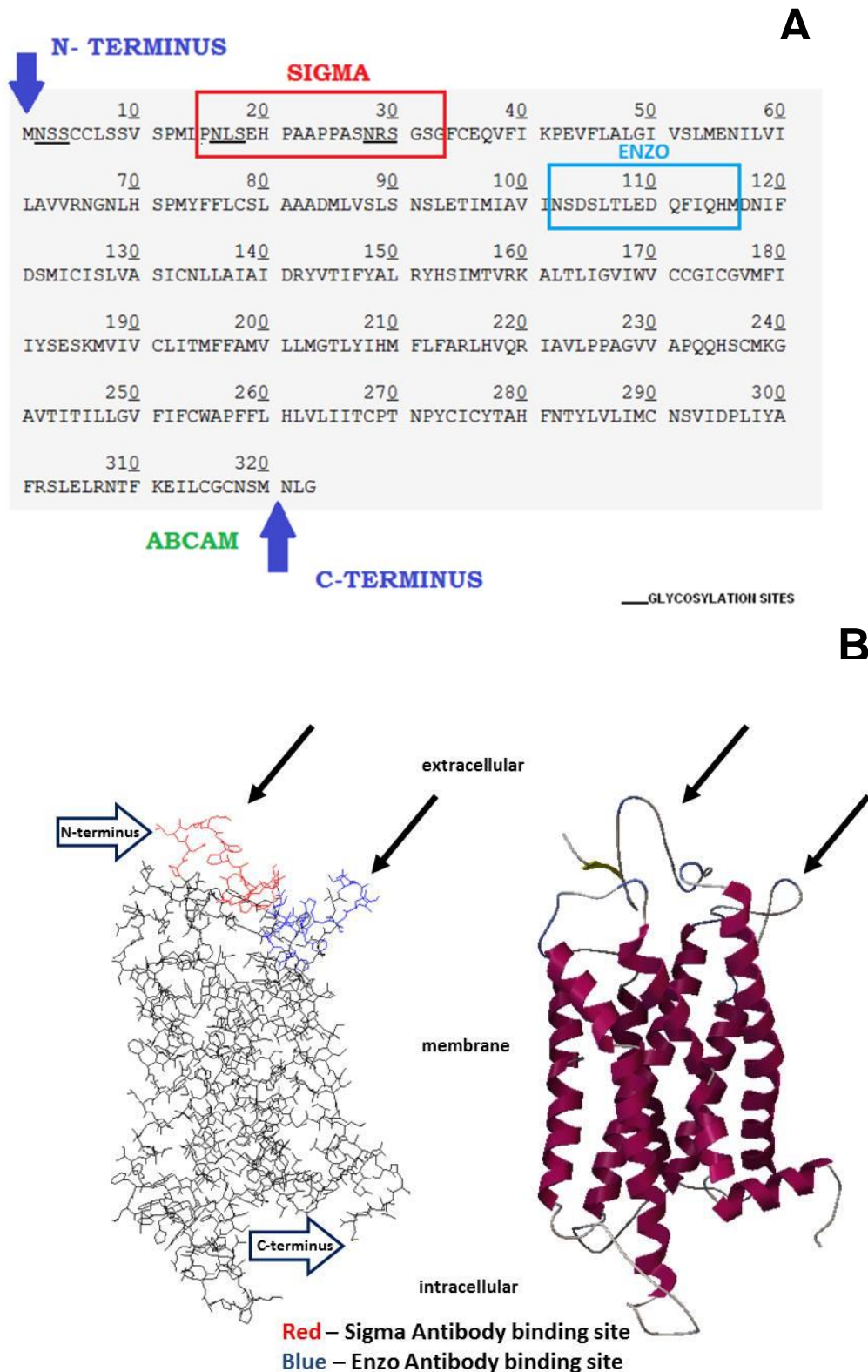
Two amplification products were detected for the ovarian tissue using POMC primers spanning across the exon 2/exon 3 boundary, one of 562 bp and the other one of approximately 500 bp (Figure 2.22 B). Interestingly, there was no detectable product using primers amplifying the truncated POMC transcript (Figure 2.22 D). Chen and colleagues (1986) reported that POMC mRNA is absent in ovaries from immature rats but increases markedly during pregnancy or in response to stimulation with gonadotropins. Similarly, POMC derivatives such as γ_3 -MSH were identified in large antral follicles and corpora lutea of cycling or pregnant mice but no immunostaining was reported in immature animals (Shaha *et al.*, 1984). Based on the fact that the expression of POMC derivatives is determined by the state of the reproductive maturity and pregnancy of the female (Shaha *et al.*, 1984; Chen *et al.*, 1986), it could be

possible that the expression of MC is regulated in a similar fashion. Surprisingly, preliminary data indicated that the mRNA expressions of most MC appeared to progressively increase at all levels of the HPG axis during pregnancy (Figure 2.16–2.19). In many cases there was a more than 1000-fold increase at day 14 of pregnancy compared to the non-pregnant female, particularly in the ovary and uterus. It is worth highlighting that the mRNA level of MC₃ was undetectable, regardless of the physiological state of female, in the uterus and very low in the ovary using this qPCR method (Figure 2.18 and 2.19). This is in contrast to Amweg and co-workers (2010) who localized the expression of MC₃ as well as MC₁ and MC₂ in various ovarian structures of adult cattle by RT-PCR. Further work is still required to determine the exact effect of the physiological state of the female on the pattern of MC expression.

The initial investigation of MC₃ protein distribution pattern was performed by Western blot using anti-MC₃ antibodies from three different companies. The three antibodies have different immunogenic sequences and bind to different sites of the MC₃ protein (Figure 2.32 A, B). A band of approximately 70 kDa was detected in all tissues tested using antibodies from Enzo and Abcam, although the actual protein size is equal to 35.5 kDa (Figure 2.26). The apparent increase in the molecular mass may be due to abnormal protein mobility in SDS-PAGE as a result of post-translational modifications such as glycosylation at the N-terminus and/or phosphorylation in the intercellular loop or at the C-terminus of the protein (Desarnaud *et al.*, 1994). Furthermore, an additional band(s) of even higher molecular weight, ranging from 95-130 kDa, was (were) identified (Figure 2.26). It is known that MC₃ and other MC may form homo- or hetero-dimers or higher order complexes of oligomers (Mandrika *et al.*, 2005). This process is very common for all receptors belonging to the GPCRs family (Milligan, 2009).

MC₃ contains a cysteine bridge in the extracellular loop 3 (Rediger *et al.*, 2012), which may mediate the process of dimerisation. MC₃ heterodimer formation with the growth hormone secretagogue receptor (GHSR)-1a (ghrelin receptor) in the arcuate nucleus has been previously reported (Rediger *et al.*, 2011). The Sigma antibody detected a faint band at 40 kDa and a number of other bands of various molecular weights (Figure 2.26). The lack of specificity may be related either to a very close homology between the MC (42-67%) or to the fact that the immunogenic sequence of the Sigma antibody correlates with a highly glycosylated region of the MC₃ protein (Wikberg, 1999; Figure 2.32 A). This may mask the amino acid sequence and prevent the formation of antigen-antibody complex (Lisowska, 2002).

Following the initial identification of what was thought to be the MC₃ protein by Western blot in tissues of the HPG axis, the antibodies were used to establish the exact cell types expressing MC₃. In the testis, the expression was detected in some cells of the seminiferous tubule and in the interstitial tissues (Figure 2.28). Further experiments localized MC₃ to Leydig cells of the interstitial islets (Figure 2.29). The exact size, molecular form and distribution of MC₃ protein in the HPG system is questionable since all of the anti-MC₃ antibodies gave positive signal when tested in tissues from MC₃^{-/-} mice by both Western blot and immunohistochemistry (Figure 2.26, 2.30 and 2.31). Kathpala and colleagues (2011) were the first to draw the attention to the fact that anti-MC₃ antibodies appear to lack specificity. The group used antibodies from different companies to those presented above but still obtained comparable data with immunoreactive MC₃-like protein being detected in both WT and MC₃^{-/-} mice.



Models were created using Python Molecule Viewer (PMV) and Swiss PDB Viewer

Figure 2.32 Anti-MC₃ antibodies – amino acid sequences and recognition sites. Panel A - relative amino acid sequences of MC₃ protein used to generate anti-MC₃ antibodies. Panel B – approximate binding sites of antibodies from Sigma (red) and Enzo (blue). Please note that information regarding the exact immunogenic sequence for the Abcam antibody is unavailable.

In this series of experiments the presence of MC₃ mRNA, and the other four MC, were determined in each tissue of the reproductive axes of both male and female mice. There are a number of factors including mouse strain, age and gender, which can affect MC mRNA levels but further investigation is required. Additionally, the full and truncated versions of POMC mRNA were detected in tissues of the HPG systems of both genders thus suggesting paracrine actions at MC. Interestingly, the reproductive (physiological) state of the animal may affect the mRNA expression levels of both MC and POMC but a larger sample size is needed before firm conclusions can be made. Although, immunoreactive MC₃-like protein was detected in the reproductive tissues of both genders by Western blot and its testicular expression was identified in cells of the seminiferous tubules and Leydig cells of the interstitial islets by immunohistochemistry, the lack of antibody specificity, tested using tissues from MC₃^{-/-} mice, means that all protein results should be regarded as unreliable. Further work using *in situ* hybridization is necessary to accurately determine the exact pattern of MC₃ expression as well as those for the other four MC. The development of specific antibodies or ligands for MC₃ and/or proteomic analysis are required to confirm MC₃ translation into protein and tissue distribution.

3 Comparison of Wild Type and MC₃ null mice

3.1 Introduction

Genetically modified animals are an invaluable tool to establish the role of ablated genes in normal physiology. MC₃ null mice (MC₃^{-/-}) were first generated in 2000 by two independent research groups (Butler *et al.*, 2000; Chen *et al.*, 2000). A neomycin-resistance cassette replaced the entire MC₃ coding region in C57BL/6 mice (Butler *et al.*, 2000; Chen *et al.*, 2000). It quickly became apparent that these animals develop a complex obesity phenotype. Despite being hypophagic, their fat mass and feed efficiency increased whilst lean mass decreased compared to wild type (WT) mice at 4-6 months of age (Chen *et al.*, 2000). Both male and female MC₃^{-/-} mice developed hyperleptinaemia, whilst males only were hyperinsulinaemic (Chen *et al.*, 2000).

Although, the two research groups (Butler *et al.*, 2000; Chen *et al.*, 2000) suggested that MC₃^{-/-} mice are able to reproduce, our experience (Stephen Getting, and some of his former colleagues at the William Harvey Research Institute, personal communications) indicated that these mice are difficult to breed. Long intervals between pregnancies and small litter sizes had been noted: unfortunately, full breeding records are not available. These anecdotal observations prompted us to investigate the effects of MC₃ ablation on reproductive physiology, since for a long time the use of MC₃^{-/-} mice was mainly devoted to study the role of MC₃ in obesity (Renquist *et al.*, 2012) and inflammation (as reviewed by Getting, 2006a). Increased or reduced intake of nutrients can directly affect reproductive functions. Hypothalamic MC₃ may have an indirect role in the control of reproductive system by regulating energy balance and it remains to be determined if there is a direct role of MC₃ in the

regulation of GnRH secretion. Watanobe and colleagues (2002) suggested that hypothalamic MC₃ could mediate the downstream effects of leptin, which is known to play a key role in weight homeostasis, on the release of LH and prolactin. The exact pathway is still unclear but some proposals exist (Chapter 1, section 1.3.1).

In contrast to the hypothalamus, the potential role(s) of MC₃ and hence its contribution to normal reproductive function at the other levels of the HPG system, particularly the gonads, has(have) not been established. The aim of this series of studies was to compare the different aspects of reproductive physiology of MC₃^{-/-} mice to WT C57BL/6 mice, which are the genetic background of the colony of MC₃^{-/-} mice. To determine the potential function(s) of MC₃ in the pituitary, the contents of all the pituitary hormones were measured in both male and female MC₃^{-/-} mice and compared to WT control mice. In gonads, the possible consequences of MC₃ ablation on normal tissue functioning were established by comparing the testicular morphology of MC₃^{-/-} to WT mice at different ages.

3.2 *Materials and Methods*

3.2.1 Comparison of pituitary hormone content in WT and MC₃^{-/-} mice

3.2.1.1 Animals

Animals and the collection of tissues were described in Chapter 2, section 2.2.1.

3.2.1.2 Radioimmunoassays (RIAs) for pituitary hormones (performed at the National Institute for Medical Research [NIMR])

Pituitaries from WT and MC₃^{-/-} male and female mice were thawed and homogenised on ice in 1 ml cold PBS (pH 7.4; 50 mM sodium dihydrogen orthophosphate dihydrate, 100 mM sodium chloride, 0.6 mM thimerosal [antiseptic/antifungal] [all from Sigma-Aldrich, UK]). The pituitary content of adrenocorticotrophic hormone (ACTH), thyroid stimulating hormone (TSH), luteinizing hormone (LH), follicle stimulating hormone (FSH), prolactin and growth hormone (GH) were measured by relevant RIA. Antibodies and hormone standards were kindly provided by Professor Parlow and the National Hormone and Pituitary Program (NHPP, Torrance, California). All hormones were iodinated at the NIMR. Each sample was initially diluted to the hormone concentrations detectable by the assay as presented in Table 3.1 and then further serially diluted 2-, 4- and 8- fold in PBS/BSA solution (3 mg/ml PBS, 0.3 % w/v BSA [Sigma-Aldrich, UK]) or in ACTH buffer (2 % v/v aprotinin [Sigma-Aldrich, UK], 0.1 % v/v Triton X-100 [Sigma-Aldrich, UK], 0.1 % w/v BSA, 0.1 % v/v β-mercaptoethanol [Sigma-Aldrich, UK], in PBS pH 7.4). Standards were prepared by serial dilution of known concentrations of each hormone in PBS/BSA solution and ranged from 0.01 ng/100 µl – 10.00 ng/100 µl. All components of the standard curve were prepared in triplicate including total counts (TC), non-specific binding (NSB) and total binding (B₀), whilst samples were prepared in duplicate. Each tube contained 100 µl of PBS/BSA buffer and 100 µl of either standard or sample, except for NSB which contained 200 µl of PBS/BSA buffer, B₀ with 100 µl of PBS/BSA buffer and TC which only contained 100 µl of tracer (hormone of interest labelled with I¹²⁵ [Perkin Elmer, UK]). Antibody (100 µl) (the antibody dilution used for each of the hormones are

provided in Table 3.2) was then added to all assay tubes (except TC). Each tube was vortexed and then 100 µl of appropriate tracer (approximately 10,000 cpm) were added. All tubes were incubated for 18-24 h at room temperature. PEG solution (600 µl) (18 % PEG prepared by mixing: 10 % Triton v/v, 0.15 % w/v bovine gamma globulin [Sigma-Aldrich, UK], 30 % w/v Tris base [Fisher Scientific, UK], 66.7 % of 27 % polyethylene glycol 6000 [Fisher Scientific, UK]) was added to all tubes (except TC) to precipitate the primary antibody-protein complexes, and incubated for 30 min at room temperature. All tubes (except TC) were then spun for 12 min at 3,000 rpm at 4 °C in a large capacity centrifuge. The supernatants were aspirated and the radioactivity of the pellet measured using a gamma counter (Wallac Wizard 1277, PerkinElmer Inc, USA). Standard curves were plotted using in-house software incorporated into the gamma counter. A summary of the RIA protocols for each of the pituitary hormones can be found in Table 3.3.

hormone analysed	initial sample dilution
ACTH	male & female 1:50
TSH	male & female 1:50
LH	male & female 1:50
FSH	male -1:20; female-1:5
prolactin	male & female 1:500
GH	male & female 1:5000

Table 3.1 Sample preparation for pituitary hormones RIAs. Initial dilutions in 100 µl that each sample was prepared as for assaying of each of different pituitary hormones.

antibody	concentrations used
Anti-ACTH	1:300
Anti-TSH	1:100
Anti-LH	1:100
Anti-FSH	1:100
Anti-prolactin	1:100
Anti-GH	1:100

Table 3.2 Initial antibody concentrations used in each of the pituitary hormones RIAs (all antibodies provided by Professor Parlow, NHPP).

tube	volume of standard/sample (μl)	PBS/BSA buffer (μl)	antibody (μl)		tracer (antigen tagged with I ¹²⁵) (μl)		PEG solution (μl)				
T _c				vortex	100	incubate at room temperature for 18-24 hours		incubate for 30 mins at room temperature; centrifuge for 12 minutes at 3 000 rpm at 4°C	aspirate and count		
NSB		200			↓		600			↓	
B ₀		100	100								↓
standards (0.01 - 10.0 ng/100 μl)	100	↓	↓								
unknowns	↓										

Table 3.3 Summary of pituitary hormones RIA protocol. TC total count, NSB- non-specific binding, B₀- total binding.

3.2.2 Histological comparisons of testes from WT and MC₃^{-/-} mice.

Tissue collection, tissue processing, tissue sectioning and slide preparation were described in section 2.2.3.2.1.

3.2.2.1 Haematoxylin and Eosin (H&E) staining

Selected sections were first cleared of wax by placing slides twice for 5 min in 100 % xylene followed by rehydration through decreasing concentrations of ethanol, starting at 100 % ethanol twice for 5 min, then 95 %, 90 %, 70 %, 50 %, and 35 % once for 5 min each. Slides were then washed twice in PBS each for 3 min and stained with Gill's haematoxylin (H-3401, Vector Laboratories, UK) for 5 min. After rinsing with running tap water (until the run-off was colourless), the slides were incubated in acid rinse solution (2 % v/v acetic acid) for 1 min, rinsed with tap water and then placed in bluing solution (1.5 % ammonium hydroxide [35614, Alfa-Aesar, UK] in 70 % ethanol) for 1 min, followed by another rinse. The slides were then stained with eosin (1 % w/v eosin in dH₂O) for 5 min and after rinsing with tap water, dehydrated with increasing concentrations of ethanol (30 %, 50 %, 70 %, 90 %, 95 %, 100 % x 2: 5 min for each concentration). Finally the slides were immersed in 100 % xylene for 5 min twice before mounting each section using DPX mounting media (HX945813, Merck, UK) with glass coverslips (631-1574, VWR, UK).

3.2.2.2 Staining Visualisation

As described in Chapter 2, section 2.2.3.2.4

3.2.2.3 Histological comparisons

Histological comparisons were made between MC₃^{-/-} and WT mice at four different ages: 3-4 weeks, 9-10 weeks, 16-17 weeks and 23-24 weeks. There were three animals per genotype (MC₃^{-/-} or WT) in each age group, and for each animal, four sections, approximately every 100 µm apart, were selected for imaging. For each section imaged, four separate frames, at distant areas within the section, were acquired.

3.2.2.4 ImageJ analyses

Acquired images were analysed using ImageJ software (ImageJ 1.47; NIH, USA). Selected quantitative measurements included: diameter and thickness of the seminiferous tubules, area of intertubular tissue and tubules as well as the total area occupied by the tissue. Tubules that appeared rounded and thus were cut at an approximately 90° angle to the length of the tubule were selected for making diameter measurements. However, if only oblique tubules were encountered in a frame, then the short axis of the tubular profile was measured. The areas of testicular structures were calculated based on the measurement for whole tubules and whole intertubular islets. Measurements obtained for a part of the structures (a part of a tubule visible on the microscopic image) were used to estimate the total area occupied by the tissue. Germinal layer (tubule) thickness was estimated by taking two measurements of the distance between basement membrane and lumen border.

For quantification verification, some of the images were remeasured by independent observers. Detailed step-by-step instructions for measurements using ImageJ can be found in Appendix 1.

3.2.2.5 Quality Controls

In order to estimate the variability in measurements between the operators the coefficient of variations (CV) for each parameter were determined. For each of the parameters the CV between operators was lower than 5 % except for the mean of tubule thickness (MC₃^{-/-}: 10.669% and WT: 9.572%) and the area of intertubular tissues (WT: 7.362% ; Table 3.4).

	animal type	mean of diameters (µm)	mean of tubule thickness (µm)	area of intertubular tissues (µm ²)	area of tubules (µm ²)
CV (%)	MC ₃ ^{-/-}	1.406	10.669	3.873	1.657
	WT	0.402	9.572	7.362	2.390

Table 3.4 Coefficients of variations (CVs) calculated to determine the variability between operators' measurements for each parameter.

3.2.3 Statistics

Comparisons between two groups were performed using unpaired Student's *t*-test (two-tailed) (Excel, Microsoft Office 2010). Statistical differences between all age groups were calculated using one-way ANOVA procedures followed by Tukey *post-hoc* tests (SPSS 18, IBM). For all statistical analyses P value is given. Data are expressed as mean ± SEM.

3.3 Results

3.3.1 The effects of MC₃ gene ablation on total pituitary hormone content

Pituitaries from WT and MC₃^{-/-} mice were homogenised and their hormone content measured by RIAs. Total pituitary content of ACTH and TSH measured by RIA were similar in the two male genotypes. However, there were reductions in the amounts of LH (WT: 1062 ± 109 ng vs. MC₃^{-/-}: 427 ± 42 ng), FSH (WT: 554 ± 21 ng vs. MC₃^{-/-}: 346 ± 13 ng), prolactin (WT: 2.12 ± 0.22 µg vs. MC₃^{-/-}: 1.30 ± 0.13 µg) and GH (WT: 64 ± 6 µg vs. MC₃^{-/-}: 35 ± 6 µg) in MC₃^{-/-} compared to WT male mice (*t*-test, *p*<0.05) (Figure 3.1). In female mice, the total pituitary contents of ACTH, TSH, LH, FSH and prolactin were unaffected by MC₃ genotype, however there was approximately 40 % decrease in the amount of GH (WT: 61 ± 8 µg vs. MC₃^{-/-}: 37 ± 5 µg) in MC₃^{-/-} compared to WT female mice (*t*-test, *p*<0.05) (Figure 3.2).

Male

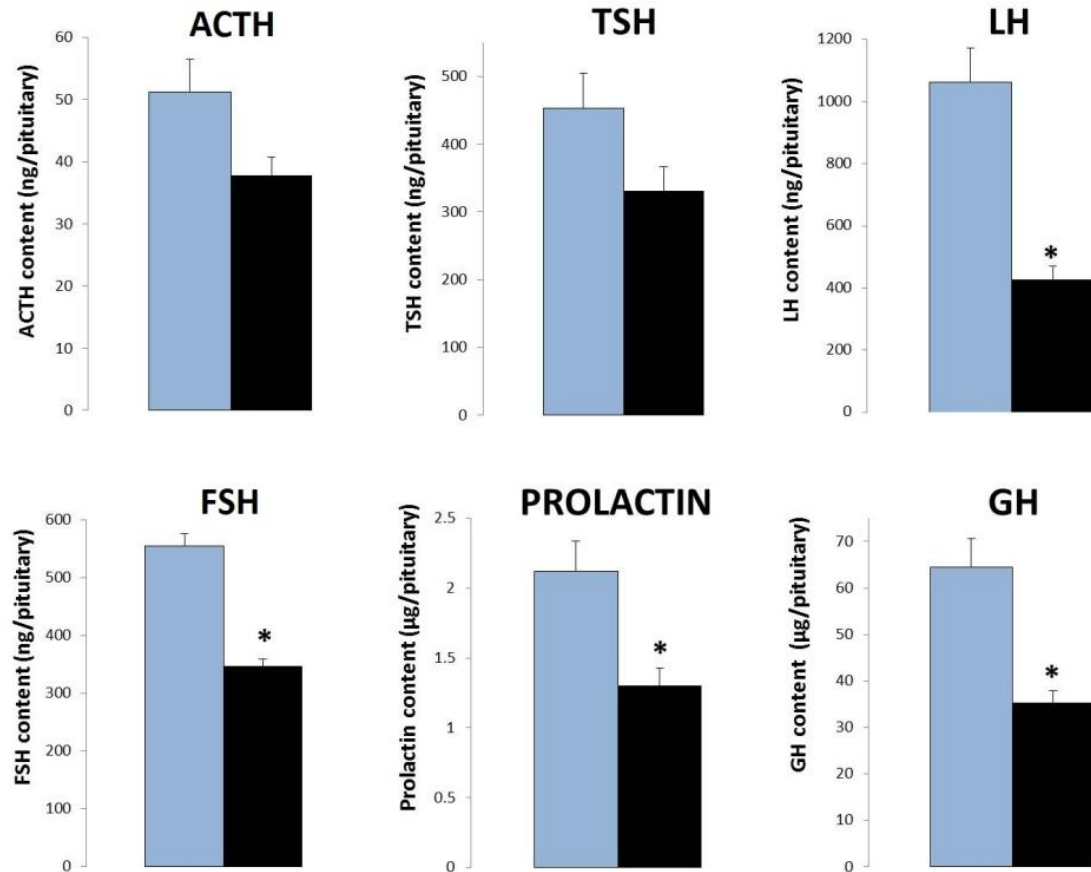


Figure 3.1 Total pituitary hormone content in wild type (blue bars) and MC₃ null (black bars) male mice. Pituitaries of sexually mature (14-16 weeks) wild type (WT; C57BL/6, n=5) and MC₃^{-/-} (n=6) male mice were removed, frozen, thawed and homogenised on ice in 1 ml cold PBS. Pituitary content of adrenocorticotrophic hormone (ACTH), thyroid-stimulating hormone (TSH), luteinizing hormone (LH), follicle stimulating hormone (FSH), prolactin and growth hormone (GH) were measured by relevant RIA. Data shown are expressed per pituitary, mean ± SEM. * p<0.05 vs. WT (*t*-test). Note the differences in scales between the hormones.

Female

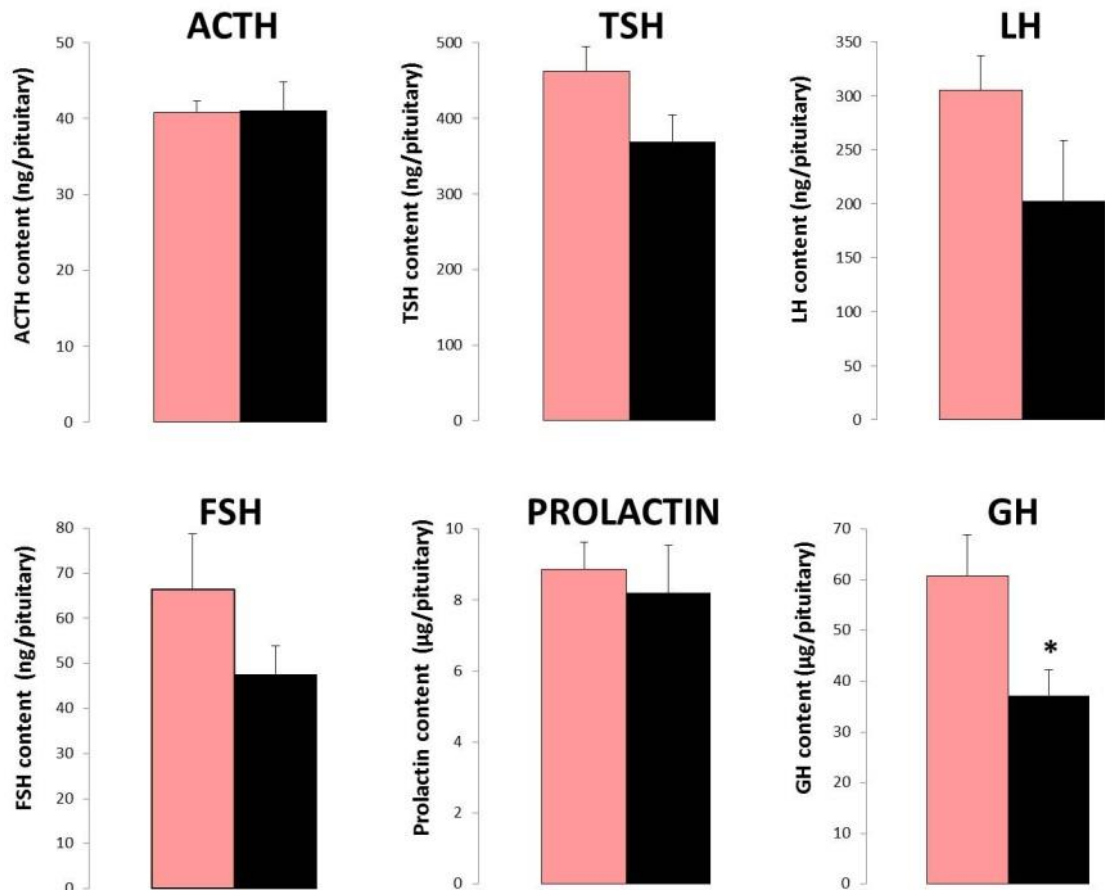


Figure 3.2 Total pituitary hormone content in wild type (pink bars) and MC₃ null (black bars) female mice. Pituitaries of sexually mature (14-16 weeks) wild type (WT; C57BL/6, n=6) and MC₃^{-/-} (n=5) female mice were removed, frozen, thawed and homogenised on ice in 1 ml cold PBS. Pituitary content of adrenocorticotrophic hormone (ACTH), thyroid-stimulating hormone (TSH), luteinizing hormone (LH), follicle stimulating hormone (FSH), prolactin and growth hormone (GH) were measured by relevant RIA. Data shown are expressed per pituitary, mean ± SEM. * p<0.05 vs. WT (*t*-test). Note the differences in scales between the hormones.

3.3.2 The effects of MC₃ gene ablation on testicular histology.

There were no gross abnormalities in the testes analysed but occasionally some histological abnormalities occurred in WT and MC₃^{-/-} mice (Figure 3.4). There were age-dependent changes in the average areas of the interstitial tissues and the seminiferous tubules in both genotypes (Figure 3.3).

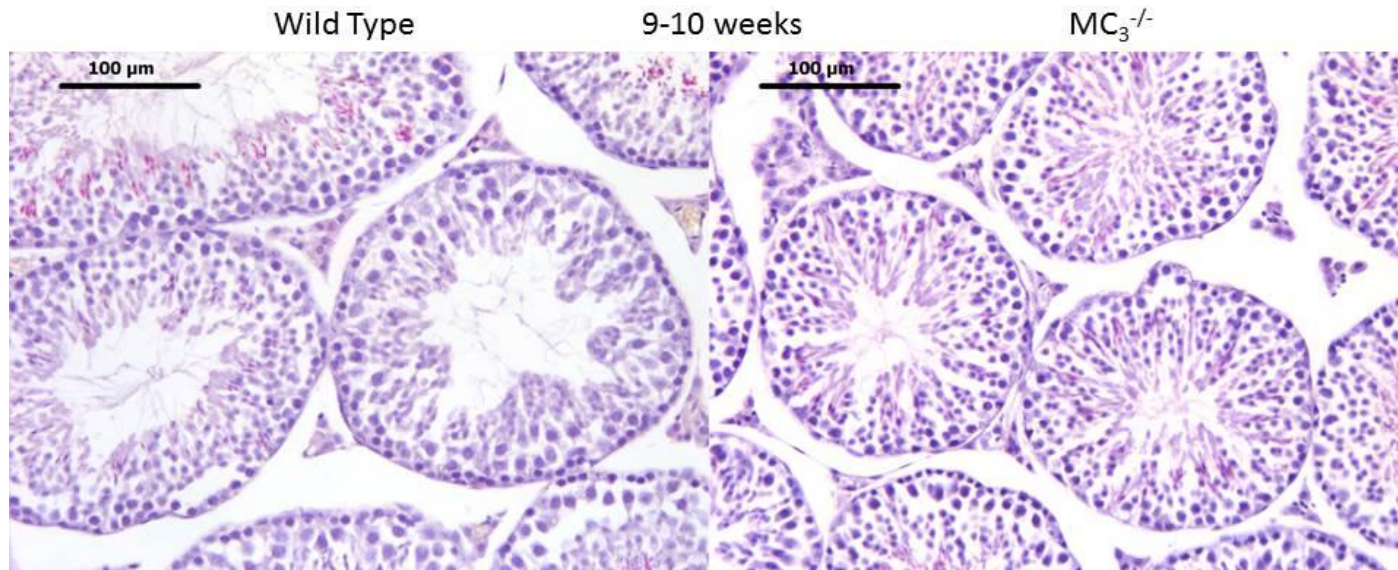
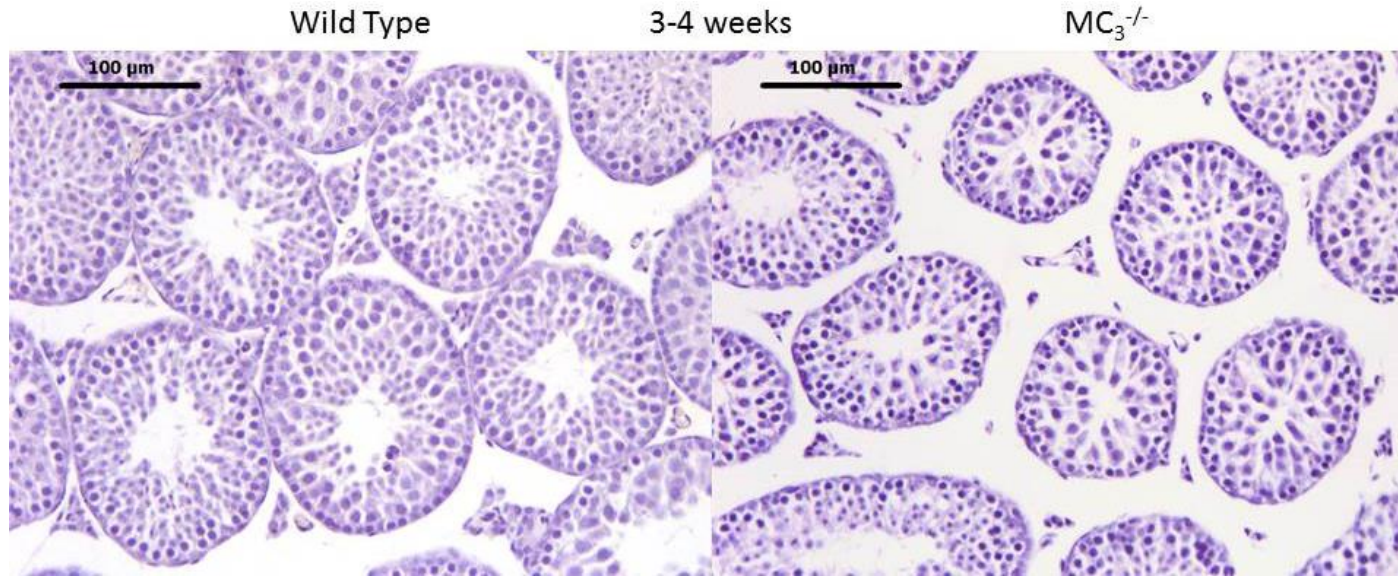
The total area occupied by testicular tissue is regarded as the total intracapsular area occupied by interstitial tissue and seminiferous tubules (Figure 3.5), this includes the areas of all seminiferous tubules and interstitial islets, either whole or only a part of them visible on the image. A greater percentage of the total tissue indicates less intertubular space (Table 3.5). The tubules occupied approximately 70-80 % of the total area whilst interstitial tissue comprised only 2-4 % of the total area. The total area (%) occupied by the tissue markedly increased following puberty between 3-4 and 9-10 weeks in both genotypes ($p < 0.05$; ANOVA, Tukey). There were no significant differences between the total tissue areas in MC₃^{-/-} and WT mice but testicular tissue occupied approximately 7-12 % less of the total area in MC₃^{-/-} mice at 3-4, 9-10 and 16-17 weeks (Figure 3.5).

The average area of interstitial islets was low at 3-4 weeks, peaked at 9-10 weeks and decreased by approximately 50 % at 16-17 weeks in both genotypes (Figure 3.6). The interstitial tissue area remained constant thereafter, until the animals reached 23-24 weeks of age. There were no significant differences between the areas of the interstitial islets in the two animal types, except in the youngest group examined (Figure 3.6). The mean area of interstitial tissues was markedly reduced in MC₃^{-/-} compared to WT mice at 3-4 weeks (t -test, $p = 0.02$; Figure 3.6).

The average diameters of the tubules increased significantly in all animals from weeks 3-4 to 9-10 ($p < 0.001$; ANOVA, Tukey) corresponding to the development of reproductive maturity at week 5 (Figure 3.7). The mean diameters of the seminiferous tubules in $MC_3^{-/-}$ mice were smaller than WT mice at 3-4 weeks ($p = 0.004$; ANOVA, Tukey) and, although not statistically significant, were also smaller at both 9-10 and 23-24 weeks (9-10 weeks: $p = 0.16$ and 23-24 weeks: $p = 0.14$; ANOVA, Tukey; Figure 3.7).

As expected, the data for the average areas of the seminiferous tubules are comparable to that of tubular diameter. There was a marked increase in the average area of tubules following puberty ($p < 0.05$; ANOVA, Tukey; Figure 3.8). There was a reduction of approximately 19-35 % in the tubule area in $MC_3^{-/-}$ mice compared to WT at 3-4, 9-10 and 23-24 weeks, with the former age group being statistically significant ($p = 0.01$; ANOVA, Tukey). In contrast, at weeks 16-17 the tubular area was markedly greater in $MC_3^{-/-}$ mice ($p = 0.002$; ANOVA, Tukey; Figure 3.8).

Similar to other tubular parameters measured, the thickness of the seminiferous tubules was markedly higher in all age groups examined compared to animals at 3-4 weeks. There were significant reductions in the thickness of tubules in $MC_3^{-/-}$ compared to WT mice at 9-10 and 23-24 weeks of age (9-10 weeks: $p = 0.02$; 23-24 weeks: $p = 0.04$; ANOVA, Tukey; Figure 3.9). Conversely, at 16-17 weeks of age the WT animals had significantly smaller tubular thicknesses ($p = 0.00091$; ANOVA, Tukey; Figure 3.9) than $MC_3^{-/-}$ mice.



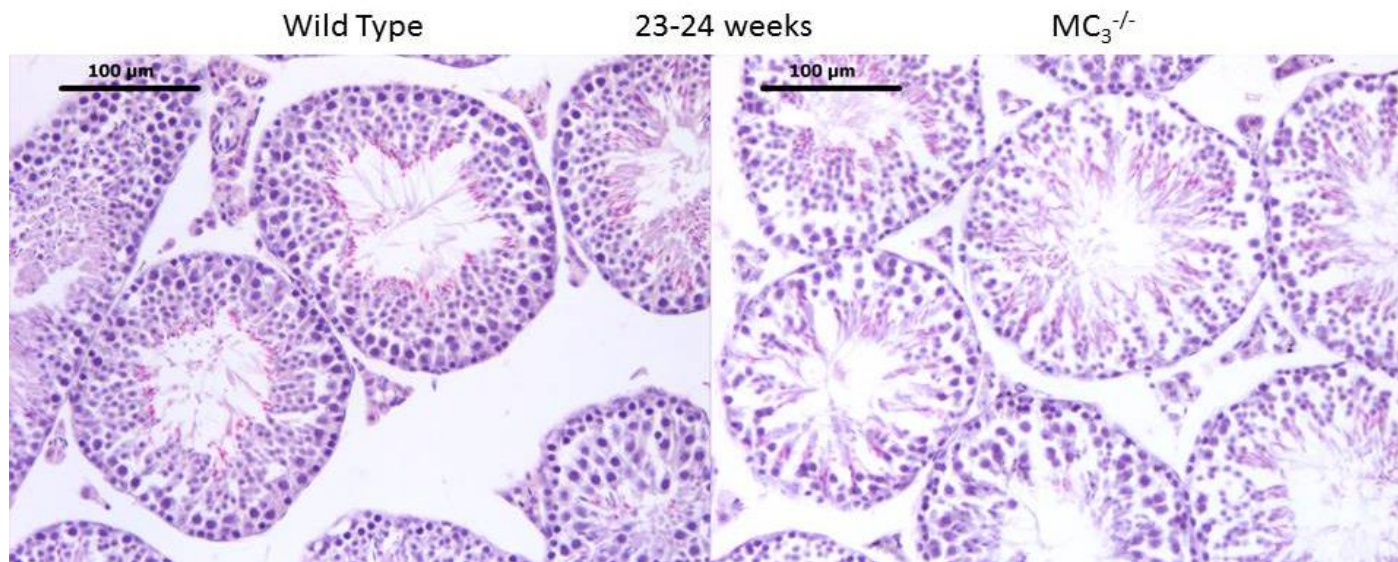
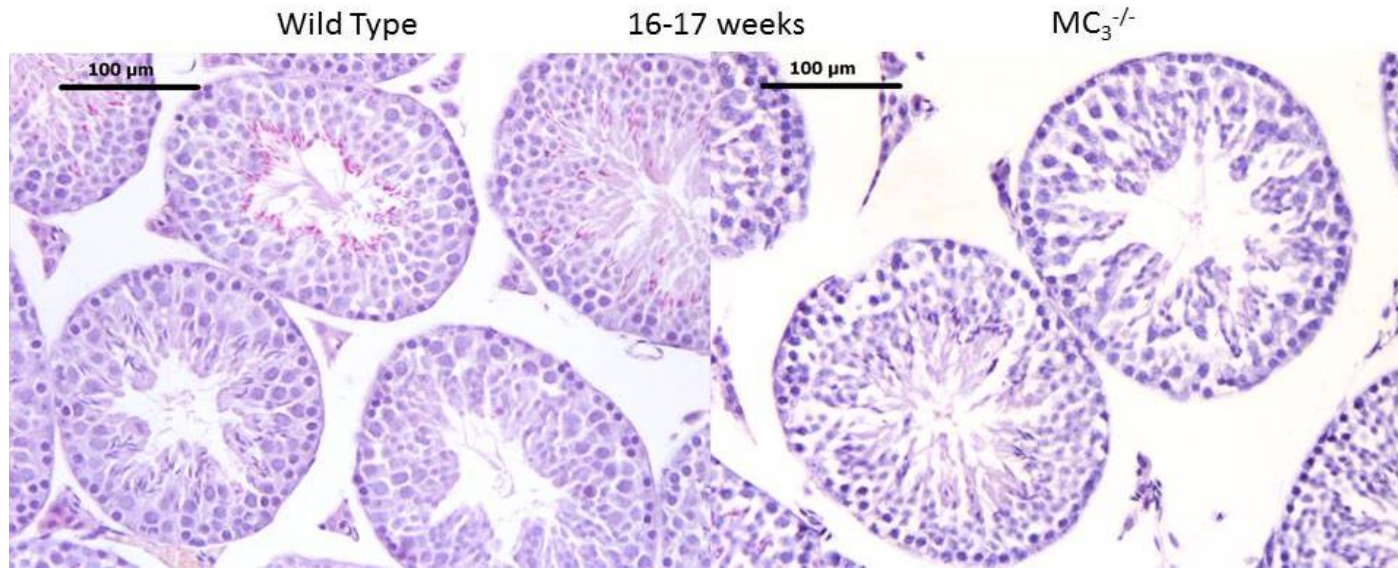


Figure 3.3 Microscopic images of testes from Wild Type (WT) and MC₃ null mice (MC₃^{-/-}) at different ages. Testes from WT (left) and MC₃^{-/-} (right) were divided into four age groups (3-4 weeks of age; 9-10 weeks of age, 16-17 weeks of age and 23-24 weeks of age) as indicated at the top of each panel. Selected sections were stained with H&E. Representative images from each group (32-36 images per group). Scale bar is present in the top right corner of each image.

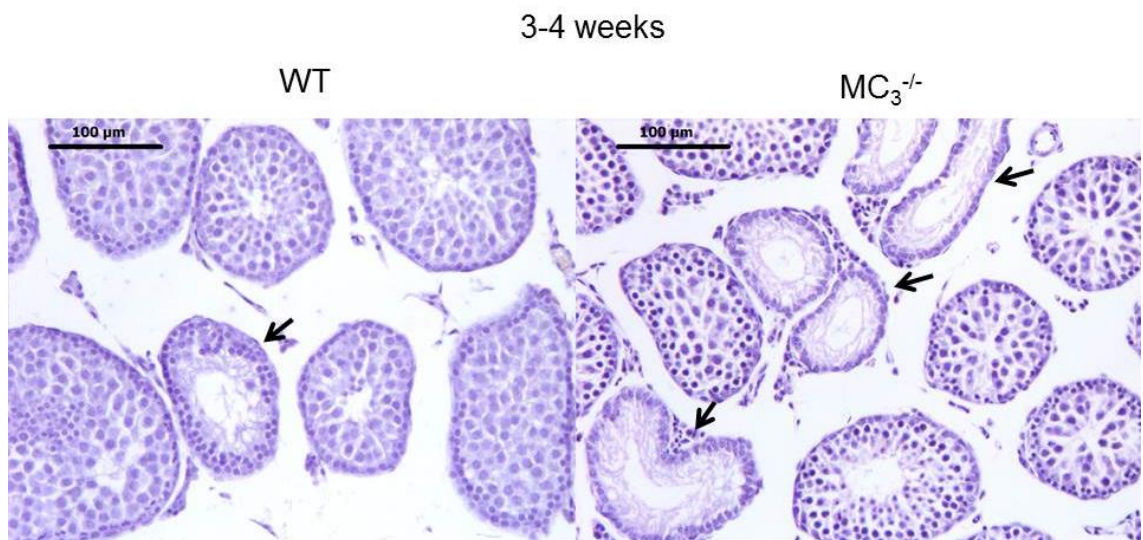


Figure 3.4 Examples of seminiferous tubules depleted of germ cells (arrow) in both WT (left) and MC₃^{-/-} (right) mice at 3-4 weeks of age.

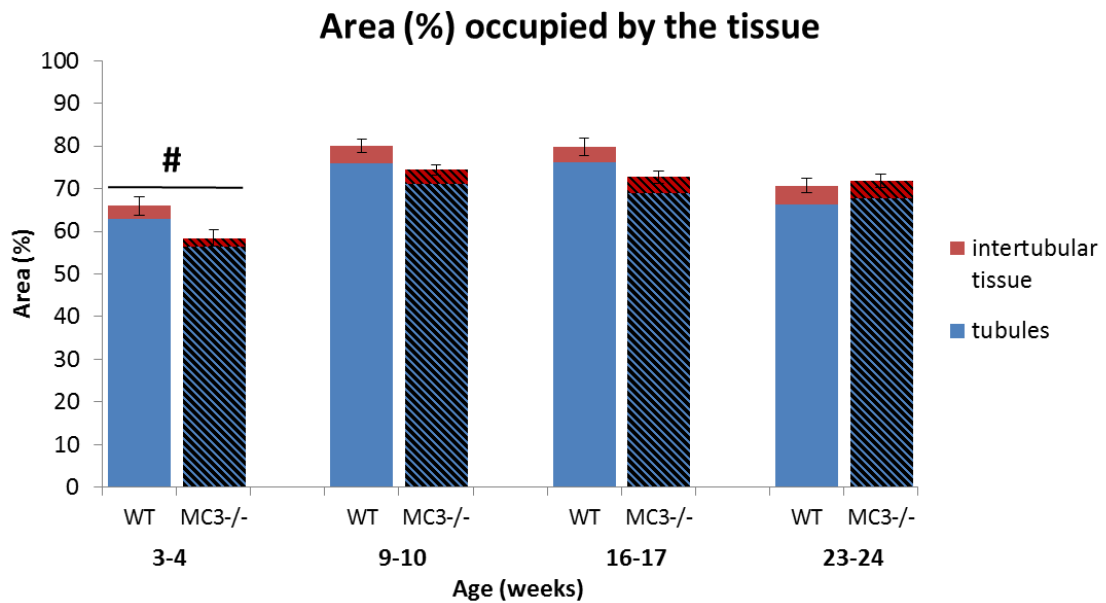


Figure 3.5 Area (%) occupied by the tissue. Testes from WT and MC₃^{-/-} mice were removed at different age (3-4 weeks of age; 9-10 weeks of age, 16-17 weeks of age and 23-24 weeks of age), fixed (4 % PFA), embedded and stained with H&E. Microscopic images were analysed using ImageJ. The total area (%) occupied by the tissue is presented for WT (non-pattern filled bars) and MC₃^{-/-} (pattern filled bars). It was subdivided into area occupied by the intertubular tissue (top, red part of the bar) and area of tubules (bottom, blue bars). Data shown are expressed as mean ± SEM of three animals (mean of 12 images per animal). #p<0.05 vs. other age groups (ANOVA, Tukey).

Age (weeks)	Animal Type	Intertubular space (%) (mean \pm SEM)
3-4	WT	34.00 \pm 2.11
	MC ₃ ^{-/-}	41.59 \pm 1.85
9-10	WT	20.03 \pm 1.58
	MC ₃ ^{-/-}	25.64 \pm 1.30
16-17	WT	20.16 \pm 2.05
	MC ₃ ^{-/-}	27.28 \pm 1.51
23-24	WT	29.33 \pm 1.71
	MC ₃ ^{-/-}	25.98 \pm 1.65

Table 3.5 Intertubular space (%) in testes from WT and MC₃^{-/-} mice at different ages. Data were calculated based on the area (%) occupied by the tissue and are presented as mean \pm SEM of three animals (mean of 12 images per animal). There were no significant differences in the intertubular space (%) between the MC₃^{-/-} and WT mice (*t*-test).

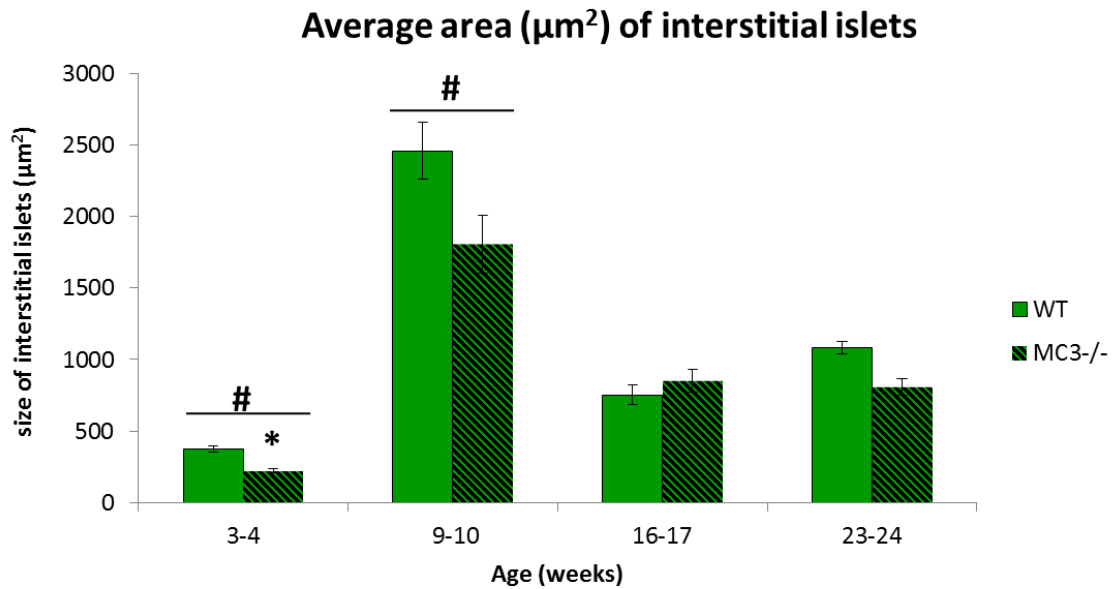


Figure 3.6 Average area (μm^2) of interstitial islets. Testes from WT and MC₃^{-/-} mice were removed at different age (3-4 weeks of age; 9-10 weeks of age, 16-17 weeks of age and 23-24 weeks of age), fixed (4 % PFA), embedded and stained with H&E. Microscopic images were analysed using ImageJ. The average size (μm^2) of interstitial islets is presented for WT (non-pattern filled bars) and MC₃^{-/-} (pattern filled bars). Data shown are expressed as mean \pm SEM of three animals (mean of 12 images per animal). * $p < 0.05$ MC₃^{-/-} vs. WT (t -test); # $p < 0.05$ vs. other age groups (ANOVA, Tukey).

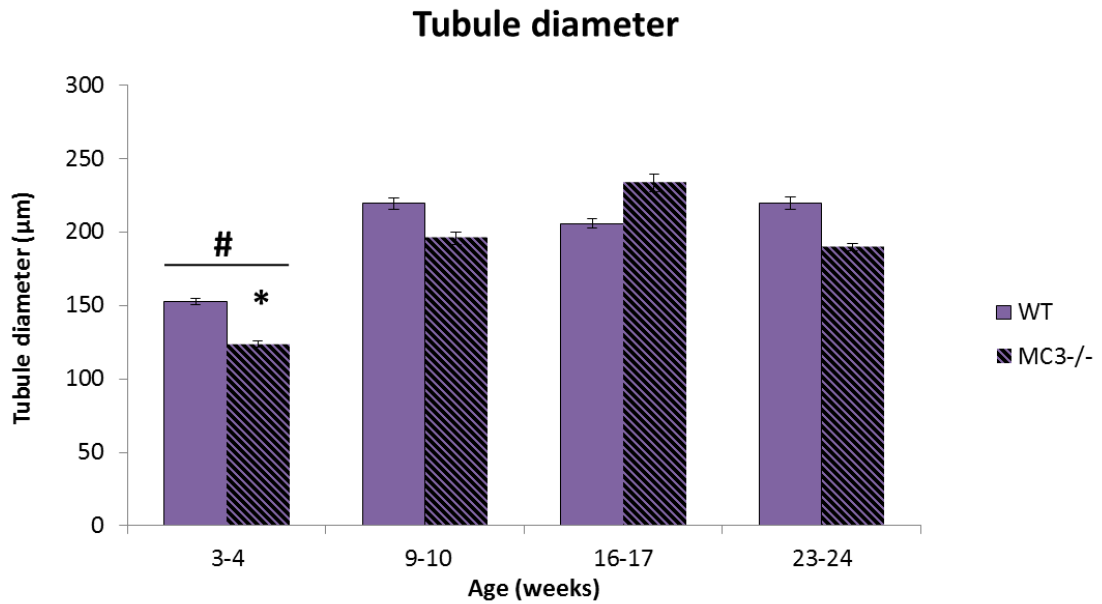


Figure 3.7 Tubule diameter (µm). Testes from WT and MC₃^{-/-} mice were removed at different age (3-4 weeks of age; 9-10 weeks of age, 16-17 weeks of age and 23-24 weeks of age), fixed (4 % PFA), embedded and stained with H&E. Microscopic images were analysed using ImageJ. The tubule diameter (µm) is presented for WT (non-pattern filled bars) and MC₃^{-/-} (pattern filled bars). Data shown are expressed as mean ± SEM of three animals (mean of 12 images per animal). *p<0.05 MC₃^{-/-} vs. WT (*t*-test); #p<0.05 vs. other age groups (ANOVA, Tukey).

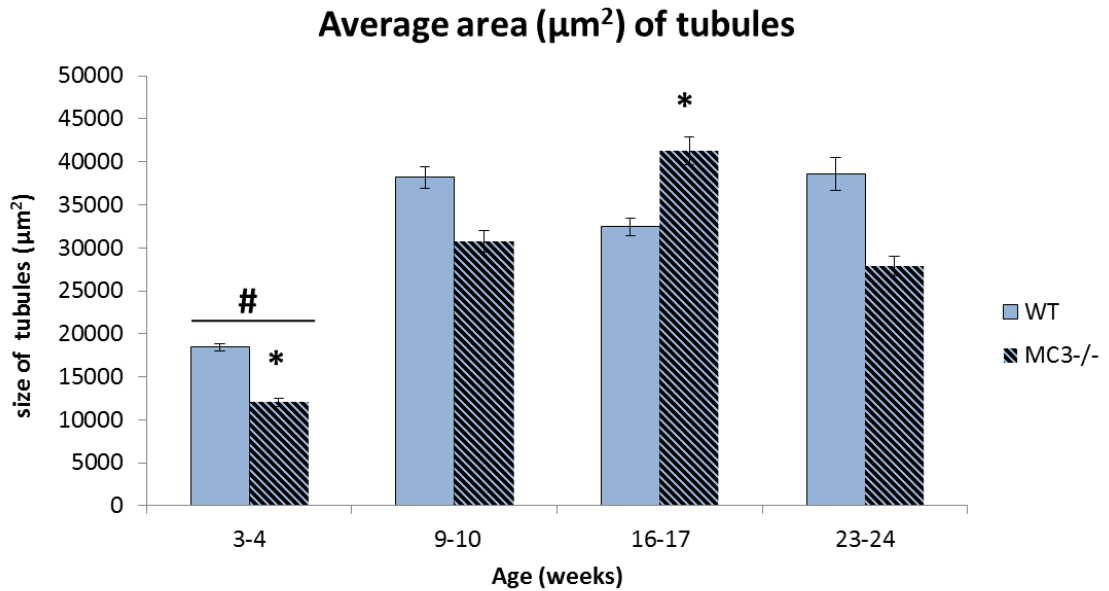


Figure 3.8 Average area (μm^2) of tubules. Testes from WT and MC₃^{-/-} mice were removed at different age (3-4 weeks of age; 9-10 weeks of age, 16-17 weeks of age and 23-24 weeks of age), fixed (4 % PFA), embedded and stained with H&E. Microscopic images were analysed using ImageJ. The average size (μm^2) of tubules is presented for WT (non-pattern filled bars) and MC₃^{-/-} (pattern filled bars). Data shown are expressed as mean \pm SEM of three animals (mean of 12 images per animal). * $p < 0.05$ vs. WT (t -test); # $p < 0.05$ vs. other age groups (ANOVA, Tukey).

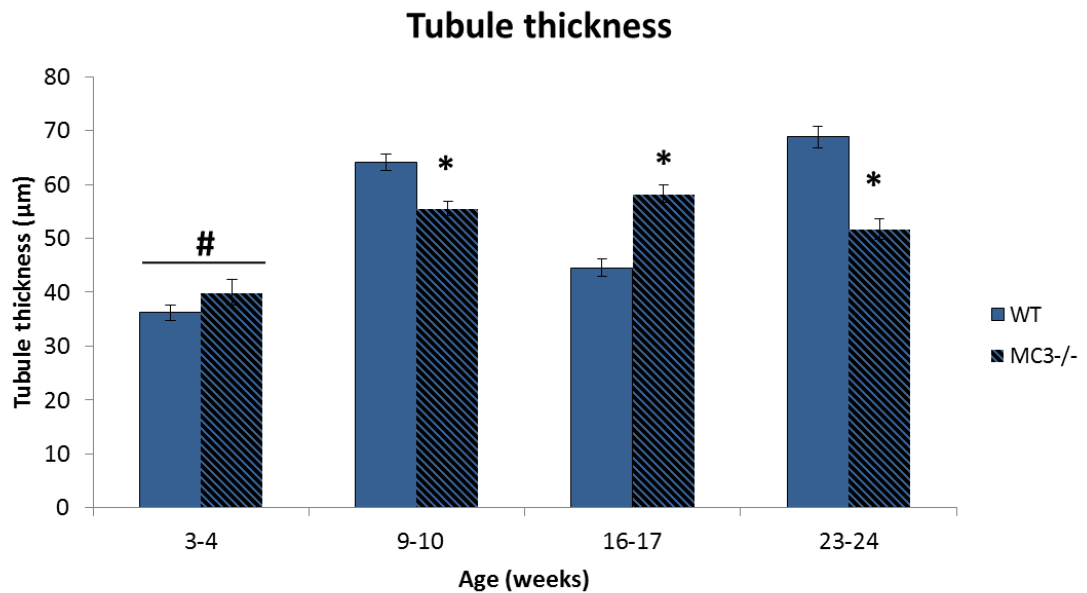


Figure 3.9 Tubule thickness (µm). Testes from WT and MC₃^{-/-} mice were removed at different age (3-4 weeks of age; 9-10 weeks of age, 16-17 weeks of age and 23-24 weeks of age), fixed (4 % PFA), embedded and stained with H&E. Microscopic images were analysed using ImageJ. The thickness (µm) of tubules is presented for WT (non-pattern filled bars) and MC₃^{-/-} (pattern filled bars). Data shown are expressed as mean ± SEM of three animals (mean of 12 images per animal). *p<0.05 MC₃^{-/-} vs. WT (*t*-test); #p<0.05 vs. other age groups (ANOVA, Tukey).

3.4 Discussion

Ablation of MC₃ led to a reduction in the content of a number of pituitary hormones, which are directly and/or indirectly implicated in the control of the reproductive system, including gonadal function. Testes from MC₃^{-/-} mice were different from that of WT with regard to a number of morphometric parameters at different ages, hence implying possible translation into functional abnormalities.

The total pituitary content of each of the anterior pituitary hormones in MC₃^{-/-} mice were determined and compared to those measured in WT animals. Overall, the absence of MC₃ had more profound effects on the total anterior pituitary hormone content of male mice (Figure 3.1 and 3.2). There was a significant reduction in GH content in both male and female MC₃^{-/-} mice. However, this content could still result in sufficient GH in the circulation to enable normal bone development and hence animal growth (McGuinness *et al.*, 2003). Phenotypically, however, MC₃^{-/-} mice have shorter body lengths compared to WT (Chen *et al.*, 2000) and this may possibly be due to a reduction in the growth plate proliferation: an effect mediated by γ_2 -MSH on MC₃-expressing chondrocytes and chondrocyte precursors (Yeh *et al.*, 2006). It is also possible that altered release of GH, either the amount or pattern, could result in reduced growth plate proliferation (Westwood *et al.*, 2010) but in the absence of a system for frequent sampling of blood for GH measurement this could not be determined. The pituitary content of ACTH and TSH in both male and female MC₃^{-/-} mice remained largely unaltered compared to WT. These data are partially supported by normal plasma concentrations of corticosterone and thyroxine (T₄) in MC₃^{-/-} male and female mice (Butler *et al.*, 2000). A

marked decrease for the two pituitary gonadotropins, LH and FSH, was seen in $MC_3^{-/-}$ of both genders but only the reduction in $MC_3^{-/-}$ male mice was significant. Female mice were sampled with no knowledge of the stage of the oestrous cycle, which accounts for the greater variability of LH, FSH and prolactin pituitary contents compared to the males. The concentrations of the three pituitary hormones are known to vary with the time of the day, the stage or any alteration of the oestrous cycle, as well as the age of the female mice (Parkening *et al.*, 1982). Additionally, in order to determine the exact effect of the MC_3 deletion on the anterior pituitary, the circadian pattern of release of the other pituitary hormones should also be measured. Overall, total content of the pituitary hormones in WT mice was comparable to that reported in the literature (McGuinness *et al.*, 2003; Waite *et al.*, 2010). The exact role of MC_3 signalling in the pituitary is not understood, but clearly, its absence in this gland or other tissues leads to a marked reduction in pituitary hormone contents, which can directly or indirectly impair functioning of the gonads. It can be hypothesized that lack of pituitary MC_3 can be compensated by activation of the other three melanocortin receptors namely MC_1 , MC_4 and MC_5 by pituitary α -MSH and γ -MSH. However, the qRT-PCR results described in Chapter 2 (Figure 2.20) showed a reduction of all MC, except for MC_1 , in pituitary of $MC_3^{-/-}$ mice compared to WT. This could indicate a type of co-dependency in melanocortin receptor expressions.

The significant reductions in the pituitary hormone contents in male $MC_3^{-/-}$ mice, particularly in the gonadotropins can indirectly affect testicular function. Therefore, the second aim was to determine the direct or indirect effects of MC_3 ablation on male gonads and ascertain whether they are age dependent. The possible functions of melanocortin receptors in the testis are described in detail

in Chapter 4. Classic methodologies for assessment of reproductive functions in mice apart from investigation of biochemical markers, also include evaluation of testicular histology and use of natural mating for fertility tests (Amann, 1986; Chubb, 1987). The histological analyses of testes applied in this study, have been routinely used in many laboratories worldwide to determine the reproductive state of an animal. There are many qualitative and quantitative histological measurements described in the literature, some provide an inexpensive but time-consuming way of assessing testicular functions. The quantitative measurements provide much stronger evidence of testicular abnormalities than the qualitative methods (Russell *et al.*, 1990). Five parameters were chosen in this study (diameter and thickness of the seminiferous tubules, area of intertubular tissues and tubules as well as total area occupied by the tissue) to compare the histology of testes from MC₃^{-/-} to WT mice and thus indirectly assess their reproductive abilities. Due to a paracrine interrelationship between the seminiferous tubules and interstitial tissue, selected parameters reflect the possible changes in both structures of the testis.

The major parameter measured in the study was the area (%) occupied by the tissue. This included the number and area of the seminiferous tubules and interstitial islets (Figure 3.5). The percentages of tubules and interstitial islets were comparable to previously published data on mice and equal to 70-80 % and 2-4 %, respectively (Hess and deFranca, 2001). The area (%) occupied by the tissue was significantly lower in the youngest animals analysed compared to all other age groups (Figure 3.5). The size of tubules and interstitial islets increased following achievement of reproductive maturity at week 5 and remained constant thereafter. There was no significant difference in the areas

(%) occupied by the tissues in $MC_3^{-/-}$ compared to WT but a marginal decrease of approximately 7 % was measured at 3-4 weeks. An increase in the percentage of interstitial space at this age (Table 3.5) could, in some cases, indicate a rise in the volume of interstitial fluid, which may exhibit infiltration of leukocytes (Kerr and Sharpe, 1989). The changes in the volume of the interstitial fluid could also be related to the fixation method, however tissues from both genotypes were prepared using the same protocol.

The average area of the intertubular islets was also compared. The interstitial tissue is mostly composed of Leydig cells but macrophages are commonly present. In rodents, Leydig cells are usually located in the central portion of the intertubular tissue, in close proximity to lymph nodes but at considerable distance to blood vessels (Setchell and Breed, 2006). All of these structures were included to determine the average area of the interstitial islets, if present within the islet boundary. Tissues from both animal types, $MC_3^{-/-}$ and WT, followed the same process of fixation and embedding to reduce the possibility of technical errors as both factors can influence the protein content of the intertubular islets and hence their size. In detail qualitative examination of the interstitial tissue, such as determination of size and appearance of individual Leydig cells or infiltration of leukocytes, has not been performed. The size of intertubular islets was approximately seven times greater at 9-10 weeks ($2,140 \pm 409 \mu\text{m}^2$) compared to the youngest age group ($299 \pm 107 \mu\text{m}^2$; Figure 3.6). A gradual increase in the volume of testicular interstitial tissue until day 90 in rodents was reported by Ariyaratne and colleagues (2000). The changes in the sizes of the interstitial islets at different age correspond with the genetic and hormonal profile of Leydig cells during their maturation. The onset of testosterone biosynthetic capacity in mice testes occurs at 3 weeks, the

maximal testosterone production appears at 7 weeks, followed by a gradual decline during the transition of immature Leydig cells into adult population (Wu *et al.*, 2010). The steroid producing capacity of newly formed adult Leydig cells is low from week 8 to 12 but their number is significantly higher (Ariyaratne *et al.*, 2000), this may explain the peak in the intertubular islet area at 9-10 weeks described herein (Figure 3.6). The increase in the area of interstitial tissues at 9-10 weeks of age was followed by reductions of approximately 60 % at 16-17 weeks and 50 % at 23-24 weeks in both genotypes (Figure 3.6). The decrease could be related to the acquisition of a full steroidogenic capacity by adult Leydig cells. Data from a study on 30 men aged between 20 and 76 years demonstrated a gradual decrease in the population of interstitial cells with increasing age (Neaves *et al.*, 1985). Although the aging process in humans is different from that in the mouse the decrease in the areas of the interstitial islets was noted in both species. The exact mechanism governing the loss of Leydig cells is unclear but phagocytosis by residual macrophages provides a possible explanation (Neaves *et al.*, 1985). In general, the mean area of the interstitial islets in $MC_3^{-/-}$ was comparable to that of WT, except in the younger groups. There were approximately 40 % and 20 % reductions in the areas of interstitial tissues at 3-4 and 9-10 weeks, respectively, compared to age matched controls.

Tubule diameter was regarded as being more accurate than the testis weight to indicate varying levels of spermatogenic abnormalities (Russel *et al.*, 1990). A positive relationship exists between the tubular diameter and the spermatogenic activity of the testis (Hikim *et al.*, 1989). In order to confirm the accuracy of the data, the areas of tubules were also measured. There were significant increases in tubule diameters and areas in both $MC_3^{-/-}$ and WT mice following puberty at week 5 (Figures 3.7 and 3.8). This is in agreement with previous

studies reporting a gradual but significant increase in the absolute volume of the seminiferous tubules until 13 weeks (Ariyaratne *et al.*, 2000). This post pubertal increase in tubular parameters coincides with a rise in the steroidogenic capacity of Leydig cells. FSH and testosterone are the key regulators of spermatogenesis. Both tubular diameter and area did not change significantly between 9-10 to 23-24 weeks in $MC_3^{-/-}$ mice and their age-matched controls (Figures 3.7 and 3.8). In contrast to C57BL/6 mice, the diameter of seminiferous tubules of Balb/c mice progressively increased until 17 weeks of age (Shukri and Shire, 1989). There was a significant reduction in both tubule diameter and area in $MC_3^{-/-}$ mice compared to controls in the youngest age group (3-4 weeks). Interestingly, tubule diameter was 10 % higher in 16-17 weeks old $MC_3^{-/-}$ mice compared to WT and this difference was more significant for tubular area (Figures 3.7 and 3.8). This is even more surprising considering the fact that no known major reproductive event is occurring at this age in mice.

The thickness of the seminiferous tubules was measured to provide an indirect assessment of the state of spermatogenesis. Moreover, it also enabled identification of possible tubular abnormalities including presence of vacuoles or blockage in the tubules or duct system indicated by shorter tubular thicknesses (Russel *et al.*, 1990). In this study, the thickness of tubules correlated with the changes in other tubular parameters. Not surprising, the thinnest germinal epithelium was estimated at 3-4 weeks, whilst the thickest at 23-24 weeks (Figure 3.9). There were approximately 15 % and 25 % reductions in $MC_3^{-/-}$ mice compared to WT at 9-10 and 23-24 weeks, respectively. Conversely, there was a significant increase in tubular thickness in $MC_3^{-/-}$ animals at 16-17 weeks in conjunction with a rise in tubular diameter and area (Figure 3.7, 3.8 and 3.9).

The length of tubular diameter and thickness vary depending on the stage of the cycle (Wing and Christensen, 1982). The latter is highest at stage V of the spermatogenic cycle followed by a gradual decrease until stage XIV, from which it increases again. The diameter of tubules significantly increases from stages I-IV to VII-VIII, followed by a decrease from stages VIII-IX caused by the depletion of the luminal contents (Wing and Christensen, 1982). Neither tubular diameters nor thicknesses were categorized according to the stage of the cycle hence the large variability in data, particularly for the latter parameter. Nevertheless, there are other examples in the existing literature of randomized tubule selection for morphometric analyses, regardless of cycle stage, which still provided insightful information (Amann, 1986; Mehraein and Negahdar, 2011; Ebadi Manas *et al.*, 2013).

There were a number of atrophic seminiferous tubules depleted of germ cells and lined mainly with Sertoli cells in both WT and MC₃^{-/-} mice, particularly in the youngest animal groups. They were regarded as sporadic, background variations of the tubules (Figure 3.4). Described results only provide preliminary indication of the differences in the histology of testes: more detailed qualitative and morphometric analyses including determination of cell numbers and volumes of tubules are still required.

Although, all tissues were fixed and embedded using the same procedure, the possibility of technical errors must be taken into consideration when interpreting the data. The paraformaldehyde fixation used in this study could lead to shrinkage of germ and Sertoli cells. This appears as separation of the cells in the germinal epithelium and further contributes to data variability for tubular thickness. This method, however, was chosen over other possible methods as it

does not affect tubule diameter or distances between them, as other fixatives like Bouins do (Scudamore, 2014).

In this part of the study, the reproductive abilities of the $MC_3^{-/-}$ mice were initially assessed at two levels of the reproductive axis. The contents of a number of anterior pituitary hormones were reduced in both male and female $MC_3^{-/-}$ mice compared to WT. The MC_3 ablation led to more than 50 % reduction in gonadotropins as well as prolactin and GH in male mice. In female, GH was the only hormone significantly affected. It is still unclear whether the reduction in the pituitary hormones is mediated by a direct loss of MC_3 in this gland, or indirectly through the hypothalamus or other tissues which interact with the pituitary gland. Furthermore, MC_3 ablation, in varying degree, affected testicular histology. The age dependent changes in testicular parameters in $MC_3^{-/-}$ mice were comparable to that of WT. In young (3-4 and 9-10) $MC_3^{-/-}$ mice, however, these measurements were significantly smaller suggesting a defect in spermatogenesis. The intratesticular, plasma or urine (Munro *et al.*, 1991; Muir *et al.*, 2001; deCatanzaro *et al.*, 2006) concentrations of testosterone could not be established due to lack of animals but it would be a good indication of the steroidogenic capacity of these animals. At present, it cannot be clarified whether the changes in testicular histology at young age are caused by direct effects of MC_3 absence in the testis, or upstream effects. A tissue specific gene ablation model would aid in establishing the exact aetiology.

C57BL/6 mice are considered good breeders (Batty, 1978; Silver, 1995) and yet $MC_3^{-/-}$ mice with this background have reduced frequency of pregnancy and litter size as anecdotally reported from our in-house observations (Stephen Getting, and some of his former colleagues at the William Harvey Research Institute, personal communications). Clearly, MC_3 ablation does not induce

complete infertility as these mice are still able to reproduce (Butler *et al.*, 2000; Chen *et al.*, 2000). It is of note, however, that the spermatozoa production in laboratory animals exceeds the number needed for fertility. Therefore, in rodents, spermatogenesis must be decreased by 90 % or even more to affect the number of offspring (Amann, 1986). In order to establish the reproductive functions of MC₃^{-/-} mice a full biochemical profile and investigation of their sexual behaviour including mount patency, frequency, intromission latency *et cetera*, is required. It is not yet clear whether MC₃ ablation affects both genders to the same degree as this study concentrated primarily on the male. Similar approaches should be taken to determine the effects in female MC₃^{-/-} mice. This would include examination of oogenesis, steroidogenesis, conception or implantation as they all may be potentially defective.

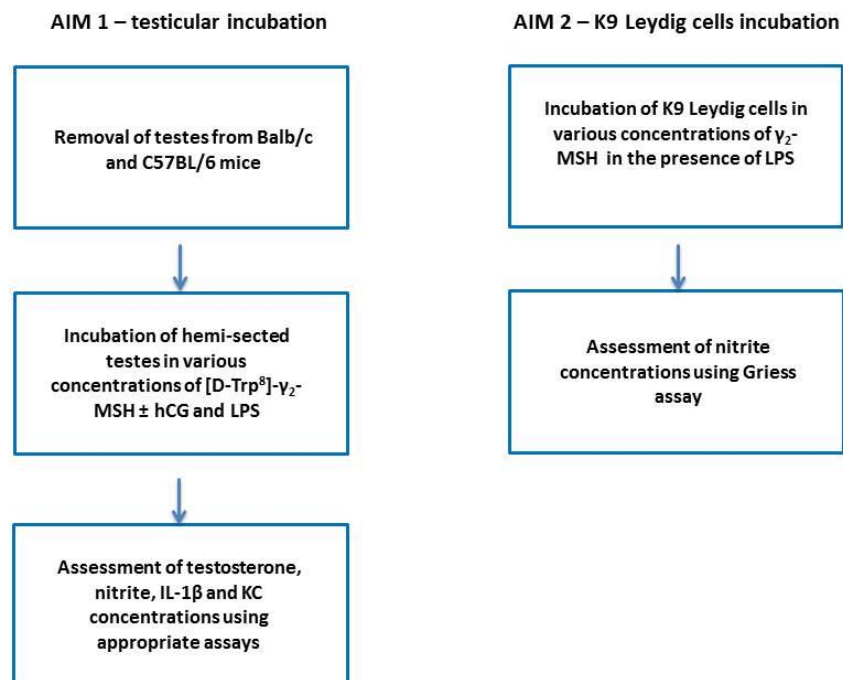
4 The effects of MC₃ activation in normal and LPS-stimulated mouse testicular tissue.

4.1 Introduction

The testis is described as an immune-privileged site, where immune responses are actively suppressed to extend survival of autoantigenic male germ cells (Meinhardt and Hedger, 2011). Failure of these protective mechanisms may result in infertility or autoimmunity. Sertoli cells are considered to be the key cell type maintaining this immune privilege (Mital *et al.*, 2010). They express several cytokines, which may modulate immune functions. Two of the cytokines interleukin 1 (IL-1) and tumour necrosis factor alpha (TNF- α), were shown to stimulate Leydig cell activity, but in the presence of acute or chronic testicular inflammation they led to a decrease in androgen secretion and hence a reduction in fertility (Gnessi *et al.*, 1997). Acute or chronic forms of infection or inflammation are often due to bacterial invasion and can be experimentally reproduced by administration of lipopolysaccharide (LPS), a component of the outer membrane of Gram-negative bacteria. Studies showed that high concentrations of LPS can inhibit testicular steroidogenesis and disrupt spermatogenesis *in vivo* by release of a number of pro-inflammatory molecules (O'Bryan *et al.*, 2000a). Prolonged inflammation may lead to partial or complete loss of fertility (Introduction, section 1.1), hence restoration to a non-inflamed state is at the heart of potential therapeutic interventions.

Among the many pleiotropic actions of MC₃, strong anti-inflammatory and immunomodulatory effects of this receptor subtype were displayed in various organs including skin, lung, heart, kidney, liver and joints (Catania *et al.*, 2004; Getting, 2006a). As determined by qRT-PCR, MC₃ as well as other MC are

present in the testes of mice (Figure 2.7). Therefore, the aim of the series of studies presented in this chapter was to determine the effects of [D-Trp⁸]- γ_2 -MSH, a synthetic compound with selectivity towards MC₃, in normal testicular function and, most importantly, during a LPS-induced inflammatory-like state. The testicular tissues were removed from two different mice strains, namely Balb/c and C57BL/6, as they are known to differ with regard to the steroidogenic activity and immune responses. The effects of the selective MC₃ agonist were assessed by measuring concentrations of testosterone as well as inflammatory markers including nitric oxide (NO), IL-1 β and KC. Additionally, the K9 Leydig cell line was used to determine whether MC₃ and/or other MC exert direct effects on Leydig cell function during inflammatory-like states or act indirectly through other cell types present in the testis such as macrophages or Sertoli cells. The summary of the aims and sequence of events in this project is presented below.



4.2 Materials and Methods

4.2.1 *In vitro* incubation of testicular tissue

4.2.1.1 Tissue collection and incubation

Testes of sexually mature (8–12 weeks) C57BL/6 and BALB/c mice were removed at the National Institute for Medical Research (London, UK) and transported to the University of Westminster in a warm DMEM media. Testes were hemi-sectioned, weighed and randomly distributed to tubes containing DMEM in varying concentrations of [D-Trp⁸]- γ ₂-MSH (selective MC₃ agonist; 0.3-30 μ g/ml) in the presence or absence of human Chorionic Gonadotropin (hCG; 50 mIU/ml; C1063-10VL, Sigma-Aldrich, UK) and/or SHU9119 (MC₃/MC₄ antagonist and MC₁/MC₅ partial agonist; 10 μ g/ml) (Table 4.1). Tissues were hemi-sectioned as opposed to dispersed cells to preserve the close cell to cell communication present *in vivo*. Incubations at 35 °C lasted for 5 h (de la Torre *et al.*, 1976; O'Shaughnessy *et al.*, 2003) and were performed in a total volume of 400 μ l of media in round bottomed, capped, test tubes (17x100 mm, 14 ml, PP, 734-0438, BD FALCON, VWR, UK) in a culture water bath. In order to induce a mild inflammatory-like response, lipopolysaccharide (LPS; 10 μ g/ml; L6529, Sigma-Aldrich, UK) (Stephan *et al.*, 1997; Aly *et al.*, 2009) was added 2 h following compound administration (Kang *et al.*, 2006; Getting *et al.*, 2008) and incubated for the remaining 3 h (O'Bryan *et al.*, 2005).

Doses of SHU9119 (Hruby *et al.*, 1995; Getting *et al.*, 1999) and hCG (de la Torre *et al.*, 1977; Mayerhofer *et al.*, 1993) were based on published reports and confirmed with dose-response experiments (Figures 4.1-4.4). The pharmacological concentrations of [D-Trp⁸]- γ ₂-MSH used in *in vitro* incubation of mice testes were also based on previous experiments (Getting *et al.*, 2006b).

Doses of the endogenous MC₃ ligand γ ₂-MSH applied *in vitro* on K9 Leydig cell line ranged from the lowest intratesticular (0.03 ng/ml) (DeBold *et al.*, 1988) to low pharmacological concentrations (3 μ g/ml).

After incubation the media were removed, aliquoted and stored at -20 °C until assayed for testosterone by RIA, nitrite by Griess Assay or cytokines by ELISA. Testicular tissue pieces were washed three times in PBS and stored at -80 °C for possible further analyses. Treatments were done in triplicates (three different testicular tissue pieces) and each experiment was repeated a minimum of three times.

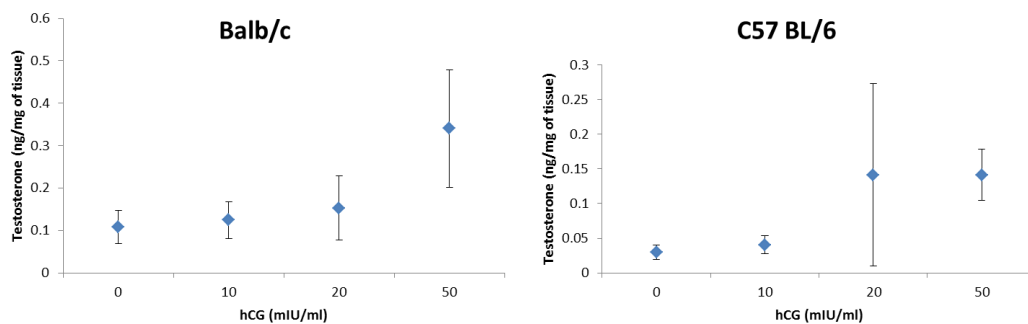


Figure 4.1 Dose response effect of hCG (mIU/ml) on *in vitro* testosterone production in Balb/c (left) and C57BL/6 (right) mice testes. Testes of sexually mature (8-12 weeks) Balb/c (left) and C57BL/6 (right) mice were hemi-sectioned and incubated in DMEM in varying concentrations of hCG (10, 20 and 50 mIU/ml) for 5 h at 35 °C in air, media were removed and assayed for testosterone by RIA. The amounts of testosterone released into the media were expressed relative to the mass of testicular tissue. Data are mean \pm SD of one experiment (n=4).

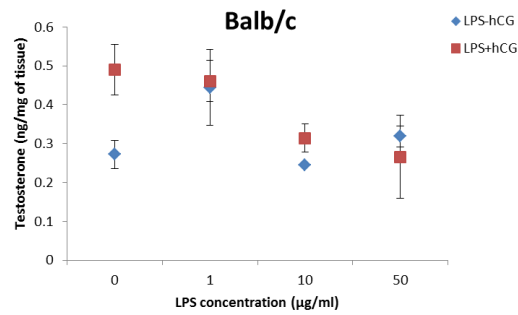


Figure 4.2 Dose response effect of LPS ($\mu\text{g/ml}$) on *in vitro* testosterone production in Balb/c mice testes. Testes of sexually mature (8-12 weeks) Balb/c mice were hemi-sected and incubated in DMEM in varying concentrations of LPS (1, 10 and 50 $\mu\text{g/ml}$) in the presence or absence of hCG (50 mIU/ml) for 5 h at 35 °C in air, media were removed and assayed for testosterone by RIA. The amounts of testosterone released into the media were expressed relative to the mass of testicular tissue. Data are mean \pm SD of one experiment (n=4).

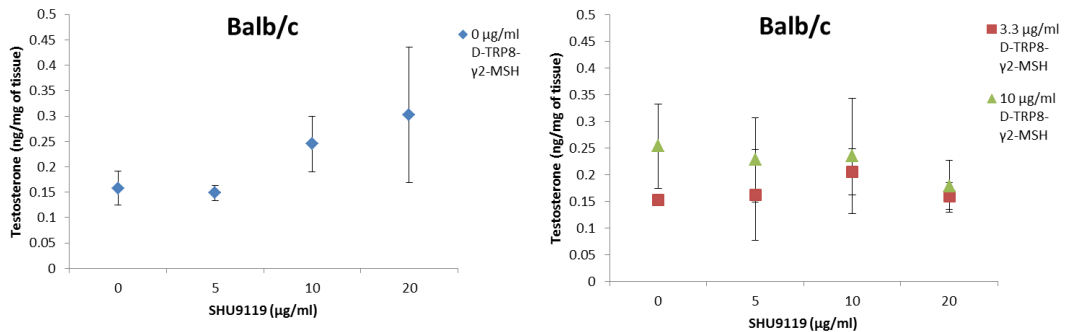


Figure 4.3 Dose response effect of SHU9119 ($\mu\text{g/ml}$) on *in vitro* testosterone production in Balb/c mice testes. Testes of sexually mature (8-12 weeks) Balb/c mice were hemi-sected and incubated in DMEM in varying concentrations of SHU9119 (5, 10 and 20 $\mu\text{g/ml}$) in the presence or absence of [D-Trp⁸]- γ_2 -MSH (3.3 or 10 $\mu\text{g/ml}$) for 5 h at 35 °C in air, media were removed and assayed for testosterone by RIA. The amounts of testosterone released into the media were expressed relative to the mass of testicular tissue. Data are mean \pm SD of one experiment (n=4).

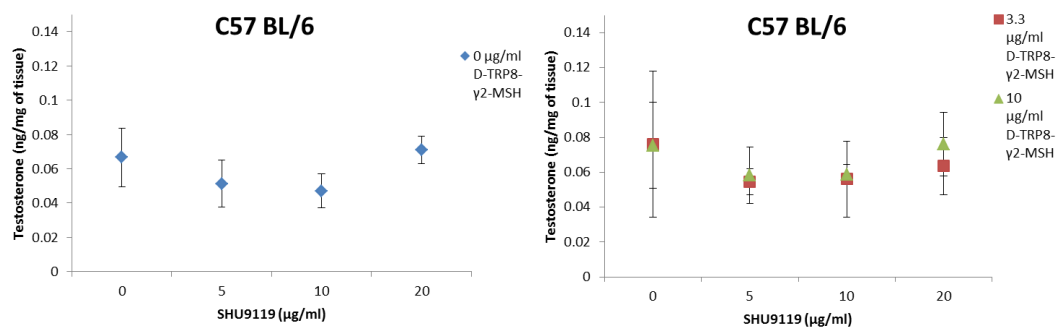


Figure 4.4 Dose response effect of SHU9119 (µg/ml) on *in vitro* testosterone production in C57BL/6 mice testes. Testis of sexually mature (8-12 weeks) C57BL/6 mice were hemi-sected and incubated in DMEM in varying concentrations of SHU9119 (5, 10 and 20 µg/ml) in the presence or absence of [D-Trp⁸]-γ₂-MSH (3.3 or 10 µg/ml) for 5 h at 35 °C in air, media were removed and assayed for testosterone by RIA. The amounts of testosterone released into the media were expressed relative to the mass of testicular tissue. Data are mean ± SD of one experiment (n=4).

4.2.1.2 Radioimmunoassay (RIA) for testosterone

The RIA was performed according to manufacturer's instructions (07189102, MPBiomedicals, UK) with minor modifications such as reducing the volume of all reagents by half. Standards were provided in the kit and ranged from 0.1 to 10.0 ng/ml. Samples were diluted 1:2–1:4 in 0.1 M PBS. All components of the standard curve including non-specific binding (NSB) and total binding (B₀) were prepared in triplicate whilst samples were assayed in duplicate. Each tube contained 25 µl of standard or sample, 50 µl of sex binding globulin inhibitor solution (SBGI) and 250 µl of testosterone ¹²⁵I. Following addition of anti-testosterone (250 µl), all tubes were vortexed, mixed and incubated at 37 °C for 120 min. After incubation 50 µl of secondary antibody were added. All tubes were vortexed, mixed and incubated for another 60 min at 37 °C. Finally, all tubes were placed in a large capacity centrifuge (2,300 rpm for 15 min; 5804R,

Eppendorf, UK). The supernatant was aspirated and the radioactivity of the pellet measured using a gamma counter (Wallac Wizard 1470, PerkinElmer Inc, USA). A summary of the testosterone RIA protocol is presented in Table 4.2. The standard curves were plotted and calculations of unknown testosterone concentrations were performed using Assayzap software (Biosoft, UK).

ligand	action	other receptors targeted	manufacturer	concentrations (µg/ml)	reference
[D-Trp ⁸]-γ ₂ -MSH	full agonist	none	kind gift from Professor Paolo Grieco, University of Naples, Italy	0.3-30.0	Grieco <i>et al.</i> , 2000
SHU9119	full antagonist	MC ₄ >MC ₃	H-3952, Bachem, Germany	10	Hruby <i>et al.</i> , 1995
	partial agonist	MC ₁ >MC ₅			

Table 4.1 Compounds used in *in vitro* studies. The rank order of affinity is based on Wikber *et al.*, 2000 and the IUPHAR/BPS Guide to Pharmacology.

161

tube	diluent buffer	standards or unknowns	SBGI solution	testosterone ¹²⁵ I	antiserum	vortex, incubate at 37°C for 120 minutes or at 37°C for 90 minutes and at 4°C overnight	secondary antibody	vortex, incubate at 37°C for 60 minutes	aspirate and count
T _c		25 µl	50 µl	250 µl	250 µl		vortex, incubate at 37°C for 120 minutes or at 37°C for 90 minutes and at 4°C overnight		
NSB	250 µl	↓	↓	↓	250 µl	↓			
B ₀									
testosterone standards (0.1 - 10.0 ng/ml)									
unknowns									

Table 4.2 Summary of testosterone RIA protocol. TC- total count, NSB- non-specific binding, B₀- total binding.

4.2.1.3 Biochemical Assays

4.2.1.3.1 Griess Assay

Nitrite is the final product of nitric oxide (NO) oxidation pathways, hence its concentrations were used to assess NO production in the testis in response to various treatments *in vitro*. Standards were prepared by serial dilution of 100 mM sodium nitrite (S2252, Sigma-Aldrich, UK) in DMEM media and ranged from 1.6–100.0 μ M, with media only as a negative control. Fifty microliters of standards or samples were loaded into each well of a 96 well plate in duplicate. An equal volume of Griess reagent mix (1:1 Solution A [1% sulphanilamide (S925, Sigma-Aldrich, UK) in 5 % phosphoric acid (452289, Sigma-Aldrich, UK)] and Solution B [0.1 % N-(1-naphthyl)ethylenediamine dihydrochloride (N9125, Sigma-Aldrich, UK)] in distilled water) was added and left for 10 min at room temperature to equilibrate. The absorbance was measured at 540 nm using VersaMax microplate reader (Molecular Devices, UK). The concentrations of nitrite in each sample were established by comparison to a standard curve (Figure 4.5).

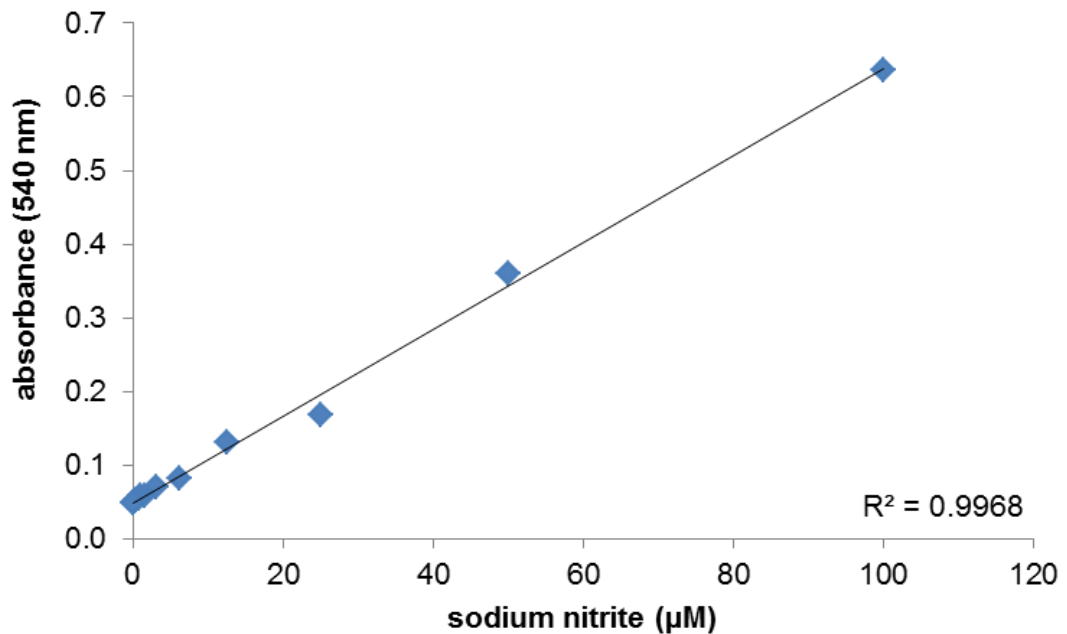


Figure 4.5 Example of a standard curve used for determination of nitrite concentrations. Value R^2 is displayed on the graph.

4.2.1.3.2 ELISA IL-1 β

Concentrations of mouse IL-1 β were determined using the DuoSet ELISA Development kit (DY401, R&D Systems, UK). Each 96-well plate (DY990, R&D Systems, UK) was coated with 100 μ l of 4 μ g/ml rat anti-mouse IL-1 β (capture antibody, supplied in the kit) diluted in PBS and incubated overnight at room temperature. The solution was removed by gentle blotting against clean paper towel and the plate was washed by filling each well (approximately 400 μ l) with wash buffer (0.05 % Tween[®] 20 in PBS, pH 7.2-7.4) using a squirt bottle. The process was repeated three times. The plate was blocked for 1 h at room temperature with 300 μ l of block buffer (1 % BSA [DY995, R&D Systems, UK] in PBS). Following blocking, the plate was washed three times as described before. Standards were prepared by serial dilution of recombinant mouse IL-1 β

(supplied) in reagent diluent (0.1 % BSA, 0.05 % Tween® 20 in Tris-buffered saline [20 mM Tris base, 150 mM sodium chloride] pH 7.2-7.4) and ranged from 0.98–1,000.00 pg/ml. The standards and samples (100 µl) were then added to each well in triplicate and duplicate, respectively, and incubated for 2 h at room temperature. After incubation the plate was washed, coated with 100 µl of 1 µg/ml biotinylated goat anti-mouse IL-1β (detection antibody, supplied) in reagent diluent and incubated for another 2 h at room temperature. The plate was then washed and 100 µl of streptavidin-HRP (1:200 dilution with reagent diluent; supplied) was added and left for 20 min at room temperature in the dark. The plate was washed again and colour developed using 100 µl of 3,3',5,5' - tetramethylbenzidine (TMB substrate; T0440-100ML, Sigma-Aldrich, UK) for 20 min at room temperature in the dark. The reaction was stopped by adding 50 µl of stop solution (2N H₂SO₄ [10765663, Thermo Fisher Scientific, UK]) and mixing. The absorbance was measured at 450 nm using a VersaMax microplate reader. The concentrations of IL-1β were determined by comparison to the standard curve (Figure 4.6). The data were linearized by plotting the log of both the IL-1β standard concentrations and the absorbance values.

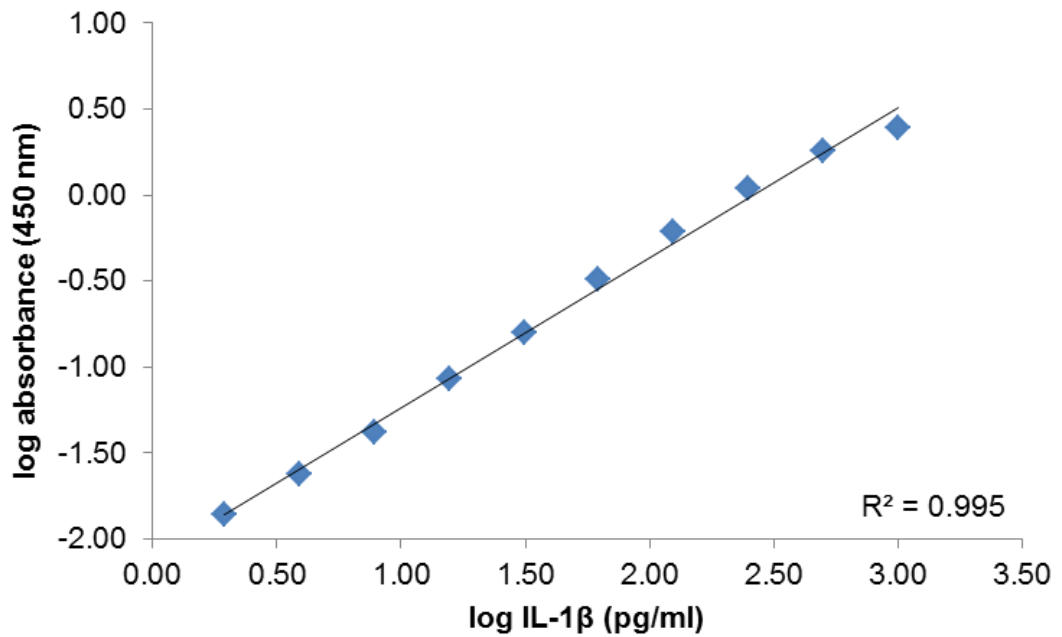


Figure 4.6 Example of a standard curve used for determination of IL-1 β concentrations. Value R^2 is displayed on the graph.

4.2.1.3.3 ELISA KC (CXCL1)

The determination of KC concentrations using the DuoSet ELISA kit (DY453, R&D Systems, UK) were performed according to the protocol described for the ELISA IL-1 β but with minor modifications. Briefly, the concentrations of capture and detection antibodies were reduced to 2 μ g/ml and 200 ng/ml, respectively. The Reagent Diluent also served as a Block Buffer and was composed of 1 % BSA in PBS (pH 7.2-7.4).

4.2.2 The K9 Leydig cell line

4.2.2.1 Maintenance of the K9 Leydig cell line

The K9 cell line is a hybrid of mouse Leydig tumor cell line (MA-10) and isolated mouse Leydig cells (Finaz *et al.*, 1987). It was kindly given by Dr Finaz (Equipe Institut National de la Santé et de la Recherche Médicale, Lyon, France). The cells were maintained in DMEM/F-12 medium (31330 – 38, Life Technologies, UK) containing 15 mM HEPES, 1.2 g/L NaHCO₃ and supplemented with 4 mM L-glutamine (G7513, Sigma-Aldrich, UK), 1 % penicillin/streptomycin (15140-122, Life Technologies, UK) and 15 % foetal calf serum (FCS; 10135552, Thermo Fisher Scientific, UK). The K9 cells were plated in 75 cm² flasks and maintained at 37 °C with 5 % CO₂ and 95 % O₂. Media were changed at least every two days due to rapid acidification. The K9 cells doubling time was 18 h in medium supplemented with 15 % FCS, hence they were passaged every three days at approximately 80 % confluency using trypsin-EDTA solution in media (10194522, Thermo Fisher Scientific, UK) to dissociate and disaggregate the cells.

4.2.2.2 *In vitro* stimulation of the K9 Leydig cell line The direct effects of γ_2 -MSH on nitrite release by Leydig cells were investigated *in vitro*. The K9 Leydig cells were plated onto a 96 well plate following trypsinization and left overnight in the incubator. Cells were then stimulated with various concentrations of γ_2 -MSH (0.3×10^{-4} –3.0 $\mu\text{g/ml}$; H-4400, Bachem, Germany) in the presence or absence of 1 $\mu\text{g/ml}$ lipopolysaccharide (LPS; L6529, Sigma-Aldrich, UK) for 6 h at 37 °C with 5 % CO₂ and 95 % O₂. The timing and dose of LPS were determined in initial experiments. Media (100 μl) from each well were then

transferred to another 96 well plate for determination of nitrite concentrations by Griess assay.

4.2.2.3 RT – PCR

4.2.2.3.1 RNA extraction

The K9 Leydig cells were plated onto a 6 well plate and incubated overnight at 37 °C with 5 % CO₂ and 95 % O₂. Media were removed and 500 µl of TriReagent (T9424, Sigma-Aldrich, UK) were added into each well to lyse the cells. The content of each well was transferred to a clean 1.5 ml tube and stored at -80 °C for future use or the RNA extraction protocol was immediately done. Chloroform (100 µl; C7559, Sigma-Aldrich, UK) was added and the mix was vortexed and partitioned by centrifugation in an IEC Micromax microcentrifuge (DJB Labcare, UK) for 30 min at 13,000 rpm at 4 °C. The colourless upper aqueous containing RNA layer was transferred into a new tube and 250 µl of isopropanol (I-9516, Sigma-Aldrich, UK) added. The content of the tube was vortexed and separated as before for 30 min at 13,000 rpm at 4 °C. Finally, the supernatant was discarded and 500 µl of 75 % ethanol were added to wash the precipitate. Following vortexing, the sample was spun for 15 min at 13,000 rpm at 4 °C. The pellet was air dried on ice, resuspended in 12 µl of DEPC water (0.1 % diethylpyrocarbonate [32490, Sigma- Aldrich, UK] in water) and stored at -80 °C. The RNA concentration and purity were assessed using a spectrophotometer as described before (Chapter 2, section 2.2.2.1).

4.2.2.3.2 cDNA synthesis

Performed as described in Chapter 2, section 2.2.2.2

4.2.2.3.3 PCR and gel electrophoresis

Performed as described in Chapter 2, section 2.2.2.3 and 2.2.2.4

4.2.3 Statistics

Normality distribution of each outcome (testosterone, nitrite, KC and IL-1 β) was checked with Kolmogorov-Smirnov test and a histogram before using the parametric tests (SPSS 18, IBM, USA). Statistical differences were calculated using one-way ANOVA procedures followed by Tukey or LSD *post-hoc* tests for inter- and intra-group comparisons (SPSS 18, IBM, USA). The Tukey *post-hoc* test is appropriate for testing large numbers of means as in the experiments presented, but it is known to be very conservative. It controls type I error (rejection of a true null hypothesis) very well but lacks statistical power, hence the probability of a type II error (acceptance of a false null hypothesis) is high (Field, 2004). There is a substantial risk of rejecting meaningful differences between the means due to small sample size using this test. Therefore, the least-significant difference (LSD) test, which is very liberal and does not control the type I error, was used in conjunction with Tukey test to reduce the risk of rejecting a drug effect that does actually exist (Field, 2004). The differences obtained using the LSD test, however, are not regarded as being significant but serve more to highlight the potential effect, which could become significant with larger sample size.

Comparison between two groups was performed using unpaired Student's t-test (two-tailed) (Excel, Microsoft Office 2010) or non-parametric Mann-Whitney test (Field, 2004). For all statistical analyses P value is given. Data are expressed as mean \pm SEM.

4.3 Results

4.3.1 Comparison of testosterone production by the testicular tissue of Balb/c and C57BL/6 mice.

There are substantial differences in the testicular tissue steroidogenic activities of Balb/c and C57BL/6 mice (Figure 4.7). Balb/c mice produce 40 % more basal testosterone than C57BL/6 mice ($p=0.065$, t -test). This difference was more striking following hCG (50 mIU/ml) stimulation ($p<0.01$, t -test). hCG increased testosterone release from the testicular tissue of Balb/c ($p=0.021$, t -test) but not from C57BL/6 mice ($p=0.314$, t -test; Figure 4.7). The low response from the testicular tissue of C57BL/6 mice could be due to generally low steroidogenic activity of these animals.

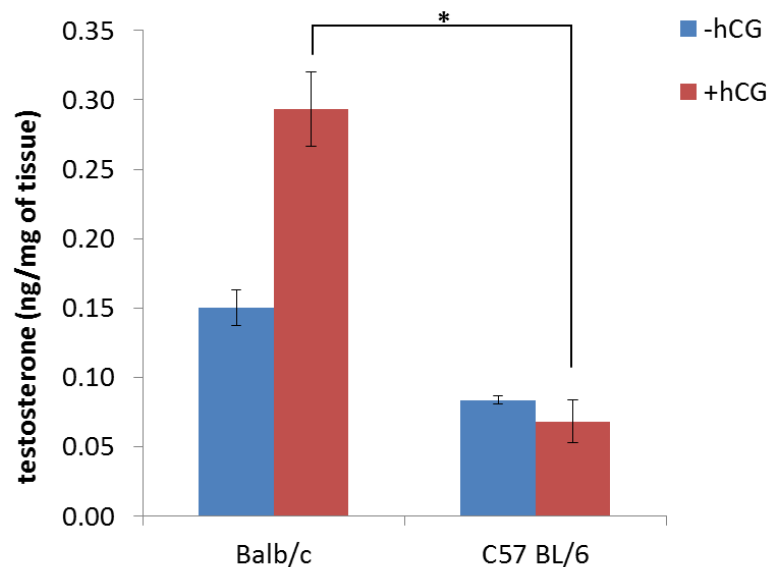


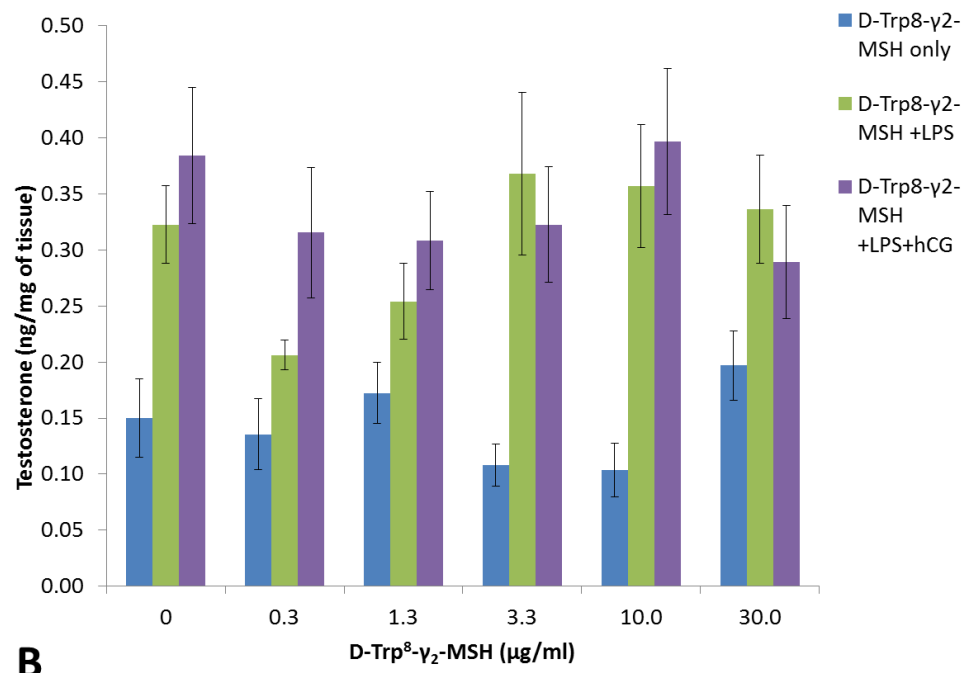
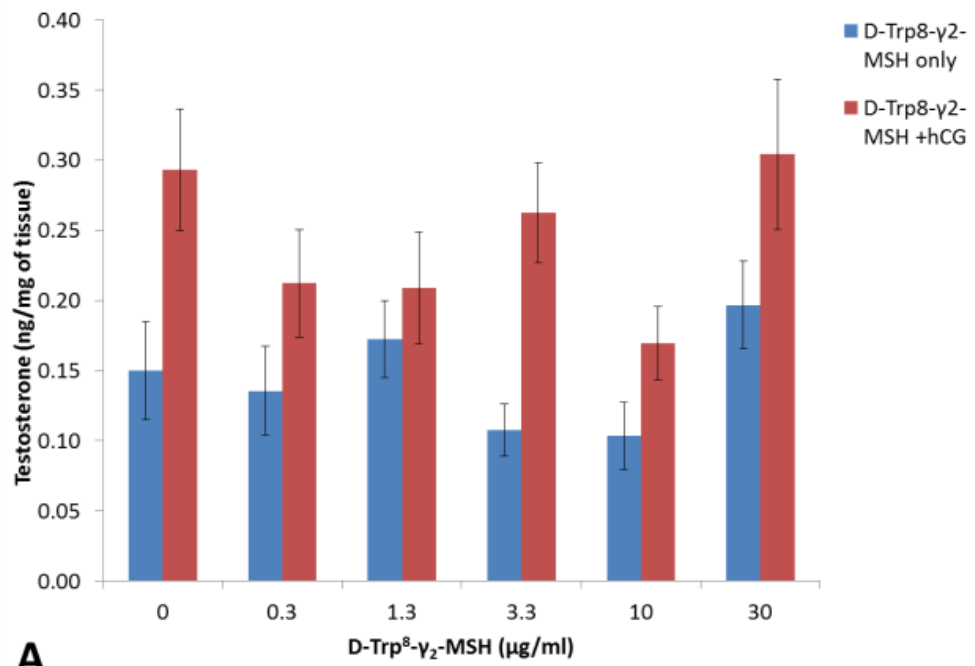
Figure 4.7 Effects of hCG (50 mIU/ml) on *in vitro* testosterone production in Balb/c and C57BL/6 mice testes. Testes of sexually mature (8-12 weeks) C57BL/6 and Balb/c mice were hemi-sectioned and incubated in DMEM in the presence or absence of 50 mIU/ml hCG for 5 h at 35 °C in air. After incubation media were removed and assayed for testosterone by RIA. The amounts of testosterone released into the media were expressed relative to the mass of the testicular tissue. Data are mean \pm SEM of four independent experiments, $n=7-10$; * $p<0.01$ for Balb/c +hCG vs. C57BL/6 +hCG (t -test).

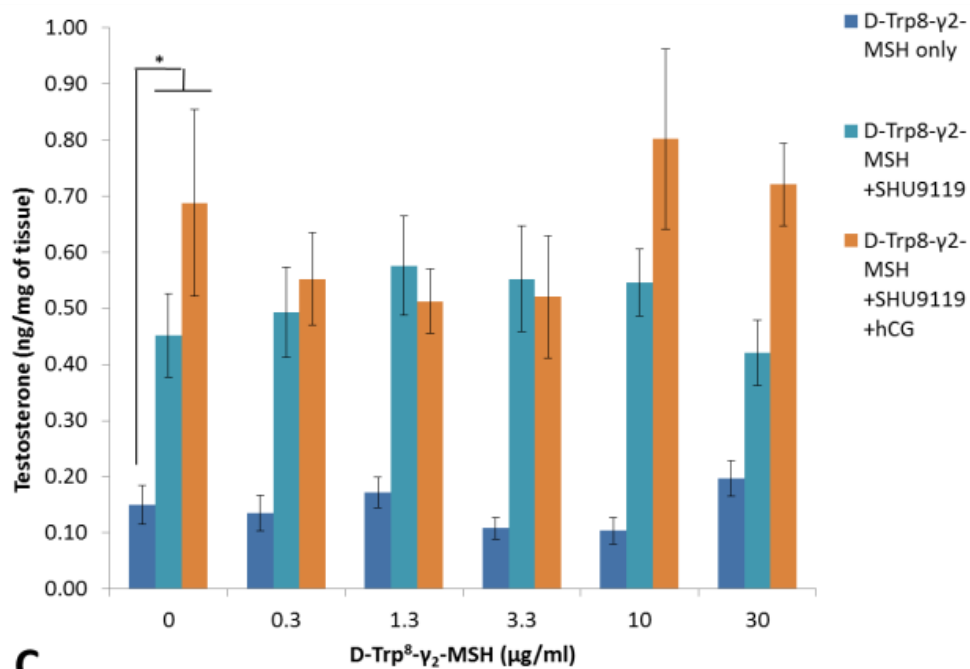
4.3.2 Effects of [D-Trp⁸]- γ ₂-MSH under various conditions on *in vitro* testosterone and inflammatory markers production from the testicular tissue of Balb/c and C57BL/6 mice

4.3.2.1 Balb/c mice

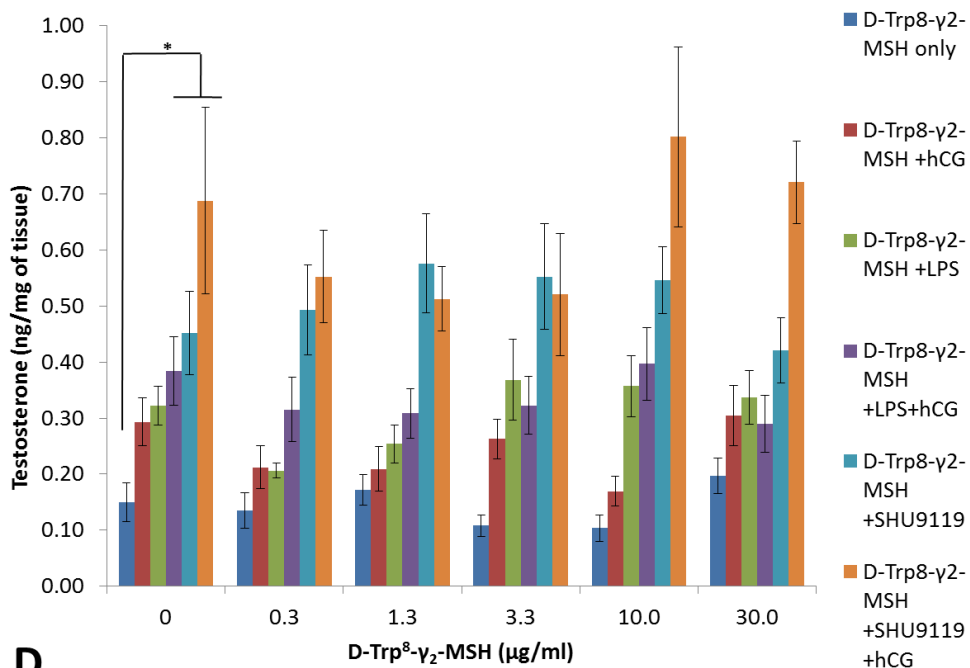
4.3.2.1.1 *In vitro* testosterone production by testicular tissue from Balb/c mice.

[D-Trp⁸]- γ ₂-MSH alone or in the presence of hCG (50 mIU/ml) had no effect on testosterone release from the testicular tissue of Balb/c mice *in vitro* ([D-Trp⁸]- γ ₂-MSH -hCG, $p=0.193$ and [D-Trp⁸]- γ ₂-MSH +hCG, $p=0.168$; ANOVA; Figure 4.8 A-D). The hCG alone increased testosterone production compared to control (0 μ g/ml) ($p=0.021$, *t*-test; Figure 4.7). In the presence of LPS alone or in combination with hCG, there were no significant differences in the amounts of testosterone released into the media from Balb/c testicular tissues in response to various concentrations of [D-Trp⁸]- γ ₂-MSH ([D-Trp⁸]- γ ₂-MSH +LPS, $p=0.155$ and [D-Trp⁸]- γ ₂-MSH +LPS +hCG, $p=0.684$; ANOVA; Figure 4.8 B and D). Similarly to other groups, [D-Trp⁸]- γ ₂-MSH had no effect on the steroidogenic activities of the testicular tissue of Balb/c mice in the presence of SHU9119 alone or in combination with hCG ([D-Trp⁸]- γ ₂-MSH +SHU9119, $p=0.673$ and [D-Trp⁸]- γ ₂-MSH +SHU9119 +hCG, $p=0.456$; ANOVA; Figure 4.8 C and D). SHU9119 alone or in the presence of hCG increased testosterone production three fold compared to basal levels independently of ligand dose ($p<0.05$, ANOVA, Tukey; Figure 4.8 C and D).





C

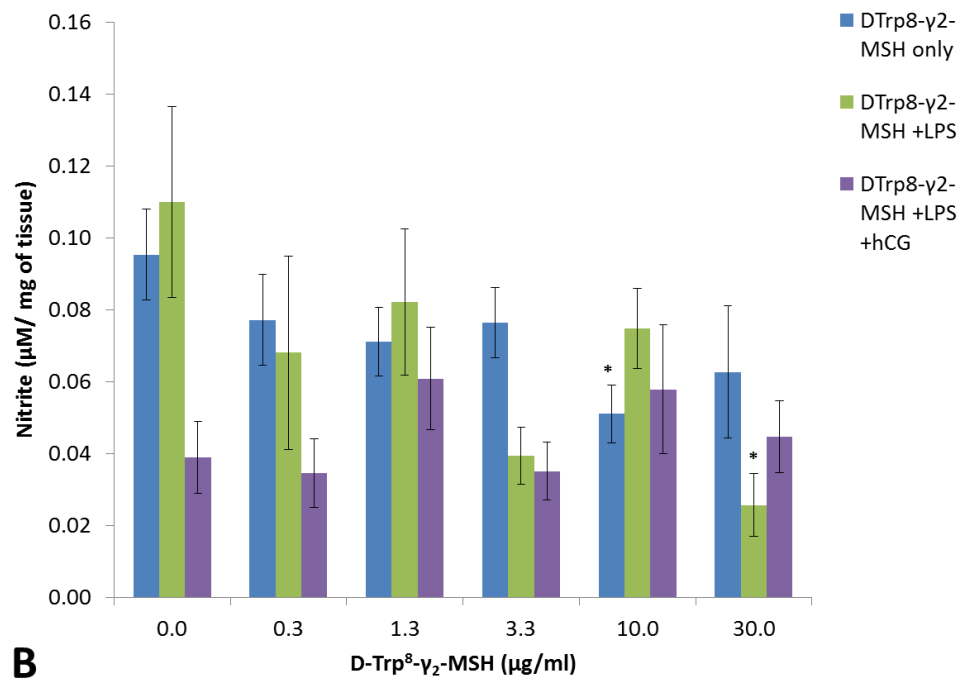
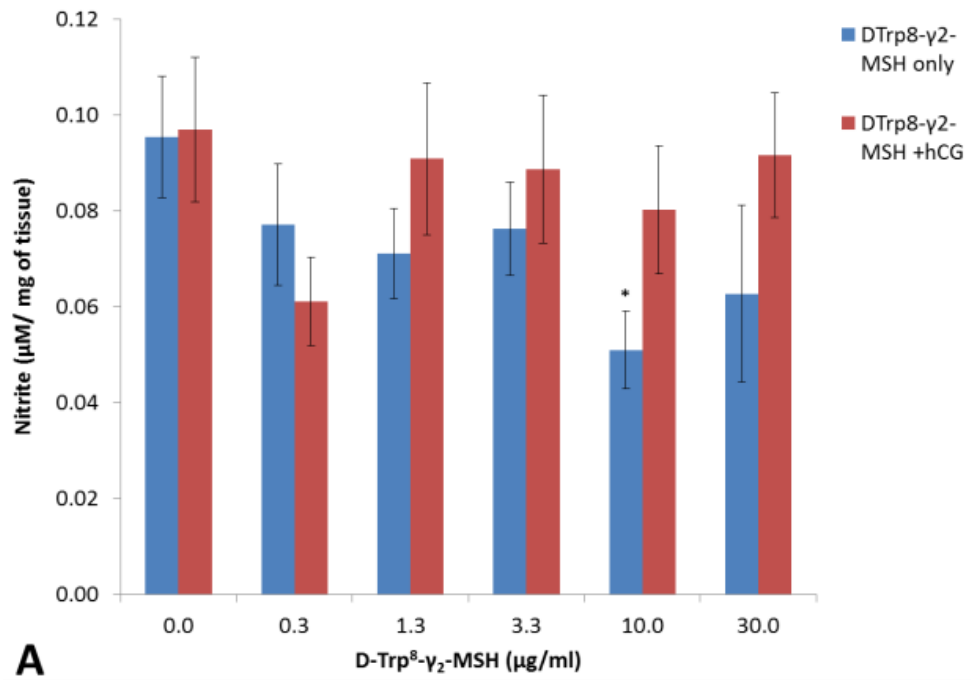


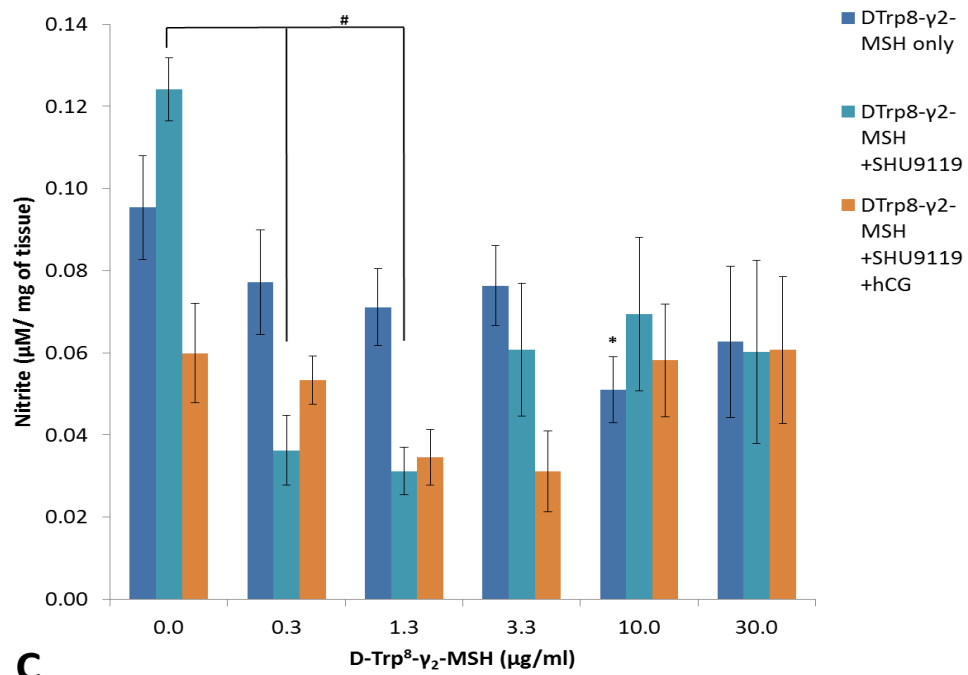
D

Figure 4.8 Effects of [D-Trp⁸]-γ₂-MSH in the presence or absence of various compounds on *in vitro* testosterone production in Balb/c mice testes. Testes of sexually mature (8-12 weeks) Balb/c mice were hemi-sectioned and incubated in DMEM in varying concentrations of [D-Trp⁸]-γ₂-MSH (0.3–30 µg/ml) in the presence or absence of LPS (10 µg/ml), SHU9119 (10 µg/ml) and hCG (50 mIU/ml) for 5 h at 35 °C in air. Media were assayed by RIA. Testosterone concentrations were expressed relative to the mass of testicular tissue. Data are mean ± SEM of two or three independent experiments, n=5-9, *p<0.05 between treatment groups indicated on the graph (ANOVA, Tukey).

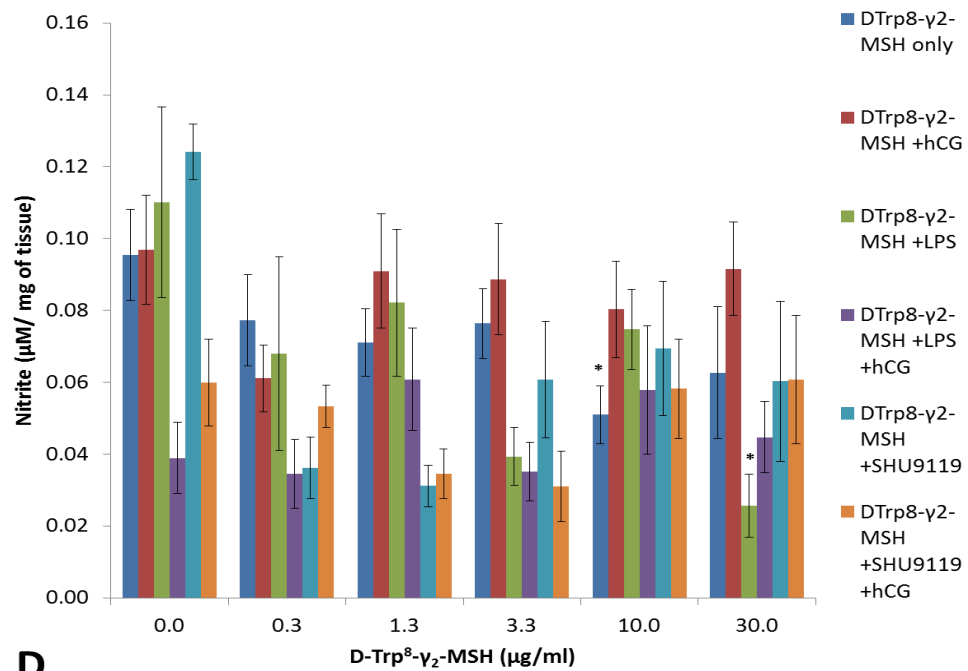
4.3.2.1.2 *In vitro* nitrite production by testicular tissue from Balb/c mice.

[D-TRP⁸]- γ ₂-MSH inhibited nitrite production under basal and LPS-stimulated conditions at 10 and 30 μ g/ml, respectively, from the testicular tissues of Balb/c mice ([D-Trp⁸]- γ ₂-MSH only, $p=0.031$ and [D-Trp⁸]- γ ₂-MSH +LPS, $p=0.049$; ANOVA, Tukey; Figure 4.9 B and D). In the presence of hCG alone there were no significant differences in the amounts of nitrite released into the media from Balb/c testicular tissues in response to various concentrations of [D-Trp⁸]- γ ₂-MSH ($p=0.475$, ANOVA; Figure 4.9 A and D). [D-Trp⁸]- γ ₂-MSH with SHU9119 in the absence of hCG decreased nitrite release at 0.3 ($p=0.025$) and 1.3 μ g/ml ($p=0.011$; ANOVA, Tukey; Figure 4.9 C and D). LPS with hCG as well as SHU9119 with hCG decreased nitrite release from the testicular tissues by 50 %, compared to control (0 μ g/ml [D-Trp⁸]- γ ₂-MSH (Figure 4.9 D).





C

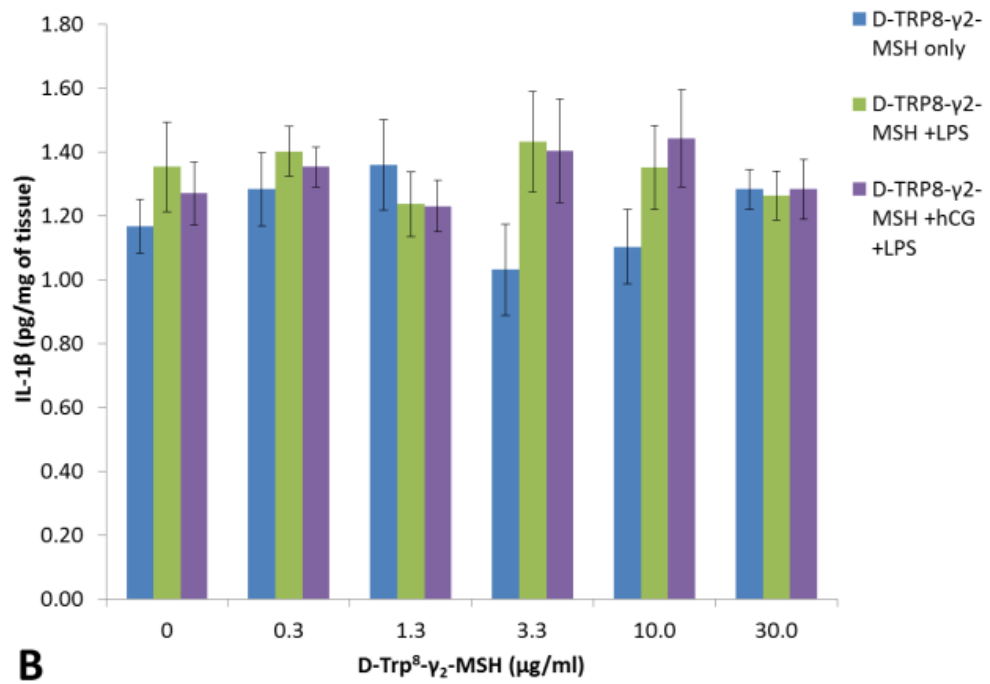
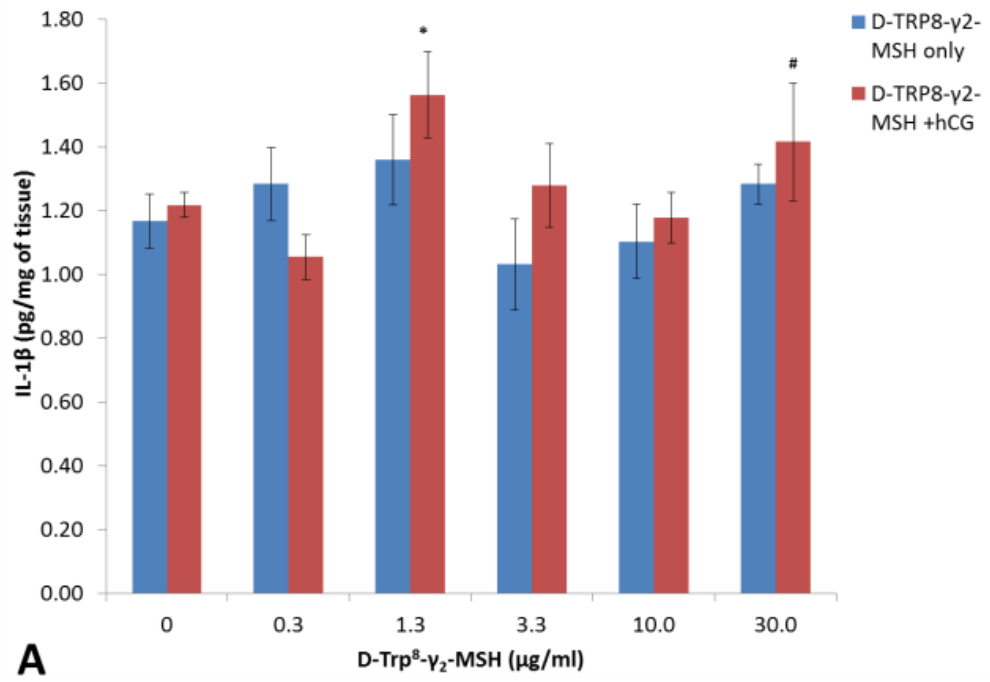


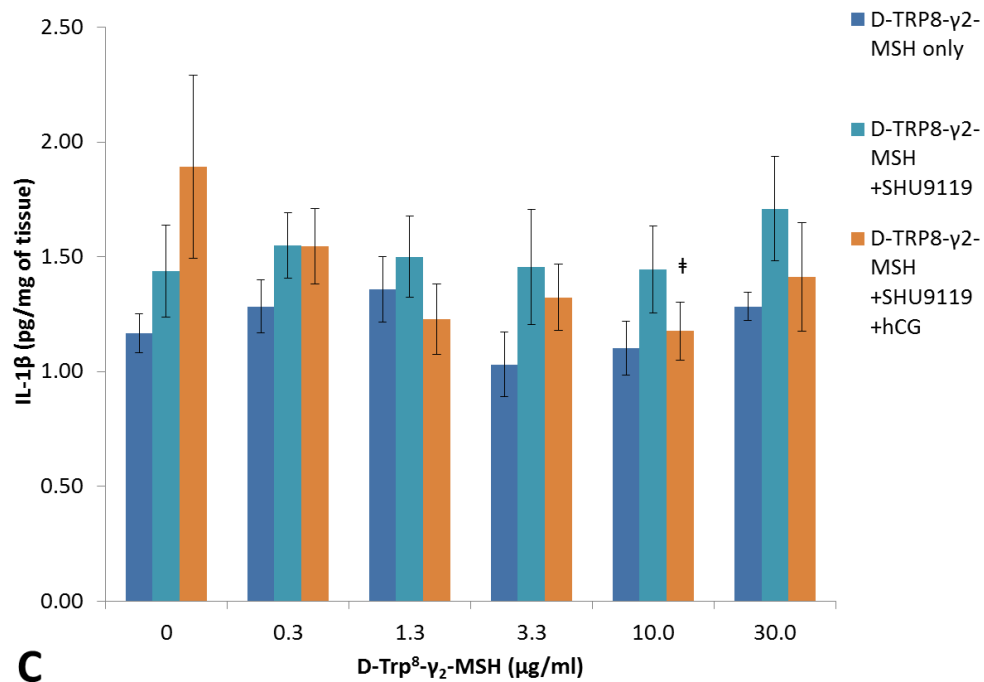
D

Figure 4.9 Effects of [D-Trp⁸]-γ₂-MSH in the presence or absence of various compounds on *in vitro* nitrite production in Balb/c mice testes. Testes of sexually mature (8-12 weeks) Balb/c mice were hemi-sectioned and incubated in DMEM in varying concentrations of [D-Trp⁸]-γ₂-MSH (0.3–30 µg/ml) in the presence or absence of LPS (10 µg/ml), SHU9119 (10 µg/ml) and hCG (50 mIU/ml) for 5 h at 35 °C in air. Media were assayed by Griess Assay. Nitrite concentrations were expressed relative to the mass of testicular tissue. Data are mean ± SEM of three independent experiments, n=4-8, *p<0.05 vs. control (0 µg/ml [D-Trp⁸]-γ₂-MSH) for appropriate treatment group, #p<0.05 between treatment groups indicated on the graph (ANOVA, Tukey).

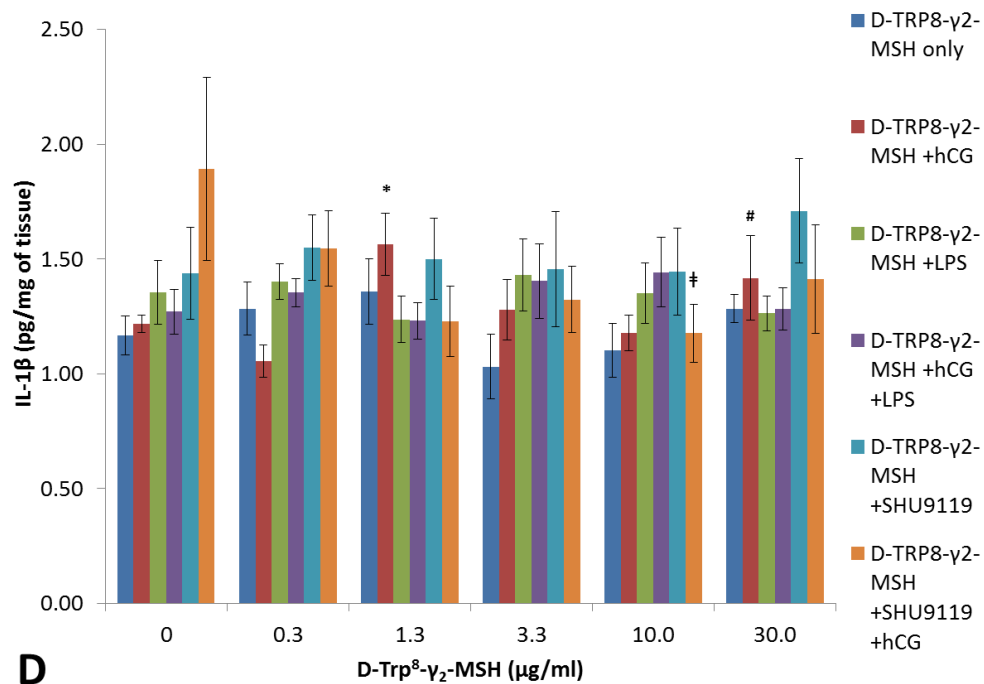
4.3.2.1.3 *In vitro* IL-1 β production by testicular tissue from Balb/c mice.

[D-Trp⁸]- γ ₂-MSH alone or in the presence of LPS and/or hCG had no effect on IL-1 β release from the testicular tissue of Balb/c mice *in vitro* ($p=0.391$ for [D-Trp⁸]- γ ₂-MSH alone; $p=0.836$ for [D-Trp⁸]- γ ₂-MSH +LPS; $p=0.754$ for [D-Trp⁸]- γ ₂-MSH +LPS +hCG; Figure 4.10 B and D). Some differences in IL-1 β concentrations for [D-Trp⁸]- γ ₂-MSH in the presence of hCG have been identified: an increase at 1.3 $\mu\text{g/ml}$ (vs. 0.3 and 10 $\mu\text{g/ml}$ [D-Trp⁸]- γ ₂-MSH +hCG); $p<0.05$; ANOVA, LSD; Figure 4.10 A and D) and 30 $\mu\text{g/ml}$ (vs. 0 $\mu\text{g/ml}$ [D-Trp⁸]- γ ₂-MSH +hCG; $p=0.027$; ANOVA, LSD; Figure 4.10 A and D). In contrast, IL-1 β production was reduced at 10 $\mu\text{g/ml}$ ($p=0.032$) of [D-Trp⁸]- γ ₂-MSH in the presence of SHU9119 and hCG (ANOVA, LSD; Figure 4.10 C and D).





C

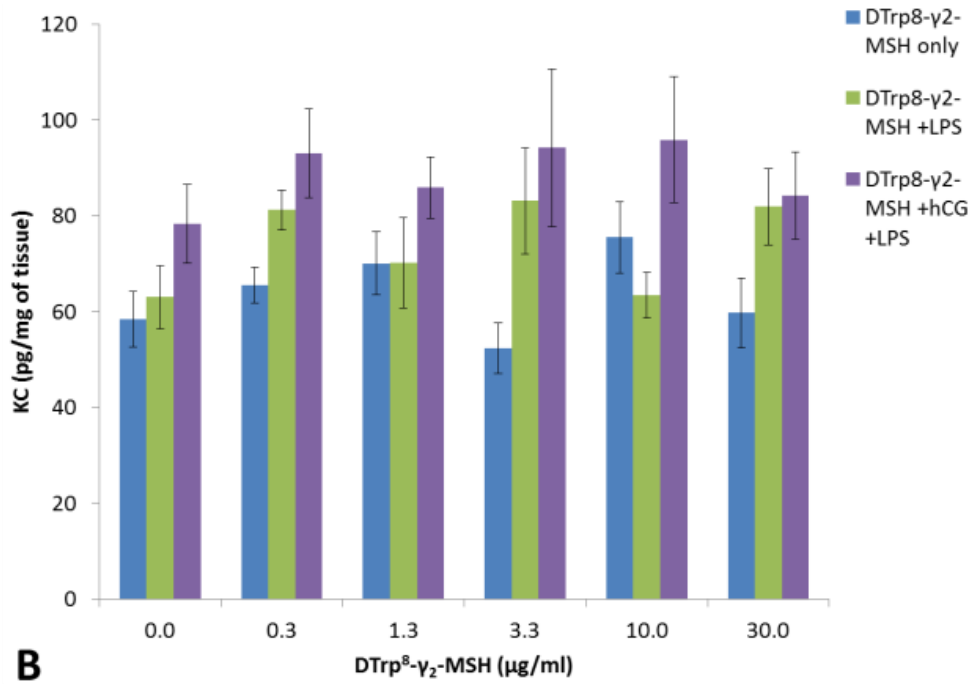
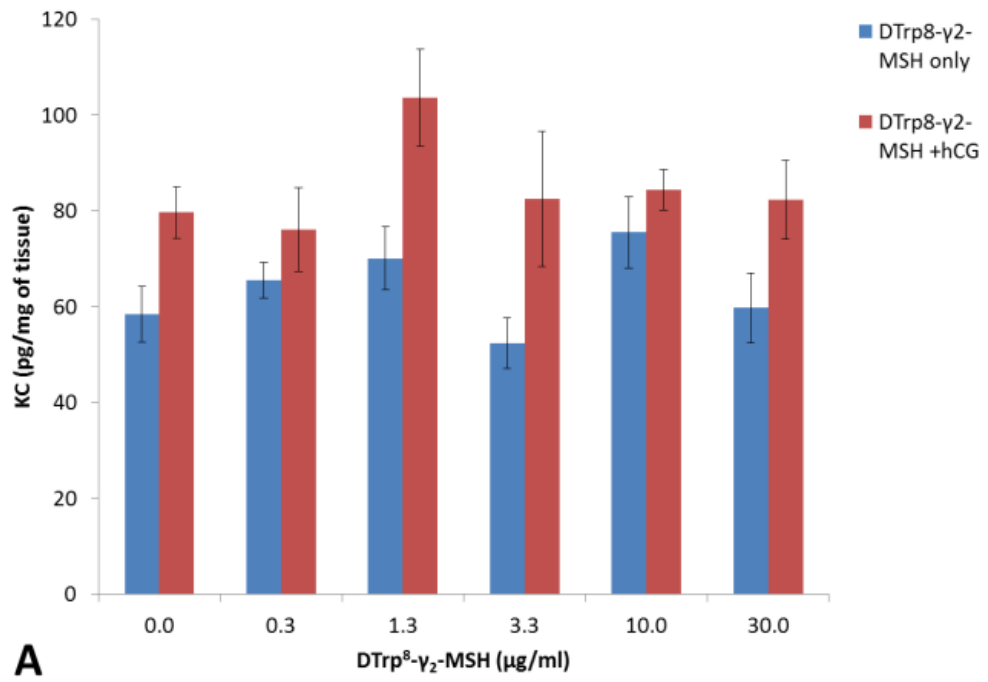


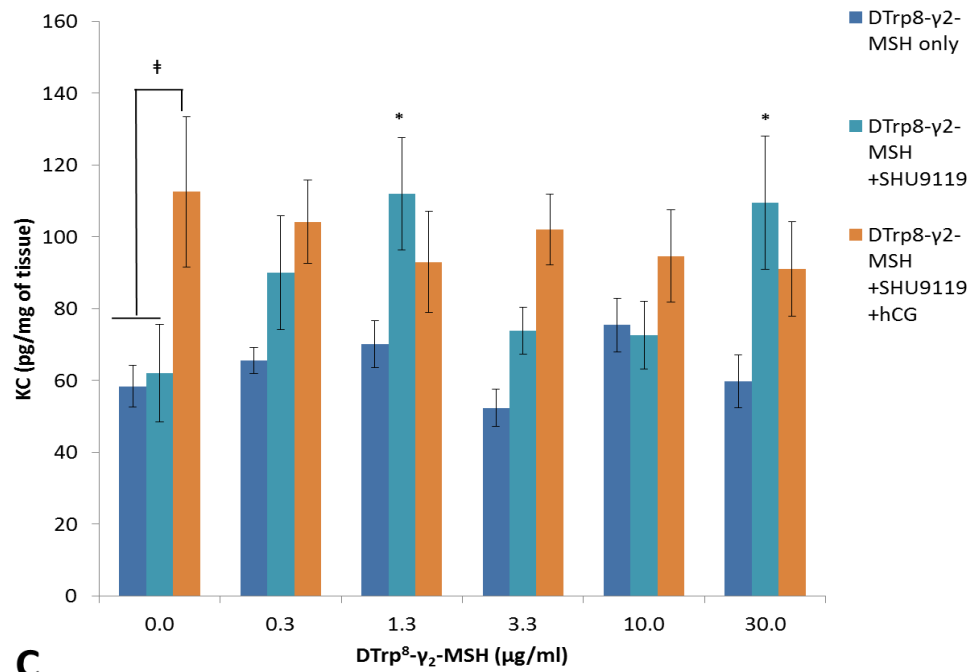
D

Figure 4.10 Effects of [D-Trp⁸]-γ₂-MSH in the presence or absence of SHU9119, LPS and hCG on *in vitro* IL-1β production in Balb/c mice testes. Testes of Balb/c mice were incubated in DMEM in varying concentrations of [D-Trp⁸]-γ₂-MSH (0.3–30 μg/ml) in the presence or absence of SHU9119 (10 μg/ml), LPS (10 μg/ml) and hCG (50 mIU/ml) for 5 h at 35 °C in air, media were assayed by ELISA. IL-1β concentrations were expressed relative to the mass of testicular tissue. Data are mean ± SEM of three independent experiments, n=5-8; *p<0.05 vs. 0.3 and 10 μg/ml [D-Trp⁸]-γ₂-MSH +hCG (ANOVA, LSD); #p=0.027 vs. control (0 μg/ml) [D-Trp⁸]-γ₂-MSH +hCG (ANOVA, LSD); ‡p=0.032 vs. control (0 μg/ml) [D-Trp⁸]-γ₂-MSH +SHU9119 +hCG (ANOVA, LSD).

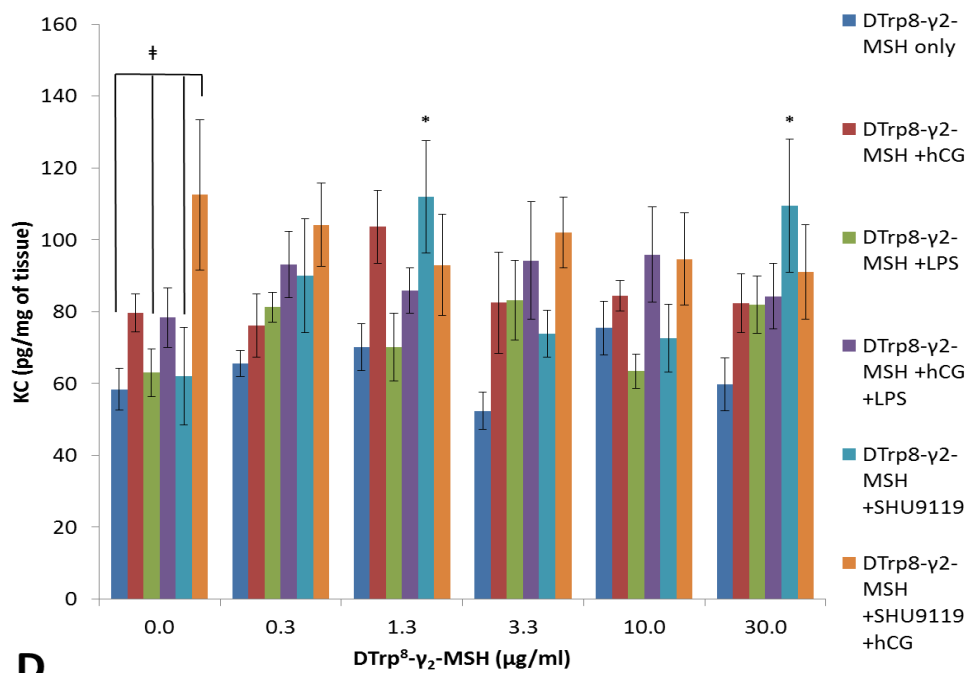
4.3.2.1.4 *In vitro* KC production by testicular tissue from Balb/c mice.

Exposure of the testicular tissue of Balb/c mice to [D-Trp⁸]- γ ₂-MSH (0.3-30.0 μ g/ml) did not affect KC production regardless of the absence or presence of hCG and LPS alone or in combination ([D-Trp⁸]- γ ₂-MSH only, $p=0.12$; [D-Trp⁸]- γ ₂-MSH +hCG, $p=0.342$; [D-Trp⁸]- γ ₂-MSH +LPS, $p=0.219$; [D-Trp⁸]- γ ₂-MSH +LPS +hCG, $p=0.854$; ANOVA; Figure 4.11 A, B, and D). There was a marked increase in KC release from the testicular tissue from Balb/c mice at 1.3 ($p=0.015$) and 30 μ g/ml ($p=0.02$) of [D-Trp⁸]- γ ₂-MSH in the presence of SHU9119 (ANOVA, LSD; Figure 4.11 C and D). SHU9119 with hCG had moderate stimulatory effects on KC production from the testicular tissue of Balb/c mice in the absence of [D-Trp⁸]- γ ₂-MSH ($P<0.05$; ANOVA, Tukey; Figure 4.11 C and D).





C

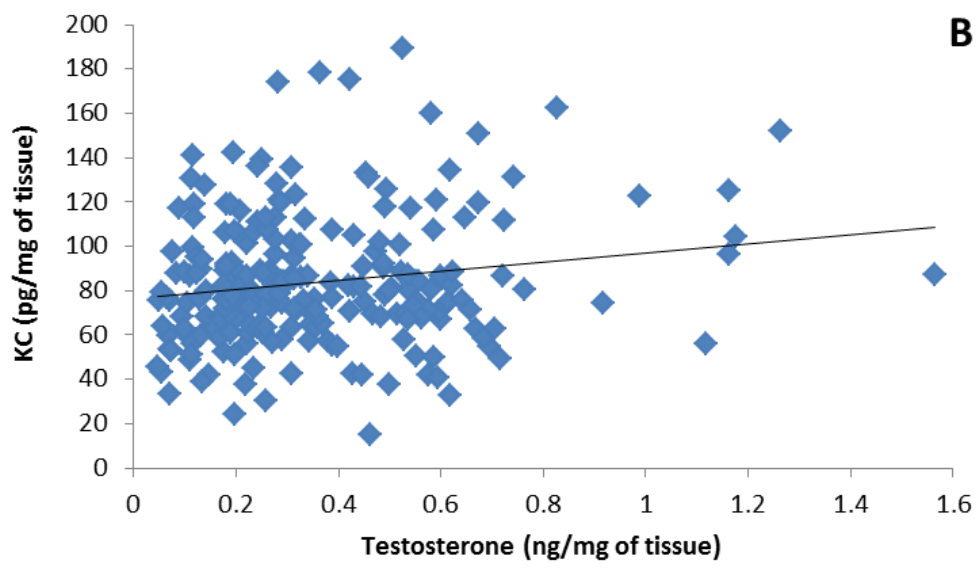
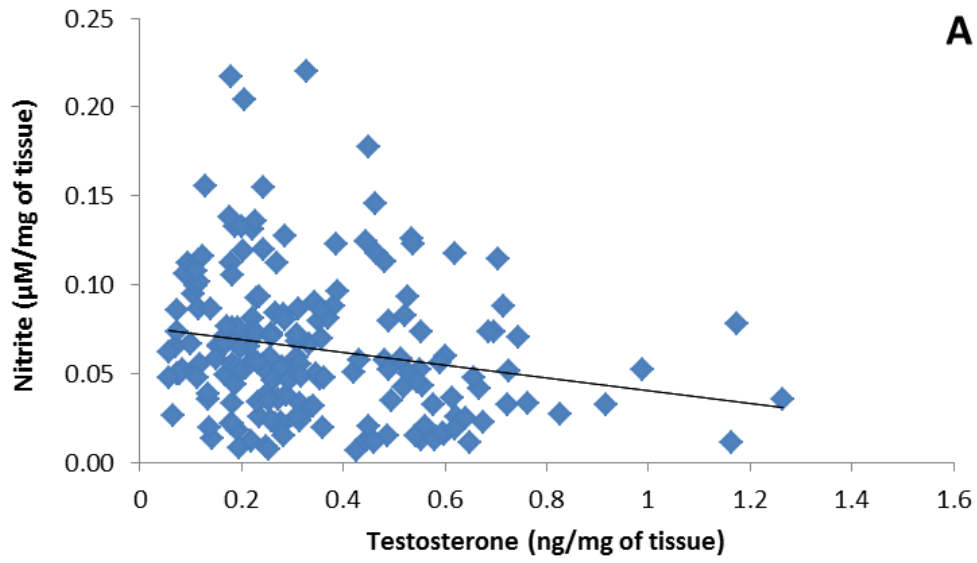


D

Figure 4.10 Effects of [D-Trp⁸]-γ₂-MSH in the presence or absence of SHU9119, LPS and hCG on *in vitro* KC production in Balb/c mice testes. Testes of sexually mature (8-12 weeks) Balb/c mice were hemi-sectioned and incubated in DMEM in varying concentrations of [D-Trp⁸]-γ₂-MSH (0.3–30 µg/ml) in the presence or absence of SHU9119 (10 µg/ml), LPS (10 µg/ml) and hCG (50 mIU/ml) for 5 h at 35 °C in air, media were assayed by ELISA. KC concentrations were expressed relative to the mass of testicular tissues. Data are mean ± SEM of three independent experiments, n=4-8; *p<0.05 vs. control [D-Trp⁸]-γ₂-MSH +SHU9119 (ANOVA, LSD); †p<0.05 between treatment groups indicated on the graph (ANOVA, Tukey).

4.3.2.1.5 Correlations

There was a moderate but significant negative correlation between testosterone and nitrite production from the testicular tissue of Balb/c mice (Pearson correlation coefficients (two-tailed) $r=-0.196$, $n=189$, $p<0.01$; Figure 4.12 A). In contrast, testosterone was positively correlated with KC (Pearson correlation coefficients (two-tailed) $r=0.268$, $n=257$, $p<0.001$; Figure 4.12 B) and IL-1 β (Pearson correlation coefficients (two-tailed) $r=0.419$, $n=257$, $p<0.001$; Figure 4.12 C) in Balb/c mice. A strong positive correlation was established between the two cytokines, KC and IL- 1 β (Pearson correlation coefficients (two-tailed) $r=0.644$, $n=257$, $p<0.001$; Figure 4.12 D). No correlations were observed between nitrite and IL-1 β (Pearson correlation coefficients (two-tailed) $r=-0.026$, $n=188$, $p=0.72$; not shown) or nitrite and KC (Pearson correlation coefficients (two-tailed) $r=-0.137$, $n=189$, $p=0.06$; not shown).



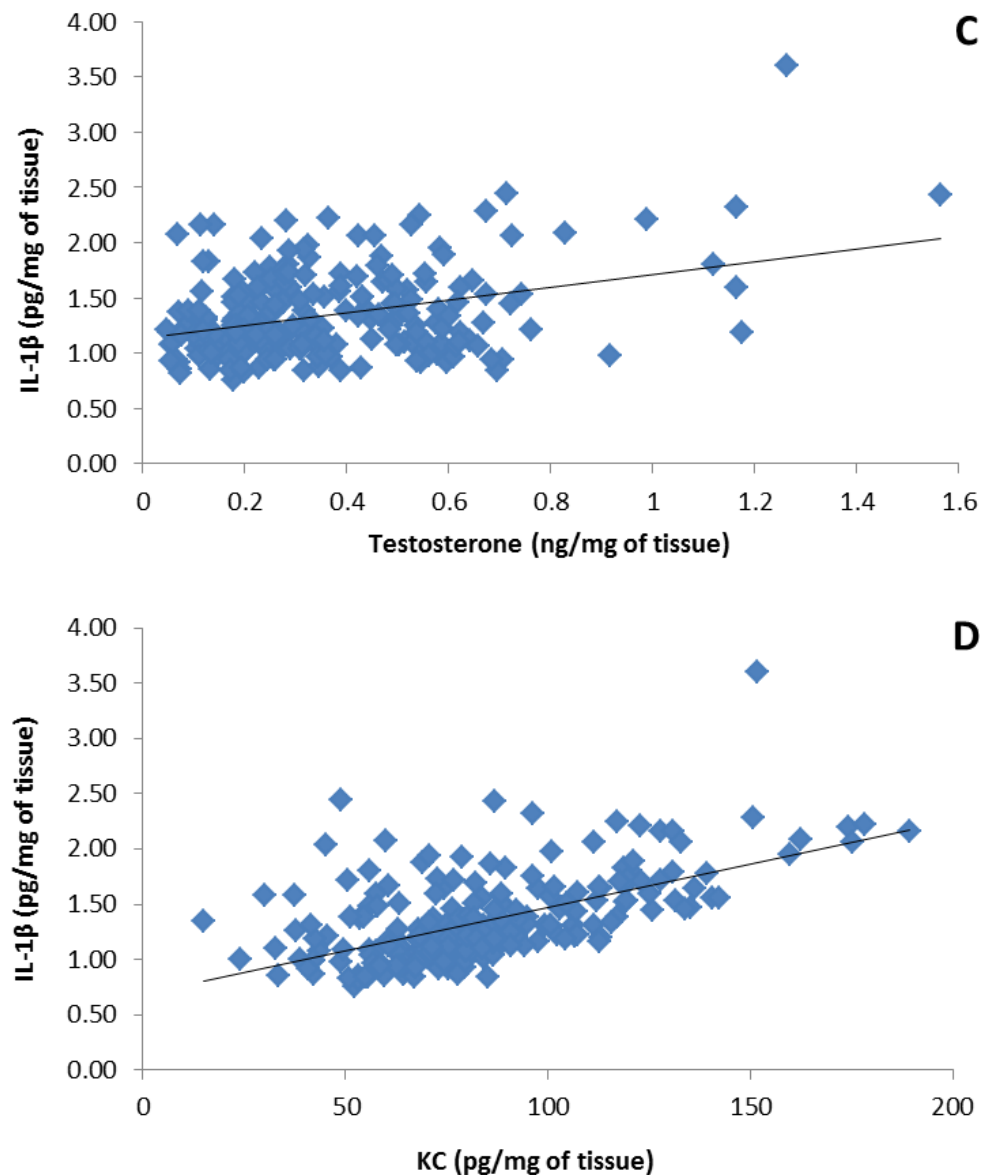
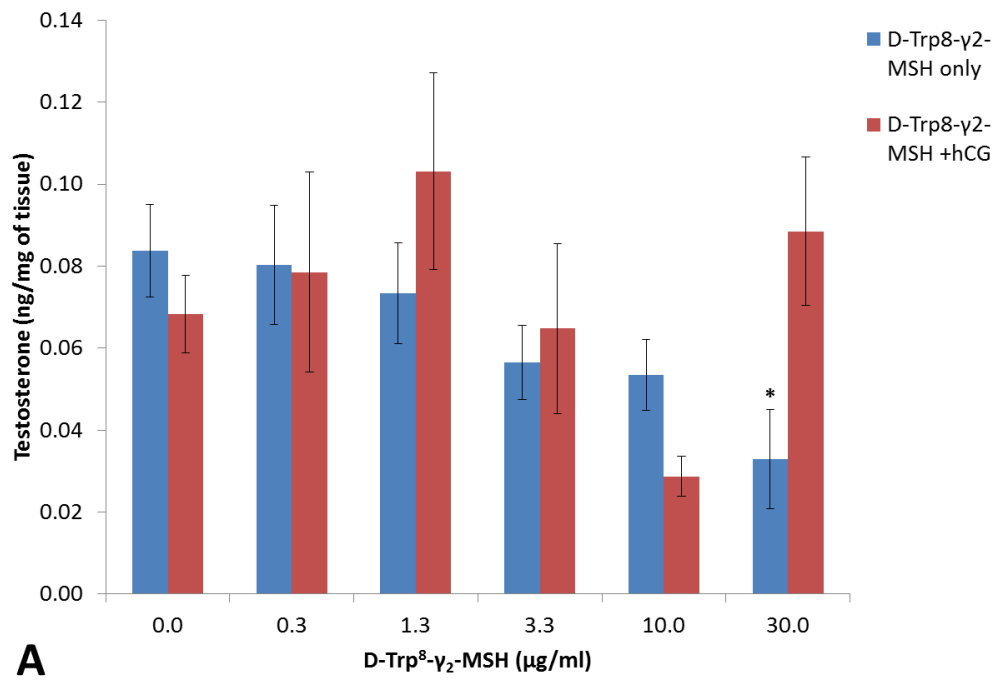


Figure 4.11 Relationship between testosterone, nitrite, KC and IL-1 β release from *in vitro* incubated testicular tissue of Balb/c mice. Testes of sexually mature (8-12 weeks) Balb/c mice were hemi-sected and incubated in DMEM in varying concentrations of [D-Trp⁸]- γ ₂-MSH (0.3–30 μ g/ml) in the presence or absence of SHU9119 (10 μ g/ml), hCG (50 mIU/ml) and LPS (10 μ g/ml) for 5 h at 35 °C in air. Panel A: Correlation between testosterone (ng/mg of tissue) and nitrite (μ M/mg of tissue); Pearson correlation coefficients (two-tailed) $r=-0.196$, $n=189$, $p<0.01$. Panel B: Correlation between testosterone (ng/mg of tissue) and KC (pg/mg of tissue); Pearson correlation coefficients (two-tailed) $r=0.268$, $n=257$, $p<0.001$. Panel C: Correlation between testosterone (ng/mg of tissue) and IL-1 β (pg/mg of tissue); Pearson correlation coefficients (two-tailed) $r=0.419$, $n=257$, $p<0.001$. Panel D: Correlation between IL-1 β (pg/mg of tissue) and KC (pg/mg of tissue); Pearson correlation coefficients (two-tailed) $r=0.644$, $n=257$, $p<0.001$.

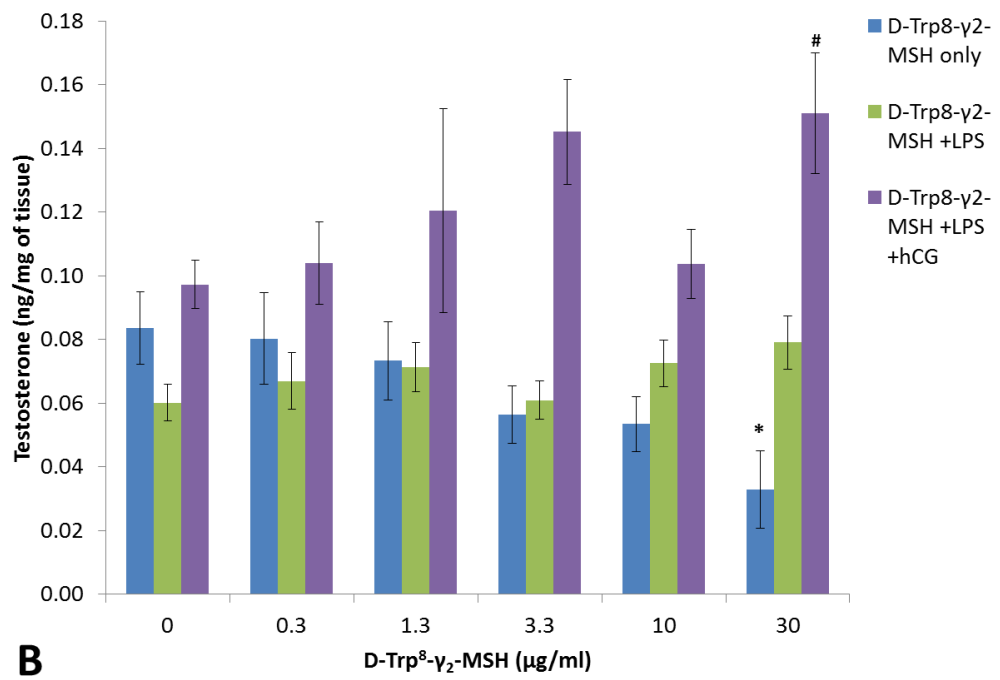
4.3.2.2 C57BL/6 mice

4.3.2.2.1 *In vitro* testosterone production by testicular tissue from C57BL/6 mice.

[D-Trp⁸]- γ ₂-MSH alone had marked inhibitory effects on testosterone production from the testicular tissues of C57BL/6 mice at the highest dose ($p=0.008$ by ANOVA, LSD and $p=0.082$ by ANOVA, Tukey; Figure 4.13 A, B and C). [D-Trp⁸]- γ ₂-MSH with hCG led to 50 % reduction in testosterone release at 10 $\mu\text{g/ml}$ ($p=0.165$, ANOVA, LSD; Figure 4.13 A, C). Exposure of testicular tissues to [D-Trp⁸]- γ ₂-MSH in the presence of LPS had no effect ($p=0.454$, ANOVA; Figure 4.13 B and C), whilst [D-Trp⁸]- γ ₂-MSH in the presence of both LPS and hCG had moderate stimulatory effects on testosterone release ($p=0.042$, ANOVA, LSD; Figure 4.13 B and C).



A



B

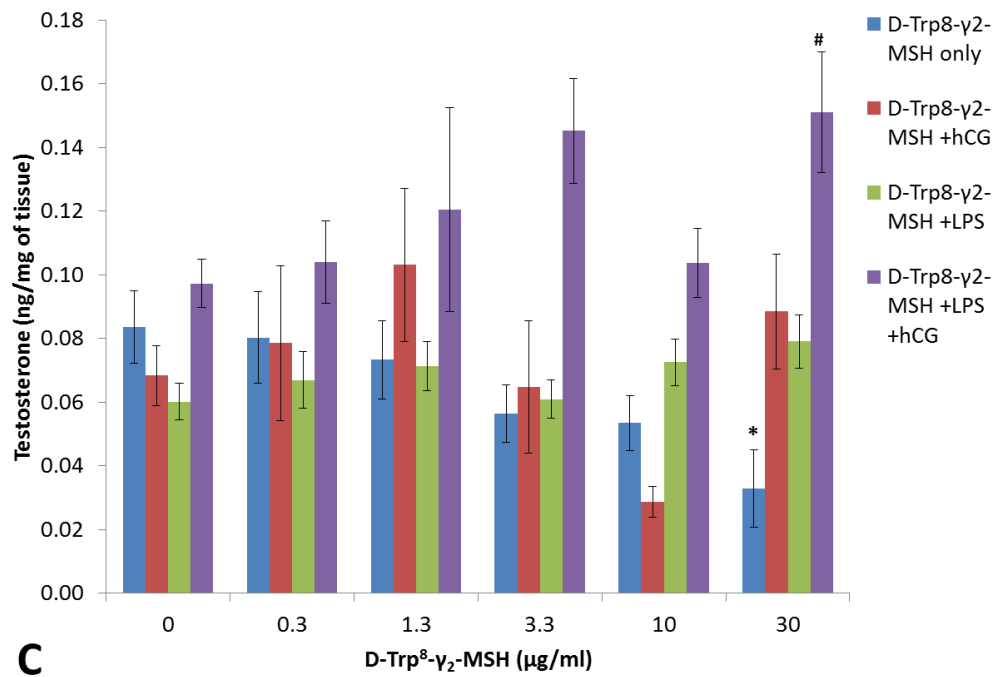
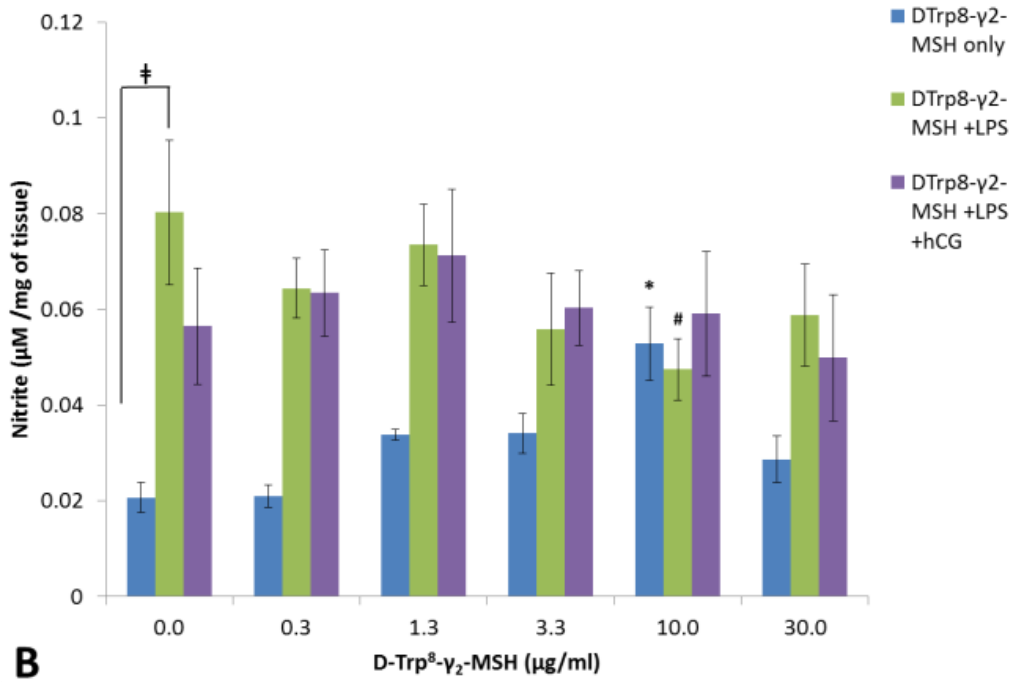
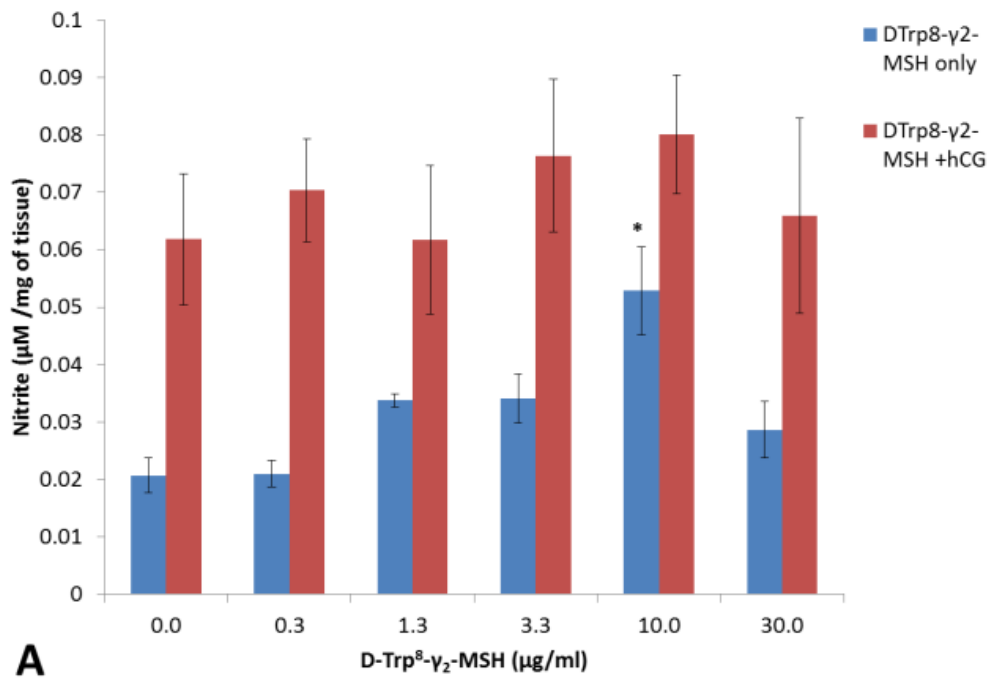


Figure 4.12 Effects of [D-Trp⁸]-γ₂-MSH in the presence or absence of LPS and hCG on *in vitro* testosterone production in C57BL/6 mice testes. Testes of sexually mature (8-12 weeks) C57BL/6 mice were hemi-sectioned and incubated in DMEM in varying concentrations of [D-Trp⁸]-γ₂-MSH (0.3–30 μg/ml) in the presence or absence of LPS (10 μg/ml) and hCG (50 mIU/ml) for 5 h at 35 °C in air, media were assayed by RIA. Testosterone concentrations were expressed relative to the mass of testicular tissue. Data are mean ± SEM of three independent experiments, n=7-15, *p=0.008 vs. control (0 μg/ml [D-Trp⁸]-γ₂-MSH) for [D-Trp⁸]-γ₂-MSH only (ANOVA, LSD); #p=0.042 vs. control (0 μg/ml [D-Trp⁸]-γ₂-MSH) [D-Trp⁸]-γ₂-MSH +hCG +LPS (ANOVA, LSD).

4.3.2.2.2 *In vitro* nitrite production by testicular tissue from C57BL/6 mice.

[D-Trp⁸]- γ ₂-MSH increased nitrite production from the testicular tissues of C57BL/6 mice under basal conditions at 10 μ g/ml ($p=0.03$, ANOVA, Tukey; Figure 4.14 A, B and C). In contrast, [D-Trp⁸]- γ ₂-MSH in the presence of LPS had moderate inhibitory effect on nitrite production at 10 μ g/ml ($p=0.027$, ANOVA, LSD and $p=0.21$, ANOVA, Tukey; Figure 4.14 B and C). [D-Trp⁸]- γ ₂-MSH with hCG and [D-Trp⁸]- γ ₂-MSH with hCG and LPS had no effect on nitrite release from the testicular tissues regardless of compound dose ($p=0.838$ for [D-TRP⁸]- γ ₂-MSH +hCG; $p= 0.862$ for [D-Trp⁸]- γ ₂-MSH +hCG +LPS, ANOVA). LPS markedly increased nitrite production from the testicular tissue of C57BL/6 mice compared to control (0 μ g/ml [D-Trp⁸]- γ ₂-MSH; $p=0.018$, ANOVA, LSD and $p=0.08$, ANOVA, Tukey; Figure 4.14 B and C).



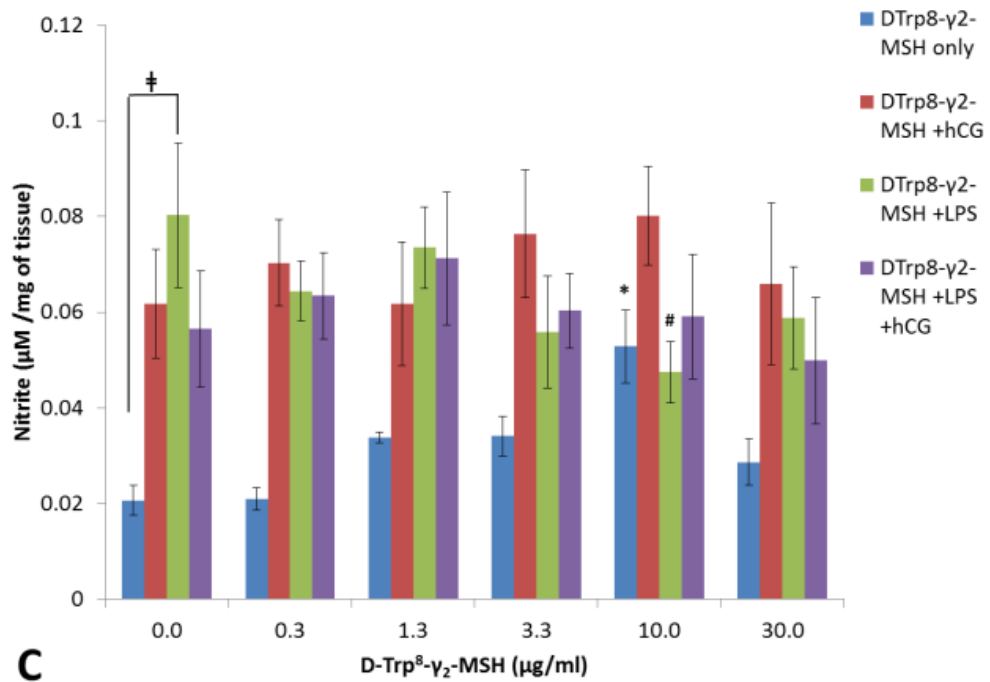
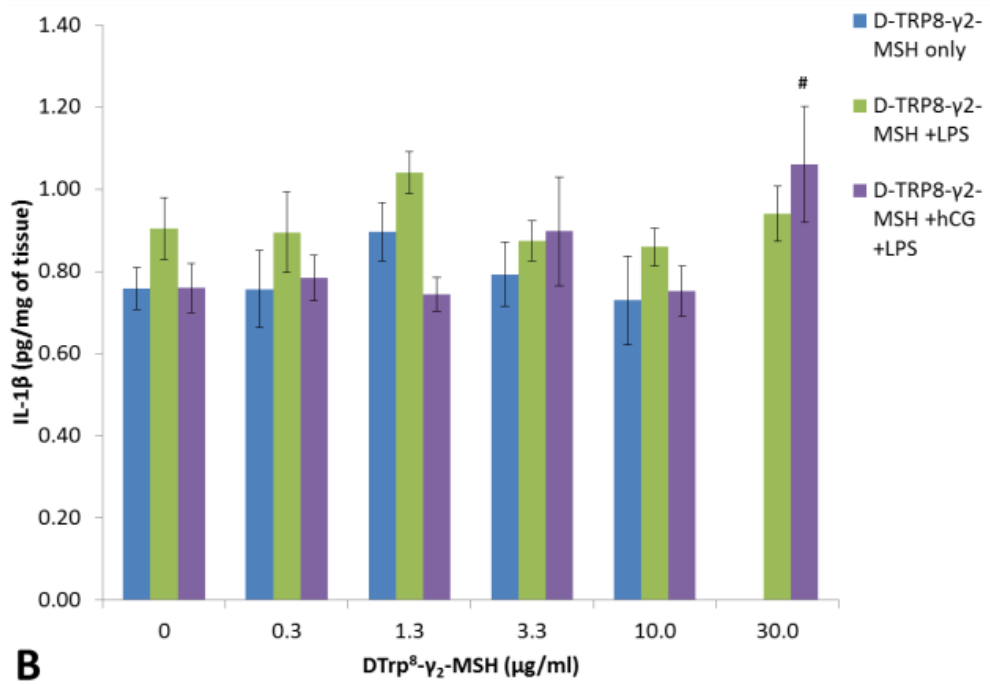
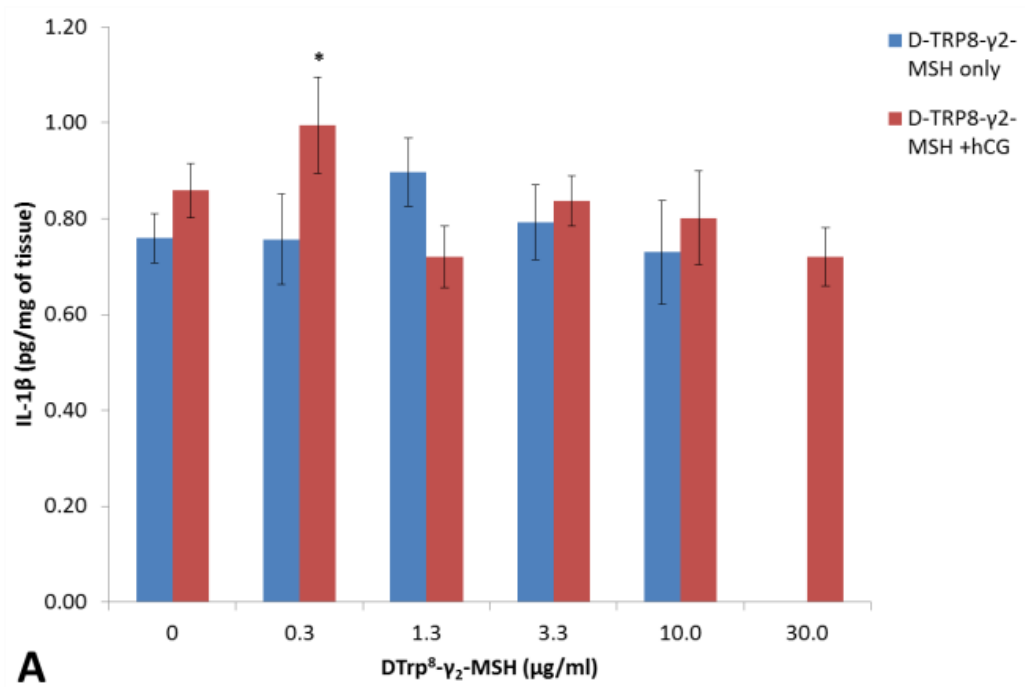


Figure 4.13 Effects of [D-Trp⁸]-γ₂-MSH in the presence or absence of hCG and LPS on *in vitro* nitrite production in C57BL/6 mice testes. Testes of sexually mature (8-12 weeks) C57BL/6 mice were hemi-sected and incubated in DMEM in varying concentrations of [D-Trp⁸]-γ₂-MSH (0.3–30 µg/ml) in the presence or absence of hCG (50 mIU/ml) and LPS (10 µg/ml) for 5 h at 35 °C in air, media were assayed by Griess Assay. Nitrite concentrations were expressed relative to the mass of testicular tissue. Data are mean ± SEM of three independent experiments, n=4-8; *p=0.03 vs. 0 and 0.3 µg/ml [D-Trp⁸]-γ₂-MSH only (ANOVA, Tukey); #p=0.027 vs. 0 µg/ml [D-Trp⁸]-γ₂-MSH +LPS (ANOVA, LSD); †p=0.018 between treatment groups indicated on the graph (ANOVA, LSD).

4.3.2.2.3 *In vitro* IL-1 β production by testicular tissue from C57BL/6 mice.

Exposure of the testicular tissue from C57BL/6 mice to [D-Trp⁸]- γ ₂-MSH (0.3-30.0 μ g/ml) did not affect IL-1 β production regardless of the absence or presence of LPS ([D-Trp⁸]- γ ₂-MSH only, $p=0.685$; [D-Trp⁸]- γ ₂-MSH +LPS, $p=0.455$; ANOVA; Figure 4.15 A, B, and C). There was an increase in IL-1 β release from the testicular tissue of C57 BL/6 mice at 0.3 and 30 μ g/ml of [D-Trp⁸]- γ ₂-MSH in the presence hCG ($p=0.013$, ANOVA, LSD) and [D-Trp⁸]- γ ₂-MSH in combination with hCG and LPS ($p=0.024$, ANOVA, LSD), respectively (Figure 4.15 A, B and C).



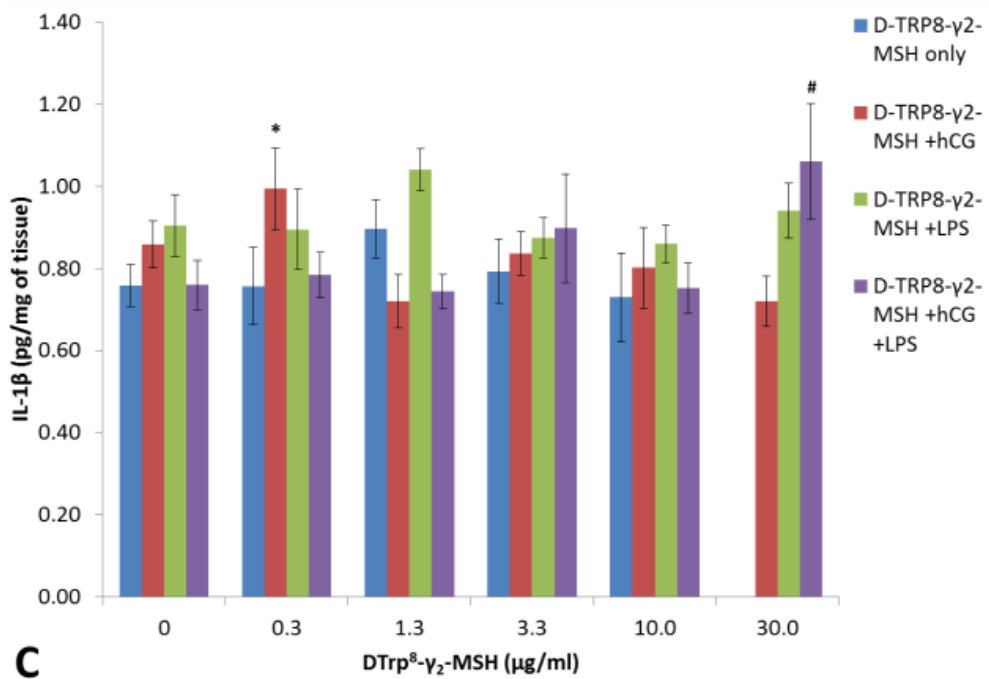
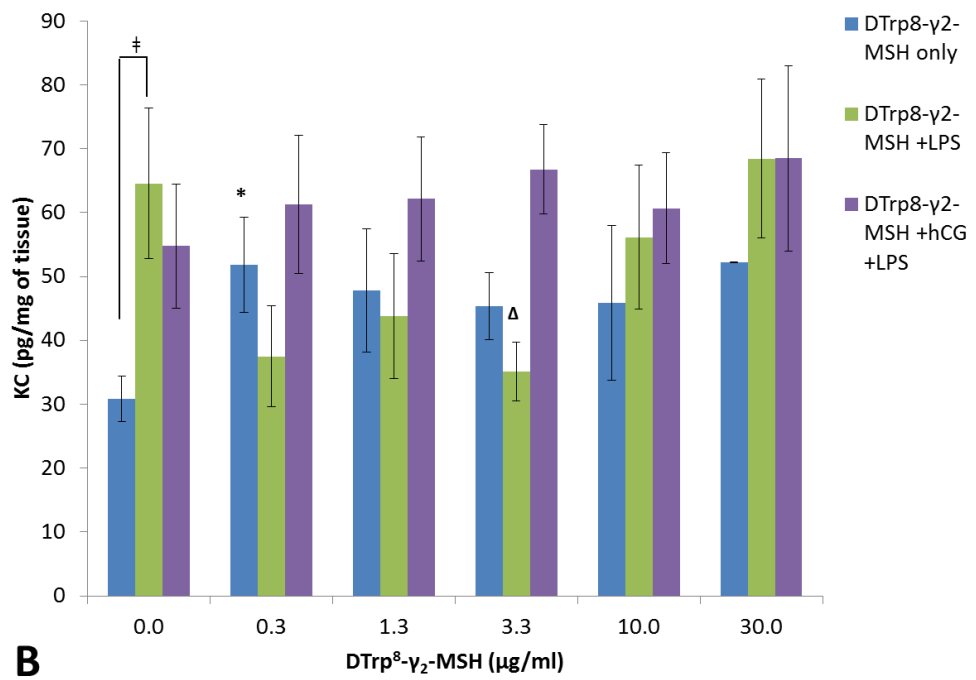
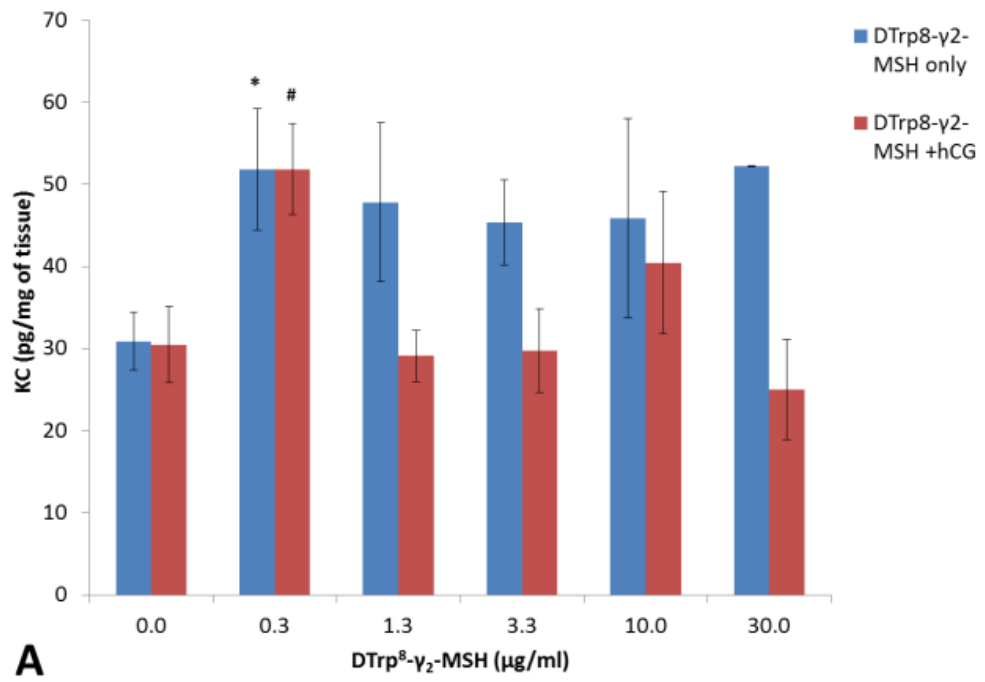


Figure 4.14 Effects of [D-Trp⁸]-γ₂-MSH in the presence or absence of hCG and LPS on *in vitro* IL-1β production in C57BL/6 mice testes. Testes of sexually mature (8-12 weeks) C57BL/6 mice were hemi-sectioned and incubated in DMEM in varying concentrations of [D-Trp⁸]-γ₂-MSH (0.3–30 μg/ml) in the presence or absence of hCG (50 mIU/ml) and LPS (10 μg/ml) 5 h at 35 °C in air, media were assayed by ELISA. IL-1β concentrations were expressed relative to the mass of testicular tissue. Data are mean ± SEM of three independent experiments, n=4-12; *p=0.013 vs. 1.3 and 30 μg/ml [D-Trp⁸]-γ₂-MSH +hCG (ANOVA, LSD); #p=0.024 vs. 0, 0.3, 1.3 and 10 μg/ml [D-Trp⁸]-γ₂-MSH +hCG +LPS (ANOVA, LSD).

4.3.2.2.4 *In vitro* KC production by testicular tissue from C57BL/6 mice.

[D-Trp⁸]- γ ₂-MSH alone and in the presence of hCG markedly increased KC release from the testicular tissue of C57BL/6 mice at 0.3 μ g/ml of compound ($p < 0.05$, ANOVA, LSD; Figure 4.16 A, B and C). In the presence of LPS there was a decrease in KC production at 3.3 μ g/ml of [D-Trp⁸]- γ ₂-MSH ($p < 0.05$, ANOVA, LSD; Figure 4.16 A, B and C). [D-Trp⁸]- γ ₂-MSH in combination with LPS and hCG had no effect on KC release from the testicular tissue of C57BL/6 mice ([D-Trp⁸]- γ ₂-MSH +LPS +hCG, $p = 0.951$, ANOVA; Figure 4.16 A, B and C). LPS alone increased KC production compared to control (0 μ g/ml [D-Trp⁸]- γ ₂-MSH, media only) or hCG alone (0 μ g/ml [D-Trp⁸]- γ ₂-MSH +hCG; $p = 0.007$, ANOVA, LSD and $p = 0.069$, ANOVA, Tukey; Figure 4.16 C).



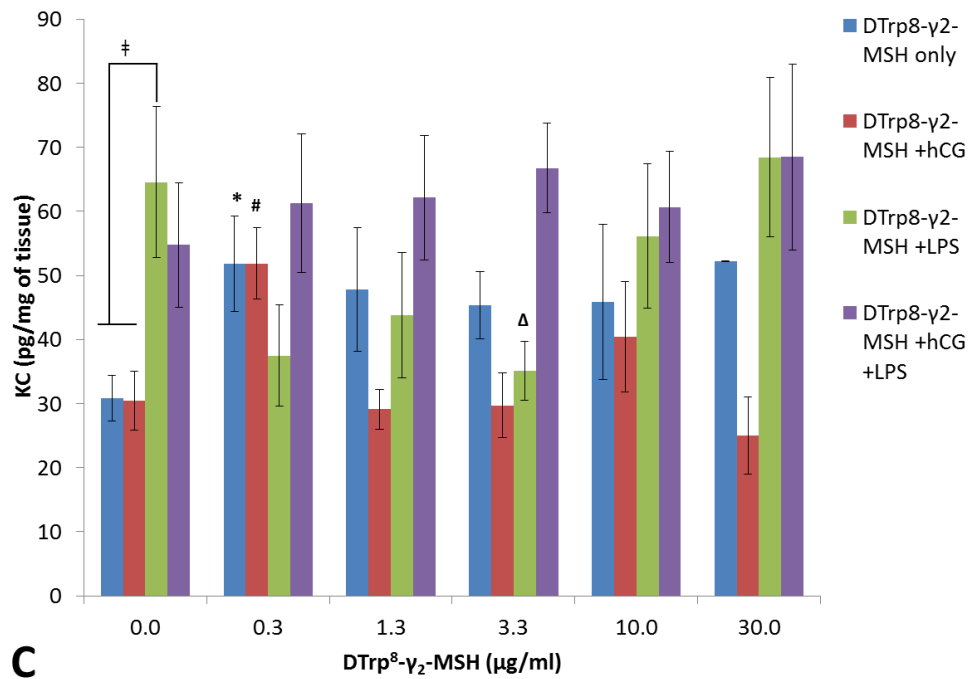
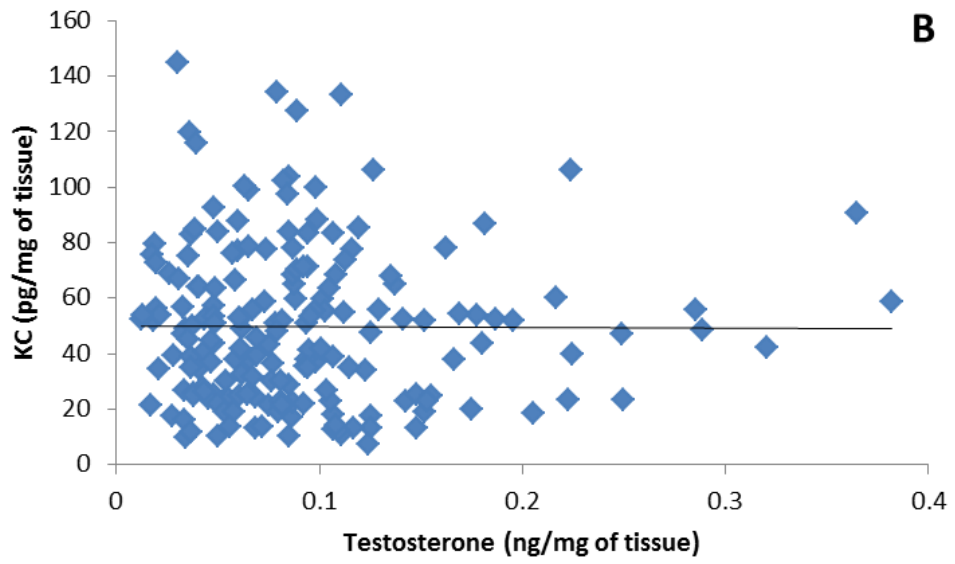
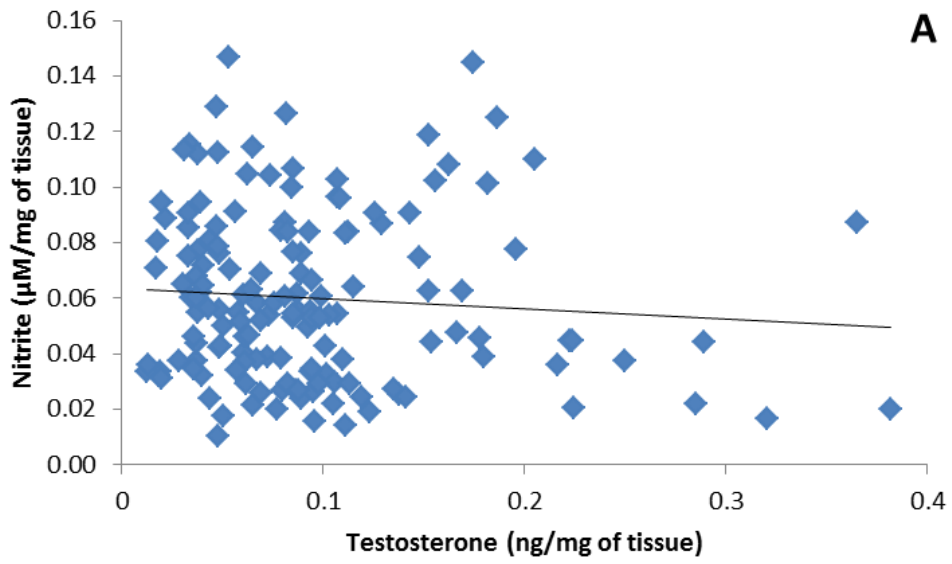


Figure 4.15 Effects of [D-Trp⁸]-γ₂-MSH in the presence or absence of LPS and hCG on *in vitro* KC production in C57BL/6 mice testes. Testes of sexually mature (8-12 weeks) C57BL/6 mice were hemi-sectioned and incubated in DMEM in varying concentrations of [D-Trp⁸]-γ₂-MSH (0.3–30 µg/ml) in the presence or absence of hCG (50 mIU/ml) and LPS (10 µg/ml) for 5 h at 35 °C in air, media were assayed by ELISA. KC concentrations were expressed relative to the mass of testicular tissue. Data are mean ± SEM of three independent experiments, n=4-8; *p<0.03 vs. 0 µg/ml [D-Trp⁸]-γ₂-MSH only (ANOVA, LSD); # p<0.05 vs. 0, 1.3, 3.3 and 30 µg/ml [D-Trp⁸]-γ₂-MSH +hCG (ANOVA, LSD); Δp<0.05 vs. 0 and 30 µg/ml [D-Trp⁸]-γ₂-MSH +LPS (ANOVA, LSD); ‡p<0.05 between treatment groups indicated on the graph (ANOVA, LSD).

4.3.2.2.5 Correlations

There was no correlation between testosterone and nitrite (Pearson correlation coefficients (two-tailed) $r=-0.08$, $n=151$, $p=0.33$; Figure 4.17 A) or testosterone and KC production from testicular tissue of C57BL/6 mice (Pearson correlation coefficients (two-tailed) $r=-0.005$, $n=164$, $p=0.94$; Figure 4.17 B). In contrast, testosterone was negatively correlated with IL-1 β (Pearson correlation coefficients (two-tailed) $r=-0.16$, $n=164$, $p=0.037$; Figure 4.17 C). Similarly to Balb/c, a strong positive correlation was established between the two cytokines, KC and IL- 1 β produced from the testicular tissue of C57BL/6 mice (Pearson correlation coefficients (two-tailed) $r=0.4$, $n=164$, $p<0.001$; Figure 4.17 D). There are no correlations between nitrite and IL-1 β (Pearson correlation coefficients (two-tailed) $r=0.048$, $n=132$, $p=0.58$; not shown) nor nitrite and KC production (Pearson correlation coefficients (two-tailed) $r=-0.132$, $n=151$, $p=0.11$; not shown).



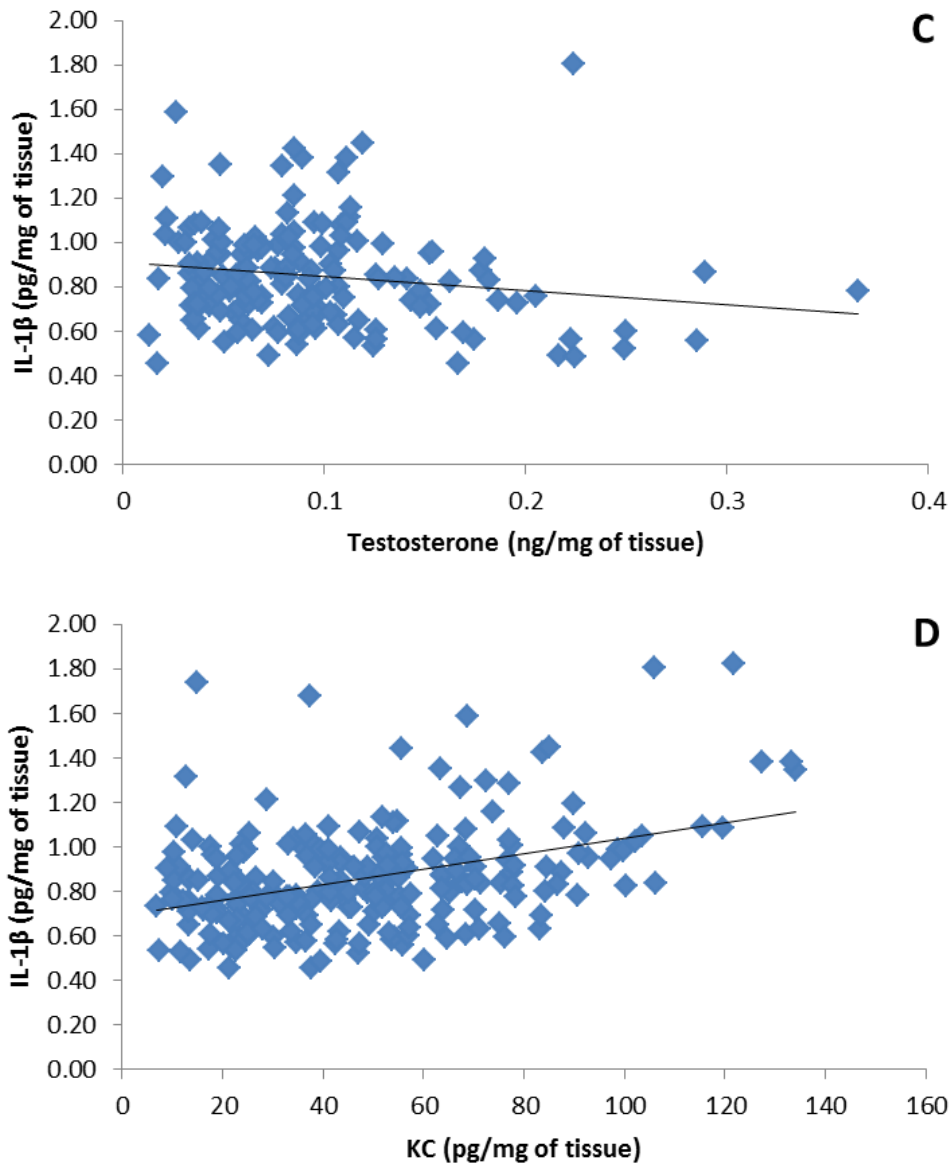
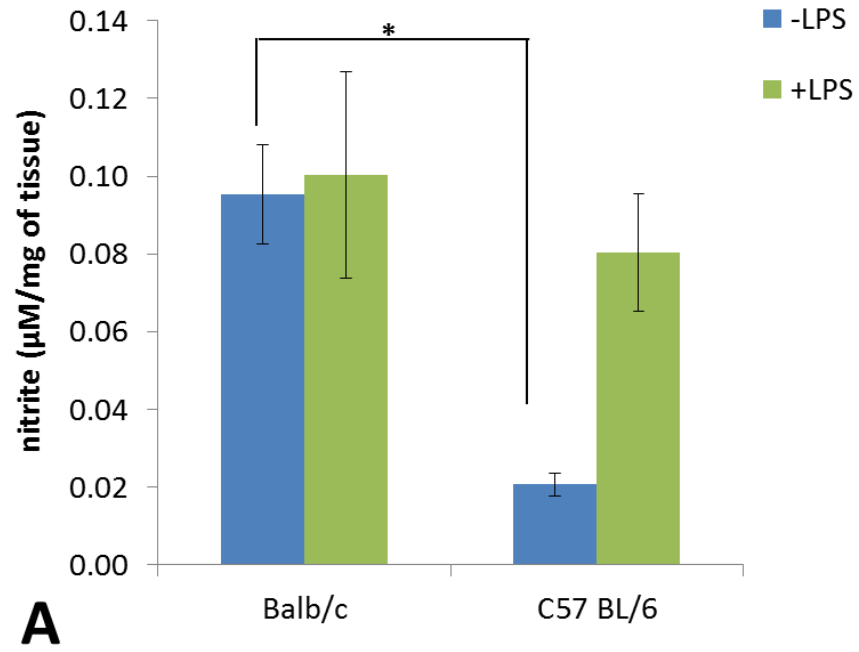


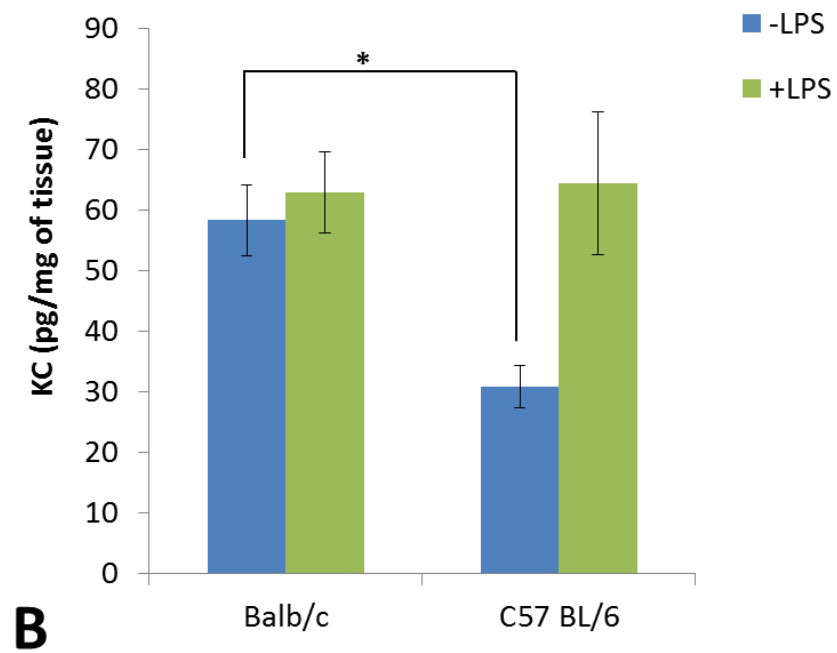
Figure 4.16 Relationship between testosterone, nitrite, KC and IL-1 β release from *in vitro* incubated testes of C57BL/6 mice. Testes of sexually mature (8-12 weeks) C57BL/6 mice were hemi-sected and incubated in DMEM in varying concentrations of [D-Trp⁸]- γ 2-MSH (0.3–30 μ g/ml) in the presence or absence of SHU9119 (10 μ g/ml), hCG (50 mIU/ml) and LPS (10 μ g/ml) for 5 h at 35 °C in air. Panel A: Correlation between testosterone (ng/mg of tissue) and nitrite (μ M/mg of tissue); Pearson correlation coefficients (two-tailed) $r = -0.08$, $n = 151$, $p = 0.33$. Panel B: Correlation between testosterone (ng/mg of tissue) and KC (pg/mg of tissue); Pearson correlation coefficients (two-tailed) $r = -0.005$, $n = 164$, $p = 0.94$. Panel C: Correlation between testosterone (ng/mg of tissue) and IL-1 β (pg/mg of tissue); Pearson correlation coefficients (two-tailed) $r = -0.16$, $n = 164$, $p = 0.037$. Panel D: Correlation between IL-1 β (pg/mg of tissue) and KC (pg/mg of tissue); Pearson correlation coefficients (two-tailed) $r = 0.4$, $n = 164$, $p < 0.001$.

4.3.3 Comparison of nitrite and cytokine production by LPS-stimulated testicular tissues of Balb/c and C57BL/6 mice.

Significant differences in basal nitrite, KC and IL-1 β production as well as in response to a mild inflammatory stimulus in the form of LPS (10 μ g/ml), from testicular tissues were measured between Balb/c and C57BL/6 mice. Balb/c mice had significantly greater basal production of nitrite, KC and IL-1 β compared to C57BL/6 mice ($p < 0.05$, t -test; Figure A, B and C). However, testicular tissue of Balb/c mice did not respond to treatment with LPS ($p < 0.05$, t -test; Figure A, B and C) In contrast, testicular tissue of C57BL/6 significantly increase production of both nitrite and KC in response to LPS ($p < 0.05$, ANOVA, LSD; Figure 20 C and 22 C). A summary of all of the effects of [D-Trp⁸]- γ ₂-MSH on testosterone and inflammatory markers production by the testicular tissue of C57BL/6 and Balb/c mice under various treatment conditions is presented in Table 4.3 and 4.4.



A



B

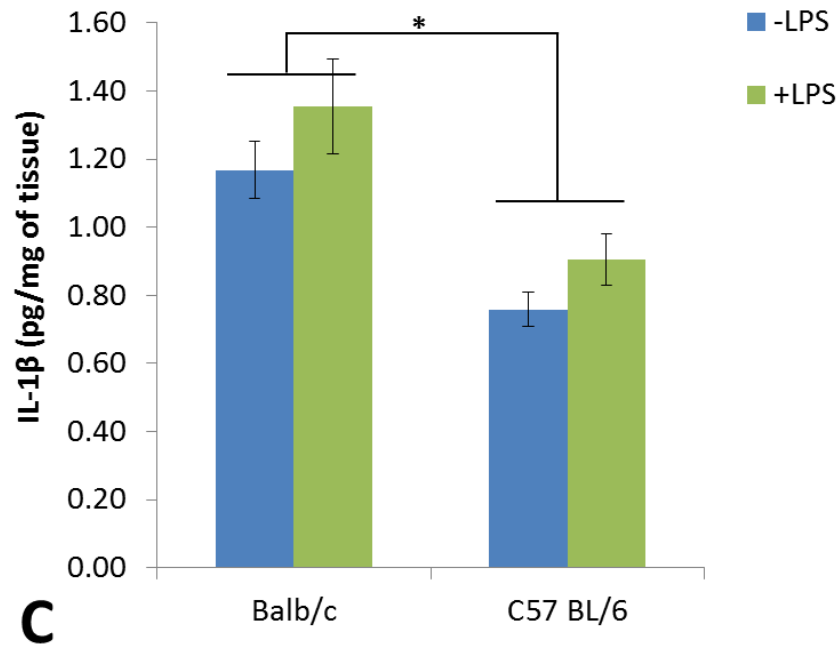


Figure 4.17 Effects of LPS (10 $\mu\text{g/ml}$) on *in vitro* nitrite and cytokines production in testicular tissue of Balb/c and C57BL/6 mice. Testes of sexually mature (8-12 weeks) C57BL/6 and Balb/c mice were hemi-sectioned and incubated in DMEM in the presence or absence of LPS (10 $\mu\text{g/ml}$) for 3 h at 35 $^{\circ}\text{C}$ in air. The concentration of nitrite and cytokines released into the media was expressed relative to the mass of testicular tissue. Data are mean \pm SEM of 4-6 independent experiments. Panel A – nitrite, $p < 0.01$ for Balb/c vs. C57BL/6 (-LPS), $n = 3-4$ (t -test). Panel B – KC, $p < 0.01$ for Balb/c vs. C57BL/6 (-LPS), $n = 8-14$ (t -test). Panel C – IL-1 β , $p < 0.02$ for Balb/c vs. C57BL/6 (-LPS and +LPS), $n = 8-12$ (t -test).

Strain	(treatment group) [D-Trp ⁸]- γ ₂ -MSH	product measured			
		Testosterone	Nitrite	IL-1 β	KC
Balb/c		Figure 4.8	Figure 4.9	Figure 4.10	Figure 4.11
	(1) [D-Trp ⁸]- γ ₂ -MSH alone	-	↓↓	-	-
	(2) +hCG	-	-	↑	-
	(3) +LPS	-	↓↓	-	-
	(4) +hCG +LPS	-	-	-	-
	(5) +SHU9119	-	↓↓	-	↑
	(6) +SHU9119 +hCG	-	-	↓	-
C57BL/6		Figure 4.13	Figure 4.14	Figure 4.15	Figure 4.16
	(1) [D-Trp ⁸]- γ ₂ -MSH alone	↓	↑↑	-	↑↑
	(2) +hCG	↓	-	-	↑
	(3) +LPS	-	↓	-	↑/↓
	(4) +hCG +LPS	↑	-	↑	-

Table 4.3 Effects of [D-Trp⁸]- γ ₂-MSH on testosterone, nitrite, IL-1 β and KC production by testicular tissue of Balb/c and C57BL/6 mice under various treatment conditions. - =no effect; ↑=slight stimulatory effect (non-significant); ↑↑=stimulatory effect; ↑↑↑= strong stimulatory effect; ↓=slight inhibitory effect (non-significant); ↓↓=inhibitory effect; ↓↓↓=strong inhibitory effect; ↑/↓=effect depends on compound concentration.

strain	treatment type	product measured			
		testosterone	nitrite	IL-1 β	KC
Balb/c		Figure 4.8	Figure 4.9	Figure 4.10	Figure 4.11
	hCG	↑	-	-	-
	LPS	↑	-	-	-
	hCG & LPS	↑↑	↓↓↓	-	-
	SHU9119	↑↑↑	-	-	-
	SHU9119 & hCG	↑↑↑	↓↓	↑	↑↑↑
C57BL/6		Figure 4.13	Figure 4.14	Figure 4.15	Figure 4.16
	hCG	-	↑↑	-	-
	LPS	-	↑↑↑	-	↑↑↑
	hCG & LPS	-	↑↑	-	↑↑

Table 4.4 Effects of various treatments on testosterone, nitrite, IL-1 β and KC production by testicular tissue of Balb/c and C57BL/6 mice. Treatments were compared against appropriate control, in the absence of compounds.- =no effect; ↑=slight stimulatory effect (non-significant); ↑↑=stimulatory effect; ↑↑↑= strong stimulatory effect; ↓=slight inhibitory effect (non-significant); ↓↓=inhibitory effect; ↓↓↓=strong inhibitory effect.

4.3.4 The K9 Leydig cell line

4.3.4.1 Relative mRNA expressions of MC in the K9 Leydig cell line

The mRNA expressions of all MC were identified in the K9 Leydig cell line. There appeared to be no significant differences in the mRNA expression levels between the receptors (Figure 4.19). The origin of the cell line was confirmed by detection of 3β -HSD mRNA, an enzyme involved in steroidogenesis and normally expressed by Leydig cells (Figure 4.20 A). The cell line also expressed iNOS (inducible nitric oxide synthase) enzyme in normal and LPS-treated cells, which indicates the ability of the K9 Leydig cells to produce nitric oxide (Figure 4.20 B).

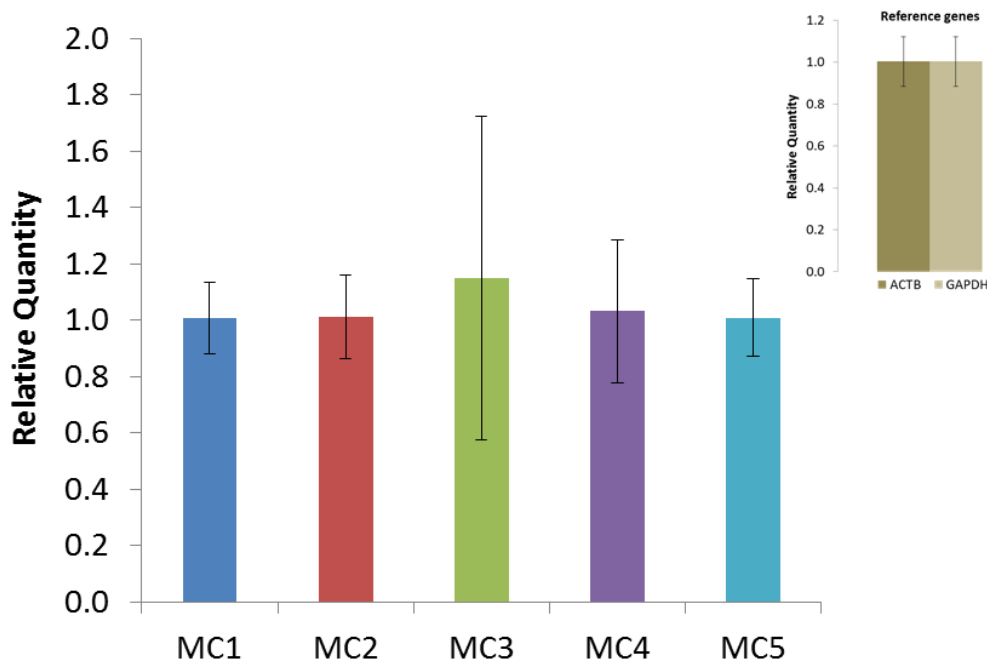


Figure 4.18 Relative mRNA expression of MC in the K9 Leydig cell line. Relative expression was determined by qPCR and results were analysed using qBase plus software including target specific amplification efficiencies. Data normalisation was performed using geometric mean of two most stable reference genes for this experimental setting, namely GAPDH and ACTB (inset in the top right corner). The average relative expression level of ACTB and GAPDH in all K9 cells samples is shown in the inset (explanation for calculation can be found on p. 67). To ensure accurate estimation of gene of interest (GOI) expression, the specificity of qRT-PCR was tested in reactions without reverse transcriptase (SuperScript; no-RT control). Data are presented as mean \pm SEM of two independent qRT-PCRs; no statistical differences were determined between the groups (ANOVA, Tukey).

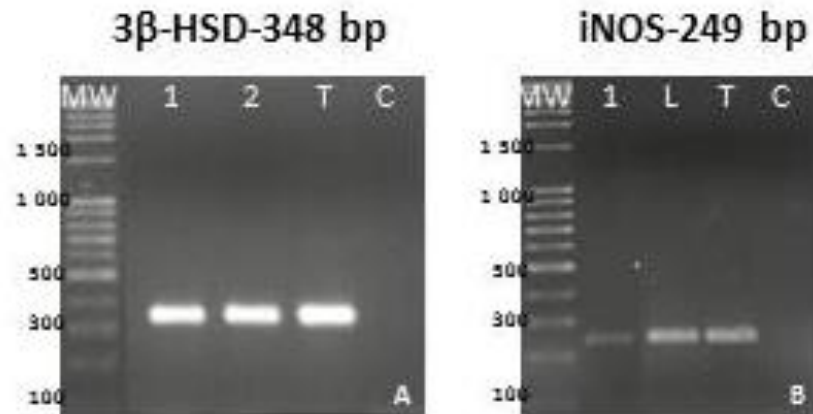


Figure 4.19 3β-HSD and iNOS mRNA expression in the K9 Leydig cell line. Panel A – RT-PCR for 3β-HSD (Leydig cells marker) mRNA. Expected product length is 348 bp. Panel B - RT-PCR for iNOS (inflammatory marker). Expected product length is 249 bp. In both panels: MW= molecular weight marker, 1=K9 cell line 1, 2=K9 cell line 2, L=LPS-treated K9 cells, T=testis, C=control, no cDNA. No PCR products were detected in parallel control samples using mRNA preparations without Super Script-reverse transcriptase. Amplification products were separated on 2 % agarose gel. Representative images of two independent PCRs.

4.3.4.2 Effects of γ_2 -MSH on *in vitro* nitrite production of the LPS-stimulated K9 Leydig cell line.

The highest concentrations of nitrite released were induced by 1 $\mu\text{g/ml}$ of LPS (Figure 4.21), hence this dose was applied in further experiments. LPS (1 $\mu\text{g/ml}$) significantly increased nitrite release compared to the untreated cells (Figure 4.22). Since mRNA expressions of all MC were identified in the K9 Leydig cell line, γ_2 -MSH, a high potency agonist at MC_3 , was used to determine the effects of MC_3 activation. There were significant reductions in nitrite concentrations in response to all doses of γ_2 -MSH ($p < 0.05$ for control vs. all other groups; ANOVA, Tukey; Figure 4.22).

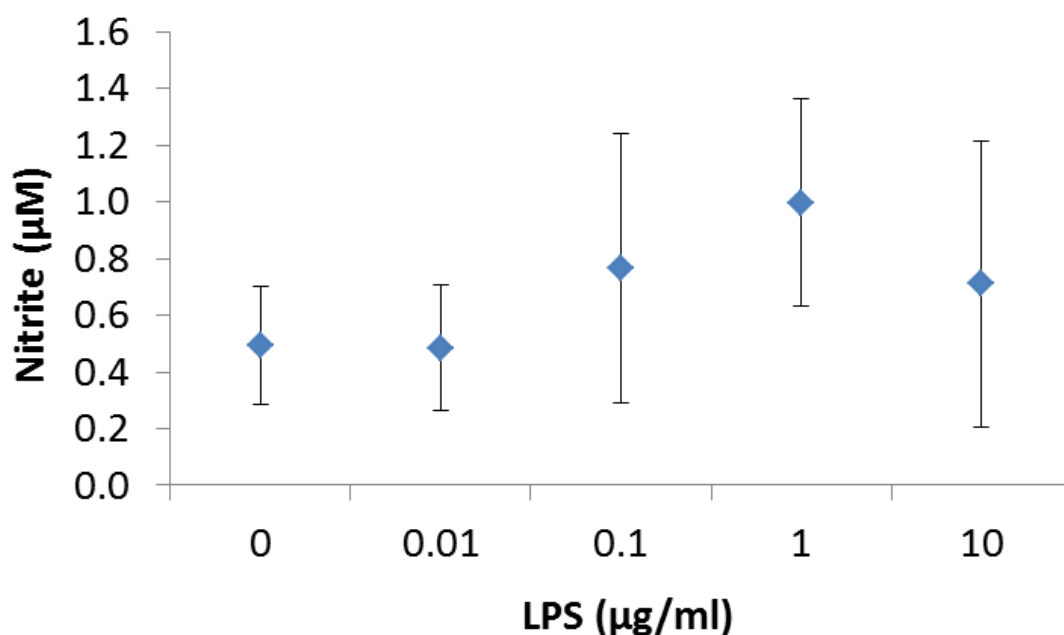


Figure 4.20 Dose response effect of LPS on nitrite release by the K9 Leydig cell line. K9 Leydig cells were stimulated with various concentrations of LPS (0.01–10 $\mu\text{g/ml}$) for 6 h at 37 $^{\circ}\text{C}$ in 5 % CO_2 and 95 % O_2 incubator. After incubation, media were collected and assayed for nitrite by Griess assay. Data are mean \pm SD of one experiment.

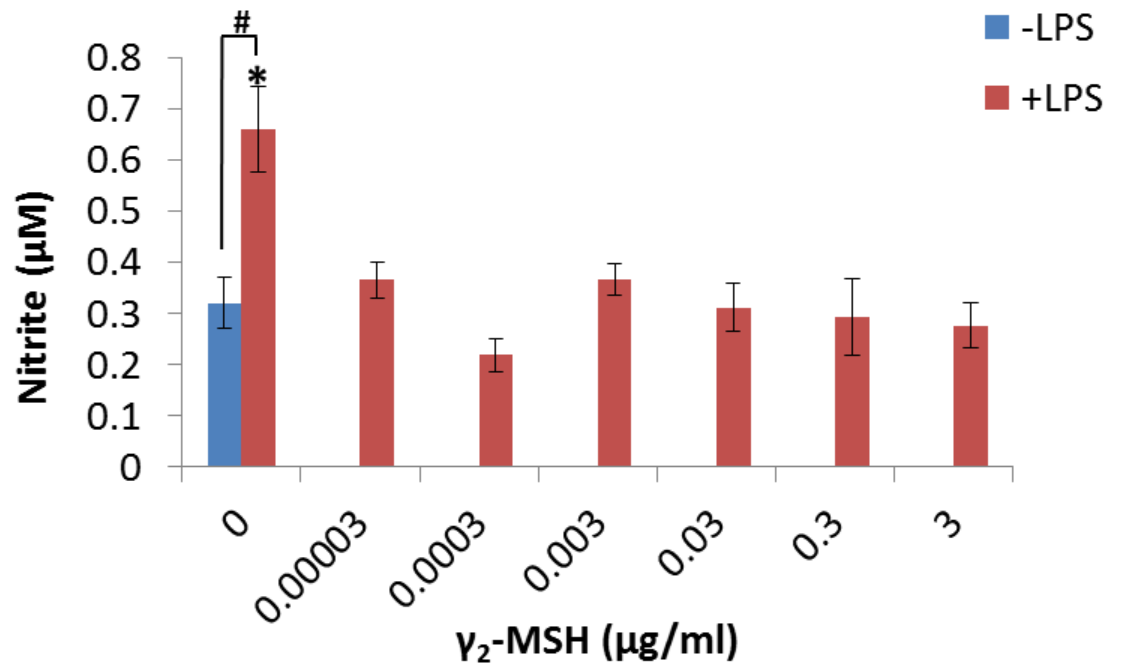


Figure 4.21 Effects of γ_2 -MSH on LPS-induced nitrite release by the K9 Leydig cell line. The K9 Leydig cells were treated with various concentrations of γ_2 -MSH in the presence of LPS (1 $\mu\text{g/ml}$) for 6 h at 37 °C in 5 % CO₂ and 95 % O₂ incubator. After incubation, media were collected and assayed for nitrite by Griess assay. Data are mean \pm SD of three experiments, n=3; *p<0.05 vs. all other groups (ANOVA, Tukey); #p<0.05 between groups indicated (t-test).

4.4 Discussion

Addition of [D-Trp⁸]- γ ₂-MSH to the incubation medium did not exert any discrete effects on steroidogenesis in Balb/c and C57BL/6 mice under normal and LPS-treated conditions. Conversely, this compound was inhibitory on nitrite release from both strain types in inflammatory-like state but had no effects on cytokines production. The decrease in nitrite production induced by LPS was also evident in the K9 Leydig cell line suggesting the involvement of Leydig cells in mediating some of the MC effects.

The two mouse strains, namely Balb/c and C57BL/6 exhibited marked differences in their levels of steroidogenic activities. C57BL/6 mice produced 40 % less testosterone than Balb/c mice basally (Figure 4.7). Additionally, Balb/c mice had a significantly greater response to stimulation with hCG (an analogue of LH), which was added to resemble the normal testicular environment (Figure 4.7). These results are in agreement with published literature investigating the testicular reproductive physiology of Balb/c and C57BL/6 mice. Shukri and Shire (1989) reported that testis of Balb/c were significantly heavier and the cross-section of their seminiferous tubules was larger compared to C57BL/6 mice. In general, C57BL/6 mice were classified as hypoandrogenic with a lower number of germinal cells (Bartke and Krzanowska, 1972), lower plasma testosterone concentrations as well as being less aggressive (Bartke, 1974).

Despite these facts, C57BL/6 mice are considered good breeders. They have 40 % higher rate of productive matings and their relative fecundity is 50 % higher than that of Balb/c mice (Silver, 1995). It appears that plasma testosterone concentrations are negatively correlated with mice copulatory behaviour, which includes its initiation (latency and frequency of mount),

execution and completion (latency and frequency of ejaculation) (Batty, 1978). Two explanations have been suggested for this phenomenon; high testosterone clearance rate and/or increased sensitivity to testosterone at the levels of the hypothalamus and the pituitary (Batty, 1978). The first explanation however, seems unlikely as intratesticular production of testosterone *in vitro*, unaffected by the clearance system, was decreased in C57BL/6 mice (Figure 4.7).

Balb/c and C57BL/6 mice are also known to differ in their immune responses. C57BL/6 mice generate responses mediated by T helper 1 lymphocytes (Th1), releasing in particular interleukin-2 (IL-2) and interferon- γ (IFN- γ), which activate macrophages (Mosmann and Coffman, 1989). In contrast, Balb/c mice are regarded as having Th2-directed responses with predominant secretion of interleukins 4, 5 and 10 (IL-4, IL-5 and IL-10), which stimulate the release of antibodies and inhibit macrophage activation (Mosmann and Moore, 1991; Mills *et al.*, 2000). The Th1-mediated responses confine protection against infections by intracellular viruses, protozoa and bacteria whilst Th2-mediated responses against extracellular pathogens (Mosmann and Coffman, 1989). This makes C57BL/6 mice display increased susceptibility to organ-specific autoimmune conditions including experimentally induced autoimmune myasthenia gravis (as reviewed by Chen *et al.*, 2005). Balb/c mice, though, are more susceptible to tumour formation such as mammary or colon tumours (as reviewed by Chen *et al.*, 2005). Upon infection with *Leishmania major*, an intracellular parasite, T lymphocytes of C57BL/6 mice release IFN- γ , which in turn stimulates production of NO by macrophages that kill the parasite (Heinzel *et al.*, 1989; Mosmann and Coffman, 1989). C57BL/6 mice display resistance to this type of infection through the generation of Th1 response. This is in contrast to Balb/c mice, which are susceptible to infection with *Leishmania major* as their subset of T

lymphocytes produce more IL-4 instead of NO to suppress macrophages and hence show a Th2-response type (Heinzel *et al.*, 1989; Mosmann and Coffman, 1989). Not only lymphocytes but also macrophages respond to the same stimuli in a different manner in C57BL/6 and Balb/c mice and can be classified into M-1 and M-2 phenotypes, respectively (Su *et al.*, 2001). M-1 macrophages are more easily induced by LPS to release NO than M-2 (Mills *et al.*, 2000). Taking into account the high number of residual macrophages present in the testis (Hedger, 2002), the lack of response by Balb/c mice to LPS stimulation displayed in this series of studies could be due to their macrophage phenotype (Figure 4.18). Conversely, C57BL/6 mice produced a marked response to the stimuli in the form of NO and KC release but not IL-1 β . Concentrations of IL-1 β were higher under normal and LPS-stimulated conditions in Balb/c compared to C57BL/6 mice (Figure 4.18 C). This is in agreement with Heinzel and colleagues (1989), who reported that mRNA expression of IL-1 β was significantly greater in Balb/c than in C57BL/6 mice. This cytokine type serves as a co-stimulator for IL-4, which acts as an autocrine growth factor for Th2 cells (Kurt-Jones *et al.*, 1987). In general, basal concentrations of all the inflammatory mediators measured were greater in Balb/c than in C57BL/6 mice (Figure 4.18). Watanobe and others (2004) reported that although Balb/c mice do not respond to LPS stimulation by release of NO, they do have elevated concentrations of inflammatory cytokines/chemokines leading to exaggerated local inflammation in response to polymicrobial infection. It now becomes clear that the effects of MC₃ agonist/antagonist on testicular functioning should be analysed taking into account the interstrain differences in both the steroidogenesis and the immune responses.

Expressions of mRNA for both MC and POMC were previously determined in mice testes (Chapter 2, section 2.3.1 and 2.3.2). It remains to be established, however, which MC subtype is involved in mediating the paracrine and/or autocrine actions of testicular melanocortins on Sertoli and Leydig cells (Chapter 1, section 1.3.3.1). Since the reported effects in the adult animals were mediated mainly by α -MSH, MC₂ can be excluded as it only binds ACTH (Bardin *et al.*, 1987). It is very likely that the action of melanocortins in the testes results from interaction with one or more of the four receptors; namely, MC₁, MC₃, MC₄ and MC₅. The main interest of this PhD project lies in MC₃ and since there is very low selectivity for endogenous melanocortin peptides between MC, a synthetic agonist for the MC₃ subtype was applied. [D-Trp⁸]- γ ₂-MSH is a stabilized γ ₂-MSH analogue developed by Grieco and colleagues (2000) with more than a 200 fold higher potency at MC₃ over MC₄ and MC₅.

Testosterone is crucial for the maintenance of spermatogenesis and thus normal fertility. Considering the potential expression of MC₃ in Leydig cells, as identified in the K9 Leydig cell line (Figure 4.19), it was of interest to determine the effects of its activation on steroidogenesis under normal physiological conditions. MC₃ agonist, [D-Trp⁸]- γ ₂-MSH had no effect on testosterone release from the testicular tissue from Balb/c mice in the absence or presence of hCG. Incubation of testicular tissue from C57BL/6 mice with [D-Trp⁸]- γ ₂-MSH alone resulted in a dose dependent inhibition in testosterone release. The inhibitory effects of [D-Trp⁸]- γ ₂-MSH were also evident in the presence of hCG but at 10 μ g/ml only. O'Shaughnessy and colleagues (2003) demonstrated that γ -MSH alone, did not affect basal testosterone production in both adult and fetal mice testes (C3H/HeJ x 101/H strain). Instead, the group reported that MC₂ activation by ACTH increased testosterone release but in the fetal testis only.

Interestingly, here MC₂ expression appeared to be the greatest in testes of adult Balb/c and C57BL/6 mice compared to other MC (Chapter 2, section 2.3.1.1).

To determine the effects of [D-Trp⁸]- γ -MSH on the release of inflammatory markers in normal physiology, NO, IL-1 β and KC were measured. A stable metabolite of NO, nitrite was measured to indicate the production of endogenous NO, which is generated through the oxidation of L-arginine to L-citrulline by NO synthases (NOSs). The three major isoforms belonging to this family of enzymes are: endothelial NOS (eNOS), neuronal NOS (nNOS) and inducible NOS (iNOS). The presence of the two constitutively expressed isoforms, eNOS and nNOS, as well as the inducible form, iNOS, were identified in normal rat testes (Middendorff *et al.*, 1997; O'Bryan *et al.*, 2000b). Interestingly, a fourth testis-specific nNOS (TnNOS) was found in Leydig cells (as reviewed by Lee and Cheng, 2008). The mRNA for iNOS was detected in normal adult mice testes and in unstimulated K9 Leydig cells (Figure 4.20 B). The presence of NO synthases in these cells indicates a possible role in testicular functioning in normal physiology.

Melanocortins are known to affect the release of NO in various tissues (Altavilla *et al.*, 2000; Nocetto *et al.*, 2004). Here, similarly to other studies, MC₃ activation by [D-Trp⁸]- γ -MSH alone had inhibitory effects on nitrite release at 10 μ g/ml in Balb/c (Figure 4.9 A). Surprisingly, this compound was stimulatory at the same concentration in C57BL/6 mice (Figure 4.14 A). There were no effects of the agonist on nitrite release in the presence of hCG in both strains. The differences in response of Balb/c and C57BL/6 mice to [D-Trp⁸]- γ -MSH in the absence of hCG may be due to differential activity of the target cell(s) – macrophages and/or Leydig cells (Mills *et al.*, 2000; Bartke, 1974). Although, macrophages are thought to be the main NO producers in the testis (Weissman

et al., 2005), other cell types including Leydig, Sertoli and germ, also express the traditional NOS isoforms; iNOS, eNOS and nNOS. Leydig cells, however, exclusively express a truncated form of nNOS called TnNOS (as reviewed by Lee and Cheng, 2004). Since both, macrophages and Leydig cells express MC₃, their nitrite releasing capacity could be directly affected by [D-Trp⁸]- γ 2-MSH under basal and hCG-stimulated conditions. The exact role of NO in normal physiology is still being unravelled but some contrasting reports exist. Welch and others (1995) suggest that intercellular and/or intracellular NO may regulate Leydig cell function as inhibitors of NO formation L-NMMA and L-NAME increased testosterone production under basal and hCG-stimulated conditions. In contrast, O'Bryan *et al.*, (2000b) reported stimulatory effects of NO in non-inflamed testes as inhibitors of NOS reduced testosterone release. Other functions of NO in normal testicular physiology include the relaxation of seminiferous tubules and dilation of blood vessels (Middendorff *et al.*, 1997). Involvement of NO in regulation of spermatogenesis cannot be excluded as NOS isoforms were identified in both Sertoli and germ cells in the normal rat testes (as reviewed by Lee and Cheng, 2008; O'Bryan *et al.*, 2000b). Furthermore, NO may control the release of cytokines and other inflammatory mediators, which take part in normal functioning of testicular interstitial cells including differentiation of the Leydig cells (Hales *et al.*, 1999).

The role of MC₃ activation on the release of cytokines in normal testicular function was also investigated. There were no effects of [D-Trp⁸]- γ 2-MSH stimulation under basal conditions on either IL-1 β or KC production in Balb/c mice (Figure 4.10 A and 4.11 A). However, in the presence of hCG, [D-Trp⁸]- γ 2-MSH had weak stimulatory effects on IL-1 β (1.3 and 30 μ g/ml) and KC (1.3 μ g/ml) in the same mouse strain (Figure 4.10 A and 4.11 A). MC₃ agonist had

no effect on basal IL-1 β but increased KC release at 0.3 μ g/ml in C57BL/6 mice (Figure 4.15 A and 4.16 A). In hCG stimulated tissue, [D-Trp⁸]- γ ₂-MSH increased production of both cytokines at the lowest concentrations in C57BL/6 mice (Figure 4.15 A and 4.16 A). In general, MC₃ activation exerted stimulatory effects at low concentrations of the agonist in the presence of hCG. Not only are immune cells, like macrophages residing in the testis, a source of inflammatory mediators. Both Sertoli and Leydig cells were shown to express mRNA for and release inflammatory mediators; including IL-1 β , which exerts paracrine or autocrine effects (Hales *et al.*, 1999). Leydig cell steroidogenic activity is also known to be affected by cytokines present in the interstitial fluid of the testis. IL-1 β was reported to stimulate testosterone release under basal and low LH-stimulated conditions (Verhoeven *et al.*, 1988). In the presence of high concentrations of LH or hCG, however, IL-1 β exerts inhibitory effect on steroidogenesis at the level of the 17 α -hydroxylase enzyme (Hales *et al.*, 1999). KC, also named CXCL1, was also detected in the media. It belongs to a small subset of cytokines known as chemokines, which display chemotactic activity for a variety of leukocytes; including, neutrophils, monocytes and lymphocytes (Borish and Steinke, 2003). There are still no reports characterising the role of this chemokine under basal conditions in the testis thus the effects of [D-Trp⁸]- γ ₂-MSH on the release of KC will be later described under inflammatory-like conditions.

To conclude, in C57BL/6 mice, MC₃ activation had inhibitory actions on basal testosterone release but had moderate stimulatory effects on nitrite release in normal testicular physiology. Conversely, in Balb/c mice, [D-Trp⁸]- γ ₂-MSH had no effect on testosterone but decreased nitrite production under basal

conditions. Both strains exhibited a weak stimulatory pattern of cytokine release at some doses of MC₃ agonist.

In general, testicular inflammation exerts inhibitory effects on steroidogenesis and spermatogenesis (Del Punta *et al.*, 1996; O'Bryan *et al.*, 2000b). In order to create an inflammatory-like environment in this study, an endotoxin was added to the incubation media. Interestingly, LPS alone increased testosterone release in the testicular tissue of Balb/c mice but not in that of C57BL/6 mice, which is in contrast to previous reports. *In vivo* studies investigating the effects of LPS indicate that inhibition in testosterone release was seen after 6 hours following endotoxin administration and that it reduced testosterone concentrations by 30 % (O'Bryan *et al.*, 2000a). Therefore, discrepancies between the results obtained in this study and the work of others could be related to the *in vitro* model, low concentrations of LPS used or the short incubation period. In the presence of hCG, [D-Trp⁸]- γ 2-MSH did not affect testosterone production under mild inflammatory-like conditions in Balb/c mice. In C57BL/6 mice, [D-Trp⁸]- γ 2-MSH in the presence of LPS had no effect on testosterone release but was stimulatory at the highest agonist dose (30 μ g/ml) in the presence of both LPS and hCG.

Although MC₃ activation did not exhibit a clear effect on testosterone release, it was inhibitory on nitrite production. The effects of LPS on steroidogenesis are known to be mediated mainly by inflammatory mediators; primarily, NO, IL-1 β and TNF- α (Del Punta *et al.*, 1996; O'Bryan *et al.*, 2000a; Shang *et al.*, 2011). A moderate but significant negative correlation between testosterone and nitrite production was found in Balb/c mice, with lower amounts of nitrite associated with higher amounts of testosterone released (Figure 4.12 A). The LPS-induced NO release was significantly higher compared to basal concentrations in

C57BL/6 mice (Figure 4.18 A). It could be related to increased expression of inducible isoform of NOS in response to LPS stimulation in Leydig cells, Sertoli cells or germ cells (O'Bryan *et al.*, 2000b) and most importantly in macrophages (Holan *et al.*, 2001). An increase in the expression of iNOS following LPS stimulation was determined in the K9 Leydig cells (Figure 4.20 B) and has been reported by others in a mouse Leydig tumour cell line MA-10 (Del Punta *et al.*, 1996), from which the K9 Leydig cells partially originate (Finaz *et al.*, 1987). High concentrations of NO released in response to inflammation inhibit steroidogenesis possibly at the level of cholesterol side-chain cleavage enzyme (cytochrome P450_{scc}) (Del Punta *et al.*, 1996). [D-Trp⁸]- γ_2 -MSH markedly reduced nitrite release at 10 and 30 $\mu\text{g/ml}$ in response to LPS stimulation in C57BL/6 and Balb/c mice, respectively, but it had no effect in the presence of both LPS and hCG in either mouse strain (Figure 4.9 B and 4.14 B). Activation of MC₃ by γ_2 -MSH also exerted inhibitory effects on nitrite release from the K9 Leydig cell line exposed to low concentration of LPS (Figure 4.22). A remarkable reduction in NO production was also observed in an *in vivo* model of LPS-induced neuroinflammation, but not under basal conditions, following the administration of different melanocortins (with an order of effectiveness of β -MSH \geq γ_1 -MSH = γ_2 -MSH > α -MSH) (Muceniece *et al.*, 2004).

LPS stimulation also led to increased production of cytokines possibly through macrophage and/or Leydig cell activities. Interestingly, the latter cell type expresses high levels of Toll-like receptors 3 and 4 (TLR3 and TLR4), which bind LPS. Upon stimulation with this endotoxin, Leydig cells are known to release IL-1 β , IL-6, TNF- α and type 1 interferons (Shang *et al.*, 2011). In contrast to nitrite, however, the effects of MC₃ activation on cytokines IL-1 β and KC were not very distinct. [D-Trp⁸]- γ_2 -MSH did not attenuate IL-1 β or KC

release in Balb/c mice in the presence of LPS in either basal or hCG-stimulated conditions (Figure 4.10 B and 4.11 B). In C57BL/6 mice, the MC₃ agonist had no effect on IL-1 β release but led to a 30 % reduction in KC production (at 0.3 - 3.3 μ g/ml) from LPS-treated testicular tissues (Figure 4.15 B and 4.16 B). Conversely, [D-Trp⁸]- γ ₂-MSH in the presence of both LPS and hCG, increased IL-1 β release at the highest concentration from the testicular tissue of C57BL/6 mice (Figure 4.15 B and 4.16 B). These results are in contrast to previous reports describing clear inhibitory actions of MC₃ on the production of both IL-1 β and KC in other models of murine and human inflammation (Getting *et al.*, 2001; Getting *et al.*, 2006b; Montero-Melendez *et al.*, 2011; Kaneva *et al.*, 2012) potentially indicating that different responses occur in other models and under different physiological conditions.

Previous *in vivo* experiments demonstrated that administration of LPS in mice leads to inhibition of steroidogenesis through reduction in the synthesis of steroidogenic acute regulatory protein (StAR) and steroidogenic enzymes including 3 β -hydroxysteroid dehydrogenase (3 β -HSD), cholesterol side-chain cleavage enzyme (cytochrome P450_{scc}) and 17 α -hydroxylase enzyme (as reviewed by Hales, 2002). A number of mediators are considered to be involved in this inhibition including NO, oxygen free radicals (Del Punta *et al.*, 1996), IL-1 β , TNF- α and IL-6 (O'Bryan *et al.*, 2005). This reduction in testosterone release during times of inflammation may allow for the generation of a full immune response, as androgens are immunosuppressive and testicular macrophages have reduced inflammatory response compared to peritoneal macrophages (Hales *et al.*, 1999). Mild inflammation appears to mainly affect the activity of the Leydig cells, as spermatogenic damage is seen only during severe inflammatory responses. The forms of the studies presented herein on

the effects of MC₃ on the functioning of the Leydig cells were for a number of reasons. Firstly, this cell type resides in close proximity to macrophages, known to affect Leydig cell function during normal and diseased states (Hedger, 2002). It was determined that macrophages release 25-hydroxycholesterol to neighbouring Leydig cells for conversion to testosterone (Hutson, 2006). Most importantly, macrophages are potential targets of melanocortins as they have previously been shown to respond to stimulation by endogenous or synthetic melanocortin compounds by reducing the release of inflammatory mediators in various models of experimental inflammation (Getting *et al.*, 2001; Getting *et al.*, 2006b). Secondly, Leydig cells contain POMC mRNA and were shown to release melanocortins (Bardin *et al.*, 1987b). Finally, expression of MC₃ and other MC were detected in the K9 Leydig cells suggesting the possibility of direct effects of melanocortins on this cell type. From the series of experiments using [D-Trp⁸]- γ ₂-MSH, it can be concluded that MC₃ may have modulatory, but not significant, effects on testosterone release in normal and LPS-stimulated testicular tissue. This modulation may be exerted directly on some of the enzymes involved in steroidogenesis and/or, most probably, indirectly through regulation of the release of inflammatory mediators. The effects of MC₃ activation on nitrite release, possibly derived from macrophages or Leydig cells, were clearly inhibitory in mild LPS-induced inflammatory-like state in both strain types and the K9 Leydig cells. Surprisingly, however, MC₃ activation had no distinct effects on the production of inflammatory mediators.

Nevertheless, there are still some doubts regarding the exact receptors mediating the described effects on the release of testosterone and inflammatory mediators. During the course of this series of studies, it was reported that [D-Trp⁸]- γ ₂-MSH may not be fully selective for MC₃ and can act as a potent agonist

at both MC₄ and MC₅ (Renquist *et al.*, 2011). Furthermore, SHU9119 (antagonist at MC₃/MC₄) with or without hCG, increased testosterone production more than three fold compared to unstimulated tissue regardless of [D-Trp⁸]- γ 2-MSH dose in Balb/c mice (Figure 4.8 C, D). The stimulatory effects of SHU9119 in the presence or absence of hCG on testosterone release, could be mediated by either MC₁ or MC₅ as it also acts as an agonist at these receptors and expressions of both subtypes were determined in the testis (Chapter 2, section 2.3.1.1) and specifically in Leydig cells (Figure 4.19). Furthermore, it was determined that both MC₁ and MC₅ may also exert anti-inflammatory and immunoregulatory functions, respectively (Chapter 1, section 1.2.3).

In summary, the effects of MC₃, or other MC activation in the testis are complex and may differ with regard to mouse strain. MC₃ may be involved in discrete paracrine and/or autocrine modulatory actions on Leydig or other cell types present in the testis. Its importance, however, is more apparent during the induction of a mild inflammatory-like response, as it inhibits the release of NO and hence may contribute to the restoration of testicular homeostasis. Nevertheless, there is still a lot to be determined; including the type of cells directly responding to melanocortins as well as the exact MC mediating these effects. Furthermore, the *in vitro* model applied in this series of studies could be substituted for an *in vivo* one. This would aid in determination of the exact effects of MC agonists during mild as well as severe testicular inflammation, characterised by an influx of leukocytes from the systemic circulation. Additionally, this model would also help establish the effects of testicular MC activation on the rest of the reproductive system.

5 General discussion

The overarching aim of the three studies was to characterise the involvement of the melanocortin system in the hypothalamo-pituitary-gonadal system. The first study demonstrated the mRNA distribution pattern of MC at each level of the reproductive axis and possible factors, which can influence, stimulate or inhibit, this expression. The second study described abnormalities in pituitary physiology and testicular morphology of MC₃^{-/-} mice, which can directly and indirectly translate into functional deficiencies in reproduction. The third study focused on the least researched topic in this area, the role of MC activation in normal testicular function. This series of experiments also investigated whether synthetic agonists for specific members of the MC family, may be used to reduce immune responses in testicular tissue during a period of inflammation, an effect reported previously in other systems.

In order to gain a holistic view of the role of the melanocortin system in the hypothalamo-pituitary-gonadal system, the effects reported here and that in the literature will be summarised and discussed below. In the hypothalamus, expressions of both MC₃ and MC₄ were confirmed in male and female mice, as extensively described before (Gantz *et al.*, 1993 a, b; Introduction, section 1.3.1). Additionally, mRNA for MC₅ was also detected in the hypothalamus. This receptor subtype was previously underestimated in the hypothalamus and only one research group has described its possible involvement in the control of GnRH release (Murray *et al.*, 2002; Murray *et al.*, 2006). Low expression of the mRNAs for MC₁ and MC₂ were also demonstrated. The hypothalamic MC mRNA expression may be influenced by age (Figure 2.9), gender (Figure 2.13) or reproductive state (Figure 2.16) of an animal. Age- and oestrous cycle-

related changes in mRNA expression were previously reported for GnRH and neighbouring neurones, and are associated with different concentrations of oestrogen and progesterone (Herbison, 2006; Gore *et al.*, 2002). As described before (Introduction; section 1.3.1), POMC neurones send inputs to GnRH neurones (Leshin *et al.*, 1988; Naftolin *et al.*, 1996) and contain oestrogen receptors (Simonian *et al.*, 1999). Evidence suggests that the hypothalamic expression of POMC (Kelly *et al.*, 2003) and possibly MC may change in response to gonadal steroids and hence contribute to the modulation of GnRH biosynthesis under different reproductive states.

Similarly to previous reports on pituitary MC, this study suggested that the most highly expressed subtype in this tissue is MC₃ (Morooka *et al.*, 1998; Roudbaraki *et al.*, 1999). All other isoforms were also identified but at considerably lower levels of expression. Therefore, it is not surprising that ablation of MC₃ led to a significant reduction in the content of a number of the pituitary hormones in both male and female mice. Although, the expression of MC₃ appears to be greater in female than in male mice as shown here (Figure 2.14) and by others (Matsumura *et al.*, 2003), lack of MC₃ had more profound effects on the total pituitary hormone content of male pituitaries. In males there was a significant reduction in all but two (ACTH and TSH) of the pituitary hormones. Theoretically, the decrease in gonadotropins should lead to a direct, whereas that in prolactin and GH to an indirect, impairment in testicular function (Chandrashekar *et al.*, 1999). It is intriguing that prolactin, the main target of pituitary MC₃ (Matsumura *et al.*, 2003), was unaffected in female MC₃^{-/-} mice and the only reduction observed was for GH. However, pituitaries for these experiments were collected from females at an unknown stage of the oestrous cycle, and there is evidence that MC₃ expression in this tissue is affected by

gonadal steroids (Matsumura *et al.*, 2004). The idea of a direct regulation of melanocortin system activity in the pituitary by the reproductive state of the female is further supported through data showing: an increase in the relative expression of pituitary MC₃ in pregnant mice (Figure 2.17) as well as a rise in pituitary (Visser and Swaab, 1979) and plasma α -MSH in pregnant women (Clark *et al.*, 1978). Additionally, an increase in circulating α -MSH concentrations, most probably of pituitary origin, was also demonstrated in the late follicular phase of women (Mauri *et al.*, 1990). These reports lead to the hypothesis that pituitary MC and POMC can directly respond to gonadotropin and/or gonadal steroids.

In comparison to the 1179 articles on the melanocortin system in the hypothalamus (822) and pituitary (357), to date only 58 research papers investigated this system in the ovary (34) and testis (24) (PubMed; accessed 26 April 2014). This area has clearly received little attention. It is surprising since some of the early studies following the cloning of the five MC subtypes demonstrated the expression of most of the receptors in the human testes, which consequently suggests a role in this tissue (Chhajlani, 1996). As described herein, all five isoforms were identified in mice testes, with MC₂ being the most highly expressed using this method (Figure 2.7 and 2.11).

In contrast, there was relatively low expression of MC in the ovary or uterus of normally cycling female mice. During pregnancy, however, expression of most of the MC significantly increased, which resembles the changes in POMC expression in this tissue (Shaha *et al.*, 1984; Chen *et al.*, 1986). These findings indicate that the ovarian melanocortin system, similarly to the hypothalamo-pituitary axis, indirectly and/or directly responds to the changing concentrations

of pituitary gonadotropins as well as prolactin and/or gonadal steroids, respectively.

Testicular MC₃ expression at the level of protein is still unclear as the antibodies used lack specificity, which could be due to high homology between the MC or inappropriate antigen site (section 2.4). However, the fact that they primarily bound to the interstitial tissue of the testis suggests at least some expression of MC₃ protein in the population of Leydig cells. This observation is further supported by: MC₃ mRNA expression in the K9 Leydig cell line (Figure 4.19) and reports showing expression of MC₁ (Thornwall *et al.*, 1997) and MC₂ (Johnston *et al.*, 2007) proteins in Leydig cells. The apparent agreement with regard to the localization of MC in the testis proposes a role for this family of receptors in Leydig cell function. However, *in vitro* incubation of testicular tissue in the presence of MC₃ agonist [D-Trp⁸]- γ -MSH did not exert any discrete effects on steroidogenesis in Balb/c and C57BL/6 mice under normal and LPS-treated conditions. Conversely, this compound was inhibitory on nitrite release from both strain types under inflammatory-like state but had no significant effect on other inflammatory markers. The decrease in LPS-induced nitrite production following γ -MSH administration was also evident in the K9 Leydig cell line supporting the idea of a direct involvement of Leydig cells in mediating some of the MC effects. These data suggest that MC₃ may be involved in the maintenance of immune homeostasis, through immune (most probably macrophages) and Leydig cells, and not directly in steroidogenesis. It cannot be excluded that other MC are involved in different activities in the testis. MC₂, for example, may have a role in the regulation of testosterone release at different time points in an animal's life (O'Shaughnessy *et al.*, 2003), whilst MC₅ may affect spermatogenesis (Nimura *et al.*, 2006).

An ablation of MC₃ in mice led to indirect (through a decrease in pituitary function) and/or direct effects on a number of testicular parameters, which could translate into reproductive deficiencies. The magnitude of the observed testicular changes seems to be age dependent. Mice at 3-4 weeks and following puberty (9-10 weeks) were more affected by the loss in MC₃ than at older ages (16-17 and 23-24 weeks). They had significantly smaller interstitial islets, which are thought to be the prime site of MC expression in this tissue (Thörnwall *et al.*, 1997; Johnston *et al.*, 2007). These observations may be explained by the pattern of testicular POMC expression, which is considerably greater during periods of high gonadotropin release in fetal and pubertal development (Bardin *et al.*, 1987b).

Summarising all of the presented evidence, a question arises about the apparent conserved ability of the MC₃^{-/-} mice to reproduce. To date, none of the studies using this mouse model have reported on their fertility. Difficulties in breeding were noted by Stephen Getting and colleagues (personal communications) but no breeding records are available to verify their observations. There is the possibility that the absence of MC₃ is compensated for by increased expression or responsiveness of the other four receptors from this or other members of the GPCR family. In contrast to this theory are preliminary data for MC mRNA in MC₃^{-/-} mice showing a marked reduction in the expression level of the majority of MC in the hypothalamus and pituitary. This would suggest that expression of MC in these tissues may be co-dependent, and ablation of one MC leads to reduction in expression or functionality of another. Formation of heterodimers between MC and other GPCRs have been reported in the hypothalamus (Rediger *et al.*, 2012). In the testis however there was no change in the pattern of expression of the other MC, except perhaps for

a slight increase in both MC₄ and MC₅ expression, implying that a compensatory mechanism could be in place there.

To conclude, the melanocortin system is present at each level of the HPG axis, and hence can affect various aspects of reproductive physiology. In the hypothalamus, MC (MC₃, MC₄ and/or MC₅) and POMC neurones comprise a part of GnRH neuronal network modulating GnRH biosynthesis in response to neuronal and hormonal cues such as oestrogen or leptin. In the pituitary, MC₃ influences the release of a number of hormones, which can directly and/or indirectly affect reproductive function. In male gonads, MC may play various functions including control of immune responses, steroidogenesis or spermatogenesis. MC may be co-localized in the same cell type and possible redundancy in functions may hence prevent a completely infertile phenotype in specific MC knockout models. The anti-inflammatory properties exerted by the synthetic and endogenous γ -MSH peptides may become a target for therapeutic applications in testicular immune imbalances. Interestingly, although still requiring confirmation, is the possibility of a direct control of MC and POMC expression by gonadotropins or gonadal steroids at each level of the reproductive axis. This implies a role for the melanocortin system in regulation of some major reproductive events, and hopefully opens new avenues that would lead to diagnosis and hence treatment of some cases of idiopathic infertility.

5.1 Recommendations for future work

Further work is still required to gain greater insight into the potential neuroendocrine, endocrine and paracrine interactions of the melanocortin system within and between tissues of the hypothalamo-pituitary-gonadal axis.

In the hypothalamus, it is still to be determined which of the three 'neural' receptors, MC₃, MC₄ and MC₅ mediate the effects of the POMC peptides on GnRH release. The localization of mRNA and protein for the above receptors with that of GnRH by *in situ* hybridization and immunohistochemistry, respectively, should provide the answer. Furthermore, determination of the exact stimuli (for example, oestrogen, progesterone, leptin, MCH, gonadotropins or prolactin), affecting the expression of MC and POMC is also of interest.

A direct effect of the MC and their ligands in gonadotroph function is unclear. In addition to the localization of MC-expressing trophs, there is a need to establish the exact source, regulation and role(s) of melanocortins, particularly α -MSH, highly detectable during pregnancy and at different stages of the oestrous/menstrual cycle in females.

Considering the expression of all five isoforms in the testis of mice and their possible co-localization, it is of interest to establish the exact, receptor-specific role in this tissue, whether it is steroidogenesis, spermatogenesis or other. In order to further explore the anti-inflammatory properties of MC₃ or other MC, a model of chronic testicular inflammation induced by higher LPS concentration or other agents should be applied. In order to conduct the functional work selective agonists and antagonists at MC are required and the possibility of homo- or

hetero-dimerisation, which can modulate ligand signalling, should be taken into account.

As mentioned, *in situ* hybridization should be used initially to localize the MC expression, however, immuno- or fluorescent staining is required to confirm that the MC mRNA is translated into protein. Nevertheless, there is a great need for the development of highly specific anti-MC₃ antibodies to undertake the protein work.

To characterise the role of MC₃ at different ages, transgenic mice with tissue specific MC₃ gene manipulation should be used. This would allow inactivation of the receptor in particular tissues at specific stages of the life cycle and thus subsequent assessment of reproductive functions of the animals.

Furthermore, it would also be interesting to determine whether changes in α -MSH expression seen in circulating females are correlated with MC and POMC expression in tissues of the reproductive axis. This would help determine the effects of gonadotropins and/or gonadal steroids on the melanocortin system.

6 References

- Abdel-Malek, Z. A. (2001). Melanocortin receptors: their functions and regulation by physiological agonists and antagonists. *Cellular and Molecular Life Sciences*, **58**, 434–441.
- Adan, R. A., Szklarczyk, A. W., Oosterom, J., Brakkee, J. H., Nijenhuis, W. A., Schaaper, W. M., Mueloen, R. H. & Gispen, W. H. (1999). Characterization of melanocortin receptor ligands on cloned brain melanocortin receptors and on grooming behavior in the rat. *European Journal of Pharmacology*, **378**, 249-58.
- Adan, R. A. (2006). Constitutive receptor activity series: endogenous inverse agonists and constitutive receptor activity in the melanocortin system. *Trends in Pharmacological Sciences*, **27**, 183-6.
- Altavilla, D., Bazzani, C., Squadrito, F., Cainazzo, M., Mioni, C., Bertolini, A. & Guarini, S. (2000). Adrenocorticotropin Inhibits Nitric Oxide Synthase II mRNA Expression In Rat Macrophages. *Life Sciences*, **66**, 2247-2254.
- Aluru, N. & Vijayan, M. M. (2008). Molecular characterization, tissue-specific expression, and regulation of melanocortin 2 receptor in rainbow trout. *Endocrinology*, **149**, 4577-88.
- Aly, H. A., Lightfoot, D. A. & El-Shemy, H. A. (2009). Modulatory role of lipoic acid on lipopolysaccharide-induced oxidative stress in adult rat Sertoli cells in vitro. *Chemico-Biological Interactions*, **182**, 112-8.
- Amann, R. P. (1986). Detection of alterations in testicular and epididymal function in laboratory animals. *Environmental Health Perspectives*, **70**, 149-58.
- Amweg, A. N., Paredesb, A., Salvettia, N. R., Larab, H. E. & Ortega, H. H. (2010). Expression of melanocortin receptors mRNA, and direct effects of ACTH on steroid secretion in the bovine ovary. *Theriogenology*, **75**, 628-37.
- Argiolas, A. (1999). Neuropeptides and sexual behaviour. *Neuroscience and Biobehavioral Reviews*, **23**, 1127-42.
- Ariyaratne, H. B. & Chamindrani Mendis-Handagama, S. (2000). Changes in the testis interstitium of Sprague Dawley rats from birth to sexual maturity. *Biology of Reproduction*, **62**, 680-90.
- Artuc, M., Grutzkau, A., Luger, T. & Henz, B. M. (1999). Expression of MC1- and MC5-receptors on the human mast cell line HMC-1. *Annals of the New York Academy of Sciences*, **885**, 364-7.
- Backholer, K., Smith, J. & Clarke, I. J. (2009). Melanocortins may stimulate reproduction by activating orexin neurons in the dorsomedial hypothalamus and

- kisspeptin neurons in the preoptic area of the ewe. *Endocrinology*, **150**, 5488-97.
- Bagnol, D., Lu, X. Y., Kaelin, C. B., Day, H. E., Ollmann, M., Gantz, I., Akil, H., Barsh, G. S. & Watson, S. J. (1999). Anatomy of an endogenous antagonist: relationship between Agouti-related protein and proopiomelanocortin in brain. *Journal of Neuroscience*, **19**, RC26.
- Baldwin, D. M., Haun, C. K. & Sawyer, C. H. (1974). Effects of intraventricular infusions of ACTH1-24 and ACTH4-10 on LH release, ovulation and behavior in the rabbit. *Brain Research*, **80**, 291-301.
- Balthasar, N., Coppari, R., McMinn, J., Liu, S. M., Lee, C. E., Tang, V., Kenny, C. D., McGovern, R. A., Chua, S. C., Jr., Elmquist, J. K. & Lowell, B. B. (2004). Leptin receptor signaling in POMC neurons is required for normal body weight homeostasis. *Neuron*, **42**, 983-91.
- Bardin, C. W., Shaha, C., Mather, J., Salomon, Y., Margioris, A. N., Liotta, A. S., Gerendai, I., Chen, C. L. & Krieger, D. T. (1984). Identification and possible function of pro-opiomelanocortin-derived peptides in the testis. *Annals of the New York Academy of Sciences*, **438**, 346-64.
- Bardin, C. W., Chen, C. L., Morris, P. L., Gerendai, I., Boitani, C., Liotta, A. S., Margioris, A. & Krieger, D. T. (1987a). Proopiomelanocortin-derived peptides in testis, ovary, and tissues of reproduction. *Recent Progress in Hormone Research*, **43**, 1-28.
- Bardin, W. C., Boitani, C., Morris, P. L., Gerendai, I. & Chen, C. L. (1987b). The Presence and Function of Beta-Endorphin, Alpha-MSH and Other Pro-opiomelanocortin-Derived Peptides in Peripheral Reproductive Tissues. *Seminars in Reproductive Endocrinology*, **5**.
- Bartke, A. & Krzanowska, H. (1972). Spermatogenesis in mouse strains with high and low abnormal spermatozoa. *The Journal of heredity*, **63**, 172-4.
- Bartke, A. (1974). Increased sensitivity of seminal vesicles to testosterone in a mouse strain with low plasma testosterone levels. *Journal of Endocrinology*, **60**, 145-8
- Bartke, A. (2004). Prolactin in the male: 25 years later. *Journal of Andrology*, **25**, 661-6.
- Batty, J. (1978). Plasma levels of testosterone and male sexual behaviour in strains of the house mouse (*Mus musculus*). *Animal Behaviour*, **26**, 339-48.
- Begrache, K., Marston, O. J., Rossi, J., Burke, L. K., McDonald, P., Heisler, L. K. & Butler, A. A. (2012). Melanocortin-3 receptors are involved in adaptation to restricted feeding. *Genes, brain, and behavior*, **11**, 291-302.

- Bertolini, A., Tacchia, R. & Vergonib, A. V. (2009). Brain effects of melanocortins. *Pharmacological Research*, **59**, 13-47.
- Bhardwaj, R., Becher, E., Mahnke, K., Hartmeyer, M., Schwarz, T., Scholzen, T. & Luger, T. A. (1997). Evidence for the differential expression of the functional alpha-melanocyte-stimulating hormone receptor MC-1 on human monocytes. *Journal of Immunology*, **158**, 3378-84.
- Bicknell, A. B. (2008). The tissue-specific processing of Pro-Opiomelanocortin. *Journal of Neuroendocrinology*, **20**, 692–699.
- Blum, M., Roberts, J. L. & Wardlaw, S. L. (1989). Androgen regulation of proopiomelanocortin gene expression and peptide content in the basal hypothalamus. *Endocrinology*, **124**, 2283-8.
- Boitani, C., Farini, D., Canipari, R. & Bardin, C. W. (1989). Estradiol and plasminogen activator secretion by cultured rat Sertoli cells in response to melanocyte-stimulating hormones. *Journal of Andrology*, **10**, 202-9.
- Borish, L. C. & Steinke, J. W. (2003). 2. Cytokines and chemokines. *The Journal of allergy and clinical immunology*, **111**, S460-75.
- Brawer, J. R. & Naftolin, F. (1978). The effects of oestrogen on hypothalamic tissue. *Ciba Foundation Symposium*, 19-40.
- Buggy, J. J. (1998). Binding of alpha-melanocyte-stimulating hormone to its G-protein-coupled receptor on B-lymphocytes activates the Jak/STAT pathway. *The Biochemical journal*, **331 (Pt 1)**, 211-6.
- Bumaschny, V. F., de Souza, F. S., Lopez Leal, R. A., Santangelo, A. M., Baetscher, M., Levi, D. H., Low, M. J. & Rubinstein, M. (2007). Transcriptional regulation of pituitary POMC is conserved at the vertebrate extremes despite great promoter sequence divergence. *Molecular Endocrinology*, **21**, 2738–2749.
- Butler, A. A., Kesterson, R. A., Khong, K., Cullen, M. J., Pelleymounter, M. A., Dekoning, J., Baetscher, M. & Cone, R. D. (2000). A unique metabolic syndrome causes obesity in the melanocortin-3 receptor-deficient mouse. *Endocrinology*, **141**, 3518-21.
- Catania, A., Rajora, N., Capsoni, F., Minonzio, F., Star, R. A. & Lipton, J. M. (1996). The neuropeptide alpha-MSH has specific receptors on neutrophils and reduces chemotaxis in vitro. *Peptides*, **17**, 675-9.
- Catania, A., Gatti, S., Colombo, G. & Lipton, J. M. (2004). Targeting melanocortin receptors as a novel strategy to control inflammation. *Pharmacological Reviews*, **56**, 1–29.

Chandrashekar, V., Bartke, A., Coschigano, K. T. & Kopchick, J. J. (1999). Pituitary and testicular function in growth hormone receptor gene knockout mice. *Endocrinology*, **140**, 1082-8.

Chen, A. S., Marsh, D. J., Trumbauer, M. E., Frazier, E. G., Guan, X. M., Yu, H., Rosenblum, C. I., Vongs, A., Feng, Y., Cao, L., Metzger, J. M., Strack, A. M., Camacho, R. E., Mellin, T. N., Nunes, C. N., Min, W., Fisher, J., Gopal-Truter, S., MacIntyre, D. E., Chen, H. Y. & Van der Ploeg, L. H. (2000). Inactivation of the mouse melanocortin-3 receptor results in increased fat mass and reduced lean body mass. *Nature Genetics*, **26**, 97-102.

Chen, C. C., Chang, C. C., Krieger, D. T. & Bardin, C. W. (1986). Expression and regulation of proopiomelanocortin-like gene in the ovary and uterus: comparison with the testis. *Endocrinology*, **118**, 2382-9.

Chen, C. L., Mather, J. P., Morris, P. L. & Bardin, C. W. (1984). Expression of pro-opiomelanocortin-like gene in the testis and epididymis. *Proceedings of the National Academy of Sciences U S A*, **81**, 5672-5.

Chen, M., Georgeson, K. E., Harmon, C. M., Haskell-Luevano, C. & Yang, Y. (2006). Functional characterization of the modified melanocortin peptides responsible for ligand selectivity at the human melanocortin receptors. *Peptides*, **27**, 2836 - 2845.

Chen, W., Kelly, M. A., Opitz-Araya, X., Thomas, R. E., Low, M. J. & Cone, R. D. (1997). Exocrine gland dysfunction in MC5-R-deficient mice: evidence for coordinated regulation of exocrine gland function by melanocortin peptides. *Cell*, **91**, 789–798.

Chen, X., Oppenheim, J. J. & Howard, O. M. (2005). BALB/c mice have more CD4+CD25+ T regulatory cells and show greater susceptibility to suppression of their CD4+CD25- responder T cells than C57BL/6 mice. *Journal of Leukocyte Biology*, **78**, 114-21.

Chhajlani, V. & Wikberg, J. E. (1992). Molecular cloning and expression of the human melanocyte stimulating hormone. *FEBS Letters*, **309**, 417-20.

Chhajlani, V., Muceniece, R. & Wikberg, J. E. (1993). Molecular cloning of a novel human melanocortin receptor. *Biochemical and Biophysical Research Communications*, **195**, 866-73.

Chhajlani, V. (1996). Distribution of cDNA for melanocortin receptor subtypes in human tissues. *Biochemistry and Molecular Biology International*, **38**, 73-80.

Childs, G. V., Ellison, D. G. & Ramaley, J. A. (1982). Storage of anterior lobe adrenocorticotropin in corticotropes and a subpopulation of gonadotropes during the stress-nonresponsive period in the neonatal male rat. *Endocrinology*, **110**, 1676-92.

- Christian, J. J. (1964). Effect of Chronic Acth Treatment on Maturation of Intact Female Mice. *Endocrinology*, **74**, 669-79.
- Chubb, C. (1987). Animal models of physiologic markers of male reproduction: genetically defined infertile mice. *Environmental Health Perspectives*, **74**, 15-29.
- Chung, T. T., Webb, T. R., Chan, L. F., Cooray, S. N., Metherell, L. A., King, P. J., Chapple, J. P. & Clark, A. J. (2008). The majority of adrenocorticotropin receptor (melanocortin 2 receptor) mutations found in familial glucocorticoid deficiency type 1 lead to defective trafficking of the receptor to the cell surface. *The Journal of clinical endocrinology and metabolism*, **93**, 4948-54.
- Clark, D., Thody, A. J., Shuster, S. & Bowers, H. (1978). Immunoreactive alpha-MSH in human plasma in pregnancy. *Nature*, **273**, 163-4.
- Cone, R. D. (2005). Anatomy and regulation of the central melanocortin system. *Nature Neuroscience*, **8**, 571-8.
- Cooper, A., Robinson, S. J., Pickard, C., Jackson, C. L., Friedmann, P. S. & Healy, E. (2005). α -melanocyte-stimulating hormone suppresses antigen-induced lymphocyte proliferation in humans independently of melanocortin 1 receptor gene status. *The Journal of Immunology*, **175**, 4806-4813.
- Cowley, M. A., Smart, J. L., Rubinstein, M., Cerdan, M. G., Diano, S., Horvath, T. L., Cone, R. D. & Low, M. J. (2001). Leptin activates anorexigenic POMC neurons through a neural network in the arcuate nucleus. *Nature*, **411**, 480-4.
- de la Torre, B., Benagiano, G. & Diczfalusy, E. (1976). Pathways of testosterone synthesis in decapsulated testes of mice. *Acta Endocrinologica*, **81**, 170-184.
- de la Torre, B., Hedman, M. & Diczfalusy, E. (1977). Species differences in steroidogenesis following the in vitro incubation of decapsulated testes. *Acta Endocrinologica (Copenhagen)*, **86**, 851-64.
- DeBold, C. R., Nicholson, W. E. & Orth, D. N. (1988). Immunoreactive proopiomelanocortin (POMC) peptides and POMC-like messenger ribonucleic acid are present in many rat nonpituitary tissues. *Endocrinology*, **122**, 2648-57.
- deCatanzaro, D., Beaton, E. A., Khan, A. & Vella, E. (2006). Urinary oestradiol and testosterone levels from novel male mice approach values sufficient to disrupt early pregnancy in nearby inseminated females. *Reproduction*, **132**, 309-17.
- Del Punta, K., Charreau, E. H. & Pignataro, O. P. (1996). Nitric oxide inhibits Leydig cell steroidogenesis. *Endocrinology*, **137**, 5337-43.

- Denko, C. W. & Gabriel, P. (1985). Effects of peptide hormones in urate crystal inflammation. *The Journal of rheumatology*, **12**, 971-5.
- Desarnaud, F., Labbe, O., Eggerickx, D., Vassart, G. & Parmentier, M. (1994). Molecular cloning, functional expression and pharmacological characterization of a mouse melanocortin receptor gene. *Biochemical Journal*, **299**, 367-73.
- Douchi, T., Kuwahata, R., Yamamoto, S., Oki, T., Yamasaki, H. & Nagata, Y. (2002). Relationship of upper body obesity to menstrual disorders. *Acta Obstetrica et Gynecologica Scandinavica*, **81**, 147-50.
- Drouin, J., Chamberland, M., Charron, J., Jeannotte, L. & Nemer, M. (1985). Structure of the rat pro-opiomelanocortin (POMC) gene. *FEBS Letters*, **193**, 54-58.
- Durando, P. E. & Celis, M. E. (1998). In vitro effect of alpha-MSH administration on steroidogenesis of prepubertal ovaries. *Peptides*, **19**, 667-675.
- Ebadi Manas, G., Hasanzadeh, S. & Parivar, K. (2013). The effects of pyridaben pesticide on the histomorphometric, hormonal alternations and reproductive functions of BALB/c mice. *Iranian journal of basic medical sciences*, **16**, 1055-64.
- Eberle, A. (2000). Proopomelanocortin and the Melanocortin Peptides. In: CONE, R. D. (ed.) *The Melanocortin Receptors*. Totowa: Humana Press.
- Einarsson, S., Ljung, A., Brandt, Y., Hager, M. & Madej, A. (2007). Impact of exogenous ACTH during pro-oestrus on endocrine profile and oestrous cycle characteristics in sows. *Reproduction in domestic animals = Zuchthygiene*, **42**, 100-4.
- Ellacott, K. L., Murphy, J. G., Marks, D. L. & Cone, R. D. (2007). Obesity-induced inflammation in white adipose tissue is attenuated by loss of melanocortin-3 receptor signaling. *Endocrinology*, **148**, 6186-94.
- Ellerkmann, E., Nagy, G. M. & Frawley, L. S. (1992). Alpha-melanocyte-stimulating hormone is a mammatrophic factor released by neurointermediate lobe cells after estrogen treatment. *Endocrinology*, **130**, 133-8.
- Fathi, Z., Iben, L. G. & Parker, E. M. (1995). Cloning, expression, and tissue distribution of a fifth melanocortin receptor subtype. *Neurochemical Research*, **20**, 107-13.
- Field, A. (2004). *Discovering Statistics using SPSS for Windows*, London, SAGE Publications.
- Finaz, C., Lefevre, A. & Dampfhofer, D. (1987). Construction of a Leydig cell line synthesizing testosterone under gonadotropin stimulation: a complex

endocrine function immortalized by cell hybridization. *Proceedings of the National Academy of Sciences of the United States of America*, **84**, 5750-3.

Fong, T., Schiöth, H., Gantz, I., Cone, R. D., Farooqi, S., Haskell-Luevano, C., Hruby, V. J., Mountjoy, K. J., Tatro, J. B. & Wikberg, J. E. S. (2013). Melanocortin receptors. *IUPHAR database (IUPHAR-DB)*, [online] Available from <http://www.iuphar-db.org/DATABASE/FamilyIntroductionForward?familyId=38>.> [Accessed 20 January 2014].

Forti, G. & Krausz, C. (1998). Clinical review 100: Evaluation and treatment of the infertile couple. *The Journal of clinical endocrinology and metabolism*, **83**, 4177-88.

Gantz, I., Konda, Y., Tashiro, T., Shimoto, Y., Miwa, H., Munzert, G., Watson, S. J., DelValle, J. & Yamada, T. (1993a). Molecular cloning of a novel melanocortin receptor. *The Journal of Biological Chemistry*, **268**, 8246-50.

Gantz, I., Miwa, H., Konda, Y., Shimoto, Y., Tashiro, T., Watson, S. J., DelValle, J. & Yamada, T. (1993b). Molecular cloning, expression, and gene localization of a fourth melanocortin receptor. *The Journal of biological chemistry*, **268**, 15174-9.

Gantz, I. & Fong, T. M. (2003). The melanocortin system. *American Journal of Physiology - Endocrinology and Metabolism*, **284**, E468-74.

Getting, S., Allcock, G. H., Flower, R. & Perretti, M. (2001). Natural and synthetic agonists of the melanocortin receptor type 3 possess anti-inflammatory properties. *Journal of Leukocyte Biology*, **69**, 98-104.

Getting, S. J., Gibbs, L., Clark, A. J., Flower, R. J. & Perretti, M. (1999). POMC gene-derived peptides activate melanocortin type 3 receptor on murine macrophages, suppress cytokine release, and inhibit neutrophil migration in acute experimental inflammation. *The Journal of Immunology*, **162**, 7446-53.

Getting, S. J., Di Filippo, C., Christian, H. C., Lam, C. W., Rossi, F., D'Amico, M. & Perretti, M. (2004). MC-3 receptor and the inflammatory mechanisms activated in acute myocardial infarct. *Journal of Leukocyte Biology*, **76**, 845-53.

Getting, S. J. (2006a). Targeting melanocortin receptors as potential novel therapeutics. *Pharmacology and Therapeutics*, **111**, 1-15.

Getting, S. J., Lam, C. W., Chen, A. S., Grieco, P. & Perretti, M. (2006b). Melanocortin 3 receptors control crystal-induced inflammation. *FASEB journal : official publication of the Federation of American Societies for Experimental Biology*, **20**, 2234-41.

Getting, S. J., Riffo-Vasquez, Y., Pitchford, S., Kaneva, M., Grieco, P., Page, C. P., Perretti, M. & Spina, D. (2008). A role for MC3R in modulating lung inflammation. *Pulmonary Pharmacology and Therapeutics*, **21**, 866-73.

Giagulli, V. A., Kaufman, J. M. & Vermeulen, A. (1994). Pathogenesis of the decreased androgen levels in obese men. *The Journal of clinical endocrinology and metabolism*, **79**, 997-1000.

Gizang-Ginsberg, E. & Wolgemuth, D. J. (1987). Expression of the proopiomelanocortin gene is developmentally regulated and affected by germ cells in the male mouse reproductive system. *Proceedings of the National Academy of Sciences USA*, **84**, 1600-1604.

Gnessi, L., Fabbri, A. & Spera, G. (1997). Gonadal peptides as mediators of development and functional control of the testis: an integrated system with hormones and local environment. *Endocrine Reviews*, **18**, 541-609.

Gonzalez, M. I., Vaziri, S. & Wilson, C. A. (1996). Behavioral effects of α -MSH and MCH after central administration in the female rat. *Peptides*, **17**, 171-177.

Gore, A. C., Oung, T. & Woller, M. J. (2002). Age-Related Changes in Hypothalamic Gonadotropin-Releasing Hormone and N-Methyl-D-Aspartate Receptor Gene Expression, and their Regulation by Oestrogen, in the Female Rat. *Journal of Neuroendocrinology*, **14**, 300-309.

Gregerson, K. A. (2006). Prolactin: Structure, Function, and Regulation of Secretion. In: NEILL, J., PLANT, T., PFAFF, D., CHALLIS, J., DE KRETZER, D., RICHARDS, J. & WASSARMAN, P. (eds.) *Knobil and Neill's Physiology of Reproduction*. 3rd ed. London: Elsevier.

Grieco, P., Balse, P. M., Weinberg, D., MacNeil, T. & Hruby, V. J. (2000). D-Amino acid scan of gamma-melanocyte-stimulating hormone: importance of Trp(8) on human MC3 receptor selectivity. *Journal of Medicinal Chemistry*, **43**, 4998-5002.

Grieco, P., Lavecchia, A., Cai, M., Trivedi, D., Weinberg, D., MacNeil, T., Van der Ploeg, L. H. & Hruby, V. J. (2002). Structure-activity studies of the melanocortin peptides: discovery of potent and selective affinity antagonists for the hMC3 and hMC4 receptors. *Journal of Medicinal Chemistry*, **45**, 5287-94.

Griffon, N., Mignon, V., Facchinetti, P., Diaz, J., Schwartz, J. & Sokoloff, P. (1994). Molecular cloning and characterization of the rat fifth melanocortin receptor. *Biochemical and Biophysical Research Communications*, **200**, 1007-1014.

Hadley, M. E. (2005). Discovery that a melanocortin regulates sexual functions in male and female humans. *Peptides*, **26**, 1687-9.

- Hales, D. B., Diemer, T. & Hales, K. H. (1999). Role of cytokines in testicular function. *Endocrine*, **10**, 201-17.
- Hales, D. B. (2002). Testicular macrophage modulation of Leydig cell steroidogenesis. *Journal of Reproductive Immunology*, **57**, 3-18.
- Hamada, A., Esteves, S. C. & Agarwal, A. (2011). The role of contemporary andrology in unraveling the mystery of unexplained male infertility. *The Open Reproductive Science Journal*, **4**, 27-41.
- Hammoud, A. O., Wilde, N., Gibson, M., Parks, A., Carrell, D. T. & Meikle, A. W. (2008). Male obesity and alteration in sperm parameters. *Fertility and Sterility*, **90**, 2222-5.
- Haskell-Luevano, C., Chen, P., Li, C., Chang, K., Smith, M. S., Cameron, J. L. & Cone, R. D. (1999). Characterization of the neuroanatomical distribution of agouti-related protein immunoreactivity in the rhesus monkey and the rat. *Endocrinology*, **140**, 1408-15.
- Hedger, M. P. (2002). Macrophages and the immune responsiveness of the testis. *Journal of Reproductive Immunology*, **57**, 19-34.
- Heinzel, F. P., Sadick, M. D., Holaday, B. J., Coffman, R. L. & Locksley, R. M. (1989). Reciprocal expression of interferon gamma or interleukin 4 during the resolution or progression of murine leishmaniasis. Evidence for expansion of distinct helper T cell subsets. *The Journal of experimental medicine*, **169**, 59-72.
- Hellemans, J., Mortier, G., De Paepe, A., Speleman, F. & Vandesompele, J. (2007). qBase relative quantification framework and software for management and automated analysis of real-time quantitative PCR data. *Genome biology*, **8**, R19.
- Hellemans, J. & Vandesompele, J. (eds.) 2011. *qPCR data analysis – unlocking the secret to successful results*: Caister Academic Press.
- Herbison, A. E. & Pape, J. R. (2001). New evidence for estrogen receptors in gonadotropin-releasing hormone neurons. *Frontiers in Neuroendocrinology*, **22**, 292-308.
- Herbison, A. E. (2006). Physiology of the Gonadotropin-Releasing Hormone Neuronal Network. In: NEILL, J., PLANT, T., PFAFF, D., CHALLIS, J., DE KRETZER, D., RICHARDS, J. & WASSARMAN, P. (eds.) *Knobil and Neill's Physiology of Reproduction*. 3rd ed. London: Elsevier.
- Hess, R. A. & deFranca, L. R. (2001). Spermatogenesis and cycle of the seminiferous epithelium. In: CHENG, C. Y. (ed.) *Molecular mechanisms in spermatogenesis*. Austin: Landes Bioscience

Hikim, A. P., Amador, A. G., Klemcke, H. G., Bartke, A. & Russell, L. D. (1989). Correlative morphology and endocrinology of Sertoli cells in hamster testes in active and inactive states of spermatogenesis. *Endocrinology*, **125**, 1829-43.

Hill, J. B., Lacy, E. R., Nagy, G. M., Gorcs, T. J. & Frawley, L. S. (1993). Does alpha-melanocyte-stimulating hormone from the pars intermedia regulate suckling-induced prolactin release? Supportive evidence from morphological and functional studies. *Endocrinology*, **133**, 2991-7.

Holan, V., Krulova, M., Pindjakova, J. & Zajicova, A. (2001). The role of macrophages and nitric oxide in the effector phase of allotransplantation reaction. *Annals of transplantation : quarterly of the Polish Transplantation Society*, **6**, 44-6.

Horvath, E., Varga, B. & Stark, E. (1986). Stimulation of progesterone production by adrenocorticotrophic hormone and prostaglandin E2 in rat luteal cells. *Biology of Reproduction*, **35**, 44-8.

Hruby, V. J., Lu, D., Sharma, S. D., Castrucci, A. L., Kesterson, R. A., al-Obeidi, F. A., Hadley, M. E. & Cone, R. D. (1995). Cyclic lactam alpha-melanotropin analogues of Ac-Nle4-cyclo[Asp5, D-Phe7,Lys10] alpha-melanocyte-stimulating hormone-(4-10)-NH2 with bulky aromatic amino acids at position 7 show high antagonist potency and selectivity at specific melanocortin receptors. *Journal of Medicinal Chemistry*, **38**, 3454-61.

Huang, L. & Li, C. (2000). Leptin: a multifunctional hormone. *Cell Research*, **10**, 81-92.

Huszar, D., Lynch, C. A., Fairchild-Huntress, V., Dunmore, J. H., Fang, Q., Berkemeier, L. R., Gu, W., Kesterson, R. A., Boston, B. A., Cone, R. D., Smith, F. J., Campfield, L. A., Burn, P. & Lee, F. (1997). Targeted disruption of the melanocortin-4 receptor results in obesity in mice. *Cell*, **88**, 131-41.

Hutson, J. C. (2006). Physiologic interactions between macrophages and Leydig cells. *Experimental Biology and Medicine*, **231**, 1-7.

Israel, D. D., Sheffer-Babila, S., de Luca, C., Jo, Y. H., Liu, S. M., Xia, Q., Spergel, D. J., Dun, S. L., Dun, N. J. & Chua, S. C., Jr. (2012). Effects of leptin and melanocortin signaling interactions on pubertal development and reproduction. *Endocrinology*, **153**, 2408-19.

Ivell, R., Walther, N. & Morley, S. (1988). Proopiomelanocortin cDNA sequences from the bovine ovary indicate alternative non-functional transcriptional initiation and a new polymorphism. *Nucleic Acids Research*, **16**, 7747.

Ivell, R. (1994). The proopiomelanocortin gene is expressed as both full-length and 5'truncated. *Reproduction, Fertility and Development*, **6**, 791-4.

Jegou, S., Boutelet, I. & Vaudry, H. (2000). Melanocortin-3 Receptor mRNA expression in Pro-Opiomelanocortin neurones of the rat arcuate nucleus. *Journal of Neuroendocrinology*, **12**, 501-505.

Johnson, M. H. (2007). *Essential Reproduction*, Oxford, Blackwell Publishing.

Johnston, H., King, P. J. & O'Shaughnessy, P. J. (2007). Effects of ACTH and expression of the melanocortin-2 receptor in the neonatal mouse testis. *Reproduction*, **133**, 1181-7.

Jungwirth, A., Diemer, T., Dohle, G., Giwercman, A., Kopa, Z., Tournaye, H. & Krausz, C. (2013). Guidelines on Male Infertility: update March 2013. *European Association of Urology*.

Juniewicz, P. E., Keeney, D. S. & Ewing, L. L. (1988). Effect of adrenocorticotropin and other proopiomelanocortin-derived peptides on testosterone secretion by the in vitro perfused testis. *Endocrinology*, **122**, 891-8.

Kaneva, M. K., Kerrigan, M. J., Grieco, P., Curley, G. P., Locke, I. C. & Getting, S. J. (2012). Chondroprotective and anti-inflammatory role of melanocortin peptides in TNF-alpha activated human C-20/A4 chondrocytes. *British Journal of Pharmacology*, **167**, 67-79.

Kang, L., McIntyre, K. W., Gillooly, K. M., Yang, Y., Haycock, J., Roberts, S., Khanna, A., Herpin, T. F., Yu, G., Wu, X., Morton, G. C., Tuerdi, H., Koplowitz, B., Walker, S. G., Wardwell-Swanson, J., Macor, J. E., Lawrence, R. M. & Carlson, K. E. (2006). A selective small molecule agonist of the melanocortin-1 receptor inhibits lipopolysaccharide-induced cytokine accumulation and leukocyte infiltration in mice. *Journal of Leukocyte Biology*, **80**, 897-904.

Kask, A., Mutulis, F., Muceniece, R., Pahkla, R., Mutule, I., Wikberg, J. E., Rago, L. & Schioth, H. B. (1998). Discovery of a novel superpotent and selective melanocortin-4 receptor antagonist (HS024): evaluation in vitro and in vivo. *Endocrinology*, **139**, 5006-14.

Kathpalia, P. P., Charlton, C., Rajagopal, M. & Pao, A. C. (2011). The natriuretic mechanism of Gamma-Melanocyte-Stimulating Hormone. *Peptides*, **32**, 1068-72.

Kelly, M. J., Qiu, J. & Ronnekleiv, O. K. (2003). Estrogen modulation of G-protein-coupled receptor activation of potassium channels in the central nervous system. *Annals of the New York Academy of Sciences*, **1007**, 6-16.

Kerr, J. B. & Sharpe, R. M. (1989). Focal disruption of spermatogenesis in the testis of adult rats after a single administration of human chorionic gonadotrophin. *Cell and Tissue Research*, **257**, 163-9.

Khong, K., Kurtz, S. E., Sykes, R. L. & Cone, R. D. (2001). Expression of functional melanocortin-4 receptor in the hypothalamic GT1-1 cell line. *Neuroendocrinology*, **74**, 193-201.

Khorram, O. & McCann, S. M. (1986). Interaction of alpha-melanocyte-stimulating hormone with beta-endorphin to influence anterior pituitary hormone secretion in the female rat. *Endocrinology*, **119**, 1071-5.

Kistler-Heer, V., Lauber, M. E. & Lichtensteiger, W. (1998). Different developmental patterns of melanocortin MC3 and MC4 receptor mRNA: predominance of Mc4 in fetal rat nervous system. *Journal of Neuroendocrinology*, **10**, 133-46.

Klovins, J., Haitina, T., Fridmanis, D., Kilianova, Z., Kapa, I., Fredriksson, R., Gallo-Payet, N. & Schioth, H. B. (2004). The Melanocortin System in Fugu: determination of POMC/AGRP/MCR gene repertoire and synteny, as well as pharmacology and anatomical distribution of the MCRs. *Molecular Biology and Evolution*, **21**, 563-579.

Konda, Y., Gantz, I., DelValle, J., Shimoto, Y., Miwa, H. & Yamada, T. (1994). Interaction of dual intracellular signaling pathways activated by the melanocortin-3 receptor. *The Journal of Biological Chemistry*, **269**, 13162-6.

Kurt-Jones, E. A., Hamberg, S., Ohara, J., Paul, W. E. & Abbas, A. K. (1987). Heterogeneity of helper/inducer T lymphocytes. I. Lymphokine production and lymphokine responsiveness. *The Journal of experimental medicine*, **166**, 1774-87.

Langouche, L., Hersmus, N., Papageorgiou, A., Vankelecom, H. & Denef, C. (2004). Melanocortin peptides stimulate prolactin gene expression and prolactin accumulation in rat pituitary aggregate cell cultures. *Journal of Neuroendocrinology*, **16**, 695-703.

Laurell, H., Iacovoni, J. S., Abot, A., Svec, D., Maoret, J. J., Arnal, J. F. & Kubista, M. (2012). Correction of RT-qPCR data for genomic DNA-derived signals with ValidPrime. *Nucleic Acids Research*, **40**, e51.

Lee, M., Kim, A., Conwell, I. M., Hruby, V., Mayorov, A., Cai, M. & Wardlaw, S. L. (2008). Effects of selective modulation of the central melanocortin-3-receptor on food intake and hypothalamic POMC expression. *Peptides*, **29**, 440-7.

Lee, N. P. & Cheng, C. Y. (2004). Nitric oxide/nitric oxide synthase, spermatogenesis, and tight junction dynamics. *Biology of Reproduction*, **70**, 267-76.

Lee, N. P. & Cheng, C. Y. (2008). Nitric oxide and cyclic nucleotides: their roles in junction dynamics and spermatogenesis. *Oxidative medicine and cellular longevity*, **1**, 25-32.

- Lerner, A. & McGuire, J. S. (1961). Effect of alpha- and beta melanocyte stimulating hormones on the skin colour of man. *Nature*, **189**, 176-179
- Leshin, L. S., Rund, L. A., Crim, J. W. & Kiser, T. E. (1988). Immunocytochemical localization of luteinizing hormone-releasing hormone and proopiomelanocortin neurons within the preoptic area and hypothalamus of the bovine brain. *Biology of Reproduction*, **39**, 963-75.
- Liakos, P., Chambaz, E. M., Feige, J. J. & Defaye, G. (2000). Expression and regulation of melanocortin receptor-5 (MC5-R) in the bovine adrenal cortex. *Molecular and Cellular Endocrinology*, **159** 99-107.
- Liotta, A. S., Advis, J. P., Krause, J. E., McKelvy, J. F. & Krieger, D. T. (1984). Demonstration of in vivo synthesis of pro-opiomelanocortin-, beta-endorphin-, and alpha-melanotropin-like species in the adult rat brain. *The Journal of neuroscience : the official journal of the Society for Neuroscience*, **4**, 956-65.
- Lipton, J. M. & Catania, A. (1997). Anti-inflammatory actions of the neuroimmunomodulator alpha-MSH. *Immunology Today*, **18**, 140-5.
- Lisowska, E. (2002). The role of glycosylation in protein antigenic properties. *Cellular and molecular life sciences : CMLS*, **59**, 445-55.
- Lorsignol, A., Vande Vijver, V., Ramaekers, D., Vankelecom, H. & Deneef, C. (1999). Detection of melanocortin-3 receptor mRNA in immature rat pituitary: functional relation to gamma3-MSH-induced changes in intracellular Ca²⁺ concentration? *Journal of Neuroendocrinology*, **11**, 171-9.
- Mandrika, I., Petrovska, R. & Wikberg, J. (2005). Melanocortin receptors form constitutive homo- and heterodimers. *Biochemical and Biophysical Research Communications*, **326**, 349-54.
- Manna, S. K. & Aggarwal, B. B. (1998). Alpha-melanocyte-stimulating hormone inhibits the nuclear transcription factor NF-kappa B activation induced by various inflammatory agents. *Journal of Immunology*, **161**, 2873-80.
- Marcinkiewicz, M., Day, R., Seidah, N. G. & Chrétien, M. (1993). Ontogeny of the prohormone convertases PC1 and PC2 in the mouse hypophysis and their colocalization with corticotropin and alpha-melanotropin. *Proceedings of the National Academy of Sciences of the United States of America*, **90**, 4922-4926.
- Matsumura, R., Takagi, C., Kakeya, T., Okuda, K., Takeuchi, S. & Takahashi, S. (2003). Alpha-melanocyte-stimulating hormone stimulates prolactin secretion through melanocortin-3 receptors expressed in mammatropes in the mouse pituitary. *Neuroendocrinology*, **78**, 96-104.
- Matsumura, R., Takeuchi, S. & Takahashi, S. (2004). Effect of estrogen on melanocortin-3 receptor mRNA expression in mouse pituitary glands in vivo and in vitro. *Neuroendocrinology*, **80**, 143-51.

- Matzuk, M. M. & Lamb, D. J. (2008). The biology of infertility: research advances and clinical challenges. *Nature Medicine*, **14**, 1197-213.
- Mauri, A., Martellotta, M. C., Melis, M. R., Caminiti, F., Serri, F. & Fratta, W. (1990). Plasma alpha-melanocyte-stimulating hormone during the menstrual cycle in women. *Hormone Research*, **34**, 66-70.
- Mayerhofer, A., Bartke, A. & Began, T. (1993). Catecholamines stimulate testicular steroidogenesis in vitro in the Siberian hamster, *Phodopus sungorus*. *Biology of Reproduction*, **48**, 883-8.
- McGuinness, L., Magoulas, C., Sesay, A. K., Mathers, K., Carmignac, D., Manneville, J., Christian, H., Phillips, J. A. & Robinson, I. C. (2003). Autosomal Dominant Growth Hormone deficiency disrupts secretory vesicles in vitro and in vivo in transgenic mice. *Endocrinology*, **144**, 720-731.
- McKinney, T. D. & Pasley, J. N. (1974). Effect of ACTH on reproductive organs of immature female northern grasshopper mice (*Onychomys leucogaster*). *Journal of Reproduction and Fertility*, **41**, 467-70.
- Mehraein, F. & Negahdar, F. (2011). Morphometric evaluation of seminiferous tubules in aged mice testes after melatonin administration. *Cell journal*, **13**, 1-4.
- Meinhardt, A. & Hedger, M. P. (2011). Immunological, paracrine and endocrine aspects of testicular immune privilege. *Molecular and Cellular Endocrinology*, **335**, 60-8.
- Middendorff, R., Muller, D., Wichers, S., Holstein, A. F. & Davidoff, M. S. (1997). Evidence for production and functional activity of nitric oxide in seminiferous tubules and blood vessels of the human testis. *The Journal of clinical endocrinology and metabolism*, **82**, 4154-61.
- Milligan, G. (2003). Constitutive activity and inverse agonists of G protein-coupled receptors: a. *Molecular Pharmacology*, **64**, 1271-6.
- Milligan, G. (2009). G protein-coupled receptor hetero-dimerization: contribution to pharmacology and function. *British Journal of Pharmacology*, **158**, 5-14.
- Mills, C. D., Kincaid, K., Alt, J. M., Heilman, M. J. & Hill, A. M. (2000). M-1/M-2 macrophages and the Th1/Th2 paradigm. *Journal of Immunology*, **164**, 6166-73.
- Mioni, C., Giuliani, D., Cainazzo, M. M., Leone, S., Bazzani, C., Grieco, P., Novellino, E., Tomasi, A., Bertolini, A. & Guarini, S. (2003). Further evidence that melanocortins prevent myocardial reperfusion injury by activating melanocortin MC3 receptors. *European Journal of Pharmacology*, **477**, 227-34.

Mital, P., Kaur, G. & Dufour, J. M. (2010). Immunoprotective sertoli cells: making allogeneic and xenogeneic transplantation feasible. *Reproduction*, **139**, 495-504.

Mizuno, T. M., Kelley, K. A., Pasinetti, G. M., Roberts, J. L. & Mobbs, C. V. (2003). Transgenic neuronal expression of proopiomelanocortin attenuates hyperphagic response to fasting and reverses metabolic impairments in leptin-deficient obese mice. *Diabetes*, **52**, 2675-83.

Moghissi, K. S., Sacco, A. G. & Borin, K. (1980). Immunologic infertility. I. Cervical mucus antibodies and postcoital test. *American Journal of Obstetrics and Gynecology*, **136**, 941-50.

Møllera, C. L., Rauna, K., Jacobsena, M. L., Pedersena, T. Å., Holstb, B., Conde-Frieboesc, K. W. & Wulffa, B. S. (2011). Characterization of murine melanocortin receptors mediating adipocyte lipolysis and examination of signalling pathways involved. *Molecular and Cellular Endocrinology*, **341**, 9-17.

Montero-Melendez, T., Patel, H. B. & Perretti, M. (2011). Role of melanocortin receptors in the regulation of gouty inflammation. *Current rheumatology reports*, **13**, 138-45.

Morooka, Y., Oomizu, S., Takeuchi, S. & Takahashi, S. (1998). Augmentation of Prolactin Release by alpha-Melanocyte Stimulating Hormone Is Possibly Mediated by Melanocortin 3-Receptors in the Mouse Anterior Pituitary Cells. *Zoological Science*, **15**, 567-72.

Morris, P. L., Cheng, C. Y. & Bardin, C. W. (1987). Identification of prolactin-responsive proteins in Leydig cell-enriched culture media. *Annals of the New York Academy of Sciences*, **513**, 390-392.

Mosmann, T. R. & Coffman, R. L. (1989). TH1 and TH2 cells: different patterns of lymphokine secretion lead to different functional properties. *Annual Review of Immunology*, **7**, 145-73.

Mosmann, T. R. & Moore, K. W. (1991). The role of IL-10 in crossregulation of TH1 and TH2 responses. *Immunology Today*, **12**, A49-53.

Mountjoy, K. G., Robbins, L. S., Mortrud, M. T. & Cone, R. D. (1992). The cloning of a family of genes that encode the melanocortin receptors. *Science*, **257**, 1248-51.

Mountjoy, K. G., Mortrud, M. T., Low, M. J., Simerly, R. B. & Cone, R. D. (1994). Localization of the melanocortin-4 receptor (MC4-R) in neuroendocrine and autonomic control circuits in the brain. *Molecular Endocrinology*, **8**, 1298-308.

Muceniece, R., Zvejniece, L., Kirjanova, O., Liepinsh, E., Krigere, L., Baumanes, L., Kalvinsh, I., Wikberg, J. E. & Dambrova, M. (2004). Beta- and gamma-

melanocortins inhibit lipopolysaccharide induced nitric oxide production in mice brain. *Brain Research*, **995**, 7-13.

Muir, C., Spironello-Vella, E., Pisani, N. & deCatanzaro, D. (2001). Enzyme immunoassay of 17 beta-estradiol, estrone conjugates, and testosterone in urinary and fecal samples from male and female mice. *Hormone and metabolic research = Hormon- und Stoffwechselforschung = Hormones et metabolisme*, **33**, 653-8.

Munro, C. J., Stabenfeldt, G. H., Cragun, J. R., Addiego, L. A., Overstreet, J. W. & Lasley, B. L. (1991). Relationship of serum estradiol and progesterone concentrations to the excretion profiles of their major urinary metabolites as measured by enzyme immunoassay and radioimmunoassay. *Clinical Chemistry*, **37**, 838-44.

Munzberg, H., Huo, L., Nilni, E. A., Hollenberg, A. N. & Bjorbaek, C. (2003). Role of signal transducer and activator of transcription 3 in regulation of hypothalamic proopiomelanocortin gene expression by leptin. *Endocrinology*, **144**, 2121-31.

Murray, J. F., Adan, R. A. H., Walker, R., Baker, B. I., Thody, A. J., Nijenhuis, W. A. J., Yukitake, J. & Wilson, C. A. (2000). Melanin-Concentrating Hormone, Melanocortin Receptors and Regulation of Luteinizing Hormone Release. *Journal of Neuroendocrinology*, **12**, 217-223.

Murray, J. F., Pellatt, L. J. & Wilson, C. A. The immunolocalization of melanocortin 5 receptors (MC5R) in the female rat hypothalamus. *In: Proceedings of the Fifth International Congress of Neuroendocrinology*, Bristol, UK, 2002: 342.

Murray, J. F., Hahn, J. D., Kennedy, A. R., Small, C. J., Bloom, S. R., Haskell-Luevano, C., Coen, C. W. & Wilson, C. A. (2006). Evidence for a stimulatory action of Melanin-Concentrating Hormone on Luteinising Hormone release involving MCH1 and Melanocortin-5 Receptors. *Journal of Neuroendocrinology*, **18**, 157-167.

Naftolin, F., Leranth, C., Horvath, T. L. & Garcia-Segura, L. M. (1996). Potential neuronal mechanisms of estrogen actions in synaptogenesis and synaptic plasticity. *Cellular and Molecular Neurobiology*, **16**, 213-23.

Neaves, W. B., Johnson, L. & Petty, C. S. (1985). Age-related change in numbers of other interstitial cells in testes of adult men: evidence bearing on the fate of Leydig cells lost with increasing age. *Biology of Reproduction*, **33**, 259-69.

Newman, C. B., Wardlaw, S. L. & Frantz, A. G. (1985). Suppression of basal and stress-induced prolactin release and stimulation of luteinizing hormone secretion by alpha-melanocyte-stimulating hormone. *Life Sciences*, **36**, 1661-8.

Ni, X., Pearce, D., Butler, A. A., Cone, R. D. & Humphreys, M. H. (2003). Genetic disruption of γ -melanocyte-stimulating hormone signaling leads to salt-sensitive hypertension in the mouse. *The Journal of Clinical Investigation*, **111**, 1251–1258.

NICE (2013). Assessment and treatment for people with fertility problems. *National Institute for Health and Clinical Excellence: Clinical Guideline 156*.

Nieschlag, E., Behre, H. & Nieschlag, S. (2010). *Male Reproductive Health and Dysfunction*, Berlin, Springer.

Nimura, M., Udagawa, J., Hatta, T., Hashimoto, R. & Otani, H. (2006). Spatial and temporal patterns of expression of melanocortin type 2 and 5 receptors in the fetal mouse tissues and organs. *Anatomy and Embryology*, **211**, 109-17.

Nocetto, C., Cragolini, A. B., Schioth, H. B. & Scimonelli, T. N. (2004). Evidence that the effect of melanocortins on female sexual behavior in preoptic area is mediated by the MC3 receptor; Participation of nitric oxide. *Behavioural Brain Research*, **153**, 537-41.

Noon, L., Bakmanidis, A., Clark, A. J. L., O'Shaughnessy, P. J. & King, P. J. (2006). Identification of a novel melanocortin 2 receptor splice variant in murine adipocytes: implications for post-transcriptional control of expression during adipogenesis. *Journal of Molecular Endocrinology*, **37**, 415-420.

Nunez, L. & Frawley, L. S. (1998). α -MSH potentiates the responsiveness of mammotropes by increasing Ca^{2+} entry. *American Journal of Physiology*, **274**, E971-7.

O'Bryan, M. K., Schlatt, S., Phillips, D. J., de Kretser, D. M. & Hedger, M. P. (2000a). Bacterial lipopolysaccharide-induced inflammation compromises testicular function at multiple levels in vivo. *Endocrinology*, **141**, 238-46.

O'Bryan, M. K., Schlatt, S., Gerdprasert, O., Phillips, D. J., de Kretser, D. M. & Hedger, M. P. (2000b). Inducible nitric oxide synthase in the rat testis: evidence for potential roles in both normal function and inflammation-mediated infertility. *Biology of Reproduction*, **63**, 1285-93.

O'Bryan, M. K., Gerdprasert, O., Nikolic-Paterson, D. J., Meinhardt, A., Muir, J. A., Foulds, L. M., Phillips, D. J., de Kretser, D. M. & Hedger, M. P. (2005). Cytokine profiles in the testes of rats treated with lipopolysaccharide reveal localized suppression of inflammatory responses. *American journal of physiology. Regulatory, integrative and comparative physiology*, **288**, R1744-55.

O'Shaughnessy, P. J., Baker, P., Sohnius, U., Haavisto, A. M., Charlton, H. M. & Huhtaniemi, I. (1998). Fetal development of Leydig cell activity in the mouse is independent of pituitary gonadotroph function. *Endocrinology*, **139**, 1141-6.

O'Shaughnessy, P. J., Fleming, L. M., Jackson, G., Hochgeschwender, U., Reed, P. & Baker, P. J. (2003). Adrenocorticotrophic hormone directly stimulates testosterone production by the fetal and neonatal mouse testis. *Endocrinology*, **144**, 3279-84.

Palatin Technologies, I. (2014). PL-6983 for female sexual dysfunction. [online] Available from < <http://www.palatin.com/products/6983.asp> > [Accessed 12 January 2014].

Parkening, T. A., Collins, T. J. & Smith, E. R. (1982). Plasma and pituitary concentrations of LH, FSH and prolactin in aging C57BL/6 mice at various times of the estrus cycles. *Neurobiology of Aging*, **3**, 31-35.

Pellati, D., Mylonakis, I., Bertoloni, G., Fiore, C., Andrisani, A., Ambrosini, G. & Armanini, D. (2008). Genital tract infections and infertility. *European Journal of Obstetrics, Gynecology, and Reproductive Biology*, **140**, 3-11.

Perdichizzi, A., Nicoletti, F., La Vignera, S., Barone, N., D'Agata, R., Vicari, E. & Calogero, A. E. (2007). Effects of tumour necrosis factor-alpha on human sperm motility and apoptosis. *Journal of Clinical Immunology*, **27**, 152-62.

Putnam, C. D., Brann, D. W. & Mahesh, V. B. (1991). Acute activation of the adrenocorticotropin-adrenal axis: effect on gonadotropin and prolactin secretion in the female rat. *Endocrinology*, **128**, 2558-66.

Quennell, J. H., Mulligan, A. C., Tups, A., Liu, X., Phipps, S. J., Kemp, C. J., Herbison, A. E., Grattan, D. R. & Anderson, G. M. (2009). Leptin indirectly regulates gonadotropin-releasing hormone neuronal function. *Endocrinology*, **150**, 2805-12.

Rajkovic, A., Pangas, S. A. & Matzuk, M. M. (2006). Follicular Development: Mouse, Sheep, and Human Models. In: NEILL, J., PLANT, T., PFAFF, D., CHALLIS, J., DE KRETZER, D., RICHARDS, J. & WASSARMAN, P. (eds.) *Knobil and Neill's Physiology of Reproduction*. 3rd ed. London: Elsevier.

Rajora, N., Ceriani, G., Catania, A., Star, R. A., Murphy, M. T. & Lipton, J. M. (1996). alpha-MSH production, receptors, and influence on neopterin in a human monocyte/macrophage cell line. *Journal of Leukocyte Biology*, **59**, 248-53.

Rajora, N., Boccoli, G., Burns, D., Sharma, S., Catania, A. & Lipton, J. (1997). alpha-MSH modulates local and circulating tumor necrosis factor-alpha in experimental brain inflammation. *The Journal of Neuroscience*, **17**, 2181-2186.

Raposo, P. D., Castillo, E., d'Alleva, V., Broqua, P., Pralong, F. P. & Aubert, M. L. (2000). Chronic blockade of the melanocortin 4 receptor subtype leads to obesity independently of neuropeptide Y action, with no adverse effects on the gonadotropic and somatotrophic axes. *Endocrinology*, **141**, 4419-27.

Ray, A., Shah, A., Gudi, A. & Homburg, R. (2012). Unexplained infertility: an update and review of practice. *Reproductive biomedicine online*, **24**, 591-602.

Rediger, A., Piechowski, C. L., Yi, C. X., Tarnow, P., Strotmann, R., Gruters, A., Krude, H., Schoneberg, T., Tschop, M. H., Kleinau, G. & Biebermann, H. (2011). Mutually opposite signal modulation by hypothalamic heterodimerization of ghrelin and melanocortin-3 receptors. *The Journal of biological chemistry*, **286**, 39623-31.

Rediger, A., Piechowski, C. L., Habegger, K., Gruters, A., Krude, H., Tschop, M. H., Kleinau, G. & Biebermann, H. (2012). MC4R dimerization in the paraventricular nucleus and GHSR/MC3R heterodimerization in the arcuate nucleus: is there relevance for body weight regulation? *Neuroendocrinology*, **95**, 277-88.

Renquist, B. J., Lippert, R. N., Sebag, J. A., Ellacott, K. L. & Cone, R. D. (2011). Physiological roles of the melanocortin MC(3) receptor. *European Journal of Pharmacology*, **660**, 13-20.

Renquist, B. J., Murphy, J. G., Larson, E. A., Olsen, D., Klein, R. F., Ellacott, K. L. & Cone, R. D. (2012). Melanocortin-3 receptor regulates the normal fasting response. *Proceedings of the National Academy of Sciences of the United States of America*, **109**, E1489-98.

Rheins, L. A., Coteleur, A. L., Kleier, R. S., Hoppenjans, W. B., Saunder, D. N. & Nordlund, J. J. (1989). Alpha-melanocyte stimulating hormone modulates contact hypersensitivity responsiveness in C57/BL6 mice. *The Journal of investigative dermatology*, **93**, 511-7.

Roa, J. & Herbison, A. E. (2012). Direct regulation of GnRH neuron excitability by arcuate nucleus POMC and NPY neuron neuropeptides in female mice. *Endocrinology*, **153**, 5587-99.

Roa, J. (2013). Role of GnRH Neurons and Their Neuronal Afferents as Key Integrators between Food Intake Regulatory Signals and the Control of Reproduction. *International journal of endocrinology*, **2013**, 518046.

Rodriguez, M. G., Rival, C., Theas, M. S. & Lustig, L. (2006). Immunohistopathology of the contralateral testis of rats undergoing experimental torsion of the spermatic cord. *Asian journal of andrology*, **8**, 576-83.

Roselli-Reh fuss, L., Mountjoy, K. G., Robbins, L. S., Mortrud, M. T., Low, M. J., Tatro, J. B., Entwistle, M. L., Simerly, R. B. & Cone, R. D. (1993). Identification of a receptor for gamma melanotropin and other proopiomelanocortin peptides in the hypothalamus and limbic system. *Proceedings of the National Academy of Sciences USA*, **90**, 8856-60.

Rosen, R. C., Diamond, L. E., Earle, D. C., Shadiack, A. M. & Molinoff, P. B. (2004). Evaluation of the safety, pharmacokinetics and pharmacodynamic effects of subcutaneously administered PT-141, a melanocortin receptor agonist, in healthy male subjects and in patients with an inadequate response to Viagra. *International Journal of Impotence Research*, **16**, 135-42.

Roudbaraki, M., Lorsignol, A., Langouche, L., Callewaert, G., Vankelecom, H. & Deneef, C. (1999). Target cells of gamma3-melanocyte-stimulating hormone detected through intracellular Ca²⁺ responses in immature rat pituitary constitute a fraction of all main pituitary cell types, but mostly express multiple hormone phenotypes at the messenger ribonucleic acid level. Refractoriness to melanocortin-3 receptor blockade in the lacto-somatotroph lineage. *Endocrinology*, **140**, 4874-85.

Russell, L. D., Ettlín, R. A., SinhaHikim, A. P. & Clegg, E. D. (1990). *Histological and histopathological evaluation of the testis*, St. Louis, Cache River Press.

Sandrock, M., Schulz, A., Merkwitz, C., Schoneberg, T., Spanel-Borowski, K. & Ricken, A. (2009). Reduction in corpora lutea number in obese melanocortin-4-receptor-deficient mice. *Reproductive biology and endocrinology : RB&E*, **7**, 24.

Sarkar, A., Sreenivasan, Y. & Manna, S. K. (2003). alpha-Melanocyte-stimulating hormone inhibits lipopolysaccharide-induced biological responses by downregulating CD14 from macrophages. *FEBS Letters*, **553**, 286-94.

Schioth, H. B., Mutulis, F., Muceniece, R., Prusis, P. & Wikberg, J. E. (1998). Discovery of novel melanocortin4 receptor selective MSH analogues. *British Journal of Pharmacology*, **124**, 75-82.

Schioth, H. B. & Watanobe, H. (2002). Melanocortins and reproduction. *Brain Research Reviews*, **38**, 340-50.

Scimonelli, T. & Celis, M. E. (1990). A central action of alpha-melanocyte-stimulating hormone on serum levels of LH and prolactin in rats. *Journal of Endocrinology*, **124**, 127-32.

Scudamore, C. L. (2014). *A practical guide to the histology of the mouse*, Chichester, John Wiley & Sons.

Sebhat, I. K., Martin, W. J., Ye, Z., Barakat, K., Mosley, R. T., Johnston, D. B., Bakshi, R., Palucki, B., Weinberg, D. H., MacNeil, T., Kalyani, R. N., Tang, R., Stearns, R. A., Miller, R. R., Tamvakopoulos, C., Strack, A. M., McGowan, E., Cashen, D. E., Drisko, J. E., Hom, G. J., Howard, A. D., MacIntyre, D. E., van der Ploeg, L. H., Patchett, A. A. & Nargund, R. P. (2002). Design and pharmacology of N-[(3R)-1,2,3,4-tetrahydroisoquinolinium-3-ylcarbonyl]-(1R)-1-(4-chlorobenzyl)-2-[4-cyclohexyl-4-(1H-1,2,4-triazol-1-ylmethyl)piperidin-1-yl]-2-oxoethylamine (1), a potent, selective, melanocortin subtype-4 receptor agonist. *Journal of Medicinal Chemistry*, **45**, 4589-93.

Setchell, B. P. & Breed, W. G. (2006). Anatomy, Vasculature, and Innervation of the Male Reproductive Tract. *In*: NEILL, J., PLANT, T., PFAFF, D., CHALLIS, J., DE KRETZER, D., RICHARDS, J. & WASSARMAN, P. (eds.) *Knobil and Neill's Physiology of Reproduction*. 3rd ed. London: Elsevier.

Shaha, C., Margioris, A., Liotta, A. S., Krieger, D. T. & Bardin, C. W. (1984). Demonstration of immunoreactive beta-endorphin- and gamma 3-melanocyte-stimulating hormone-related peptides in the ovaries of neonatal, cyclic, and pregnant mice. *Endocrinology*, **115**, 378-84.

Shang, T., Zhang, X., Wang, T., Sun, B., Deng, T. & Han, D. (2011). Toll-like receptor-initiated testicular innate immune responses in mouse Leydig cells. *Endocrinology*, **152**, 2827-36.

Shukri, N. M. & Shire, J. G. (1989). Genetic variation in testicular development in mice of the C57BL/10ScSn, C57BL/6By and BALB/cBy strains and the CXB recombinant-inbred lines. *Journal of Reproduction and Fertility*, **87**, 587-92.

Shupnik, M. A. (2002). Oestrogen receptors, receptor variants and oestrogen actions in the hypothalamic-pituitary axis. *Journal of Neuroendocrinology*, **14**, 85-94.

Silver, L. M. (1995). *Mouse Genetics: Concepts and Applications*, Oxford, Oxford University Press.

Simonian, S. X., Spratt, D. P. & Herbison, A. E. (1999). Identification and Characterization of Estrogen Receptor α -Containing Neurons Projecting to the Vicinity of the Gonadotropin-Releasing Hormone Perikarya in the Rostral Preoptic Area of the Rat. *The Journal of Comparative Neurology*, **411**, 346-358.

Sortino, M. A. & Wise, P. M. (1989). Effect of hyperprolactinemia on luteinizing hormone and prolactin secretion assessed using the reverse hemolytic plaque assay. *Biology of Reproduction*, **41**, 618-25.

Stanley, S. A., Small, C. J., Kim, M. S., Heath, M. M., Seal, L. J., Russell, S. H., Ghatei, M. A. & Bloom, S. R. (1999). Agouti related peptide (Agrp) stimulates the hypothalamo pituitary gonadal axis in vivo & in vitro in male rats. *Endocrinology*, **140**, 5459-62.

Stanley, S. A., Davies, S., Small, C. J., Gardiner, J. V., Ghatei, M. A., Smith, D. M. & Bloom, S. R. (2003). gamma-MSH increases intracellular cAMP accumulation and GnRH release in vitro and LH release in vivo. *FEBS Letters*, **543**, 66-70.

Star, R. A., Rajora, N., Huang, J., Stock, R. C., Catania, A. & Lipton, J. M. (1995). Evidence of autocrine modulation of macrophage nitric oxide synthase by α -melanocyte-stimulating hormone. *Proceedings of the National Academy of Sciences USA*, **92**, 8016-8020.

- Stephan, J. P., Syed, V. & Jegou, B. (1997). Regulation of Sertoli cell IL-1 and IL-6 production in vitro. *Molecular and Cellular Endocrinology*, **134**, 109-18.
- Su, S. H., Chen, H. & Jen, C. J. (2001). C57BL/6 and BALB/c bronchoalveolar macrophages respond differently to exercise. *Journal of Immunology*, **167**, 5084-91.
- Sutton, G. M., Begriche, K., Kumar, K. G., Gimble, J. M., Perez-Tilve, D., Nogueiras, R., McMillan, R. P., Hulver, M. W., Tschop, M. H. & Butler, A. A. (2010). Central nervous system melanocortin-3 receptors are required for synchronizing metabolism during entrainment to restricted feeding during the light cycle. *FASEB journal : official publication of the Federation of American Societies for Experimental Biology*, **24**, 862-72.
- Szardenings, M., Muceniece, R., Mutule, I., Mutulis, F. & Wikberg, J. E. (2000). New highly specific agonistic peptides for human melanocortin MC(1) receptor. *Peptides*, **21**, 239-43.
- Taherzadeh, S., Sharma, S., Chhajlani, V., Gantz, I., Rajora, N., Demitri, M. T., Kelly, L., Zhao, H., Ichiyama, T., Catania, A. & Lipton, J. M. (1999). alpha-MSH and its receptors in regulation of tumor necrosis factor-alpha. *American Journal of Physiology*, **276**, 1289-94.
- Takeuchi, S. & Takahashi, S. (1999). A possible involvement of melanocortin 3 receptor in the regulation of adrenal gland function in the chicken. *Biochimica et Biophysica Acta*, **1448**, 512-518.
- Tao, Y. X. (2010). The melanocortin-4 receptor: physiology, pharmacology, and pathophysiology. *Endocrine Reviews*, **31**, 506-43.
- Thornwall, M., Dimitriou, A., Xu, X., Larsson, E. & Chhajlani, V. (1997). Immunohistochemical detection of the melanocortin 1 receptor in human testis, ovary and placenta using specific monoclonal antibody. *Hormone Research*, **48**, 215-8.
- Tilemans, D., Ramaekers, D., Andries, M. & Deneef, C. (1997). Effect of POMC(1-76), its C-terminal fragment gamma3-MSH and anti-POMC(1-76) antibodies on DNA replication in lactotrophs in aggregate cell cultures of immature rat pituitary. *Journal of Neuroendocrinology*, **9**, 627-37.
- Trojian, T. H., Lishnak, T. S. & Heiman, D. (2009). Epididymitis and orchitis: an overview. *American Family Physician*, **79**, 583-7.
- Turek, P. J. & Lipshultz, L. I. (1994). Immunologic infertility. *The Urologic clinics of North America*, **21**, 447-68.
- Vaisse, C., Clement, K., Durand, E., Hercberg, S., Guy-Grand, B. & Froguel, P. (2000). Melanocortin-4 receptor mutations are a frequent and heterogeneous cause of morbid obesity. *The Journal of clinical investigation*, **106**, 253-62.

Van Bael, A., Vande Vijver, V., Devreese, B., Van Beeumen, J. & Deneef, C. (1996). N-terminal 10- and 12-kDa POMC fragments stimulate differentiation of lactotrophs. *Peptides*, **17**, 1219-28.

Van der Ploeg, L. H., Martin, W. J., Howard, A. D., Nargund, R. P., P., A., Guan, X., Drisko, J., Cashen, D., Sebhat, I., Patchett, A. A., Figueroa, D. J., DiLella, A. G., Connolly, B. M., Weinberg, D. H., Tan, C. P., Palyha, O. C., Pong, S., MacNeil, T., Rosenblum, C., Vongs, A., Tang, R., Yu, H., Sailer, A. W., Fong, T. M., Huang, C., Tota, M. R., Chang, R. S., Stearns, R., Tamvakopoulos, C., Christ, G., Drazen, D. L., Spar, B. D., Nelson, R. J. & MacIntyre, D. E. (2004). A role for the melanocortin 4 receptor in sexual function. *Proceedings of the National Academy of Sciences USA*, **99**, 11381–11386.

Varga, B., Stark, E. & Horvath, E. (1986). Direct effects of ACTH on the ovary. *Acta Physiologica Hungarica*, **67**, 3-11.

Verhoeven, G., Cailleau, J., Van Damme, J. & Billiau, A. (1988). Interleukin-1 stimulates steroidogenesis in cultured rat Leydig cells. *Molecular and Cellular Endocrinology*, **57**, 51-60.

Visser, M. & Swaab, D. F. (1979). Life span changes in the presence of alpha-melanocyte-stimulating-hormone-containing cells in the human pituitary. *Journal of Developmental Physiology*, **1**, 161-78.

Voogt, J. L., de Greef, W. J., Visser, T. J., de Koning, J., Vreeburg, J. T. & Weber, R. F. (1987). In vivo release of dopamine, luteinizing hormone-releasing hormone and thyrotropin-releasing hormone in male rats bearing a prolactin-secreting tumor. *Neuroendocrinology*, **46**, 110-6.

Wachira, S. J., Hughes-Darden, C. A., Taylor, C. V., Ochillo, R. & Robinson, T. J. (2003). Evidence for the interaction of protein kinase C and melanocortin 3-receptor signaling pathways. *Neuropeptides*, **37**, 201–210.

Waite, E., Lafont, C., Carmignac, D., Chauvet, N., Coutry, N., Christian, H., Robinson, I., Mollard, P. & Le Tissier, P. (2010). Different degrees of somatotroph ablation compromise pituitary growth hormone cell network structure and other pituitary endocrine cell types. *Endocrinology*, **151**, 234-243.

Ward, D. R., Dear, F. M., Ward, I. A., Anderson, S. I., Spergel, D. J., Smith, P. A. & Ebling, F. J. (2009). Innervation of gonadotropin-releasing hormone neurons by peptidergic neurons conveying circadian or energy balance information in the mouse. *PloS one*, **4**, e5322.

Watanabe, H., Numata, K., Ito, T., Takagi, K. & Matsukawa, A. (2004). Innate immune response in Th1- and Th2-dominant mouse strains. *Shock*, **22**, 460-6.

Watanobe, H., Suda, T., Wikberg, J. E. & Schioth, H. B. (1999). Evidence that physiological levels of circulating leptin exert a stimulatory effect on luteinizing

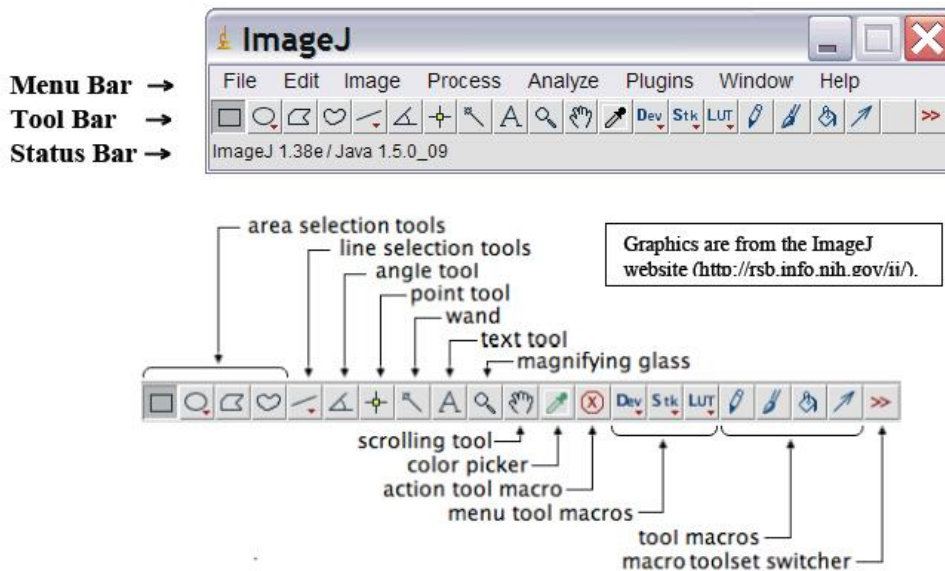
- hormone and prolactin surges in rats. *Biochemical and Biophysical Research Communications*, **263**, 162-5.
- Weissman, B. A., Niu, E., Ge, R., Sottas, C. M., Holmes, M., Hutson, J. C. & Hardy, M. P. (2005). Paracrine modulation of androgen synthesis in rat leydig cells by nitric oxide. *Journal of Andrology*, **26**, 369-78.
- Welch, C., Watson, M. E., Poth, M., Hong, T. & Francis, G. L. (1995). Evidence to suggest nitric oxide is an interstitial regulator of Leydig cell steroidogenesis. *Metabolism: Clinical and Experimental*, **44**, 234-8.
- Westwood, M., Maqsood, A. R., Solomon, M., Whatmore, A. J., Davis, J. R., Baxter, R. C., Gevers, E. F., Robinson, I. C. & Clayton, P. E. (2010). The effect of different patterns of growth hormone administration on the IGF axis and somatic and skeletal growth of the dwarf rat. *American journal of physiology. Endocrinology and metabolism*, **298**, E467-76.
- Wikberg, J. E. (1999). Melanocortin receptors: perspectives for novel drugs. *European Journal of Pharmacology*, **375**, 295-310.
- Wikberg, J. E. S., Muceniece, R., Mandrika, I., Prusis, P., Lindblom, J., Post, C. & Skottner, A. (2000). New aspects on the melanocortins and their receptors. *Pharmacological Research*, **42**, 393-420.
- Wilkinson, C. W. (2006). Roles of acetylation and other post-translational modifications in melanocortin function and interactions with endorphins. *Peptides*, **27**, 453-71.
- Wing, T. Y. & Christensen, A. K. (1982). Morphometric studies on rat seminiferous tubules. *The American journal of anatomy*, **165**, 13-25.
- Wu, X., Arumugam, R., Zhang, N. & Lee, M. M. (2010). Androgen profiles during pubertal Leydig cell development in mice. *Reproduction*, **140**, 113-21.
- Yang, F. & Tao, Y. X. (2012). Functional characterization of nine novel naturally occurring human melanocortin-3 receptor mutations. *Biochimica et Biophysica Acta*, **1822**, 1752-61.
- Yang, Y. (2011). Structure, function and regulation of the melanocortin receptors. *European Journal of Pharmacology*, **660**, 125-30.
- Yang, Y. & Honaramooz, A. (2012). Characterization and quenching of autofluorescence in piglet testis tissue and cells. *Anatomy research international*, **2012**, 820120.
- Yeh, J. K., Evans, J. F., Niu, Q. & Aloia, J. F. (2006). A possible role for melanocortin peptides in longitudinal growth. *Journal of Endocrinology*, **191**, 677-686.

7 Appendices

7.1 Appendix 1: Image J instructions

1. Open ImageJ software. The ImageJ window will appear on the desktop; do not enlarge this window.

Note that this window has a Menu Bar, a Tool Bar and a Status Bar.



2. Select **File – Open** – to select folder with images from Disk E (removable disk)
3. Set Measurement Scale. Select straight line drawing option on the Image J tool bar. Draw a line between two points of the scale (black bar in the top left corner) on the photograph. Go to **Analyze - Set Scale**. In the Set Scale window the length of the line, in pixels, will be displayed. Type the

known distance (100) and units of measure (um) in the appropriate boxes and click OK. Measurements will now be shown using these settings. Check 'global' to apply this scale to other image frames.

4. Choose tubules that appear rounded and thus are cross-sectioned for making diameter measurements. If slightly oblique tubules are encountered, then the short axis of the tubular profile should be measured.
5. Measure **tubule diameter**. Draw a line between two points. The status bar will show the length. To transfer the values to a data window simply type M on the keyboard. Perform two measurements for each tubule. Transfer the measurements to the excel spreadsheet.
6. Measure **thickness of the tubule**. Select the points between the base of the tubule and lumen. Perform two measurements for each tubule. Transfer the measurements to the excel spreadsheet.
7. Measure **total area** of the image by typing M. Transfer the measurement to the excel spreadsheet.
8. Measure the **area of each intertubular tissue**. Surround an area with a perimeter. This can be done with an area selection tool, the freehand. Type in M to transfer the area measurement to a data window. Transfer the measurement to the excel spreadsheet. Highlight the measurements for whole intertubular islets.
9. Repeat the measurement for all intertubular tissues. Transfer the measurements to the excel spreadsheet.

10. Measure **the area of each tubule**. Surround an area with a perimeter.

This can be done with an area selection tool, the freehand. Type in M to transfer the area measurement to a data window then type in the measurement to the excel spreadsheet. Highlight the measurements for whole tubules.

11. Remember to clearly indicate the slide number on the spreadsheet.

7.2 Appendix 2: Ethics forms

OFFICE USE: ___ / ___ / ___

University of Westminster
Research Ethics sub-Committee

Application for Research Ethics Consideration

COVER SHEET
(To be completed by all applicants)

Section 1 – PROJECT AND APPLICANT DETAILS

To be completed by all applicants

1.1 Project Title:

The effect of age on fertility: melanocortin signalling in the male and female reproductive axes.

1.2 Applicant Details

Name: Monika Dowejko

Email Address:

monika.horanin@my.westminster.ac.uk

Contact Address:

1 Farrant House,
Winstanley Road
London, SW11 2EJ

Telephone Number:

07885990906

Please check the relevant box:

Undergraduate Postgraduate MPhil/PhD Student Staff

1.3 Supervisor/Dean of School/ School Research Director details

Please note that all applicants with a supervisor(s) must ensure that the supervisor signs the declaration at the bottom of this page if completing Part A only or in **Section 10.3** if completing Part B

All staff must ensure that their Dean of School, or School Research Director (or nominee), as appropriate, signs the declaration at the bottom of this page if completing Part A only or in **Section 10.3** if completing Part B

Name: Dr Joanne Murray

Email Address:

j.f.murray@westminster.ac.uk

School/Centre/Unit: School of Life Sciences	Telephone Number: 020 7911 5000 ext 3566
---	--

NOW COMPLETE PART A

PART A

Section 2 – Project Details

2.1 Please provide a description of the background to your study including a literature review (250 words maximum):

Melanocortins are the products of posttranslational modification of proopiomelanocortin (POMC) prohormone. This family of POMC peptides includes adrenocorticotrophic hormone (ACTH), as well as α -, β -, and γ - Melanocyte Stimulating Hormones (MSH) (Gantz and Fong, 2003). Melanocortins exert their effects by binding and activating one of five melanocortin receptors (MC₁ through to MC₅), which belong to the family of G-protein-coupled receptors, and are widely distributed throughout the body (Getting, 2006). The melanocortins are involved in a number of physiological roles, including regulation of food intake, memory, behaviour and inflammation. MC₃, to be investigated in this study, is predominantly expressed in the CNS but has also been found in periphery (including placenta, gastrointestinal tract, heart, and immune cells) (Gantz et al., 1993). Furthermore, MC₃ has been detected in the pituitary and testis of adult mice, but its exact function in reproductive physiology is still not clear. Some evidence, however, suggests that MC₃ may play serve as a potential link between energy metabolism and reproductive function (Watanobe, 2002).

2.2. Please provide a brief description of your study (250 words maximum):

The overarching aim of the project is to characterize the expression and role of MC₃ in the reproductive systems of both the male and the female.
The first part of the project will determine the expression of MC₃ in the hypothalamus, pituitary, gonads and other reproductive organs of mice at different ages.
The next part will evaluate the physiological effects and mode of action of MC₃ in various tissues and/or cell lines by administration of agonists/antagonists of this melanocortin receptor subtype.

2.3. What are the specific aims of the study? (250 words maximum):

- To determine the distribution pattern of MC₃ in mice tissue and/or cell line at the level of mRNA and protein.
- To determine the functional role of MC₃ in reproductive physiology.

2.4. Please outline the design and methodology of your study [attach extra information as necessary] (250 words maximum in total):

Reproductive organs of sexually mature wild type mice will be obtained from a range of animal houses licensed by the Home Office following a schedule 1 procedure and cell lines will be purchased.

The presence or absence of melanocortin receptor 3 in mouse tissue and/or cell line will be determined:

- at the level of mRNA by Reverse Transcriptase-PCR (RT-PCR) or qRT-PCR,
- at the level of protein by Western Blot and immunohistochemistry.

Radioimmunoassay or ELISA will be performed to measure hormone output following *in vitro* incubation of mouse tissue and/or cell line with MC₃ agonist/antagonist.

2.5 Timescales

Start Date (DD/MM/YY): 1/10/2010

Estimated duration of work: 46 months

Section 3 RISK OF HARM				
		Yes	No	N/A
1	Is pain or more than mild discomfort likely to result from the study		X	
2	Could the study induce psychological stress or anxiety or cause harm or negative consequences beyond the risks encountered in normal life?		X	
3	Will the study involve prolonged or repetitive testing?		X	
4	Will the study involve raising sensitive topics (e.g. sexual activity, drug use, revelation of medical history and/or illegal activities)		X	
5	Does your work involve any material containing human cells (e.g. blood, urine, saliva, body tissues) from living or deceased persons? (Such work must take account of the Human Tissue Act).		X	
6	Will DNA samples be taken from human participants? (Such work must take account of the Human Tissue Act).		X	
7	Does your study raise any issues of personal safety for you or other researchers involved in the project? (Especially relevant if taking place outside working hours or off University premises)		X	
8	Does your study involve deliberately misleading the participants (e.g. deception, covert observation)		X	
9	Does your work involve administration of a non-food substance in abnormally large amounts or one that is known to cause allergic reaction(s) in some people?		X	
PARTICIPANTSx				
Does your work involve any of the following:				
		Yes	No	N/A
10	Human participants in health settings (e.g. private patients in private clinics)		X	
11	Human participants in health settings (e.g. NHS patients in NHS clinics/hospitals)		X	
12	Human participants who are in the care of a social worker		X	
13	Expectant or new mothers		X	
14	Refugees		X	
15	Minors (under the age of 18 years old)		X	
16	Participants in custody (e.g. prisoners or arrestees)		X	
17	Participants with impaired mental capacity (e.g. severe mental illness, brain damaged, sectioned under Mental Health Act, lowered or reduced sense of consciousness)		X	
INFORMATION TO PARTICIPANTS				
		Yes	No	N/A
18	Will you provide participants with a Participant Information Sheet prior to obtaining consent which can be taken away by the participant?			X
19	Will you describe the procedures to participants in advance, so that they are informed about what to expect?			X
20	Will you obtain consent for participation? (normally written)			X
21	Will you tell participants that they may withdraw from the research at any time and for any reason?			X
22	With questionnaires, will you give participants the option of omitting questions they do not want to answer?			X
23	Will you tell participants that their data will be treated with full confidentiality and that, if published, it will not be identifiable as theirs?			X
24	Will you debrief participants at the end of their participation (e.g. give them a brief explanation of their study)?			X

If you have answered NO to questions 1-17 (inclusive) and YES to questions 18-24 (inclusive), you do not need to complete the Full Research Ethics Approval Form (Part B). Please keep this form for your records.

If you have answered YES to any of the questions 1-17 (inclusive) or NO to any of the questions 18-24 the Full Research Ethics Approval Form (Part B) MUST be completed.

If you are applying for external Ethical Approval, please send an electronic *copy* of the Cover Sheet and Part A of the form to Huzma Kelly, Senior Research Officer (Policy and Governance), Academic Registrar's Department, Copland Building, New Cavendish Street.